

Niche Adaptation in *Campylobacter jejuni* and *Helicobacter pylori*

Stephen Russell Thompson



A thesis submitted in fulfilment of the requirements
of Nottingham Trent University for the degree of
Doctor of Philosophy (PhD)

October 2022

Declaration

The written content of this thesis including analysis, discussion and conclusions are my own unless referenced. All experimental work presented in this body of work is original and conducted by the author, at Nottingham Trent University unless otherwise stated.

Antrum/Corpus paired isolate genomes compared in Chapter three were provided by Dr Daniel Wilkinson, former NTU PhD student.

RNA extraction and RNA sequencing in Chapter four was performed by Macrogen Inc, South Korea with samples prepared by the author at Nottingham Trent University.

Some bioinformatic analyses and subsequent production of images in Chapter four were generated by Professor Lesley Hoyles. These instances are referred to as they arise in the relevant methods, results and discussion sections of Chapter four.

The copyright in this work is held by the author. You may copy up to 5% of this work for private study, or personal, non-commercial research. Any re-use of the information contained within this document should be fully referenced, quoting the author, title, university, degree level and pagination. Queries or requests for any other use, or if a more substantial copy is required, should be directed to the author.

Abstract

Campylobacter jejuni and *Helicobacter pylori* represent two major human pathogens. *C. jejuni* related gastroenteritis (campylobacteriosis) is considered the leading cause of human bacterial gastroenteritis cases worldwide and *H. pylori* infection although asymptomatic in the majority of cases can increase the risk of developing peptic ulcers and gastric adenocarcinoma. This thesis investigates different populations within these two bacteria and how they vary phenotypically and genomically from each other and how this may relate to niche adaptation ability.

In *C. jejuni*, research was focussed on strains belonging to the 403 Clonal-Complex (MLST). The 403CC represents a lineage that seemingly demonstrates a near inability to colonise poultry hosts which is atypical, given poultry are a major zoonotic reservoir for *C. jejuni* carriage. Phenotypic testing found no significant differences between 403CC isolates and chicken isolates, except that during initial growth at 42°C (6-9 h) chicken isolates grew statistically significantly faster. Genome analysis showed a 403CC lineage specific genome content particularly a restriction-modification system (*HhaIm*) has been described in previous research and this association still holds true.

In *H. pylori* the aim was to characterise the phenotypic and genomic properties of antrum/corpus paired strains isolated from the respective regions of patient's stomachs. No statistically significant differences were observed in phenotypic ability between antrum and corpus strains across a range of assays or genomically. The transcriptional effect of sub-MIC concentrations of menadione on *H. pylori* 322A was demonstrated by whole RNA-Sequencing. Menadione generates superoxides by redox cycling thus replicating niche oxidative stress in the gastric niche. Treatment with menadione compared to untreated samples caused 1312 significantly differentially expressed genes. 89 metabolic pathways, particularly epithelial cell signalling in *H. pylori* infection were affected. Major genes *cagA*, *vacA*, *ureA/B/I luxS*, and *ruvC* were all downregulated.

Niches play an important role in both *C. jejuni* and *H. pylori* in the wider context of the organisms as human pathogens. The research presented compares niche adaptation within these organisms and demonstrates for the first time the effect of menadione on the whole *H. pylori* transcriptome.

Acknowledgements

First of all, I would like to thank Nottingham Trent University for the VC Scholarship that funded this PhD, and the resources that allowed me to generate the work presented in this thesis.

Professor John Atherton and the team at the University of Nottingham, for obtaining patient biopsies from Queens Medical Centre Hospital, Nottingham, and providing the subsequent antrum and corpus isolates for use in this thesis.

My supervisory team past and present, Dr Gina Manning for the 1st year of my PhD and all of her input into the *Campylobacter* work. Dr Michael Loughlin for stepping in as a second supervisor and providing great feedback, whilst re-assuring me on my presenting skills. Most importantly Dr Jody Winter, not only for stepping up as my Director of Studies but navigating me through what turned out to be a tricky PhD, with endless support, kindness and knowledge that was above and beyond what most supervisors would do.

All of the AROM group, students and lecturers. Not only for your feedback, but also creating a warm and welcoming environment for everybody to work.

Dr Daniel Wilkinson for providing me with *H. pylori* genomes and showing me the ropes of how *Helicobacter* should be handled. Professor Alan McNally (Uni of Birmingham) for overseeing my *C. jejuni* genome analysis at UoB. Professor Lesley Hoyles on her contribution in Chapter 4 and showing me all things transcriptomics.

Two personal acknowledgements, to my parents who have gone through every up and down with me over the years but believed I would always find a way through. Finally, my best friend Harry. Sometimes family are the people you choose, and one amazing friend can do more for you than a crowd of people. I will always be indebted to you.

Table of Contents

Declaration	i
Abstract	ii
Acknowledgements	iii
List of tables	ix
List of figures	x
Abbreviations	xii
Chapter One: Introduction	1
1.1 General features of <i>Campylobacter jejuni</i>	1
1.1.1 Transmission routes of <i>C. jejuni</i>	2
1.1.2 <i>C. jejuni</i> in humans.....	4
1.1.3 <i>C. jejuni</i> in chickens.....	4
1.1.4 Diagnosis of <i>C. jejuni</i> infection.....	5
1.1.5 Treatment of <i>C. jejuni</i> infection.....	6
1.1.6 Global impact of <i>C. jejuni</i>	7
1.1.7 Rationale for the current study.....	9
1.2 General features of <i>Helicobacter pylori</i>	11
1.2.1 Transmission routes of <i>H. pylori</i>	12
1.2.2 <i>H. pylori</i> colonisation.....	13
1.2.3 Clinical presentation of <i>H. pylori</i>	17
1.2.4 Diagnosis of <i>H. pylori</i> infection.....	19
1.2.5 Sydney Scoring System of <i>H. pylori</i> gastritis.....	21
1.2.6 Treatment of <i>H. pylori</i> infection.....	21
1.2.7 Antibiotic resistance and global impact of <i>H. pylori</i>	22
1.2.8 Rationale of <i>H. pylori</i> study.....	24
1.2.9 <i>C. jejuni</i> and <i>H. pylori</i> comparisons.....	25
1.2.10 Thesis aims.....	27
Chapter Two: Materials and Methods	
2.1 <i>C. jejuni</i> strains used in phenotypic assays	28
2.1.1 Maintenance, storage and general culture of strains.....	29
2.1.2 Temperature growth curves.....	29
2.1.3 Biofilm formation.....	29

2.1.4	Motility.....	30
2.1.5	Chemotaxis.....	30
2.1.6	Vitamin B5 Synthesis.....	31
2.1.7	Oxidative stress.....	32
2.1.8	Purity checks.....	32
2.1.9	Genomic analysis.....	33
2.1.10	Statistical analysis.....	33
2.2	<i>H. pylori</i> strains used in phenotypic assays.....	34
2.2.1	Maintenance, storage and general culture of strains.....	35
2.2.2	Growth curves.....	35
2.2.3	Motility.....	36
2.2.4	Oxidative stress.....	36
2.2.5	Menadione resistance.....	37
2.2.6	Biofilm formation.....	39
2.2.7	Purity checks.....	39
2.2.8	Genome analysis.....	39
2.2.9	Statistical analysis.....	40
2.3	Directed evolution and transcriptomics.....	40
2.3.1	Strain selection for <i>H. pylori</i> transcriptomics.....	41
2.3.2	Culture and preparation.....	41
2.3.3	RNA extraction and Library construction.....	43
2.3.4	RNA sequencing and output.....	43
2.3.5	Bioinformatics analyses.....	43
2.3.6	Principal component analysis.....	44
2.3.7	Visualisation of data for significantly differentially expressed genes.....	44
2.3.8	Pathway over-representation analysis.....	44
Chapter Three: Phenotypic and genomic comparisons within <i>Campylobacter jejuni</i>.....		
3.1 Introduction.....		
3.1.1	Temperature based growth.....	46
3.1.2	Biofilm formation.....	47
3.1.3	Motility and Chemotaxis.....	48
3.1.4	Vitamin B5 synthesis.....	49

3.1.5	Oxidative stress survival.....	50
3.1.6	Genome analysis.....	51
3.1.7	Aims.....	52
3.2	Results.....	53
3.2.1	Growth of strains at 42°C shows faster initial growth of chicken isolate group.....	53
3.2.2	Biofilm formation is highly variable with no consensus on optimal conditions.....	56
3.2.3	Motility is highly variable between strains but is not significant between groups.....	59
3.2.4	Chemotactic mediated migration increases at higher concentrations of fucose.....	61
3.2.5	Vitamin B5 depleted media does not significantly impair <i>C. jejuni</i> growth	63
3.2.6	Oxidative stress survival does not significantly differ between strain groups.....	65
3.2.7	Genes related to phenotypic assays and niche adaptation are largely conserved across 403CC and Campylobacter specialist genomes	67
3.2.7.1	Biofilm genes.....	67
3.2.7.2	Motility genes.....	67
3.2.7.3	Chemotaxis genes.....	68
3.2.7.4	Vitamin B5 synthesis genes.....	68
3.2.7.5	Oxidative stress genes.....	68
3.2.7.6	Other genes of potential relevance.....	68
3.3	Discussion.....	70
3.3.1	Temperature growth curves.....	71
3.3.2	Biofilm formation.....	73
3.3.3	Motility.....	75
3.3.4	Chemotaxis.....	76
3.3.5	Vitamin B5 synthesis.....	78
3.3.6	Oxidative stress.....	79
3.3.7	Genome analysis.....	80
3.3.8	Conclusions and Recommendations.....	83

Chapter Four: Phenotypic and genomic comparisons within <i>Helicobacter pylori</i>	87
4.1 Introduction	87
4.1.1 Growth curve	87
4.1.2 Motility	88
4.1.3 Oxidative stress survival	88
4.1.4 Menadione resistance	89
4.1.5 Biofilm formation	90
4.1.6 Genome analysis	90
4.1.7 Aims	92
4.2 Results	92
4.2.1 Growth curves show uniform growth across all isolates	92
4.2.2 Motile ability varies by strain but not significantly between antrum and corpus group	94
4.2.3 Oxidative stress survival is not significantly different between antrum and corpus isolates	96
4.2.4 Menadione MIC is consistent across all strains	98
4.2.5 Biofilm formation was significantly different between strains but not by isolate group	100
4.2.6 Genome analysis by heatmap shows paired antrum/corpus isolates differ in gene presence/absence	102
4.3 Discussion	103
4.3.1 Growth curves	104
4.3.2 Motility	105
4.3.3 Oxidative stress survival	106
4.3.4 Menadione resistance	107
4.3.5 Biofilm formation	108
4.3.6 Genome analysis	109
4.3.7 Conclusion and Recommendations	110
Chapter Five: Transcriptomic effect of menadione on <i>H. pylori</i> strain 322A	114
5.1 Introduction	114
5.2 Results	115

5.2.1	Principal component analysis shows sample clustering by treatment group.....	115
5.2.2	Heatmap shows 1312 significantly differentially expressed genes clustered by treatment group.....	117
5.2.3	Top ten most significantly differentially expressed genes show menadione treatment causes both down and upregulation of genes.....	119
5.2.4	Pathway over-representation shows ‘Epithelial cell signalling in <i>H. pylori</i> infection’ as the most significantly affected metabolic pathway by menadione treatment.....	121
5.3	Discussion.....	125
5.3.1	Principal component analysis.....	125
5.3.2	Heatmap of significantly differentially expressed genes.....	126
5.3.3	Top ten significantly differentially expressed genes.....	126
5.3.4	Pathway over-representation analysis.....	130
5.3.5	Conclusion and Recommendations.....	132
Chapter Six:	Final Discussion.....	136
6.1	Discussion.....	135
6.2	Future work.....	141
6.3	Conclusion.....	142
7.0	References.....	144
8.0	Appendix.....	177
8.1	<i>Helicobacter pylori</i> ethical approval.....	177
8.2	<i>C. jejuni</i> genome analysis presence/absence list.....	178
8.3	Original heatmap of differentially expressed genes in 5.2.2.....	192
8.4	KEGG over-representation metabolic pathways with menadione treated significantly differentially expressed genes mapped to them.....	193

List of Tables

Table 1.1: Direct comparison of key features of <i>C. jejuni</i> and <i>H. pylori</i>	26
Table 2.1: <i>C. jejuni</i> strains used in phenotypic analysis.....	28
Table 2.2: <i>H. pylori</i> strains used phenotypic analysis with associated patient Sydney scores.....	35
Table 2.3: Flask designations (T) or (U) with menadione in RNA-Seq sample prep with randomised ST (named designation)	42
Table 3.1: <i>C. jejuni</i> genes identified to be not present across all 403CC and ST21/45 generalist genomes.....	69
Table 5.1: Log2 fold changes between menadione treatment groups for the top 10 most significantly differentially expressed genes.....	119
Table 5.2: List of significant KEGG over-production metabolic pathways the 1312 significantly differentially expressed genes were mapped to.....	122

List of Figures

Figure 1.1: Transmission routes of <i>C. jejuni</i> in the ecosystem.....	3
Figure 1.2: Stool Gram-stain of <i>C. jejuni</i>	6
Figure 1.3: <i>C. jejuni</i> outbreaks in more economically developed countries (2007-2013).....	8
Figure 1.4: <i>H. pylori</i> colonisation sites and potential clinical outcomes by colonisation region.....	14
Figure 1.5: Presence and arrangement of cells in antrum and corpus glands.....	14
Figure 1.6: Polymorphic regions of the CagA protein, EPIYA motifs and the geographic regions associated with different EPIYA motifs.....	16
Figure 1.7: Potential allelic variations of s- i- d- and m- domains of <i>vacA</i>	17
Figure 1.8: Gastric precancerous cascade associated with <i>H. pylori</i> ‘Correa’s cascade of gastric carcinogenesis’	19
Figure 1.9: Global map of reported rates of <i>H. pylori</i> clarithromycin, metronidazole and levofloxacin resistance in WHO countries in 2018.....	23
Figure 2.1: 96-well plate dilution series used in the menadione MIC assay.....	38
Figure 3.1: <i>C. jejuni</i> chicken isolate growth is initially faster at 42°C than 403CC isolates	54
Figure 3.2: <i>C. jejuni</i> biofilm formation is highly variable under standard atmospheric oxygen.....	57
Figure 3.3: <i>C. jejuni</i> biofilm formation is highly variable under microaerobic oxygen levels.....	58
Figure 3.4: <i>C. jejuni</i> motility is highly variable between strains but does not show significance by strain group.....	60
Figure 3.5: Increase in fucose concentration increases <i>C. jejuni</i> migration by chemoattraction.....	62
Figure 3.6: Absence of vitamin B5 does not significantly affect <i>C. jejuni</i> growth.....	64
Figure 3.7: Oxidative stress survival does not differ significantly between <i>C. jejuni</i> strain groups.....	66
Figure 4.1: Proposed mechanism of menadione production of ROS by redox cycling.....	89
Figure 4.2: Growth curve shows growth of <i>H. pylori</i> was tightly grouped across all strains	93

Figure 4.3: <i>H. pylori</i> motility varies greatly by strain but did not cluster by antrum or corpus group.....	95
Figure 4.4 <i>H. pylori</i> oxidative stress survival was not significantly different between antrum and corpus isolates.....	97
Figure 4.5 MIC value obtained for menadione was consistent across all <i>H. pylori</i> strains	99
Figure 4.6: <i>H. pylori</i> biofilm formation was variable by strain with corpus isolates showing a tighter clustering in biofilm performance.....	101
Figure 4.7: <i>H. pylori</i> genome analysis, bidirectional heatmap showing clustering of present or absent genes.....	102
Figure 5.1-5.2: Principal component analysis shows samples cluster by menadione treatment condition.....	116
Figure 5.3: Heatmap showing clustering of 1312 significantly differentially expressed genes between menadione treated and untreated samples.....	118
Figure 5.4: Box plots of log ₂ transformed gene count data for the top ten most significantly differentially expressed genes.....	120
Figure 5.5: Box plots of log ₂ transformed gene count data for <i>cagA</i> and <i>vacA</i> with the epithelial cell signalling pathway for <i>H. pylori</i> infection showing log ₂ changes created by menadione treated significantly differentially expressed genes.....	124

Abbreviations

ANOVA	Analysis of Variance
CC	Clonal Complex
CDC	Centre for Disease Control
Cfu/ml	Colony forming units per millilitre
DALY	Disability-adjusted life years
EPIYA	(Glu-Pro-Ile-Tyr-Ala) sequence
FCS	Fetal Calf Serum
GBS	Guillan-Barre Syndrome
KEGG	Kyoto Encyclopaedia of Genes and Genomes
MIC	Minimum Inhibitory Concentration
MBEC	Minimum Biofilm Eradication Concentration
MHB	Mueller-Hinton Broth
MCCDA	Modified Charcoal-Cefoperazone-Deoxycholate Agar
NCTC	National Collection of Type Cultures
OD	Optical Density
PBS	Phosphate-Buffered Saline
PCA	Principal Component Analysis
PCR	Polymerase Chain Reaction
R-M	Restriction-Modification
RNA	Ribonucleic Acid
ROS	Reactive Oxygen Species
ST	Sequence Type (Except chapter five)
ST1-12	Random sample allocation for RNA extraction (Chapter five)
V/V	Volume per Volume
WHO	World Health Organisation

Chapter One: Introduction

Bacteria are ubiquitous in ecological niches on Earth. Species that have evolved with humans and other organisms have become more proficient in their ability to colonise and persist in these niches as they mutate and over time adapt to the specific conditions of their surroundings. This thesis looks at two such bacterial species and their adaptation to these niches. *Campylobacter jejuni* is a multi-species host pathogen that adapts to life across many different animal species, which will be referred to as inter-host niche adaptation. *Helicobacter pylori* is a bacterial species that has evolved with humans that encounters variable conditions in the different areas of the stomach in that it colonises, which will be referred to as intra-host niche adaptation. The thesis will explore how different populations within these bacterial species are differentially adapted to intra or inter specific niches and also how these species compare and contrast.

1.1 General features of *Campylobacter jejuni*

Campylobacter jejuni is a curved, rod shaped, Gram-negative, microaerophilic bacterium causing acute gastroenteritis (campylobacteriosis). It is one of the major leading causes of food and waterborne infections worldwide (Igwaran and Okoh 2019) and one of the most widespread infectious diseases of the last century (Kaakoush *et al* 2015).

The *Campylobacter* genus was taxonomically recognised in 1963 following the reclassification of *Vibrio fetus* to *Campylobacter fetus* (Sebald and Veron 1963). Since 2018 the World Health Organisation has recognised 17 species and six subspecies assigned to the *Campylobacter* genus of which the most prevalent is *C. jejuni*. *Campylobacter jejuni* was first described in relation to the intestinal disorders of cows in 1931 as *Vibrio jejuni* (Jones *et al* 1931) and was added to the *Campylobacter* genus taxonomic nomenclature as *Campylobacter jejuni* in 1973 (Veron and Chatelain 1973).

C. jejuni isolates are categorised and grouped through multilocus sequence typing. Multilocus sequence typing is a system that relies on genetic variation of seven 'housekeeping' loci and can be used to group strains within a species.

The MLST typing system for *C. jejuni* was proposed by Dingle *et al* (2001) that began with 194 isolates that were divided into 155 distinct sequence types (STs) and resolved into 62 clonal lineages/complexes (CC). PubMLST (Jolley *et al* 2018) one of the largest databases for MLST typing of bacteria currently holds 102,761 isolates in the *Campylobacter* database 81,950 *C. jejuni* and 20,811 *C. coli* (August 2022). Isolates comprise approximately 10,000 distinct sequence types divided into 44 clonal complexes.

Another facet of *C. jejuni* grouping designation is the notion of generalist and specialist lineages. In a multi host species pathogen such as *C. jejuni* it could be assumed that strains are adapted for transmission and colonisation across multiple species. Despite this it appears that some *C. jejuni* lineages have evolved to be associated primarily with a specific host species, known as host association. Currently there are no specific criteria on which an ST group or CC is designated as a generalist or specialist lineage. One study suggested an arbitrary cut off point of '70-30%' where if 70% of non-human isolates in the pubMLST database for a lineage came from one specific host species they would be designated the label of specialist lineage in regards to that host. If fewer than 70% of isolates were obtained for a specific host species then the lineage would be considered a generalist lineage (Sheppard *et al* 2014).

1.1.1 Transmission routes of *C. jejuni*

C. jejuni infection is widespread in the ecosystem. From the perspective of human infection there are many zoonotic reservoirs by which transmission can occur as shown in figure 1.1. The largest reservoir that humans acquire *C. jejuni* infection is through consumption of undercooked infected poultry, particularly chicken. A recent study found that in New Zealand an estimated 84% of campylobacteriosis cases were attributed to strains associated with poultry and 14% attributed to cattle (Lake *et al* 2021). *C. jejuni* is also routinely isolated from cattle, sheep, pigs, many bird species, domestic animals such as dogs and cats and from the environment such as farms, slaughterhouses and from environmental water sampling.

The magnitude of isolation points of *C. jejuni* highlights its problematic nature as a zoonotic pathogen. A recent study found that in a poultry supply chain in Valencia Spain, sampling retail equipment found a 36.7% *Campylobacter spp.* isolation rate in the broilers and an 80% isolation rate in packaging (Bort *et al* 2022). As multi species host colonisers a large proportion of *C. jejuni* are host generalists the largest clonal complexes being ST-21 and ST-45 as seen on the pubMLST database (Jolley *et al* 2018). Through phylogeographic analysis it is estimated that zoonotic transmission host species jumps occur approximately every 1.6-1.8 years. It is also suggested that due to this rapid host switching there is no association between genetic structure and host species and that generalists are equally adapted to inter-species host transmission as intra-species host transmission (Dearlove *et al* 2016).

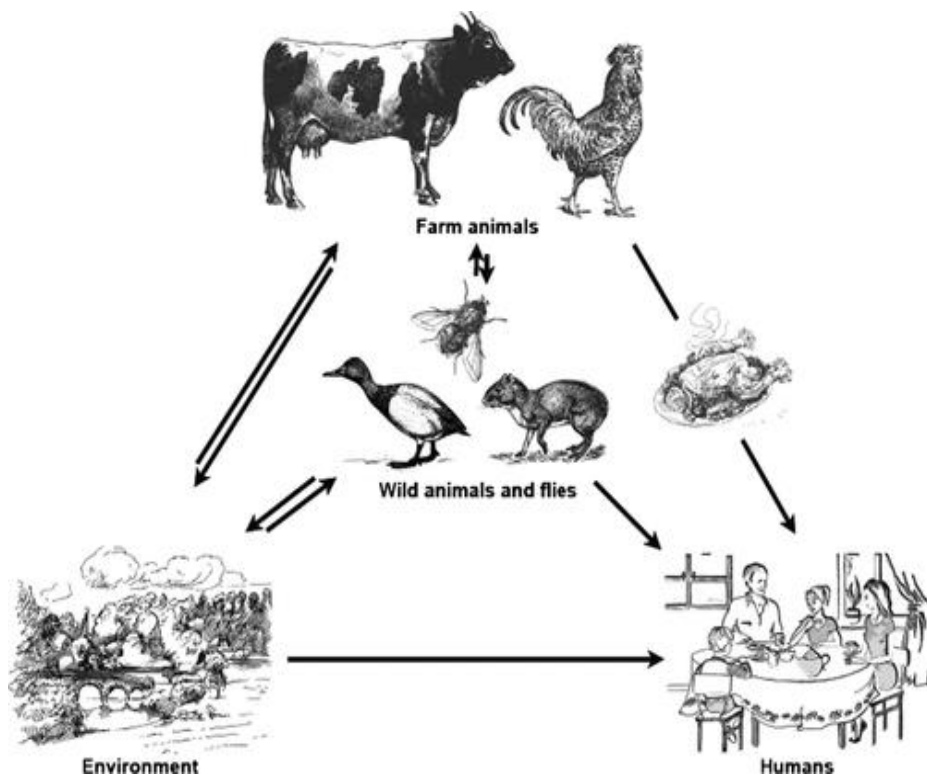


Figure 1.1 adapted from Bronowski, James and Winstanley (2014) showing transmission routes of *C. jejuni* in the ecosystem. Permission to reproduce this figure has been granted by publisher.

1.1.2 *C. jejuni* in humans

C. jejuni infection is the causative agent of a specific gastroenteritis, namely campylobacteriosis in humans. It is suggested that a dose as small as 360 CFU can cause symptomatic campylobacteriosis (Hara-Kudo and Takatori 2011), however mathematical modelling suggests an intermediate dose of 9×10^4 CFU/ml has the highest ratio of illness to infection (Medema *et al* 1996). Colonisation of the human host occurs in the small intestine and symptoms typically occur two to five days post infection. Commonly associated symptoms of campylobacteriosis are acute bloody or watery diarrhoea, fever and abdominal cramps lasting on average six days (Man 2011).

The major complication associated with *C. jejuni* infection is the triggering of Guillain-Barré Syndrome (GBS). GBS is an acute immune mediated disorder causing flaccid paralysis. The disorder affects the peripheral nervous system and is the leading cause of acute neuromuscular paralysis since the decline of the prevalence of polio in recent decades (Ho, McKhann and Griffin 1998). *C. jejuni* associated GBS is mediated by the molecular mimicry between microbial and nerve agents. This causes an unwanted autoimmune response that causes progressive acute limb weakness that peaks at two to four weeks post triggering. Artificial ventilation is required in 25% of patients and recovery post peak can take months or even years. In 2019 there were approximately 150,095 cases of GBS globally roughly equating to 1.9 prevalence per 100,000 of the population (Bragazzi *et al* 2021). Approximately 1 in 1,000 develop GBS following a *C. jejuni* infection. (Huizinga *et al* 2015).

1.1.3 *C. jejuni* in chickens

As noted, chickens are the largest reservoir of *C. jejuni* and has the largest impact on human campylobacteriosis cases. Given this, and the abnormal colonisation pattern displayed by the *C. jejuni* strains studied in this thesis it is important to understand why *C. jejuni* is so prevalent in chickens. Chicks receive maternal antibodies, to protect the animal until it can mount a robust immune system of its own. Maternal immunoglobulin Y antibodies are particularly important in the early life of the chick.

One to two-week-old birds are less susceptible to *C. jejuni* infection than three-week-old birds and this correlates with the decline in maternal antibodies (Cawthraw & Newell 2010). A similar study concluded that by the four-week period maternal antibodies had depleted to background levels (Sahin *et al* 2003). Given the intensive nature of commercial chicken farming, with many broiler houses keeping birds in close vicinity, it is unsurprising that *C. jejuni* can run rampant within the population. Once infected most chickens do not clear *C. jejuni* fully, and this is due to the fact that they are slaughtered at six weeks of age before the immune response would have fully matured.

It was long thought that within the chicken *C. jejuni* held a commensal relationship with the host. Not only does the organism reside in the cecal crypts of the intestine in very high levels in the order of 10^{10} cfu/g whilst being potentially asymptomatic. *C. jejuni* also cannot invade intestinal epithelium (Larson *et al* 2008, Looft *et al* 2019). This conclusion however has been challenged by observations on the pathogenicity of the organism, immune response mounted by the host and fitness deterioration of the host. The immune response mounted by a chicken against *C. jejuni* far surpasses that at which a commensal would be tolerated, although this varies by bird species and strain. It was observed that a strong inflammatory response caused diarrhoea, leading to leg and foot damage through standing on wet litter and thus decreasing the bird's fitness (Humphrey *et al* 2014). Research has also found that *C. jejuni* does not confine itself to the gastric tract and can spread to muscle tissue and the liver. Infact the disease levels observed in the liver correlated with *C. jejuni* colonisation levels (Williams, Fonseca & Humphrey 2016). From this it can be concluded that the blanket statement of *C. jejuni* commensalism in chickens is not accurate.

1.1.4 Diagnosis of *C. jejuni* infection

As *C. jejuni* is often self-limiting most cases are not reported, however in more severe cases *C. jejuni* infection is routinely diagnosed from stool sample, from which organism isolation and culture can be achieved for confirmatory diagnosis. Alongside sample culture, rapid detection can be achieved by stool sample Gram staining (Figure 1.2) (Kamata and Tokuda 2014) and for more thorough confirmation PCR tests can be used, particularly those targeting the *cdtC* and *hipO* genes (Kabir *et al* 2019).

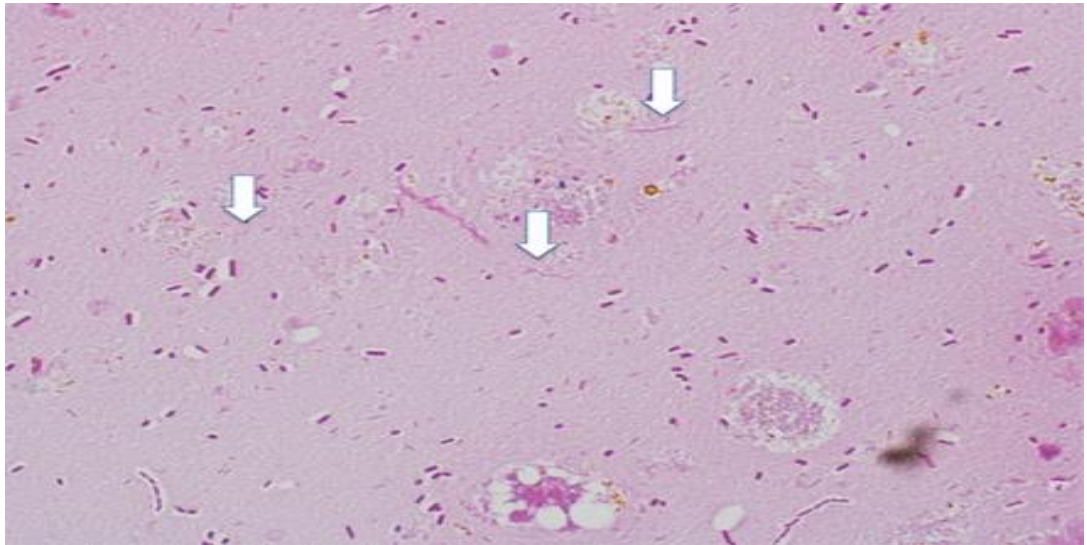


Figure 1.2 Adapted from Kamata and Tokuda (2014) showing a stool Gram stain. Arrows pointing to gull wing shaped Gram-negative rods suggests *C. jejuni* presence. Permission to reproduce figure has been granted by publisher.

1.1.5 Treatment of *C. jejuni* infection

The infection is generally self-limiting however more severe cases can result in hospitalisation requiring Oral Rehydration Therapy (ORT) and potential antibiotic treatment. Historically fluoroquinolone class antibiotics were used as first line in diarrhoeal illnesses however resistance rates are rising in *C. jejuni* (Whelan *et al* 2019). Macrolides such as erythromycin and azithromycin are now more commonly used as first line choices in treatment dependant cases of campylobacteriosis as resistance rates remain lower (Bolinger and Kathariou 2017). A 2012 WHO report stated that in 2010 in the USA 1% of *C. jejuni* isolates from human sources were resistant to erythromycin, 36% to tetracycline and 22% to ciprofloxacin with similar resistance rates of 1%, 36% and 22% respectively in chicken broiler meat isolates. In the EU in the same year resistance rates of 2% erythromycin, 21% tetracycline and 52% fluoroquinolone were observed in human *C. jejuni* isolates with comparable rates of 2%, 22% and 50% respectively in chicken broiler meat isolates.

A more recent study in Irish broiler houses from 2017 and 2018 suggested 45% of *Campylobacter* spp. isolates were resistant to at least one antimicrobial. Tetracycline resistance was most prevalent in *C. jejuni* in 38% of isolates, followed by ciprofloxacin and nalidixic acid resistance at 29%. It was noted that resistance rates have remained consistent over the last 20 years, interestingly ciprofloxacin resistance rates have failed to fall despite fluoroquinolone use being banned as a growth supplement in Europe since 2006 (Lynch *et al* 2020).

1.1.6 Global impact of *C. jejuni*

In 2012 the WHO published a report entitled “The Global View of Campylobacteriosis”. This report looked at the global impact of *Campylobacter* spp. as a whole. The report recognises that the true incidence rate of gastroenteritis caused by *Campylobacter* spp. is poorly known, particularly in low- and middle-income countries (LMIC). In high income countries annual incidence rates are estimated at between 4.4 and 9.3 per 1000 population. Even within high income countries there is a disparity in disability-adjusted life years (DALY) from *Campylobacter* spp. with estimates that range from 0.4 per 100,000 population in France to 109 DALY per population in Poland. With overall foodborne disease burden estimates ranging from 0.5 DALYs per 100000 in Greece up to 21.2 DALYs per 100000 in New Zealand (Lackner *et al* 2019). There has been a number of well publicised *Campylobacter* outbreaks across higher economically developed countries across the globe in recent years with a majority coming from poultry examples of which are shown in figure 1.3. Not only does the impact of *C. jejuni* campylobacteriosis result in DALY that affect individuals but the economic impact of *C. jejuni* should also not be underestimated. There is pressure on poultry farmers selectively using antibiotic in feed, through to food processing plants in broiler houses and slaughterhouses and then to food packaging companies to reduce the burden of *C. jejuni* in product for human consumption. Measures in biosecurity bring considerable cost to the industries. At the other end of the “farm to fork” spectrum there is an economic cost involved in public engagement and health campaigns. As the infectious dose of *C. jejuni* is so low and the bacteria is so prevalent in commercial chickens, public health campaigns are critical in raising awareness on correct preparation and cooking of poultry products.

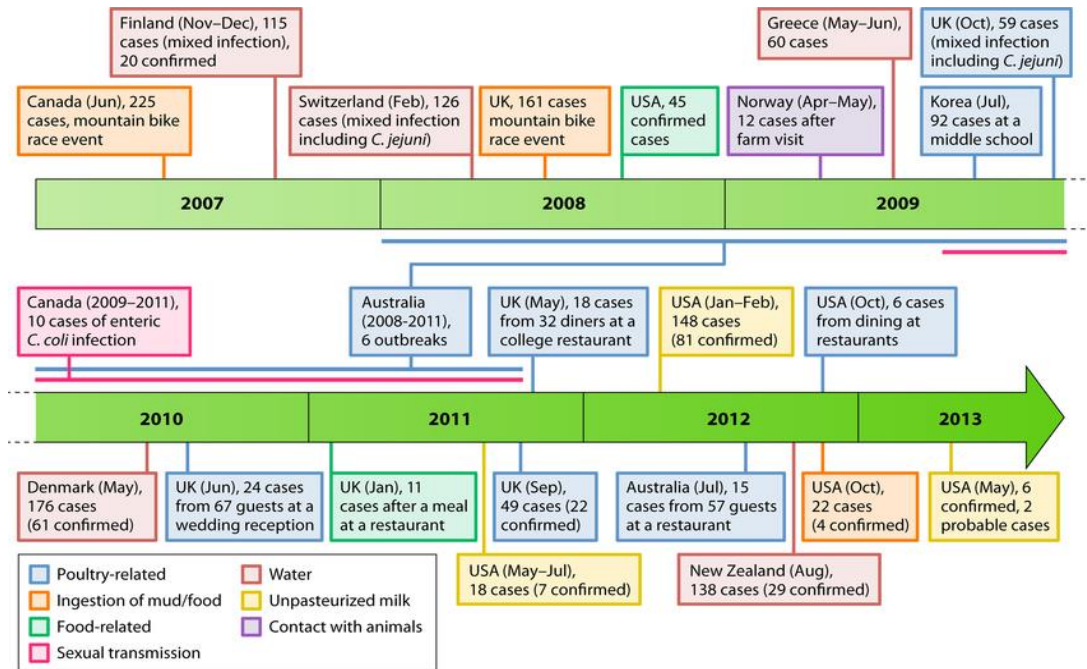


Figure 1.3 Adapted from Kaakoush *et al* (2015) showing outbreaks in economically developed countries between 2007-2013. Permission to reproduce has been granted by publisher.

In more recent years there was a substantial outbreak associated with the consumption of raw dairy milk (unpasteurised) that by law is permissible to sell direct to consumer as long as the consumers are made aware of what this entails. 69 cases of campylobacteriosis were recorded from a dairy farm in North West England in 2016, the last recorded outbreak of campylobacteriosis in the UK in relation to unpasteurised milk occurred in 1996 (Kenyon *et al* 2020).

More recently the CDC reported several outbreaks from a less common transmission route of *C. jejuni*. Infected puppies purchased from pet stores in the USA. The first outbreak between 2016-2018 saw 113 individuals infected with a multidrug resistant strain of *C. jejuni*, the same strain resurging in 2019 with a further 56 confirmed cases (CDC 2021).

The 2012 WHO report highlighted the need to tackle campylobacteriosis cases, detection, identification and treatment and there were recommendations made for each of these points. It was recommended that surveillance and monitoring of *C. jejuni* cases was paramount to understanding the human and economic impact of campylobacteriosis cases and how successful potential intervention strategies were.

Surveillance also should inform on emerging trends in observed antibiotic resistance rates in both human and poultry isolates and how this relates to preventative and post infection treatment for veterinarians and healthcare professionals. Standardisation and validation of laboratory diagnostic measures should be introduced, and culture independent diagnostic tests will allow better monitoring of *C. jejuni* spread. Action should be taken to reduce bacterial load in poultry products for human consumption and it was acknowledged that this must take place at each stage of the food processing chain, in farming, slaughterhouse and food packaging. It was also acknowledged that although poultry is the major reservoir for campylobacteriosis infections other routes are present in the ecosystem and these must also be tackled through biosecurity and sanitation measures such as pasteurisation of milk and chlorination of water supplies (World Health Organisation 2013).

1.1.7 Rationale for the current study

C. jejuni is a multi-species host pathogen that poses a significant global impact to health. By researching the niche colonisation patterns of this zoonotic infective organism we may better understand how transmission occurs and the role it plays in foodborne and waterborne acquired infections in humans. Of particular interest are strains that do not fit the general niche colonisation patterns associated with the majority of *C. jejuni* infections.

As mentioned in section 1.1 multi locus sequence typing is the means by which *C. jejuni* isolates are grouped together. One of the largest databases of *C. jejuni* isolates that uses the MLST system is pubMLST (Jolley *et al* 2018) that houses 102,761 isolates in the *Campylobacter* database where isolates comprise approximately 10,000 distinct sequence types divided into 44 clonal complexes. A sequence type (ST) is a group of isolates that have identical allelic profiles of the seven housekeeping genes, this is then expanded to a clonal complex (CC) where all isolates share similarities to a central allelic profile.

The two largest clonal complexes are the ST-21CC and ST-45CC that account for 18,541 and 7,266 of the total database isolates respectively. These two clonal complexes are the major ‘generalist’ complexes, an identifier used when 70% of recorded isolates in the database are not attributed to a single host source, distinguishing it from specialist lineages. Examples of specialist clonal complex groups are the ST-61CC (Cattle), ST-257CC and ST-573CC (Chickens) and ST-682CC (Wild birds/Environmental).

The 403 clonal complex of *C. jejuni* represents a population of strains that are ill-adapted to colonise the chicken niche. The rationale for this is the low reported isolation rate of 403CC strains from chickens on the PubMLST *C. jejuni* strain collection database. The 403CC is a generalist lineage yet interestingly of the 997 recorded 403CC isolates in the PubMLST database only five (0.5%) are attributed to chicken hosts. In comparison the most populous generalist CC ST-21 and ST-45 have an 8.5% and 13.9% chicken isolate rate respectively. Given that chickens are a major reservoir of *C. jejuni*, the 403CC provides a unique example of niche restriction compared to the norm. Several unanswered key questions can be posed about the 403 clonal complex:

- Why is the isolation rate of 403CC strains from poultry so low?
- What barriers do 403CC strains face in regard to colonising poultry?
- What physical properties do 403CC strains possess or lack that affect this colonisation ability?
- What genomic properties do 403CC strains possess or lack that affect this colonisation ability?

To address these key questions phenotypic analysis was conducted on 403CC *C. jejuni* isolates and directly compared to isolates of chicken origin. Assays were chosen that reflected niche adaptation or niche transmission barriers. Genomic analysis was also conducted. Given that 403CC is the only recorded generalist lineage with near inability to colonise chicken hosts, it was decided to compare the genomes of 403CC to successful generalist chicken colonisers to look for the presence/absence of genes that may be indicative of this anomaly. All work in relation to *C. jejuni* can be found in chapter three.

1.2. General features of *Helicobacter pylori*

Helicobacter pylori is a helical, Gram-negative, microaerophilic organism that chronically infects approximately 33-50% of the world's adult population with strong variance depending on geographic region, with lower infection rates in North America and Northern Europe (Peleteiro *et al* 2014). Infection is asymptomatic in a large percentage of cases. Despite this, carriage can lead to the development of peptic ulcer disease in approximately 10-20% of cases and in some cases lead to the development of gastric adenocarcinoma in approximately 1-2% of carriers (Kamogawa-Schifter *et al* 2018).

H. pylori is the only currently recognised bacterial carcinogen and was categorised as a type 1 carcinogen by the International Agency for Research on Cancer (IARC) in 1994 as reported in Møller, Heseltine and Vainio (1995).

Although the early history of *H. pylori* is full of observations of the bacterium, the discovery of *H. pylori* and its role in gastric disease is largely credited to Warren and Marshall (1983) who reported on an “unidentified curved bacilli” and its presence in active chronic gastritis cases. It was during this work that *H. pylori* was first successfully cultured from a patient and was the basis of the follow up breakthrough work Marshall *et al* (1985). In 1985 in order to fulfil Koch's postulates for this “unidentified curved bacilli” now tentatively called a “pyloric *Campylobacter*” due to its morphological similarities to *Campylobacter spp.*, Marshall ingested bacteria cultured from a patient, subsequently developing infection and gastritis as proven by endoscopy approximately four weeks later. This work into the discovery of *H. pylori* as a gastric pathogen earned Warren and Marshall the Nobel Prize in Physiology or Medicine in 2005.

Taxonomically *H. pylori* was originally assigned to the *Campylobacter* genus as *Campylobacter pylori* for several years until its reclassification when the *Helicobacter* genus was proposed in 1989 (Goodwin *et al* 1989) and *H. pylori* was established.

1.2.1 Transmission routes of *H. pylori*

The transmission route of *H. pylori* is yet to be fully elucidated. It is likely that a complex web of potential transmission routes are involved in *H. pylori* acquisition. What is known is that infection by *H. pylori* is thought to occur predominantly in early childhood and will persist as a chronic infection in the absence of eradication treatment. Transmission routes of *H. pylori* can be broken down into horizontal and vertical transmission events.

Person to person transmission events are most likely the predominant source of *H. pylori* acquisition and these can be classed as vertical (ascendant to descendant down a familial line) or horizontal (contact with members outside of the family) (Kayali *et al* 2018). Interestingly, a 2008 study found that members of families in the developed western world were more likely to share identical strains of *H. pylori* suggesting vertical parental or sibling transmission than in developing countries where strains acquired were more varied suggesting horizontal transmission (Schwarz 2008). In familial transmission although sibling and paternal infection may factor in acquisition of *H. pylori* infection it is suggested that it is the maternal carriage status that has the greatest impact on childhood infection (Weyermann, Rothenbacher and Brenner 2009). *H. pylori* infection can also occur in later life for example through saliva from adult partner to partner (Gisbert *et al* 2002). Transmission can occur through gastro-oral (Bürgers *et al* 2008), oral-oral (Gebara *et al* 2006) and fecal-oral (Oderda *et al* 2000) routes. The prevalence of transmission through these routes will be dependent on sanitation infrastructure and hygiene practices. There is also the potential for *H. pylori* infection from environmental sources, for example in a 2019 study of water and wastewater samples *H. pylori* was found in 8% and 36% of samples respectively (Farhadkhani *et al* 2019).

1.2.2 *H. pylori* colonisation

H. pylori colonises the gastric mucosa and gastric epithelium of the human stomach. The human stomach is a dynamic system and is comprised of two distinct anatomical regions or gastric niches due to differences in environmental conditions, local cell types and general functions. The corpus that is proximal to the oesophagus forms the main “body” of the stomach and the antrum that is distal to the oesophagus and proximal to the duodenum forms the other main niche (Figure 1.4). The main difference between these two regions are the cell types that are present in the glands (Figure 1.5). As shown in Figure 1.5 the cells present in antrum and corpus glands show variation due to their differing roles in maintenance of the stomach environment. Antral glands contain mucus producing cells, alongside somatostatin cells (D cells) and gastrin cells (G cells). The role of D and G cells are to inhibit and stimulate gastric acid secretion respectively, although there are no acid secreting cells in the antrum itself. The corpus glands contain the parietal cells that secrete gastric acid alongside chief cells that produce pepsinogen, a protease precursor.

The greatest challenge to *H. pylori* survival in the human stomach is the highly acidic environment. *H. pylori* tackles this potential colonisation barrier through generation of a localised neutral micro-environment by secreting urease to hydrolyse gastric urea into ammonia and carbon dioxide (Scott *et al* 2002). *H. pylori* survival is also promoted through motility, using its helical shape to traverse through the viscous gastric mucosa mediated by chemotactic signalling. Chemotactic systems in *H. pylori* are mediated primarily by core chemotaxis proteins belonging to the Tlp or Transducer like proteins family, containing TlpA, TlpB, TlpC and TlpD. Tlp chemoreceptors working in conjunction with other chemotaxis proteins such as CheW, CheA and CheY facilitate motility based chemoattraction to host urea and arginine and chemorepellence to acidic pH, reactive oxygen species and bile salts (Johnson and Ottemann 2018).

The next step in persistent colonisation is adhesion to the gastric epithelium. Outer membrane proteins (OMPs) play the predominant role in achieving adhesion. Several OMPs called adhesins are thought to be vital to adhesion in *H. pylori* the main ones being blood group antigen-binding adhesion (BabA), sialic acid-binding adhesion (SabA), outer membrane inflammatory protein (OipA) and adherence associated lipoproteins (AlpA and AlpB) (Huang *et al* 2016).

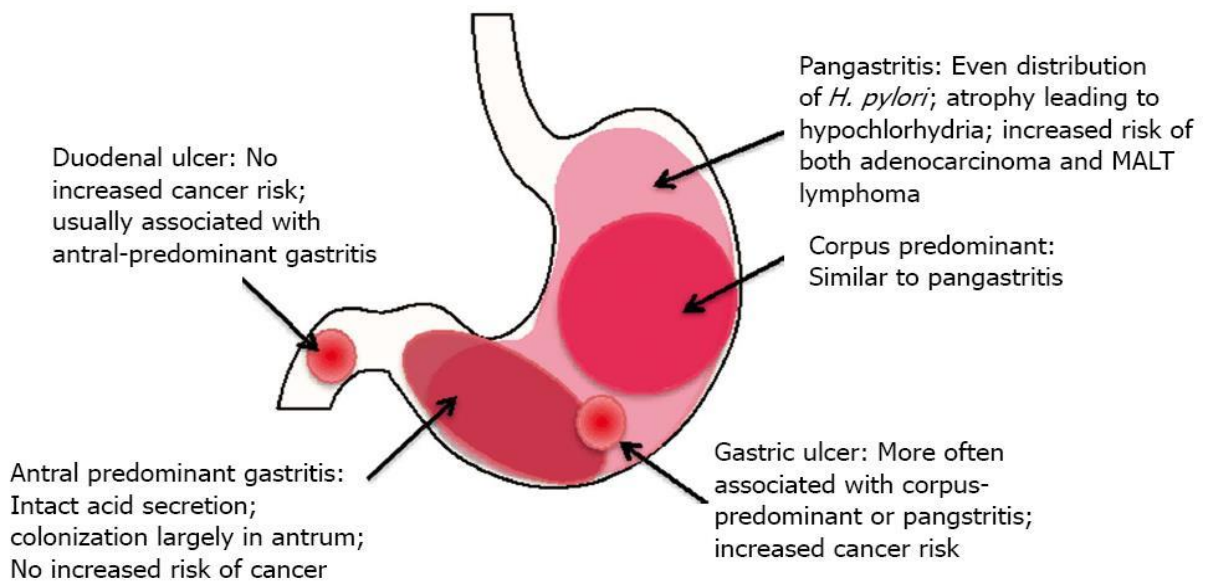


Figure 1.4 Adapted from Testerman and Morris (2014) showing *H. pylori* colonisation sites and potential clinical outcomes due to colonisation of a particular region of the stomach. Figure reproduced under open access creative commons freedom.

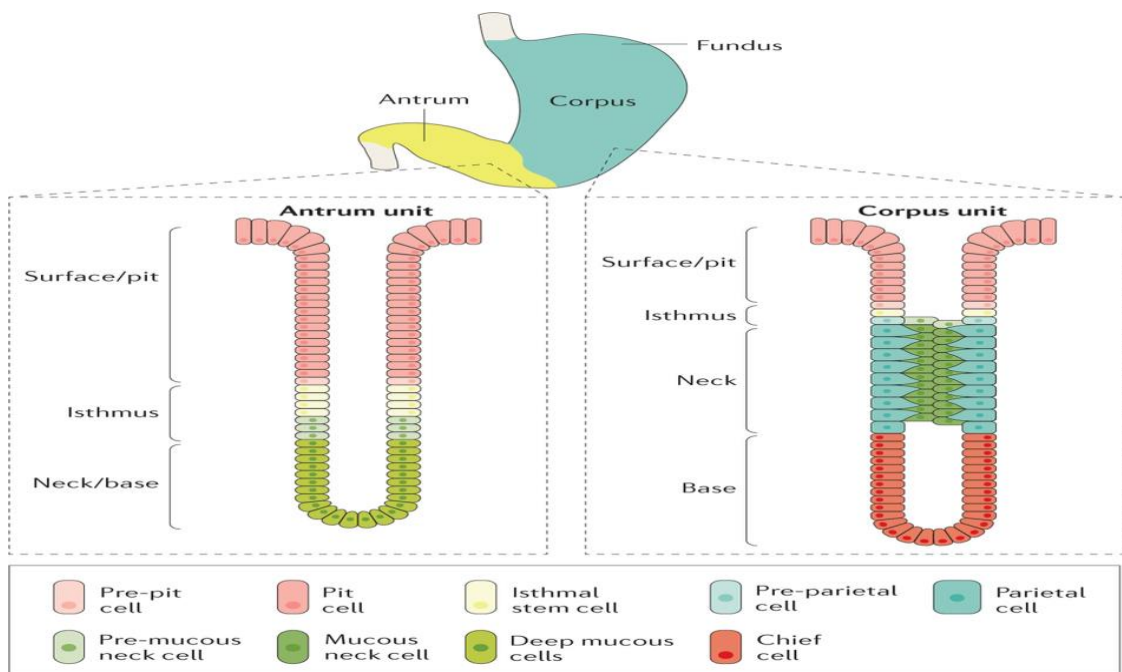


Figure 1.5 Adapted from Saenz and Mills (2018) showing presence and arrangement of cells in antrum and corpus glands. Permission to reproduce figure granted by authors.

H. pylori can also modulate gastric epithelium by employing two key toxins CagA and VacA. Cytotoxin-associated gene A (CagA) is an effector oncoprotein that is part of the *cag* pathogenicity island (*cagPAI*) that may be present or absent in *H. pylori* strains and makes them highly virulent. The *cagPAI* is approximately 40kb in size containing 27-31 genes including *cagA* and the protein components of the Type IV secretion system (T4SS) required for translocation of the CagA toxin into a host gastric epithelial cell. CagA undergoes phosphorylation-dependant and independent pathways modulating signalling cascades that are involved in proliferation, inflammation, disruption of cell junctions, suppression of apoptosis, cytoskeletal rearrangements amongst others (Backert, Tegtmeyer and Fischer 2015).

At the base level *cagA* positive strains are strongly associated with ulcers and gastric cancer (Khadir *et al* 2017). However, the CagA protein is polymorphic in nature and these variants of the CagA protein are thought to contribute differentially in terms of potential disease outcome. The C-Terminus region of the CagA protein has a geographically conserved variable region known as the EPIYA motif region. The EPIYA motif region consists of Glu-Pro-Ile-Tyr-Ala residues and the number of EPIYA motif repeats and variation in amino acids flanking this region have distinguished the polymorphic nature of the CagA protein. Tyrosine in the EPIYA motif is a site of phosphorylation in the CagA protein. EPIYA motif regions are designated the nomenclature EPIYA-A, -B, -C and -D as shown in figure 1.6. For example, CagA is termed 'Western' when EPIYA-A, -B and -C are present where the C motif may be duplicated multiple times. East Asian CagA by contrast contains EPIYA-A, -B and -D. More severe infection outcomes are observed in Western countries with EPIYA-ABC with more EPIYA-C repeats, and in East Asia EPIYA-ABD is associated with a higher risk of gastric cancer (Bridge and Merrell 2013).

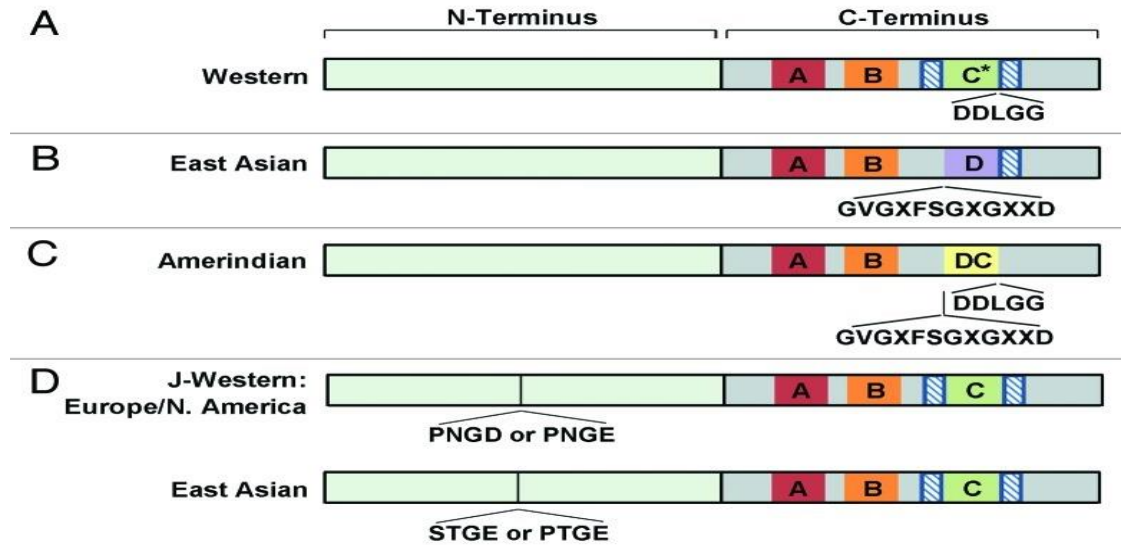


Figure 1.6 Adapted from Bridge and Merrell (2013) showing the polymorphic regions of the CagA protein, their assigned EPIYA motif initial and which geographic region the motif belongs to. Permission to reproduce figure granted by publisher.

Vacuolating cytotoxin A (VacA) is a multifunctional toxin named due to its ability to cause vacuole like structures in the cytoplasm of gastric epithelial cells. Unlike *cagA* that may be present or absent the *vacA* gene is ubiquitously present in *H. pylori* strains. When locally secreted VacA is endocytosed into gastric epithelium where it modulates components of the cell. VacA causes vacuolation of endosomes, targets mitochondrial DNA replication machinery, alters gastric cell integrity to provide of flow of nutrients into the lumen from the gastric mucosa and induces apoptosis pathways. VacA is also an immune modulatory toxin that inhibits activation and proliferation of T-cells, interferes with MHC class II B cell antigen presenting and inhibits INF- β causing apoptosis in macrophages (Chauhan *et al* 2019).

Like the CagA protein VacA is highly polymorphic. The signal region (s-region), intermediate region (i-region), deletion region (d-region) and mid region (m-region) can all show allelic diversity as shown in figure 1.7. The s, d and m regions show allelic diversity as termed s1/s2, i1/i2/i3 and m1/m2/m3. The d-region is either present (d1) or there is 69-89bp deletion as shown in figure 1.7 B and this is termed d2. Strains with type 1 alleles s1/i1/d1/m1 are more strongly associated with the development of gastric cancer (Bridge and Merrell 2013).

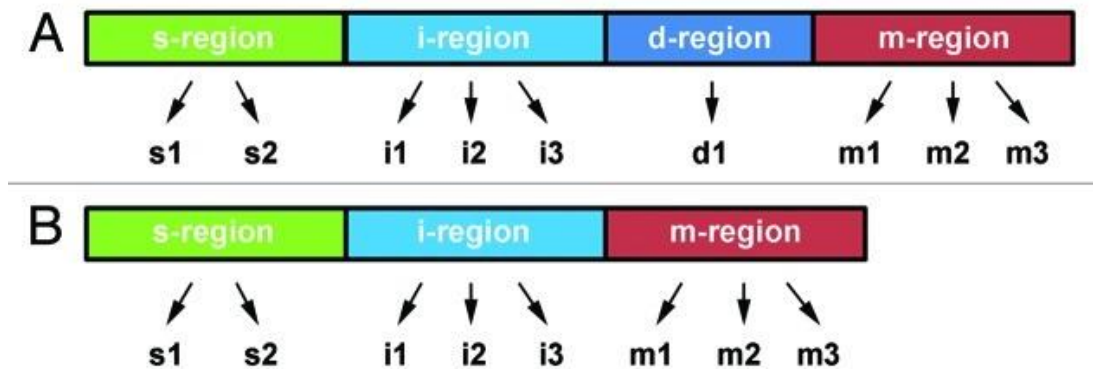


Figure 1.7 Adapted from Bridge and Merrell (2013) showing the potential allelic variations of the s-,i-,d- and m- regions of the *vacA* gene producing the VacA toxin. A) shows a d1 variant of *vacA* and B) shows a *vacA* gene with a 69-89bp deletion therefore termed d2 where the d-region is absent. Permission to reproduce figure granted by publisher.

Interestingly for two toxins that are produced by the same organism there is significant interplay between VacA and CagA. CagA and VacA are largely thought to work antagonistically to each other at the protein signalling level downregulating the effect of the other. CagA is known to actively inhibit the endocytosis of VacA into host cells (Akada *et al* 2010). It was theorised by this work that the interplay between toxins is a means by which establishing a localised niche, disrupting distant cells with VacA whilst protecting the cells *H. pylori* requires with the VacA downregulating effects of CagA. This notion may be further bolstered by evidence suggesting that VacA promotes CagA accumulation in gastric epithelial cells (Abdullah *et al* 2019).

1.2.3 Clinical presentations of *H. pylori* infection

As stated in section 1.2, *H. pylori* infections are largely asymptomatic in a majority of cases, however symptomatic presentations such as persistent untreatable acid reflux, dyspepsia, abdominal pain, loss of appetite and weight loss often warrant further investigation.

Chronic gastritis, inflammation of the gastric epithelium, is the most likely disease outcome of *H. pylori* infection and infections of this kind are the leading cause of gastritis worldwide (Sugano *et al* 2015). Chronic damage to the gastric mucosa is also a precursor to further gastric complications. From the Kyoto global consensus meeting on gastritis classification (As reported by Sugano *et al* 2015) there is clarification on classification of gastritis particularly in which *H. pylori* is the causative agent. Gastritis can be categorised as pangastritis or antrum/corpus predominant and this is achieved through histology and/or endoscopy. Gastritis severity should be categorised by histology looking at inflammation, atrophy and intestinal metaplasia and this will be further discussed in section 1.2.5.

H. pylori is also a causative agent of both gastric and duodenal ulcers. Antral predominant gastritis is associated with duodenal ulcers whereas corpus predominant gastritis is associated with gastric ulceration (De Brito *et al* 2019). Ulceration may be asymptomatic however patients with duodenal ulcers often report worsening abdominal pain on an empty stomach, at night, and within two to three hours after a meal. This contrasts with patients found to have gastric ulcers that often report nausea, vomiting and post-prandial pain (Narayanan, Reddy and Marsicano 2018).

The most serious disease outcomes associated with *H. pylori* infection are gastric adenocarcinoma and mucosa associated lymphoid tissue (MALT) lymphoma. Gastric cancer is the fifth most commonly diagnosed cancer worldwide and as a gastric bacterial carcinogen, *H. pylori* is heavily implicated as a strong risk factor in a large proportion of gastric cancer cases (Eusebi *et al* 2020).

It is estimated that 17.8% of cancer cases worldwide are caused by infectious agents. Of those 5.5% are attributed to *H. pylori* which corresponds to approximately 60% of gastric cancer cases (Correa and Piazzuelo 2011). The stages of developing gastric cancer are outlined in “Correa’s cascade of gastric carcinogenesis” (Correa and Piazzuelo 2012) as shown in figure 1.3. As well as *cagA*⁺ status the genotype combination *vacA*⁺/*oipA*⁺/*babA2*⁺ was recently linked to an increased risk of developing gastric cancer (Bartpho *et al* 2020).

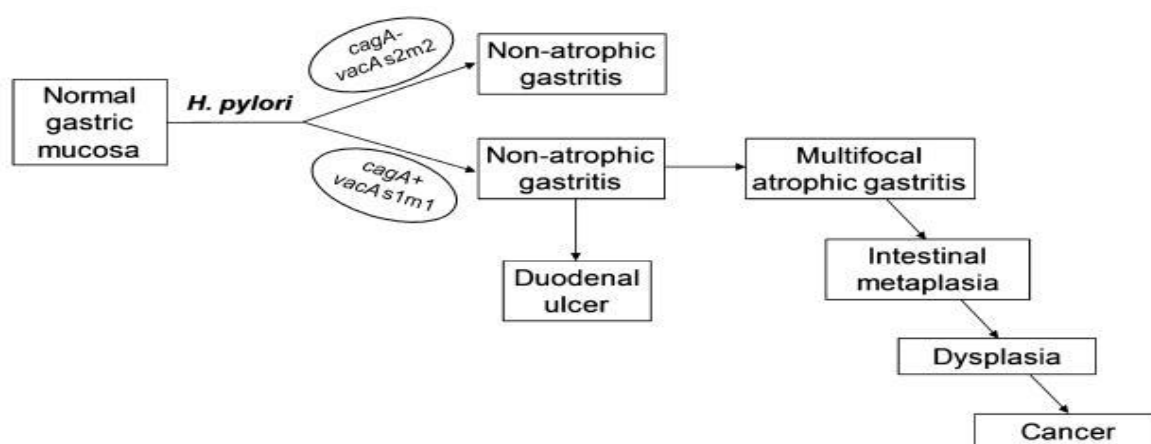


Figure 1.8 The gastric precancerous cascade associated with *H. pylori* infection “Correa’s cascade of gastric carcinogenesis” as adapted from Correa and Piazeolo (2012). Permission to reproduce figure granted by publisher.

H. pylori infection also plays a causative role in the development of mucosa associated lymphoid tissue (MALT) lymphoma in the gastric mucosa. Chronic infection by *H. pylori* causes a sustained mounted immune response at the gastric mucosa. T-cell dependent pathways generates reactive T and B cells. Reactive T cells causing prolonged proliferation of reactive B cells alongside inflammatory cytokines, ROS and activation of the CD40 pathway by *H. pylori* contribute to lymphoma development. *H. pylori* eradication leads to remission in 50-90% of these cases (Nakamura and Matsumoto 2013).

1.2.4 Diagnosis of *H. pylori* infection

Due to the high prevalence of *H. pylori* in the general population and given the largely asymptomatic nature of carriage, *H. pylori* is not routinely screened for in the UK. In fact, there is an absence of mass screening strategies globally and a country has yet to achieve this (Lee *et al* 2016). There is one noted example of a screening programme conducted on residents of Matsu Island, Taiwan that showed how community screening for *H. pylori* could be effective at lowering gastric disease rates particularly involving outcomes such as gastric cancer however the cost effectiveness of this type of programme is debated (Lee *et al* 2013). Patients presenting with unresolved symptoms of gastric upset as described in 1.2.3 are diagnosed on a “test and treat” strategy.

There are a plethora of diagnostic tests for *H. pylori* infection and these can be divided into invasive and non-invasive tests. As of yet there is no definitive gold standard of test that combines sensitivity, accuracy, cost effectiveness, speed of diagnosis and ease of use and therefore any number of these tests are routinely employed.

Non-invasive tests include Urea breath tests (UBTs), Stool antigen tests (SATs) and serology. UBTs rely on the *H. pylori* survival strategy of secreting urease to hydrolyse urea into ammonia and carbon dioxide to generate its localised neutral microenvironment. Ingestion of urea labelled with ^{13}C or ^{14}C isotopes can indicate *H. pylori* infection based on $^{13/14}\text{CO}_2$ being expelled in the breath caused by a *H. pylori* urease mediated breakdown in the stomach. A meta-analysis of urease breath test studies concluded a pooled sensitivity and specificity of 96% and 93% respectively (Ferwana *et al* 2015).

Stool antigen tests primarily employ an enzyme-linked immunosorbent assay (ELISA) to test for presence of *H. pylori* antigens. A 2014 meta-analysis of SATs found that monoclonal antibody-based ELISA had the highest sensitivity and specificity of all stool antigen test methods with an overall sensitivity and specificity of 92.1% and 94.1% respectively (Zhou *et al* 2014).

Serological testing for *H. pylori* also employs an ELISA based method and several commercial kits are available for the testing of anti *H. pylori* IgG antibody. A study that looked at the specificity and sensitivity of three commercial serological ELISA kits reported sensitivities of 89.7%, 100% and 100% and specificities of 85.5%, 75.4% and 80.7%, respectively (Lee *et al* 2015)

Invasive testing for *H. pylori* is centred around endoscopy. Whilst invasive procedures may be considered more technically demanding and often provide more discomfort for the patient not only can they inform on the presence of a likely *H. pylori* infection but also associated changes to the gastric mucosa due to this. A study investigating the sensitivity and specificity of the ability of endoscopy to predict histology of the gastric mucosa in real time reported sensitivity and specificity of 85.4 and 81.7% for gastric inflammation, 71.8 and 95.2% for gastric intestinal metaplasia, and 80 and 98.9% for gastric carcinoma, respectively (Liu *et al* 2014).

There are several other diagnostic tools available to clinicians that are less commonly used due to a lack of sensitivity or specificity, classed as invasive as they are follow-up tests from biopsy. These include a rapid urease test (RUT), standard culture methods and several developed PCR assays that are usually employed in screening for potential antibiotic resistance markers (Patel *et al* 2014) (Mentis, Lehours and Mégraud 2015).

1.2.5 Sydney Scoring

As mentioned in the diagnosis of *H. pylori* infection, invasive testing can inform on the status of a patient's gastric epithelium and the potential severity of a present *H. pylori* infection. The Sydney scoring classification was first proposed in 1990 and then updated by a panel of worldwide gastrointestinal pathologists in 1994. The updated scoring system that is used to grade gastric epithelial gastritis to this day was published in 1996 (Dixon *et al* 1996). The scoring system is number based where 0= normal, 1= mild, 2= moderate and 3= severe. There are four observable histopathological characteristics by which gastritis is classified. Inflammation, as defined by lymphocyte and plasma cells in the lamina propria. Neutrophil activation sometimes referred to as "activity", as observed by neutrophilic infiltration in the superficial epithelium. Glandular atrophy or "atrophy" as observed by the loss of specialised corpus and antral glands. Finally, intestinal metaplasia, observed as the transformation of mucosal epithelium of the stomach to resemble the structure of intestinal epithelium. Inflammation and activity are often variable as will be discussed in later chapters *H. pylori* creates a chronic inflammatory environment that it in part tunes using a biological rheostat. Atrophy and intestinal metaplasia in particular are of interest as they are mentioned in figure 1.8 as stages of the gastric precancerous cascade associated with *H. pylori* infection, "Correa's cascade of gastric carcinogenesis".

1.2.6 Treatment of *H. pylori*

As previously mentioned, the UK operates on a "test and treat" basis and there are several lines of treatment available to treat *H. pylori* infection, which is commonly called *H. pylori* eradication therapy. The NICE guidelines for testing and eradication of *H. pylori* as of October 2019 provide recommendations on first, second and third lines of treatment for the eradication of *H. pylori* (National Institute for Health and Care Excellence 2019 "*Helicobacter pylori* testing and eradication in adults" pathway).

For first line treatment it is recommended to use a 7-day course of amoxicillin, with a protein pump inhibitor (PPI) such as omeprazole and either clarithromycin or metronidazole taking into account potential previous exposure to clarithromycin or metronidazole. For those with penicillin allergies a PPI with both clarithromycin and metronidazole is advised. If patients are symptomatic after first-line eradication treatment a second 7-day course can be administered of amoxicillin with a PPI and either clarithromycin or metronidazole whichever was not used in first line. For those with penicillin allergies a PPI with metronidazole and levofloxacin is advised. Third line treatments are often used for those with previous exposure to clarithromycin and metronidazole and use a PPI with amoxicillin and tetracycline or levofloxacin. In the case of those with a penicillin allergy a PPI with bismuth, metronidazole and tetracycline is used. There are also several triple/quadruple therapy combinations that are saved as “rescue treatments” following unsuccessful eradication by other means. A study of all current suggested rescue treatments suggests by meta-analysis that a 10-d TL quadruple therapy comprised of PPI, bismuth, tetracycline and levofloxacin has a 98% eradication rate in patients who have failed to respond to less complex eradication treatment lines, and should therefore be considered the universal rescue treatment (Lin and Hsu 2018).

1.2.7 Antibiotic resistance and the global impact of *H. pylori*

H. pylori was listed in the 2017 World Health Organisations global priority list of 12 antibiotic resistant bacteria in urgent need of antibiotics with particular reference being made to the clarithromycin resistance rates rising in *H. pylori* (Tacconelli *et al* 2018). Despite this, more recent reports of European countries showed that none of 28 EU and 4 EU trade member states assessed required reporting of resistance rates of *H. pylori* to antibiotics (Rajendran *et al* 2019). It is also worth noting that antibiotic susceptibility profiles are not routinely generated for all *H. pylori* positive clinical cases.

A meta-analysis of studies reporting antibiotic resistance rates in WHO countries noted that primary and secondary resistance rates to clarithromycin, metronidazole, and levofloxacin were $\geq 15\%$ in all WHO regions, except primary clarithromycin resistance in the Americas and South-East Asia and primary levofloxacin resistance in the European region (Savoldi *et al* 2018)(Figure 1.9).

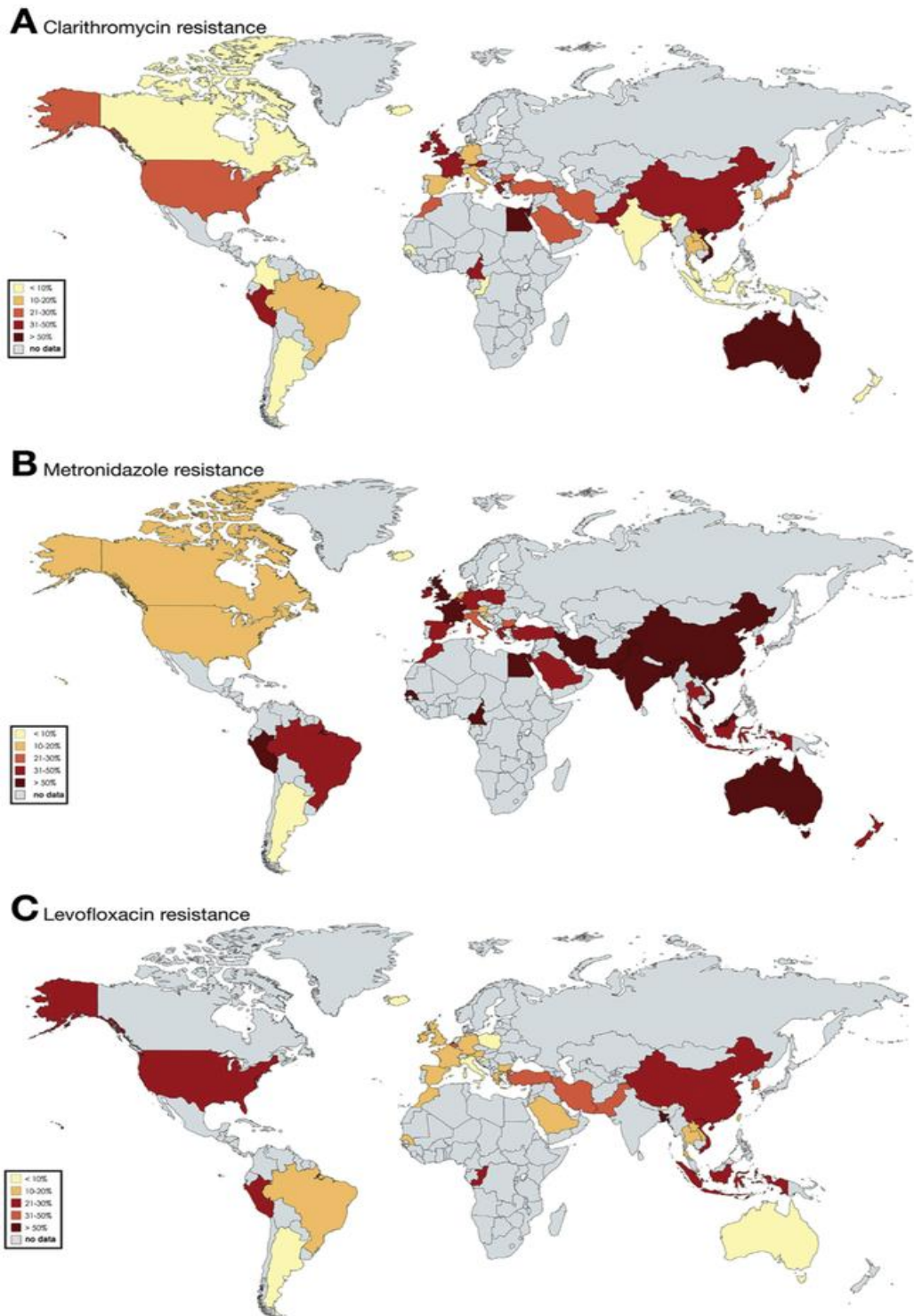


Figure 1.9 Adapted from Savoldi *et al* (2018) showing meta-analysis results of studies reporting resistance rates to Clarithromycin, Metronidazole and Levofloxacin in WHO countries. Permission to reproduce figure granted by publisher.

In 2018 there were 2.2 million infection attributed cancer cases diagnosed worldwide and of these approximately 810,000 were said to be primarily caused by *H. pylori* infection (De Martel *et al* 2020). Due to the generic symptomatic complaints associated with gastric cancer, diagnosis can be later on in the disease's progression. This leads to poor prognosis once gastric cancer is diagnosed. For example, in England Cancer Research UK cites 5-year survival rates ranging from 65% for stage 1 gastric cancer to as low as 25% for stage 3 (Cancer Research UK 2019). Other complications caused by *H. pylori* also factor into the burden of the bacteria for example *H. pylori* can be causative of peptic ulcers in 10-20% of infection cases as noted in section 1.2. In 2013 it was estimated that approximately 300,000 deaths worldwide were attributed to peptic ulcer disease (Peiffer *et al* 2020).

Rates of *H. pylori* infection are falling worldwide particularly in the west however they still remain relatively high in lesser economically developed countries particularly in the sub Saharan African area. Gastric cancer incidence rates are predicted to continue decreasing in the majority of countries, with 16 approaching the "rare disease" threshold status of 6 per 100,000 person-years by 2035. However, the overall number of new diagnosed cases remains high and is set to rise in some countries particularly in the under 50 age group that may be associated with increased risk lifestyle choices, such as smoking, alcohol consumption and salt consumption (Arnold *et al* 2020).

1.2.8 Rationale of *H. pylori* study

H. pylori still presents a major issue of global concern as shown in section 1.2.6 by both the potential severity of infection outcomes and the global incidence rates. As mentioned in section 1.2.1 *H. pylori* infection is most often acquired in early childhood and presents as a chronic often lifelong infection. The ability of the bacterium to persist in the host for this long span of time is of great interest in *H. pylori* research.

Given the duration of colonisation within a specific host, and the high mutation and recombination rate of *H. pylori*, the ancestral infecting strain often branches off into diverse sub-populations or quasispecies due to microevolution over generations (Ailloud *et al* 2019) (Morelli *et al* 2010). One influence of this and potential driver of microevolution may be due to the dynamic system of the human stomach. As described in section 1.2.2 the stomach is comprised of two anatomically distinct regions the antrum and corpus and given the variation in their environments may be considered two separate intra-host niches as described in Chapter four (Section 4.1).

This thesis seeks to determine how paired strains isolated from a single host, one from antrum biopsy and one from corpus biopsy may show variation in observed phenotypic ability and genome content. Phenotypic assays were selected to test niche colonisation conditions or stressors and the performance of the antrum/corpus isolates as described in Chapter four (Section 4.2). Genome analysis of *H. pylori* antrum and corpus grouped strains was also conducted to look at whether genotype was clustered by ancestral strain or by niche area, as described in Chapter four (Section 4.2). Chapter five of the thesis is dedicated to how an *in-vitro* niche stressor mimicker can affect *H. pylori* transcription. A brief overall discussion and evaluation of the thesis in its entirety will then conclude the thesis (Chapter six).

1.2.9 *C. jejuni* and *H. pylori* comparisons

H. pylori was originally assigned to the *Campylobacter* genus as *Campylobacter pylori* before its reclassification when the *Helicobacter* genus was introduced in 1989. This was based upon initial light microscopy and preliminary DNA analysis at the time that concluded similarities between this new bacterium and the members of the *Campylobacter* genus. It was only after deeper research using the bacterial classification system of ultrastructure, fatty-acid profiles, respiratory quinones, growth characteristics, and enzyme capabilities that it was decided distinct enough to form a new genus (Luning *et al* 1989). Much more is now known about these two bacterial species and the similarities and differences are outlined in table 1.1. As can be seen from table 1.1 there were considerable similarities between the two organisms to initially conclude they were closely related.

Both organisms are Gram negative microaerobic fastidious mesophiles associated with the gastrointestinal system. Despite these similarities the course of infection is distinctly different with *C. jejuni* presenting as an acute infection and *H. pylori* as a chronic often lifelong infection. Disease outcomes are also distinctly different with *C. jejuni* routinely causing gastroenteritis (campylobacteriosis) with rarer instances of Guillan-Barre syndrome as discussed in section 1.1.2. With *H. pylori* being asymptomatic in approximately 90% of cases but with complications of peptic ulcers and gastric cancers as discussed in sections 1.2 and 1.2.3. In respect of genome both organisms have a similar sized relatively modest genome with low GC contents and are both highly recombinant and with high mutation rates.

	<i>Campylobacter jejuni</i>	<i>Helicobacter pylori</i>
Gram stain	Gram-negative	Gram-negative
Morphology	Curved rod	Helical
Optimal growth	37-42°C Microaerobic	37-42°C Microaerobic
Growth rate/needs	Fastidious slow grower	Fastidious slow grower
Site of colonisation	Gastric (intestinal)	Gastric (stomach)
Host switching capability	Multiple species	Human restricted
Duration of infection	Acute	Chronic
Infection outcome	Campylobacteriosis/ Guillan-Barre Syndrome	Largely asymptomatic, 10- 20% rate of peptic ulcers 1- 2% gastric cancer
Treatment	Largely self-limiting occasionally antibiotics	Antibiotic and protein pump inhibitor eradication
Genome size	1,641,481bp	1,667,867bp
GC content	30.6%	39%
Mutation rate	High	High
Recombination rate	High	High

Table 1.1 Direct comparison of key features of *C. jejuni* and *H. pylori*

1.2.10 Thesis aims

In this thesis the niche adaptation of *C. jejuni* and *H. pylori* were studied, in different contexts.

In *C. jejuni* inter-host niche adaptation focussing on the 403 clonal complex was studied alongside chicken isolates. Chapter three will set out all work pertaining to *C. jejuni*, brief background, results and discussion.

In *H. pylori* intra-host niche adaptation was studied focussing on the different niches within human stomachs namely the antrum and the corpus. In chapter four potential phenotypic differences between antrum and corpus strains were explored. In chapter five the transcriptomic effect of a niche mimicking stressor on *H. pylori* strain 322A is shown in full.

Therefore, the overall aims of the thesis were to:

- Test for potential phenotypic differences between 403CC *C. jejuni* isolates and chicken isolates and how this may relate to genome content (chapter three)
- Test for potential phenotypic differences between antrum and corpus *H. pylori* isolates and if antrum and corpus strains show distinctly different genome content (chapter four)
- To test the transcriptomic effect of menadione as a niche stressor mimicker on *H. pylori* strain 322A (chapter five)

Chapter Two: Materials and Methods

As two bacterial species were used in this thesis for separate assays, the material and methods section mirrors the subsequent chapters. All methodology pertaining to *C. jejuni* work (chapter three) can be found in section 2.1. *H. pylori* work as it related to chapter four can be found in section 2.2. Finally work pertaining to *H. pylori* transcriptomics work (chapter five) can be found in section 2.3.

2.1 *C. jejuni* strains used in phenotypic assays

For phenotypic analysis, initially twelve *C. jejuni* strains were chosen. Six belonging to the 403CC, which showed the chicken niche restriction that was to be investigated and six strains of chicken origin that provided a suitable comparison as chicken colonising strains. Three strains of chicken origin (B2/12, B2/10 and B1/25) were unrecoverable from several culturing attempts at the beginning of the work and therefore analysis proceeded with six 403CC strains and three chicken isolates. The list of isolates used for phenotypic analysis are detailed in Table 2.1

Strain	Country of isolation	Year of isolation	Host source	Sequence Type	Clonal complex
PS857	U.K	2000	Pig	ST-270	ST-403 CC
PS549.1	U.K	1999	Pig	ST-403	ST-403 CC
PS623	U.K	1999	Pig	ST-552	ST-403 CC
PS304	U.K	1999	Pig	ST-551	ST-403 CC
PS484	U.K	1999	Pig	ST-435	ST-403 CC
PS444	U.K	1999	Pig	ST-553	ST-403 CC
C2/3	Canada	2009	Chicken	ST-45	ST-45 CC
RM1221	U.S.A	1997	Chicken	ST-354	ST-354 CC
B1/41	Botswana	2015	Chicken	ST-9027	ST-354 CC

Table 2.1 *C. jejuni* strains used in all phenotypic *C. jejuni* assays, belonging to the 403CC (N=6) or isolates of chicken origin (N=3)

2.1.1 Maintenance, Storage & General Culture of Strains

All strains were made into frozen stocks and stored at -80°C in Muller-Hinton broth (Oxoid) made to standard specifications containing 10% (v/v) glycerol (Fisher Scientific) until needed. Unless otherwise stated for specific assays, strains were cultured from the frozen stocks onto Modified Charcoal Cefoperazone Deoxycholate Agar (MCCDA) (Oxoid) made to manufacturers specifications and non-supplemented with blood or antibiotics. Plates were then incubated microaerobically in a microaerobic cabinet (Don Whitley Scientific) at constant 37°C temperature and under gas controlled atmospheric conditions of 5% O₂, 10% CO₂ and 85% N₂ for 48 h prior to use.

2.1.2 Temperature Growth Curves

Strains were prepared as stated in section 2.1.1 and standardised in MHB to an optical density (OD_{600nm}) of 0.1. 100 µl of each strain suspension was added to a well of a sterile 96-well plate in triplicate alongside triplicate wells containing MHB only, as a control. The plate was then incubated in a micro-titer plate reader with temperature and microaerobic environment controls (BioTek) at either 37°C or 42°C under gas controlled atmospheric conditions of 5% O₂, 10% CO₂ and 85% N₂ to simulate mammalian and chicken body temperatures, respectively, for a total of 42 h with automatic readings at OD_{600nm} being taken at hourly intervals. Sampling was taken from the wells at the conclusion of the assay, this was incubated on MCCDA under *C. jejuni* conditions to test for purity based on plate colony morphology, and further to this Gram stained for confirmation.

2.1.3 Biofilm formation

Strains were prepared as stated in section 2.1.1. To simulate a variety of environmental conditions it was decided to test 12 variations based on media (rich/poor nutrient), atmospheric composition (aerobic/microaerobic) and a variety of temperatures to simulate ideal host (37°C), warm external temperature (25°C) and cold external temperature (6°C). Strains were standardised to an OD_{600nm} 0.1 in either phosphate buffered saline (PBS) or MHB.

150 μ l of each suspension was transferred to wells of a 96-well plate in triplicate alongside a PBS or MHB only control triplicate. Three temperature-controlled aerobic incubators were used for 37°C, 25°C and 6°C respectively. Plates incubated for microaerobic conditions were placed in these incubators in anaerobic jars with a CampyGen pack (ThermoFisher) and a small beaker of distilled water to generate and maintain microaerobic conditions and humidity. Following 48 h incubation, plates were emptied and washed with deionised water before being stained with 200 μ l 0.01% (v/v) crystal violet (Sigma). Crystal violet was left for 15 minutes at room temperature to develop before washing the wells thoroughly with deionised water to remove excess dye. The biofilm stain was then solubilised with the addition of 150 μ l 70% ethanol to each well and left at room temperature for 15 minutes. Wells were then read at OD_{600nm} in a micro-titer plate reader.

2.1.4 Motility

Strains were prepared as stated in section 2.1.1 before being standardised to an OD_{600nm} of 0.05 in MHB. Semi-solid motility agar plates were made with MHB supplemented with 0.6% agar (w/v) (Sigma) with care being taken not to disrupt or invert the agar plates during movement, storage or incubation. All plates contained exactly 20 ml of agar to ensure depth remained consistent. The method employed was a simple agar stab. 10 μ l of each prepared suspension was inoculated into the centre of a motility agar plate by penetrating the agar surface with a pipette tip and gently releasing the bacterial suspension without touching the bottom of the plate. This was repeated across triplicate plates for each strain. Plates were then incubated microaerobically for 48 h at 37°C before the diameter of the growth “halo” around each stab inoculum was measured.

2.1.5 Chemotaxis

Method was adapted from Elgamoudi et al (2018) using fucose (Sigma) as a chemoattractant. Fucose powder was dissolved in sterile distilled water. Strains were prepared as stated in section 2.1.1 before being standardised to OD_{600nm} of 1 in MHB. 4% MHB-agar plates were made with fucose final concentrations of 10 mM, 50 mM and 100 mM. Plugs approximately 5 mm in diameter and 10 mm deep were cut out and placed in empty petri dishes.

For each concentration plug plate 15 ml of media was poured in containing 7.5 ml of MHB strain suspension and 7.5 ml 0.6% agar and left ten minutes to set. Each concentration was repeated in triplicate for each strain alongside a non-fucose control plug. Plates were then incubated at 37°C microaerobically for 24 h. After incubation, bacteria that had migrated to a plug were recovered by extracting plugs from the plates and harvesting the bacteria by transferring the plugs into 1 ml of MHB and vortexing thoroughly and incubating at 42°C for 30 minutes. Viable counts were then performed to calculate cfu/ml recovered from each plug. The percentage increase in migration associated with a 10-fold increase in chemoattractant concentration was also calculated using the following calculation:

$$100 \times \left[\frac{\text{Cfu/ml bacteria from 10 mM fucose plugs}}{\text{Cfu/ml bacteria from 100 mM fucose plugs}} \right]$$

2.1.6 Vitamin B5 synthesis

Method was adapted from Sheppard *et al* (2013). Strains were prepared as stated in section 2.1.1 before being standardised to an OD_{600nm} of 0.05 in MHB. 10 µl of each suspension was inoculated in triplicate into wells of a sterile 96-well plate containing 150 µl of synthetic media. Synthetic media was composed of 1x Earle's balanced salt solution (EBSS)(Sigma), 1x MEM essential amino acid solution (Sigma), 1x MEM nonessential amino acids (Sigma), 1 mM sodium pyruvate (Sigma), 20 µM FeSO₄ (Sigma) and 2.1 µM pantothenic acid (Sigma). The strains were inoculated with a composition of this media containing pantothenic acid (vitamin B5) and the same media without pantothenic acid. The inoculated 96-well plates were incubated for 72 h under microaerobic conditions at 37°C and growth was examined by reading plates at OD_{600nm} in a micro-titer plate reader at 0, 24, 48 and 72 h. Alongside OD data for growth in B5- and B5+ media, the effect of B5- media on growth for each strain was directly compared to B5 enriched media as a percentage using the calculation:

$$\% = 100 \times \left[\frac{\text{OD in B5 depleted media}}{\text{OD in B5 enriched media}} \right]$$

2.1.7 Oxidative stress

Method was adapted from Oh, McMullen and Jeon (2015). Strains were prepared as stated in section 2.1.1 before being standardised to an OD_{600nm} of 0.1 in MHB. 100 µl of each suspension was inoculated into wells of a 96 well plate in 18 wells, for six time points in triplicate. This was repeated on a plate with a duplicate layout. Plates were incubated either microaerobically or aerobically at 37°C for a total of 24 h. At 0,4,6,8 and 24 h marks plates were read at OD_{600nm}. For a more accurate measure of environmental oxidative stress survival, a Bac-Titer cell viability assay was used. This assay determines cell viability by lysing the bacteria and generating a luminescent signal that is proportional to the amount of cellular ATP released. Since ATP is a very short-lived molecule, this can be used as a measure of the number of viable cells present.

At each time point, a set of triplicates for each strain on both plates were transferred to an opaque 96 well plate. 100 µl of BacTiter-Glo (Promega) was added to each of the 100 µl of bacterial suspensions and placed on a low speed orbital shaker for five minutes before reading luminescence units (arbitrary) on a micro titer plate reader with luminescence equipment (BioTek).

2.1.8 Purity checks

For each of the assays described above endpoint purity checks were carried out. The purpose of these checks is to ensure that the data retrieved reflected the phenotypic behaviour of the *C. jejuni* strains tested and not by a contaminant that may have been introduced at any point of the assay. MCCDA plates were pre-warmed to 37°C to ensure that no contaminants were present on the purity test plates themselves. Aliquots were taken for each strain at the endpoint of each assay and streaked onto the pre-warmed agar plates that were then incubated for 48 h at standard microaerobic conditions as described in section 2.1.1. After reviewing for potential contaminants based on general appearance and morphology Gram staining was performed where possible for confirmation of purity.

2.1.9 Genomic analysis

For genomic comparison between 403CC isolates and chicken colonising lineages, 121 ST-21/ST-45 isolate whole genome sequences were obtained from the pubMLST *C. jejuni* database. 14 403CC isolate sequences were provided by Professor Alan McNally of the University of Birmingham. Under the supervision of Professor McNally, sequences were annotated using Prokka v1.11 (Seemann 2014). Pan genome analysis was conducted using Roary v.3.7.1 (Page *et al* 2015). The gene presence/absence list produced was then sorted to group isolates into ST-21/ST-45 or 403CC using Scoary v.1.0 (Brynildsrud *et al* 2016) to tag individual genomes within the gene presence/absence list to the correct isolate group. Genome groups were then compared for presence or absence of genes that may relate to chicken colonisation, and/or the phenotypic properties tested in chapter three.

2.1.10 Statistical analysis

Statistical analysis was performed using GraphPad Prism (Version 9). Statistical tests employed in this section were One-way ANOVA (Analysis Of Variance) with post hoc Tukey's multiple comparison test, Two-way ANOVA with post hoc Sidak's multiple comparisons and unpaired or paired, parametric, two-tailed T-tests. One-way ANOVA was used to compare means amongst single isolates where multiple T tests would produce higher type I error rates, with post hoc Tukey's multiple comparison to compare the means of each isolates with each of the other isolates. T tests were performed to directly compare the means of two groups, in this instance where data was presented as 403CC isolate group vs chicken isolate group that may include post hoc multiple comparisons where multiple time points are present. A two-way ANOVA was performed for the chemotaxis HAP count assay due to there being 3 concentration conditions with post hoc Sidak's multiple comparisons test. All statistics presented use a confidence interval (CI) of 95% (P=0.05).

2.2 *H. pylori* strains used in phenotypic assays

Clinical isolates were originally obtained by antrum/corpus paired biopsy from patients undergoing gastric endoscopy for suspected *H. pylori* infection at the Queens Medical Centre Hospital in Nottingham by Professor John Atherton and team at the University of Nottingham. Alongside biopsy, histopathologic features of observed gastritis were scored in each region of the stomach for each patient by the updated Sydney scoring system for gastritis (Dixon *et al* 1996) looking at inflammation, activity, atrophy and intestinal metaplasia. *H. pylori* was cultured from biopsy samples by Professor Atherton and team at the University of Nottingham by plating onto blood base agar #2 (Oxoid) supplemented with 5% (v/v) defibrinated horse blood (TCS Biosciences). Plates were incubated for approximately 48 h at 37°C under microaerobic conditions (5% O₂, 10% CO₂ and 85% N₂) before being checked for purity and stored at -80°C in iso-sensitest broth (Oxoid) supplemented with 15% (v/v) glycerol (Sigma Aldrich). Frozen stocks alongside anonymised patient data was provided to Nottingham Trent Universities' Antibiotic Resistance, Omics and Microbiota (AROM) team by Professor Atherton and team. Ethical approval for use of these clinical isolates for research purposes was granted by the NHS National Research Ethics Service, Nottingham Research Ethics Committee (Ref: 08/H0408/195) dated 27th January 2009 (see appendix).

Four pairs of antrum/corpus strains were chosen from the NTU AROM collection that showed distinct within pair differences in Sydney scores provided. The list of strains used, shown in table 2.2 were used in all phenotypic assays in this chapter.

Strain ID	Antrum/Corpus	Inflammation	Activity	Atrophy	Intestinal metaplasia
265A	Antrum	3	2	0	0
265C	Corpus	1	0	0	0
295A	Antrum	2	2	0	0
295C	Corpus	1	0	0	0
322A	Antrum	1	0	1	3
322C	Corpus	3	2	0	1
791A	Antrum	2	3	0	0
791C	Corpus	1	0	0	0

Table 2.2 *H. pylori* strains used in all phenotypic assays with gastric site of biopsy isolate was obtained from and Sydney scores for inflammation, activity, atrophy and intestinal metaplasia where 0= absent, 1= mild, 2 = moderate and 3= severe.

2.2.1 Maintenance, Storage & General Culture of Strains

All strains were made into frozen stocks and stored at -80°C in Iso-sensitest broth (Oxoid) containing 15% (v/v) glycerol until needed. Unless otherwise stated for specific assays strains, when required, were cultured from the frozen stocks onto blood agar base #2 supplemented with 5% (v/v) defibrinated horse blood. Plates were then incubated microaerobically in a microaerobic cabinet (Don Whitley Scientific) at constant 37°C temperature and under gas controlled atmospheric conditions of 5% O₂, 10% CO₂ and 85% N₂ for 48h before being subcultured onto fresh blood agar plates for a further 48 h before use.

2.2.2 Growth curves

Strains were prepared as stated in section 2.2.1 before being standardised to an OD_{600nm} of 0.5 in brucella broth (Oxoid) supplemented with 7% (v/v) heat-inactivated foetal calf serum (Sigma Aldrich). 1 ml of each strain of bacterial suspension was inoculated in triplicate into separate T25 tissue culture flasks containing 20 ml of brucella broth supplemented with 7% (v/v) FCS and gently mixed.

An untreated control flask containing media only without bacteria was included. 1 ml was taken from each of these initial flasks into a cuvette and measured for OD_{600nm} in a spectrophotometer. Flasks were incubated in a microaerobic cabinet with gentle shaking (75rpm) for 72 h, with daily 1 ml samples being taken from each flask and OD_{600nm} measured. With the final readings an additional volume of 100 µl was sampled from each flask and this was plated onto a blood agar plate to test for purity.

2.2.3 Motility

Strains were prepared as stated in section 2.2.1 before being standardised to an OD_{600nm} of 1.0 in brucella broth supplemented with 5% FCS. Semi-solid motility agar plates were made with brucella broth supplemented with 0.4% agar (w/v) and 5% FCS with care being taken not to disrupt or invert the agar plates during movement, storage or incubation. All plates contained exactly 20 ml of agar to ensure depth remained consistent. The method employed was a simple agar stab. 10 µl of each prepared suspension was inoculated into the centre of a motility agar plate by permeating the agar surface with a pipette tip and releasing the suspension without touching the bottom of the plate. This was repeated across triplicate plates for each strain. Plates were then incubated microaerobically for 7 days at 37°C before the diameter of the growth “halo” around each stab inoculum was measured.

2.2.4 Oxidative Stress

Method was adapted from Oh, McMullen and Jeon (2015). Strains were prepared as stated in section 2.2.1 before being standardised to an OD_{600nm} of 0.1 in MHB. 100 µl of each suspension was inoculated into wells of a 96 well plate in 18 wells, for six time points in triplicate. This was repeated on a plate with a duplicate layout. Plates were incubated either microaerobically or aerobically at 37°C for a total of 24 h. At 0,2,4,8 and 24 h marks plates were read at OD_{600nm}. For a more accurate measure of environmental oxidative stress survival, A Bac-Titer cell viability assay was used. At each time point, a set of triplicates for each strain on both plates were transferred to an opaque 96 well plate. 100 µl of BacTiter-Glo was added to each of the 100 µl of bacterial suspensions and placed on a low speed orbital shaker for five minutes before reading luminescence units (arbitrary) on a micro titer plate reader with luminescence equipment.

2.2.5 Menadione resistance

A 96-well plate minimum inhibitory concentration (MIC) assay was developed to test resistance of *H. pylori* to varying concentrations of menadione. A water-soluble form of menadione, menadione bisulfite (Sigma Aldrich) was used throughout this thesis and was dissolved in sterile distilled water. Strains were prepared as stated in section 2.2.1 before being standardised to an OD_{600nm} of 0.05 in brucella broth. 96 well plates were prepared with 100 µl of brucella broth supplemented with 5% FCS added to every well. 100 µl of 20 mM menadione was added to the top row of wells and then two-fold serially diluted down to 0.01953125 mM. Two control rows were also set up one containing no bacteria and one containing no menadione (see figure 3.2). 10 µl of bacterial suspension was added to each well so that each strain was inoculated in triplicate at each menadione concentration. All well plates were incubated at 37°C under microaerobic conditions. OD_{600nm} was recorded at 0, 24, 48, 72 and 96 h.

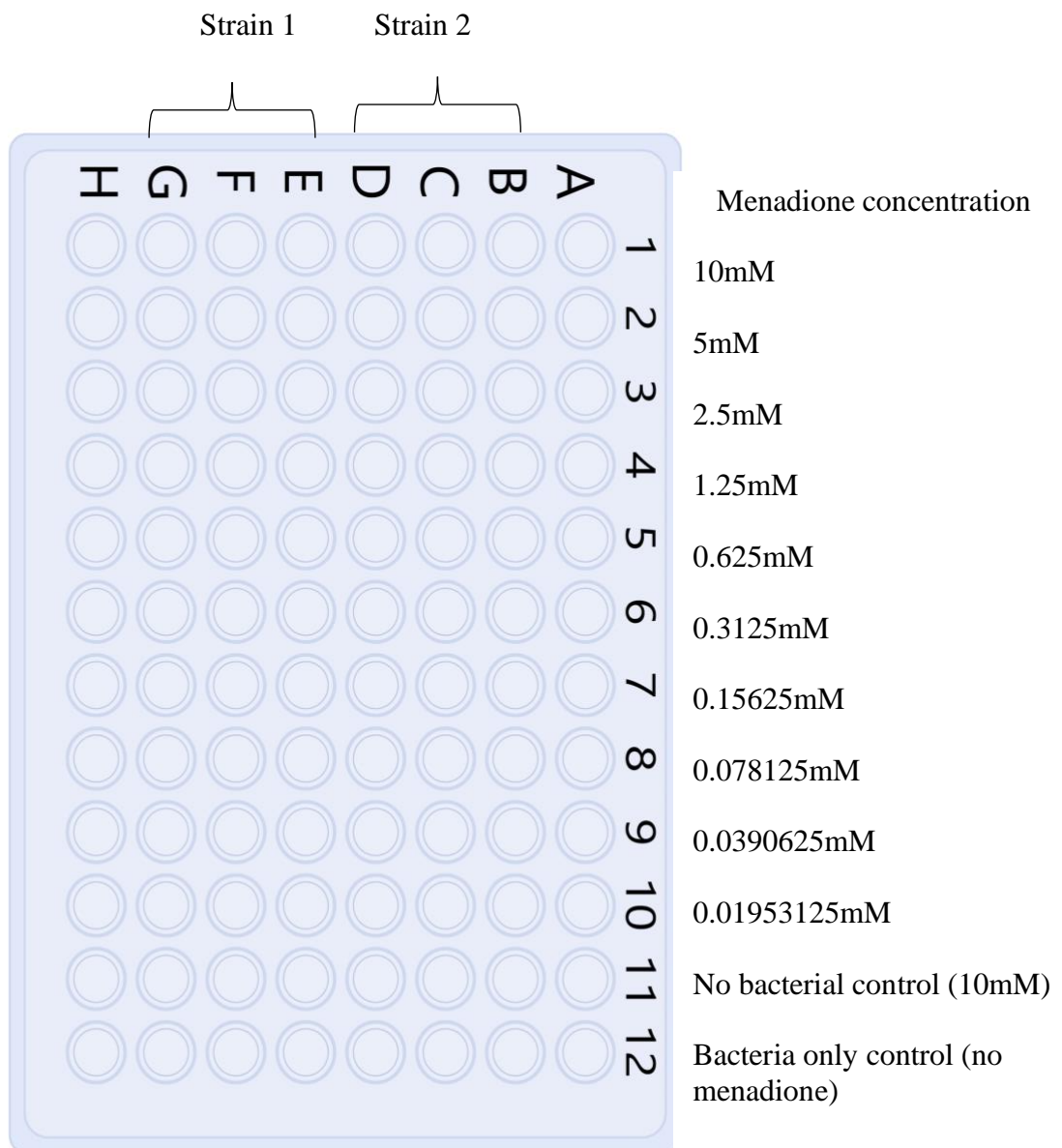


Figure 2.1 Dilution series used for menadione MIC assay. Menadione concentration (right) represents the concentration in each corresponding row of the 96 well plate (left) including controls. Due to the need for triplicate results two strains were tested per plate in columns E,F and G for one strain and B, C and D for the other.

2.2.6 Biofilm formation

Strains were prepared as stated in section 2.2.1 before being standardised to an OD_{600nm} of 0.3 in brucella broth supplemented with 5% FCS. 2 ml of each bacterial suspension was pipetted in triplicate into wells of a 12-well plate alongside three wells containing media without bacteria as a control. 22x22 mm sterile cover slips were placed in each well sitting at an angle in the broth to allow biofilm formation on the slips at the air-liquid interface. Plates were incubated at 37°C under microaerobic conditions with gentle shaking (65rpm) for seven days. After seven days incubation, a crystal violet assay for biofilm intensity was performed. Each glass cover slip was washed with PBS before allowing to dry for an hour. Each slip was then stained with crystal violet for 30 seconds before being washed with distilled water and then left to dry for an 1 h. Each cover slip was then placed into a clean well and washed with 1 ml of ethanol and placed on a flatbed shaker for five minutes to wash dye into the well. 200 µl of dye solution was transferred into triplicate wells of a 96 well plate and OD_{600nm} was read.

2.2.7 Purity checks

For each of the assays described above endpoint purity checks were carried out for the purpose described in section 2.1.8. For *H. pylori*, blood agar plates were pre-warmed to 37°C and aliquots were taken for each strain at the endpoint of each assay. This sample was then streaked onto the pre-warmed agar plates and incubated for 48 h at standard microaerobic conditions as described in section 2.2.1. After reviewing for potential contaminants based on general appearance and morphology Gram staining was performed where possible for confirmation of purity.

2.2.8 Genome analysis

13 pairs of antrum corpus isolate genome sequences were provided by Dr Daniel Wilkinson (Wilkinson *et al* 2022), plus reference strain J99 were used for genomic comparison. Sequences were annotated using Prokka v1.11 (Seemann 2014). Pan genome analysis was conducted using Roary v.3.7.1 (Page *et al* 2015). The output was then given to Professor Lesley Hoyles (NTU) who converted this into a binary gene presence/absence file in Excel. The binary file was then used in R to create a bidirectional heatmap using Heatmap.2 (Warnes *et al* 2015).

2.2.9 Statistical analysis

To assess the significance of the phenotypic data statistical analysis was performed using GraphPad Prism (Version 9). Statistical tests employed in this section were One-way ANOVA (Analysis Of Variance) with post hoc Tukey's multiple comparison test, Two-way ANOVA with post hoc Sidak's multiple comparisons and unpaired or paired, parametric, two-tailed T-tests.

One-way ANOVA was used to compare means amongst single isolates where multiple T tests would produce higher type I error rates, with post hoc Tukey's multiple comparison to compare the means of each isolates with each of the other isolates. T tests were performed to directly compare the means of two groups, in this instance where data was presented as antrum isolate group vs corpus isolate group that may include post hoc multiple comparisons where multiple time points are present. All statistics presented use a confidence interval (CI) of 95% (P=0.05).

2.3 Directed evolution

From the menadione resistance assays (results shown in section 3.3.4) *H. pylori* strain 322A was selected due to the consistency of the results. The 96-well plate minimum inhibitory concentration (MIC) assay used in section 3.2.6 was continued to test resistance of 322A to menadione in an effort to screen for mutants. A directed evolution approach was initially attempted, in the hope that by exposing strain 322A to menadione some resistant mutants might emerge, which could be used to study adaptations to menadione at the genome level. 322A was prepared from frozen stocks and stored at -80°C in Iso-sensitest broth containing 15% (v/v) glycerol until needed. When required, 322A was cultured from the frozen stocks onto blood agar base #2 supplemented with 5% (v/v) defibrinated horse blood. Plates were then incubated microaerobically in a microaerobic cabinet at constant 37°C temperature and under gas controlled atmospheric conditions of 5% O₂, 10% CO₂ and 85% N₂ for 48 h before being subcultured onto fresh blood agar plates for a further 48 h before use. 322A then standardised to an OD_{600nm} of 0.05 in brucella broth. 96 well plates were prepared with 100 µl of brucella broth supplemented with 5% FCS added to every well.

100 μ l of 20 mM menadione was added to the top row of wells and then two-fold serially diluted down to 0.01953125 mM. Two control rows were also set up one containing no bacteria and one containing no menadione. 10 μ l of 322A suspension was added to each well so there were eight replicates of 322A at each menadione concentration. This was done over two identical well plates for a total of 16 replicates at each concentration. Both well plates were incubated at 37°C under microaerobic conditions. OD_{600nm} was recorded at 0, 24 and 48 h. This methodology was repeated to observe over 100 replicates.

2.3.1 Strain selection for *H. pylori* transcriptomics

Of the eight strains used in chapter four it was decided that 322A would be used for transcriptomic analyses, as the results were highly consistent across all strains. Any of the strains would have been appropriate for use however 322A was chosen as it lay in between the strains most and least resistant strains to menadione. 322A was prepared from frozen stocks and stored at -80°C in Iso-sensitest broth containing 15% (v/v) glycerol until needed. When required, 322A was cultured from the frozen stocks onto blood agar base #2 supplemented with 5% (v/v) defibrinated horse blood. Plates were then incubated microaerobically in a microaerobic cabinet at constant 37°C temperature and under gas controlled atmospheric conditions of 5% O₂, 10% CO₂ and 85% N₂ for 48 h before being subcultured onto fresh blood agar plates for a further 48 h before use.

2.3.2 Culture and preparation

322A was taken from blood agar plates cultured as described above in section 2.3.1 and was grown under the aforementioned microaerobic growth conditions in a tissue culture flask containing 400 ml of Brucella broth supplemented with 5% FCS on an orbital shaker to an OD₆₀₀ of 0.4. This was to ensure homogeneity of starter culture for all samples. At this point purity checks were done on the master flask of broth through streaking onto agar and Gram staining. 15 ml of broth culture from the master flask was pipetted into 12 smaller flasks, as it was decided for the transcriptomic comparison six menadione treated and six untreated flasks were to be submitted for RNA extraction and RNA-Seq at Macrogen Inc, South Korea. Flasks were randomly allocated either U (untreated) or T (menadione treated). Samples were labelled ST1-ST12 to ensure they were easily identifiable when the post-sequencing data was returned, without indicating during the

process which samples were treated (See table 2.3). In the treated flasks, 10 µl of stock menadione was added for a final concentration in the flask of 0.15625 mM, the sub-MIC concentration determined for use from the menadione assays in section 3.3.4. All 12 flasks were then re-incubated for a further 24 h to allow for the menadione to take effect, if any. Second round contamination checks were carried out on each of the flasks and cfu/ml was determined through Miles & Misra (T average 1.5×10^8 cfu/ml and U average 3×10^8 cfu/ml). U3 shown in figure 4.1 was discarded due to contamination post incubation during the second round contamination check. As MacroGen required $>1 \times 10^9$ cells per sample, the entirety of the 15ml in each flask was pelleted down into an Eppendorf tube and submerged in 1 ml of Trizol (Thermo Fisher). The 11 tubes were labelled by ST number allocation, and shipped on dry ice to MacroGen, South Korea for RNA extraction and RNA-Seq. Samples were randomised before sending to the sequencing provider to avoid any potential for introduction of a technical batch effect based on which group (T or U) the samples belonged to (i.e. to stop the sequencing provider extracting RNA from all T samples and then all U samples).

Untreated or Treated Sample	ST Designation
U1	ST10
U2	ST7
U3*	ST12*
U4	ST2
U5	ST6
U6	ST1
T1	ST8
T2	ST9
T3	ST3
T4	ST11
T5	ST5
T6	ST4

Table 2.3 List of flasks that were randomly assigned to be treated with menadione or untreated, and corresponding random ST sample identifier. Note untreated sample 3 (U3, designation ST12) marked with asterisk, as this sample was discarded due to contamination during the second round of purity checks.

2.3.3 RNA Extraction and Library Construction

Total RNA extraction was conducted by Macrogen Inc. The RNA samples then went through a quality control check where all 11 samples were of acceptable RNA Integrity Number (RIN, >7) and thus proceeded to the library construction stage. Library construction done by Macrogen used the Illumina TruSeq Stranded Total RNA (Illumina Inc, San Diego) protocol with ribosomal RNA depletion (Ribo-Zero).

2.3.4 RNA Sequencing and Output

All sequencing was done by Macrogen Inc. For mRNA sequencing, the barcoded library was loaded into the flow cell of an Illumina NovaSeq 6000 machine to generate 40M 100-bp paired-end reads/sample. Post sequencing the raw data of binary base calls (BCL) was converted into FASTQ files using the Illumina package bcl2fastq. The fastq files were returned to NTU by Macrogen Inc., with all downstream processing and analyses of the sequence data done at NTU.

2.3.5 Bioinformatics analyses

Analysis of the raw RNA-Seq data to look for significantly differentially expressed genes used the US web-based platform Galaxy (<http://usegalaxy.org/>) (Afgan *et al* 2018). Firstly, the genome sequence (fasta file) and annotations (gff file) for 322A (provided by NTU) were uploaded to Galaxy as the reference genome followed by the FASTQ output files for each sample from the RNA-Seq run. Quality control of the transcriptome sequence reads was assessed using FastQC v0.11.9 (Andrews 2010) within Galaxy. Sequence reads were then mapped to the 322A reference genome using HISAT2 v2.2.1 set to paired-end library (Kim, Paggi, Park *et al* 2019) before counting the number of reads that mapped to genes using featureCounts (Galaxy v2.0.1+galaxy2) (Liao, Smyth & Shi 2014). To test for differential gene expression between the treated (T) and untreated (U) samples DESeq2 v1.34.0 (Love, Huber & Anders 2014) used the count data from the featureCounts outputs and generated a normalised counts file and principal component analysis plot for the entire dataset. Genes were considered significantly differentially expressed based on $P < 0.05$ (Benjamini-Hochberg adjusted P values).

2.3.6 Principal Component Analysis

Principal component analysis plots were generated by DESeq2 using count data from featureCounts showing clustering of samples based on their similarities. 2 PCA plots were generated in this analysis, one with ST9 and one with ST9 omitted. This will be shown in the results section and elaborated upon in the discussion.

2.3.7 Visualisation of data for significantly differentially expressed genes

The log₂-transformed gene count data for the 1312 significantly differentially expressed genes ($P < 0.05$, Benjamini-Hochberg adjusted values) identified by the DESeq2 analysis were visualised in heatmaps. One heatmap was generated in GraphPad v9.0 by the author, a second version was generated using the R package heatmap.2 from gplots v3.0.1 by Professor Lesley Hoyles found in the appendix (section 8.3). Boxplots showing log₂ gene counts for the top ten most significantly differentially expressed genes between the T and U groups were generated using the R package tidyverse v1.2.1. Boxplots were also generated for *cagA* and *vacA* gene data. These visualizations were made by Professor Lesley Hoyles, NTU. Alongside these, log₂ fold change for the respective genes is shown in figure 5.4 and added to figure 5.5A. This data was obtained and visualised from DESeq2 analysis by the author.

2.3.8 Pathway over-representation analysis

Analysis was performed by Professor Lesley Hoyles, NTU. All protein sequences (amino acid format) for strain 322A were uploaded to the Kyoto Encyclopedia of Genes and Genomes (KEGG) Automatic Annotation Server (<https://www.genome.jp/kegg/kaas/>) on 8 March 2020 (Kanehisa & Goto 2020), to map the strain's genes against metabolic pathways. 668 of strain 322A's genes mapped to one or more KEGG entries. The R package KEGGREST v1.26.1 (Tenenbaum & Maintainer 2022) was used to identify all KEGG-mapped pathways and genes for *Helicobacter pylori* 26695 (KEGG release 93.0+, accessed on 13 March 2020), which was taken as the reference against which strain 322A would be compared. KEGG mapping data were available for 93 pathways in the reference strain, covering 1619 KEGG orthology (KO) entries. The KEGG entries for *H. pylori*

26695 were matched with those of 322A to get KEGG gene annotations for the 322A genes associated with KEGG entries. The number of significantly (adjusted P value < 0.05, Benjamini-Hochberg) differentially expressed genes in 322A that mapped to genes in each of the 93 *H. pylori* 26695 pathways was determined, with a one-sided Fisher's exact test used to determine the significance of gene over-representation. P values were subject to adjustment using the Benjamini-Hochberg method, with P < 0.05 the threshold for significance.

Chapter Three: Phenotypic and genomic comparisons within *Campylobacter jejuni*

3.1 Introduction

Phenotypic properties of six *C. jejuni* strains belonging to the ST-403 MLST clonal complex and three *C. jejuni* isolated from chickens (ST-354CC, ST-354CC and ST-45CC) were compared to investigate potential association between phenotype and niche adaptation ability. As described in chapter one, (section 1.1.7) 403CC strains show a near inability to colonise chicken hosts and the reason for this has yet to be elucidated in the field of *C. jejuni* research. It was hypothesised that 403CC strains may display a distinctly different phenotypic profile to known chicken colonisers and that this could partially explain the lack of observed chicken colonisation by strains of the 403 complex. Phenotypic assays were selected based on known colonisation factors and potential barriers to transmission. The 403CC isolates used in this work have previously been studied phenotypically by Morley (2014) with some overlap in the properties tested. The experiments conducted in this thesis directly compared phenotypes between 403CC and chicken isolate strain groups and thus differ from previously published studies. The secondary component of this chapter was to compare the genomes of 403CC isolates to those belonging to the most prominent host generalist *C. jejuni* groups, ST21 and ST45 and look for the presence or absence of genes that may be related to host colonisation and/or transmission routes between hosts.

3.1.1 Temperature based growth

C. jejuni is a mesophile that can survive at temperatures ranging from 4-55°C and can grow in the range of 30-45°C (Klancnik *et al* 2014, Habib, Uyttendaele and De Zutter 2010). The ability to survive temperatures is paramount to the success of *C. jejuni* as a multi-host pathogen that may spend extended periods of time between hosts, in an external environment. A flexible growth temperature within this range of temperatures is also key to *C. jejuni* as a zoonotic pathogen that can infect a variety of species that range in internal body temperatures, with mammalian and avian colonisation being prime examples.

An existing study (Aroori, Cogan and Humphrey 2013) on the effect of growth temperature on *Campylobacter spp.* concluded that growth was similar at 37°C and 42°C, that are human and poultry internal body temperatures respectively. Although strains showed different growth patterns at the different temperatures, ultimately the final OD for both temperature curves were not significantly different at the 48 h endpoint. The study worked under the hypothesis that temperature may be a factor in a colonising organism 'recognising' they had entered a specific host (avian vs mammalian) and changing gene expression to adapt to the niche. They called this a switch from pathogenic to commensal behaviour however this is disputed (section 1.1.3). The same study also found that some strains were more motile at 42°C and some were more invasive at 37°C (Aroori, Cogan and Humphrey 2013). Increased motility at 42°C was concluded to may be an indicator of how *C. jejuni* can spread through chicken populations more readily, it was also supported that *flgH* expression was higher at 42°C although this was not statistically significant. Increased invasiveness at 37°C may account for why *C. jejuni* invades mammalian intestinal epithelium but does not in avian hosts. There is some debate that temperature does not affect pathogenicity and specifically invasiveness, rather it is the difference in avian and human mucosa. This has not been demonstrated to a level of statistical significance at this time (Byrne, Clyne & Bourke 2007). There is no currently published work on the effects of temperature on the growth of 403CC *C. jejuni*. Although Morley (2014) previously demonstrated that 403CC strains have the ability to grow at both poultry and human temperatures, comprehensive growth curves at each temperature have not been done to date. Since 403CC *C. jejuni* strains do not colonise chickens, and sustained growth at 42°C is a specific adaptation for the colonisation of chickens, it was hypothesised that 403CC strains may display impaired growth rates at 42°C compared to a group of chicken isolates. This is because 403CC strains would have no reason to maintain this adaptation.

3.1.2 Biofilm formation

Biofilm formation is an important survival strategy for *C. jejuni* to persist in the environment between host transmission events. It must withstand desiccation, temperature fluctuations and perhaps most importantly oxidative stress. In the context of *C. jejuni* as a foodborne pathogen, particularly in poultry processing from farm to fork, biofilm formation is of importance when considering levels of antibiotic usage and potential biofilm formation on food processing equipment and surfaces.

C. jejuni can form mono- and multi- species biofilm. *C. jejuni* can form dual-species biofilms with organisms such as *Pseudomonas aeruginosa*, *Salmonella enterica* and *Staphylococcus aureus* (Feng *et al* 2016), and a dual-species biofilm with *C. jejuni* and *P. aeruginosa* was much more robust at surviving environmental stresses than a *C. jejuni* mono-culture (Ica *et al* 2012). Studies of biofilm formation in *C. jejuni* are relatively scarce compared to other bacterial species. Recent work by Teh *et al* (2017) looking at the effects of oxygen level and growth medium on *C. jejuni* biofilm formation showed that biofilm levels were highly variable between strains, with no consensus on preference towards aerobic or microaerobic conditions nor on differing nutrient growth conditions. The hypothesis in this thesis was that 403CC *C. jejuni* may have impaired biofilm forming ability compared to the chicken isolate group, relating to an inability to persist in a farm environment for cattle to poultry transmission.

3.1.3 Motility and Chemotaxis

C. jejuni flagella are bipolar and facilitate tumbling motility that is essential to colonisation and persistence within a host (Lertsethtakarn *et al* 2011). Motility allows *C. jejuni* to traverse the thick mucus layer of the intestinal lining, the niche that *C. jejuni* inhabits within a host (Almeka, Corcionivoschi & Bourke 2012). As with many organisms, motility in *C. jejuni* is mediated by chemotactic systems that are crucial to *C. jejuni* establishing colonisation in its intestinal niche (Hendrixson & DiRita 2004). Fucosylated glycoprotein structures of intestinal mucin are often a chemoattractant to *C. jejuni* and the degradation of this carbohydrate in the localised area means that some *C. jejuni* isolates are able to utilise this carbon source for a competitive growth advantage (Stahl *et al* 2011). When looking at niche adaptation in *C. jejuni* particularly between chicken and mammalian hosts it is important to consider the differences in these host organisms. For example, as noted in section 3.1.1, the body temperature of the host can affect motility. Motility and chemotaxis genes are upregulated at 42°C compared to 37°C (Stintzi 2003) and this may affect colonisation ability. It is also important to consider the physiology of the host organism and the nature of infection. The mucin layer of the intestine, the colonisation site of *C. jejuni*, differs biochemically between chickens and mammals. Different types of mucin are produced within the intestinal system of a host, and these are encoded by mucin (MUC) genes.

Duangnumsawang, Zentek & Borojani (2021) reported that there are 20 types of mucin produced in the human intestinal tract, 11 in the small intestine and nine in the large intestine. Comparatively there are six types of mucin in the chicken intestine, four in the small and two in the large intestine. The review also stated that the conformational structure of these different mucin types may determine viscosity and permeability of the mucus. Although it is well established that *C. jejuni* is pathogenic in humans, there has been debate about commensalism in chickens as discussed in section 1.1.3. Although the mechanisms underpinning this are not yet clear, chicken mucin may attenuate the pathogenicity of *C. jejuni in-vitro* (Alemka *et al* 2010). It was therefore hypothesised that 403CC *C. jejuni* would be less motile and chemotactic than strains adapted to colonise and persist in a chicken host.

3.1.4 Vitamin B5 synthesis

Vitamin B5 also known as pantothenic acid is synthesised by some *C. jejuni* strains, that possess the genes *panBCD*. Vitamin B5 may be a host specificity factor and the *pan* genes are part of a cattle associated region of the *Campylobacter* genome (Sheppard *et al* 2013). One rationale for *panBCD* being present in the majority of cattle colonising strains is due to host diet. Vitamin B5 is present in higher quantities in commercial chicken feed but it is present in low amounts in grass that grazing cattle consume.

Therefore, *pan* genes are essential as a host specificity factor for persistence in a cattle host. Interestingly the 403CC strains that readily colonise cattle are largely devoid of this set of genes, whilst chicken isolates that do not require the genes in the host that they were isolated from retain these genes. This raises the possibility that vitamin B5 plays a broader role in transmission through multiple host niches. It was hypothesised for this work that 403CC *C. jejuni* would have impaired growth *in-vitro* in B5 depleted media.

2.1.5 Oxidative stress

As a microaerophilic bacterium and multi host pathogen *C. jejuni* must be able to persist in a range of oxygen rich environments in order to transmit between organisms. Oxidative stress caused by these external environments provide one of the greatest challenges to the organisms' survival and viability during transmission events. Oxidative stress survival defence mechanisms in *C. jejuni* are multifaceted and incorporate motility, biofilm formation and even morphological changes to coccoid and filamentous structures (Oh, McMullen and Jeon 2015). The organism also has an array of antioxidant genes, producing proteins that protect the organism against reactive oxygen species (ROS). In *C. jejuni* the primary three responsible are *sodB*, *katA* and *ahpC* (Flint *et al* 2014). Strains that are better adapted to cope with these hostile conditions are more likely to be transmissible particularly across species that are geographically separated. However, *C. jejuni* is often detected in many environmental sample types such as soil, pasture and stock drinking water (Rapp *et al* 2020) that supports the idea the species is robust enough to live outside a host for an extended time. In farming and agriculture settings, strains may be exposed to atmospheric levels of oxygen for extended periods of time to transmit between cattle and poultry. It is suggested that a host species jump occurs in generalist lineages such as ST-21/ST-45 every 1.6-1.8 years (Dearlove *et al* 2016). This contrasts wildly to the confinement of a broiler house or indeed even cattle farming that has seen a dramatic rise in *C. jejuni* carriage due to intensive farming practices (Mourkas *et al* 2020). Given that 403CC *C. jejuni* strains exhibit a host species generalist lifestyle aside from their apparent near inability to colonise chickens, it is improbable that they are severely restricted in transmission by environmental factors such as oxidative stress. This does not however sufficiently exclude the possibility that the clonal complex as a whole may have impaired ability to deal with oxidative stress and are therefore less likely to make a species to species host jump, and this hypothesis will be tested in this work.

3.1.6 Genomic analysis

Given that *C. jejuni* has over 10,000 distinct sequence types over 44 clonal complexes (Chapter one, Section 1.1), and is found across many host species and environmental sites it is likely that the species shows significant genetic variation. As noted in Table 1.1 *C. jejuni* has a relatively high mutation and recombination rate. The first whole genome sequence of *C. jejuni* was published in 2000 using the NCTC11168 strain originally isolated from human faeces in a case of food poisoning by Dr Skirrow at Public Health England in 1977. From the 2000 study it was revealed that *C. jejuni* had a modest genome size of 1,641,481 base pairs in length with a low GC content of 30.6% and approximately 1,654 coding sequences (CDS). It was noted that there were few insertion sequences of phage associated sequences and very few repeat sequences. There were however many present hypervariable sequences in the form of short homopolymeric nucleotide runs in genes encoding for biosynthesis or modification of surface structures (Parkhill *et al* 2000). Sequencing of prominent strains such as RM1221 and highly virulent strain *C. jejuni* 81-176 have revealed the genomic diversity of the bacterial species (Parker *et al* 2006, Hofreuter *et al* 2006).

The total mutation rate for *C. jejuni* including synonymous and non synonymous mutations has been estimated at approximately $3.23 \times 10^{-2} \text{ kb}^{-1} \text{ year}^{-1}$ and recombination rates have been estimated at approximately $3.07 \times 10^{-3} \text{ kb}^{-1} \text{ year}^{-1}$ (Wilson *et al* 2009) though this will be greatly varied between strains. For example, 403 clonal complex strains that are investigated in this thesis have already been demonstrated to show a much lower rate of recombination events compared to non 403CC isolates (Morley *et al* 2015).

Due to *C. jejuni* having the ability for multi species host niche colonisation it is even suggested that regions of the genome are associated to a specific host for example the “cattle associated genome region” as referred to in Sheppard (2013). Morley (2014) who originally conducted genomic analysis on 403CC isolates found that the clonal complex had a 403CC exclusive restriction-modification system from the gene *HhaIm*. Therefore, the work in this chapter will test whether this exclusivity is still true, when compared to ST21/ST45 genomes. It will also look for other present or absent genes of interest, which may play a role in the niche colonisation ability of 403CC isolates.

3.1.7 Aims

The overriding aim of this chapter was to consider the phenotypic and genomic properties of a set of strains belonging to the 403CC of *C. jejuni* that possess near inability to colonise chickens and compare them phenotypically to *C. jejuni* isolates from chickens and genomically to other host generalists that readily colonise chickens. Phenotypic assays were chosen that reflect potential niche transmission or niche colonisation factors. The *in-vitro* performance of 403CC strains versus chicken isolates were determined. Genome analysis also determined potential genes of interest that may separate 403CC isolates from their other host generalist counterparts, and how this may explain the observed pattern of near absent colonisation rate of 403CC in chickens.

The aims of this chapter were:

- To compare the growth of 403CC and chicken isolate *C. jejuni* strains at 37°C and 42°C.
- To compare the biofilm formation ability of 403CC and chicken isolate *C. jejuni* strains.
- To compare the motility and chemotactic properties of 403CC and chicken isolate *C. jejuni* strains.
- To compare the ability of 403CC and chicken isolate *C. jejuni* strains to grow in vitamin B5 depleted media.
- To compare the viability of 403CC and chicken isolate *C. jejuni* strains when exposed to environmental oxidative stress.
- To consider whether across these phenotypic assays, there were sufficient differences between 403CC and chicken isolates to explain the observed pattern of differing niche transmission/colonisation between the two groups of strains.
- To compare the genomes of 403CC isolates to ST21/45 generalist isolates.

3.2 Results

A range of assays were undertaken to compare the phenotypic ability of six strains belonging to the *C. jejuni* 403 clonal complex against three *C. jejuni* strains of chicken host origin. Results are presented for testing of temperature dependent growth, biofilm formation, motility, chemotaxis, vitamin B5 synthesis and oxidative stress resistance. Unless otherwise stated the data presented are means calculated from triplicate data for each isolate. Results are presented with errors bars that represent the standard deviation calculated for the mean based on the range of data collected for each strain individually. At the end of the phenotypic analysis results a brief summary of the genome analysis results (see methods section 2.2.8) is provided.

3.2.1 Growth of strains at different temperatures shows faster initial growth for chicken isolates at 42°C

Temperature dependent growth curves were constructed using optical density at 600 nm readings at two temperatures - 37°C and 42°C over 42 h and were constructed into temperature growth curves as described in section 2.1.2. Data shown are the triplicate means at each time point for each strain grouped into their respective groups of 403 clonal complex strains and chicken host isolate strains. Results for each individual strain's temperature-dependent growth are presented in figure 3.1 A-B. Group-based summary data of temperature-dependent growth are shown in figure 3.1 C-D.

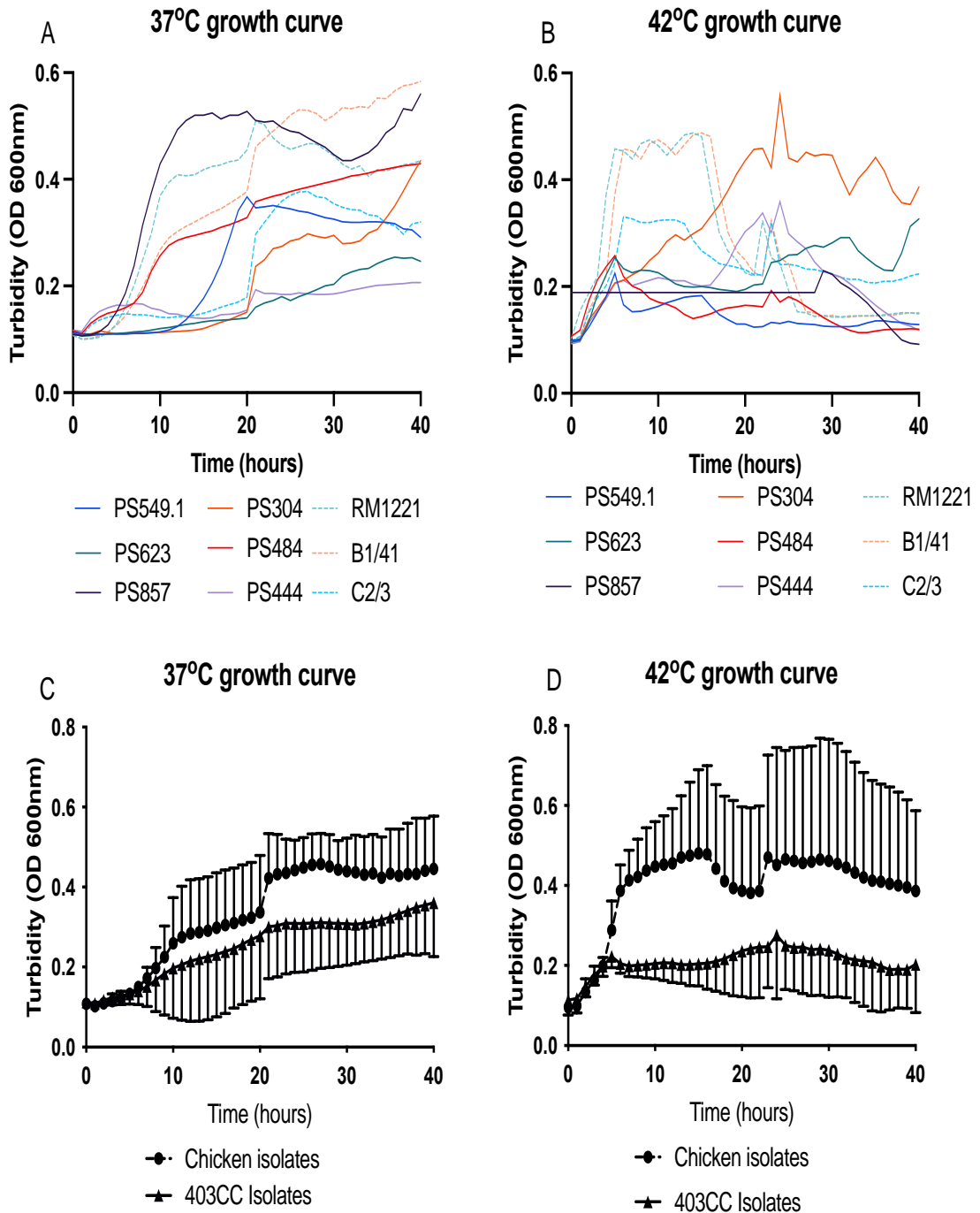


Figure 3.1 Chicken isolate growth is initially faster at 42°C. 37°C and 42°C growth curves measured at hourly time points for OD_{600nm}. (A-B) Growth curves by individual isolate where dotted lines represent chicken isolates and full lines represent 403CC isolates. (C-D) growth curves by group where the line with circular points represents the chicken isolate group and the line with triangular points represents the 403CC isolate group. Error bars are only shown unidirectionally for ease of viewing.

The individual strain data (Figures 3.1A and 3.1B) show that there was considerable variation between isolates and the differences in growth between strains became more pronounced over time ($P < 0.0001$ at both temperatures). Across the 37°C and 42°C datasets combined there were 16 instances of statistically significant higher mean growth between isolates and this was a mixture of 403CC isolates showing higher growth than chicken strains and vice versa, demonstrating variance between individual strains. The most important data of note is that in 10 of the 16 instances where there were statistically significant growth differences between isolates, the chicken isolates had statistically higher mean growth than 403CC isolates at 42°C. This is evident in figure 3.1B that clearly shows much more rapid growth by the chicken isolates than 403CC isolates at earlier time points in the experiment. The OD did fall for many strains as the assay went on, particularly the fast-initial growing chicken isolates at 42°C and commentary on this will follow in the discussion. The grouped analysis data, (shown in figures 3.1C and 3.1D) found that there were no statistically significant differences in growth between the chicken and 403CC isolates at 37°C however, at 42°C the chicken isolate group grew significantly faster than the 403CC isolate group between the 6-9 h timepoints where the chicken isolate group showed higher growth ($p < 0.05$).

3.2.2 Biofilm formation is highly variable between strains with no consensus on optimal conditions for formation

Biofilm formation data was gathered under twelve varying combinations of temperature, nutrient and environmental oxygen conditions as described in section 2.1.3. The biofilm forming ability of 403CC strains and chicken isolates are compared in figures 3.2 and 3.3. There was substantial variation in biofilm forming ability across temperature, nutrient and environmental oxygen conditions. Under microaerobic conditions, the chicken isolates produced significantly more biofilm than the 403CC isolates at 6°C ($p < 0.05$) and at 37°C ($p < 0.01$). Of the 12 conditions B1/41 produced the most biofilm within the chicken isolates group in 11 conditions, with the exception of 25°C microaerobic conditions in MHB where RM1221 was superior, suggesting B1/41 may be a strong biofilm former. In the 403CC group strain PS857 showed highest biofilm in eight of the conditions spanning all combinations of atmospheric condition, temperature and growth media. Under certain conditions however PS444, PS484 and PS623 all demonstrated higher biofilm formation. PS623 for example had highest biofilm of the group at 6°C atmospheric in MHB but also 25°C microaerobic in PBS leading to the idea that individual strains are not necessarily fixed to an optimum environment for biofilm production.

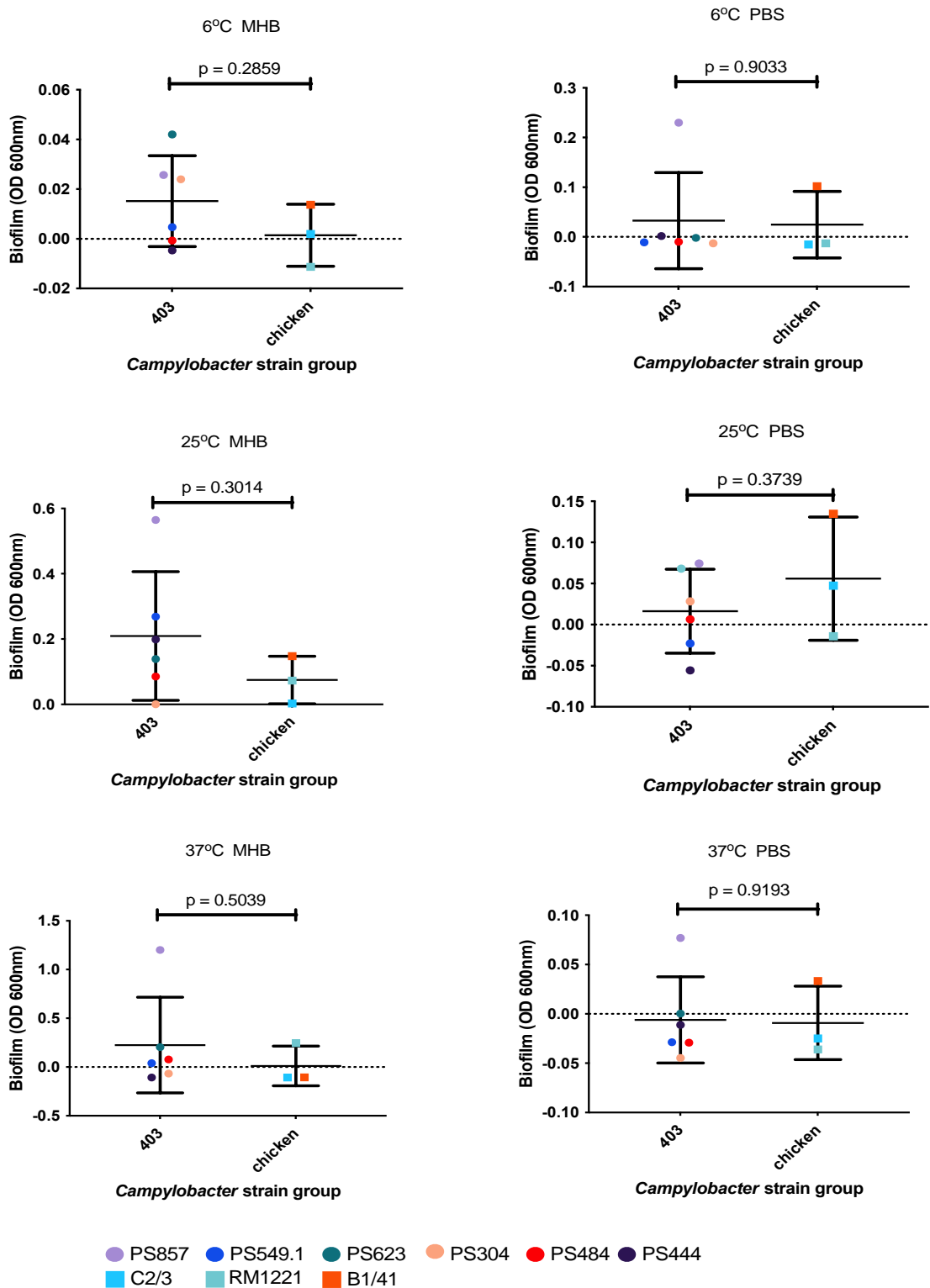


Figure 3.2 Biofilm formation is variable across all strains under atmospheric conditions. Biofilm measured by OD_{600nm}. Each experiment was conducted with variable temperature (6°C, 25°C or 37°C) and media (PBS or MHB) conditions. Results shown are grouped data with triplicate mean shown for each individual strain within the group. Individual strains are shown as circles for 403CC isolates and squares for chicken isolates. The bars and error bars indicate the mean and SD, respectively, for each group. P values were generated by unpaired t-test.

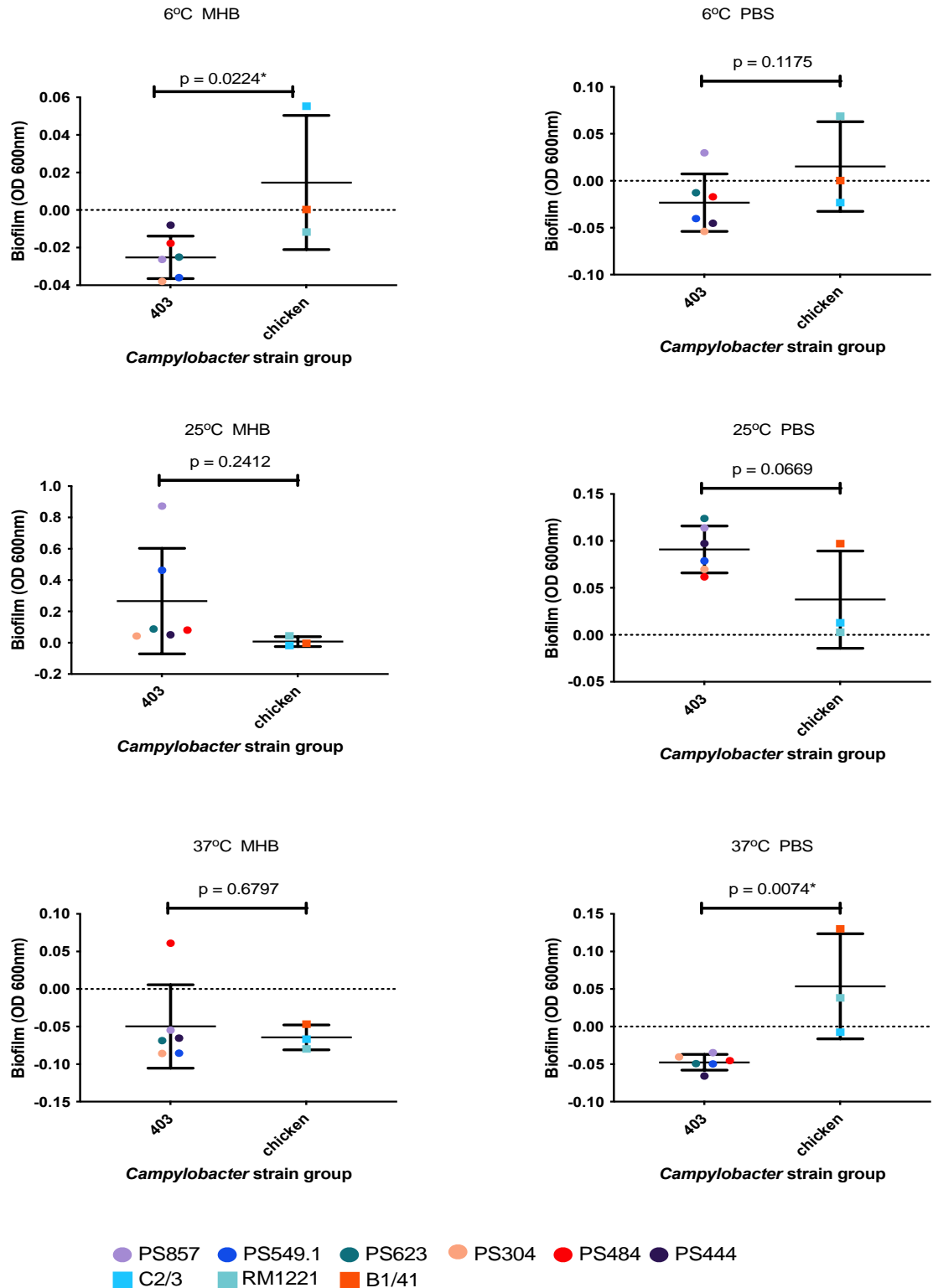


Figure 3.3 Chicken group biofilm formation is significantly higher under specific microaerobic conditions. Biofilm measured by OD_{600nm}. Each experiment was conducted with variable temperature (6°C, 25°C or 37°C) and media (PBS or MHB) conditions. Results shown are grouped data with triplicate mean shown for each individual strain within the group. Individual strains are shown as circles for 403CC isolates and squares for chicken isolates. The bars and error bars indicate the mean and SD, respectively, for each group. P values were generated by unpaired t-test.

3.2.3 Motility is variable between isolates but shows no significant difference between strain groups

Motility data was gathered by an agar stab motility assay as described in section 2.1.4. *Micrococcus luteus* was used as a non-motile control to correct for false positives, such as the observed “halo” being the result of the actual initial inoculum into the soft agar rather than observable motility. The motility of individual strains is shown in figure 3.4A and grouped results in figure 3.4B. As can be seen in figure 3.4A there was considerable variation in motility between individual strains ($P < 0.0001$). Within the 403CC isolates group, there was large variation as all strains behaved differently whereas the chicken isolates had two strains that were similarly motile (C2/3 and RM1221) while isolate B1/41 showed lower motility. Analysis of data from individual strains revealed that there were 4 statistically significant instances of a 403CC isolate showing higher motility than a chicken isolate, and ten instances of a chicken isolate showing higher motility than a 403CC isolate ($p < 0.05$). Grouped analysis showed no overall statistically significant difference in motility between the 403CC and chicken isolate groups ($P = 0.4681$, figure 3.4B, unpaired t-test).

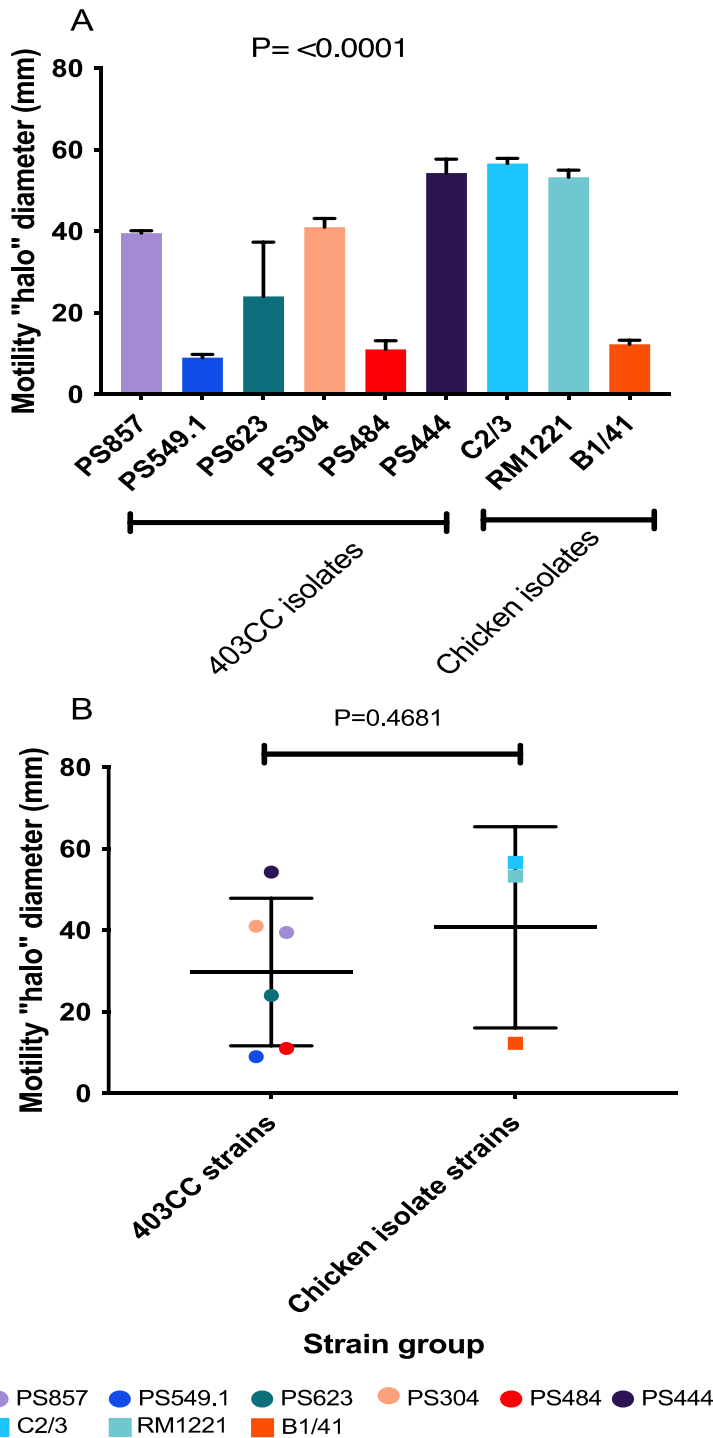


Figure 3.4 Motility is highly variable between strains but is not significant between the 403CC and chicken isolate groups. Agar stab motility assay results showing diameter of zone of motility in millimetres. 3.4A shows motility by isolate. Error bars show standard deviation from the triplicate mean recorded for each isolate. 3.4B shows motility by strain group where each isolate triplicate mean is displayed as a circle for 403CC isolate and square for chicken isolate. Bars show mean for the group and error bars indicate standard deviation.

3.2.4 Chemotaxis migration increases at higher concentrations of fucose

Chemotactic properties of *C. jejuni* strains were observed using a fucose chemoattractant hard agar plug (HAP) assay as described in section 2.1.5. Strains were grouped into 403CC and chicken isolate group results for chemoattraction at 10 mM, 50 mM, and 100 mM fucose based on viable count of bacteria recovered from each agar plug. The % increase in migration to the agar plug observed when increasing fucose concentration from 10 mM to 100 mM was also recorded, both for individual isolates and in the aforementioned groups. The grouped viable counts are shown in figure 3.5A and percentage increase in chemoattraction migration when increasing fucose concentration 10-fold for individual (Figure 3.5B) and grouped (Figure 3.5C) strains. Increasing fucose concentration resulted in an increased viable count of bacteria retrieved from the agar plugs (Figure 3.5A, $p < 0.0001$, two-way ANOVA). There were no statistically significant differences in viable count between the 403CC and chicken isolate groups at any of the fucose concentrations tested (Figure 3.5A, Sidak's multiple comparisons tests). Increasing fucose concentration 10-fold from 10 mM to 100 mM caused 20%-90% increase in viable counts of 403CC strains recovered from the agar plugs and a similar 22-83% increase in viable counts of chicken strains (figure 3.5 B, $P = 0.699$, t-test).

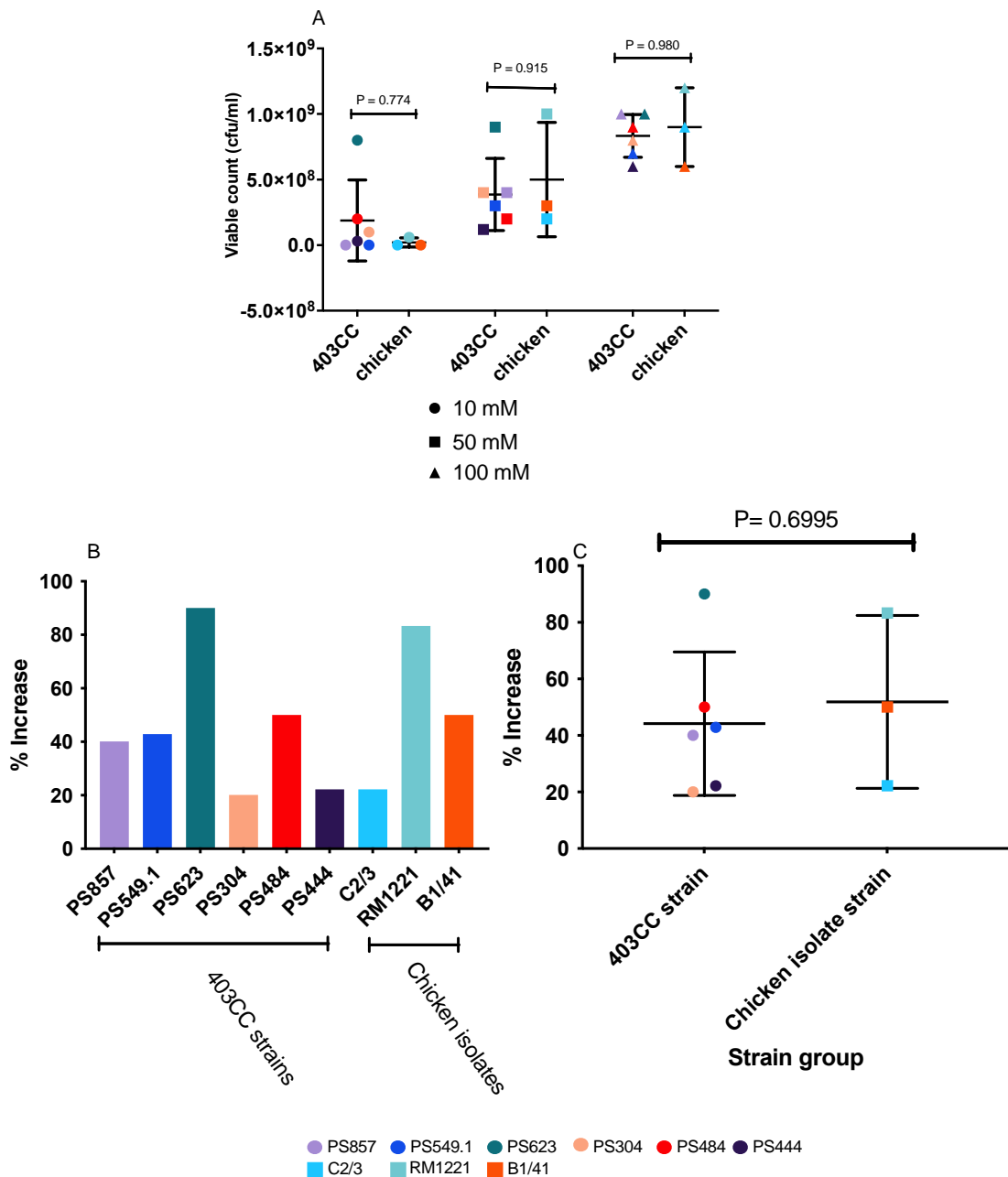


Figure 3.5 Increasing fucose concentration improves chemoattraction based migration. Fucose chemotaxis assay as performed by chemoattractant hard agar plug (HAP) viable count. Figure 3.5A shows viable counts (cfu/ml) obtained from agar plugs containing 10 mM, 50 mM and 100 mM of fucose respectively. Results are separated into 403CC and chicken isolate groups with each point representing a triplicate mean of an isolate within the group, error bars show standard deviation and bars show mean for each group. P values displayed are generated from Sidaks multiple comparison test. Figure 3.5B shows percentage increase in viable count for each individual strain observed when increasing fucose plug concentration from 10 mM to 100 mM. Figure 2.5C shows

percentage increase to viable count by strain group when increasing fucose plug concentration from 10 mM to 100 mM. Each isolate triplicate mean is depicted as a circle for 403CC isolates and square for chicken isolates, error bars show standard deviation and bars show mean for each group.

3.2.5 Vitamin B5 depleted media does not significantly impair growth of *C. jejuni* isolates

Growth in vitamin B5 enriched and B5 depleted media was recorded based on OD_{600nm} growth readings as described in section 2.1.6. Data was recorded for each strain in the presence and absence of B5 before being grouped into the respective 403CC/Chicken isolate groups to examine the percentage decrease in growth rate in B5 depleted media compared with “normal growth” in B5 enriched media. Figure 3.6A shows the mean recorded growth OD for the 403CC and chicken isolate groups over time, up to 72 h. Paired endpoint comparisons of individual strain growth in B5 depleted and B5 enriched conditions are shown in Figure 3.6 B. Finally, relative growth between media types is shown in figure 3.6 C. No significant differences in growth were seen between the 403CC and chicken isolates, or between media with and without B5, at any time point (Figures 2.6A and 2.6B, two-way ANOVA with Tukey’s multiple comparisons). Grouped analysis showed no statistically significant difference between the 403CC and chicken isolate groups, when comparing growth change between B5 depleted and B5 enriched media (figure 2.6, P= 0.3686, unpaired t-test).

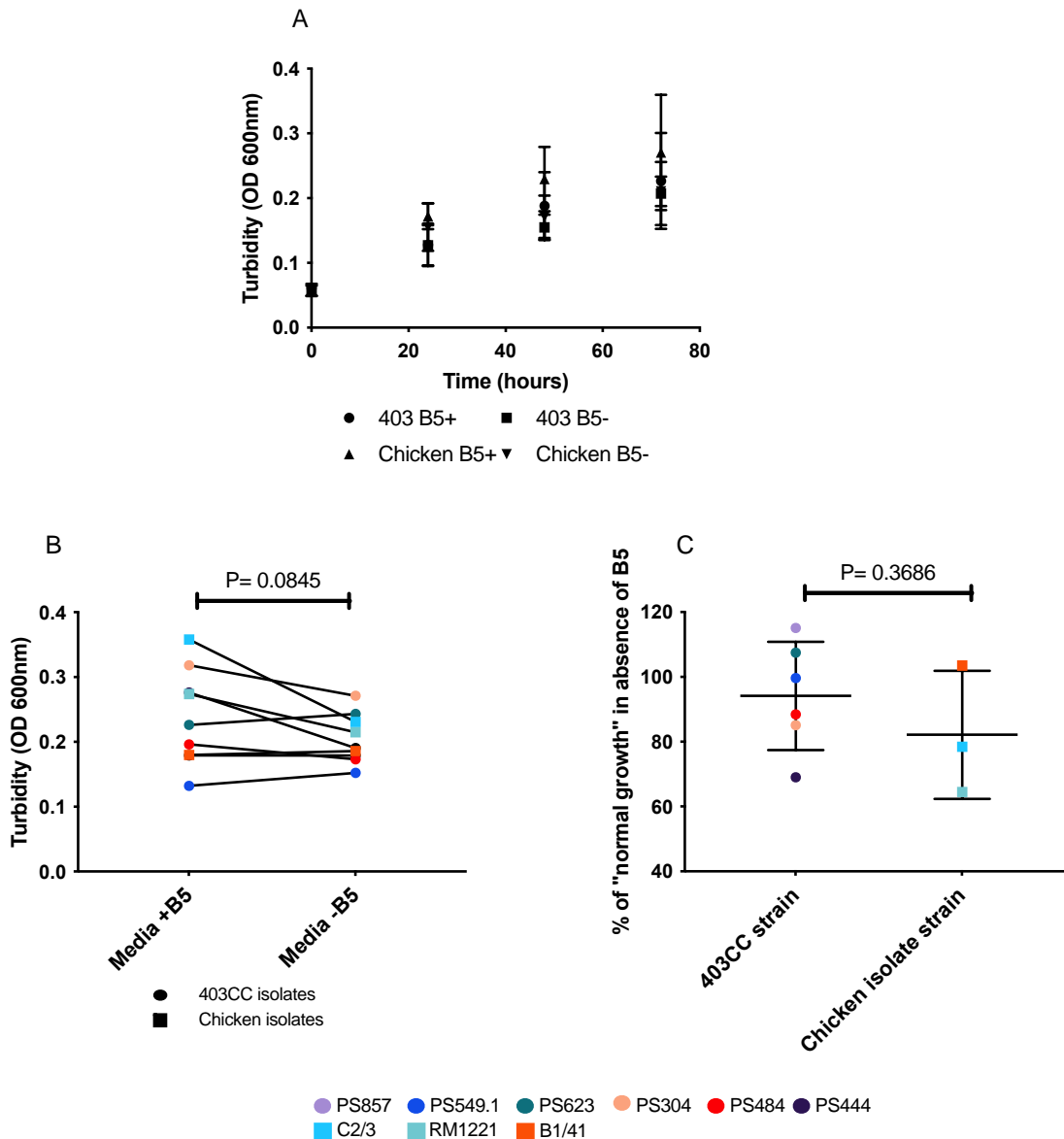


Figure 3.6 Absence of Vitamin B5 does not significantly affect isolate growth Pantothenic acid (Vitamin B5) depletion assay. Figure 3.6A shows OD_{600nm} growth readings at 0,24,48 and 72 h for chicken isolate group and 403CC group in the presence and absence of B5, each data point represents the mean for the group obtained from triplicate means for each strain within the group. The bars and error bars indicate the mean and SD, respectively, for each group. Figure 3.6B shows paired analysis of the growth of individual strains at 72 h endpoint in B5+ and B5- media, 403CC strains are indicated by circles and chicken isolates by triangles. Figure 3.6C shows relative growth in B5- media compared to growth in B5+ media, expressed as a percentage of “normal growth” in B5+ media for each strain. Triplicate means for each isolate within the group are indicated by circles for 403CC isolates and squares for chicken isolates. The bars and error bars indicate the mean and SD, respectively, for each group.

3.2.6 Oxidative stress survival does not significantly differ between strain groups

To assess each strain's ability to survive oxidative stress, bacterial growth and viability in microaerobic (5% O₂) and standard atmospheric (20% O₂) conditions were monitored over time by measuring the OD_{600nm} and BacTiter Glo luminescence (arbitrary units), respectively as described in section 2.1.7. Strains were grouped into 403CC and chicken isolates. Figure 3.7 panels A-B show OD readings for the groups under both microaerobic and normal atmospheric oxygen conditions and panels C-D show the corresponding luminescence results. No statistically significant difference was found between the chicken isolate and 403CC isolate groups when measuring OD (growth) in both microaerobic and atmospheric conditions (figure 2.7 panel A-B, P= 0.810 and P= 0.776 respectively, multiple t-test). No statistically significant difference was found between the groups when measuring luminescence (viability) either (figure 3.7 panel C-D, P= 0.697 and P=0.096 respectively, multiple t-test).

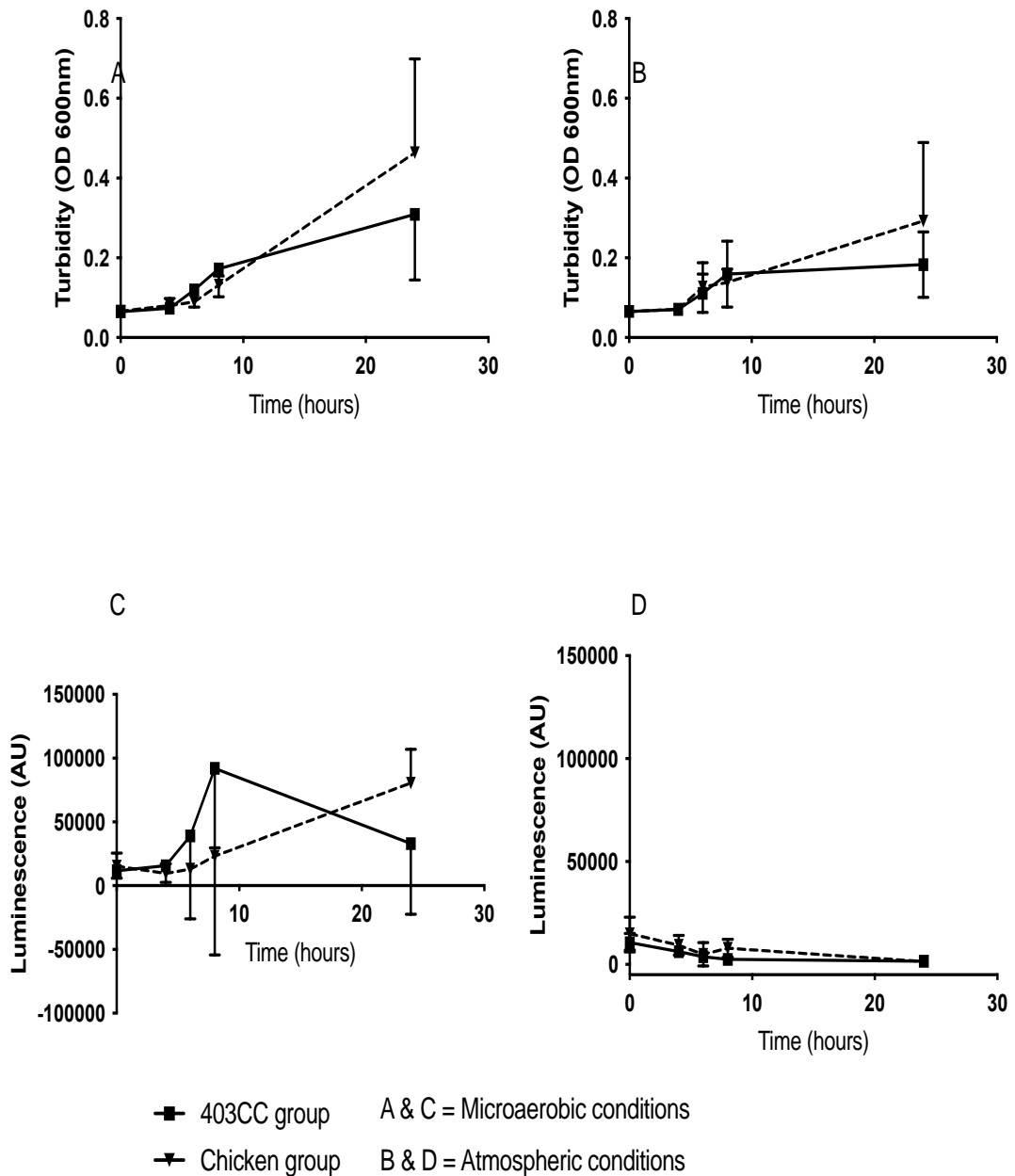


Figure 3.7 Oxidative stress survival does not significantly differ between strain groups. Figure 3.7 (A-B) shows OD_{600nm} at 0, 4, 6, 8 and 24 h for 403CC and chicken isolate groups under microaerobic (A) and atmospheric (B) oxygen conditions. Figure 3.7 (C-D) shows luminescence (arbitrary units) at 0, 4, 6, 8 and 24 h for 403CC and chicken isolate groups under microaerobic (2.7C) and normal atmospheric oxygen (2.7D) conditions. Error bars are displayed unidirectionally for ease of viewing. The bars and error bars indicate the mean and SD, respectively, for each group.

3.2.7 Genes related to phenotypic assays and niche adaptation are largely conserved across 403CC and *C. jejuni* generalist genomes

Pan genome construction of host generalist ST-21/ST-45 isolates and 403CC isolates was performed. Post pan genome construction, isolates were separated out into the ST21/45 and 403CC groupings. A presence/absence gene list then showed how many isolates a gene was present or absent for within that grouping (see methods 2.1.9). The presence/absence list was then used to look for genes that may relate to chicken colonisation and/or genes that relate to the phenotypic assays in this chapter that may explain phenotypic performance. Below are known genes for each phenotypic assay, the findings of which will be elaborated in the discussion (section 3.3.7). Genes identified that are not present in all genomes across both groups are compiled in table 3.1. A full list of genes that were exclusively or comparatively highly present in one group compared to the other can be found in the appendix.

3.2.7.1 Biofilm genes

13 known biofilm genes were identified, 11 of which were present in all generalist and all 403CC genomes. *ilvE*, *fabZ*, *lpxA*, *carB*, *serB*, *cheA*, *htpG*, *mrdB*, *kpsT*, *nuoC* and *flgE2* were present in 14/14 403CC isolates and 121/121 generalist isolates. There were however two biofilm genes that showed a strong difference between groups, *tal* was found in only 1/14 403CC genomes but 116/121 generalist genomes. *bioC* was absent from the 403CC genomes but was present in 77/121 generalist genomes.

3.2.7.2 Motility genes

Motility genes of interest were grouped into three prominent motility gene groups, *fli*, *flg* and *fla*. There were 12 *fli* genes that were present in all genomes across both groups *fliA/D/E/F/G/M/N/P/Q/R/S/W/Y*. Similarly, *flg* genes were also conserved. Six *flg* genes were identified and were present in all genomes, *flgB/C/G/H/I/K*. Two *fla* genes were also identified however these were not ubiquitous *flaA* was present in all 403CC isolates but only 62/121 generalist isolates. *flaB* was present in all 403CC isolates but only present in 39/121 generalist isolates.

3.2.7.3 Chemotaxis genes

The first group of chemotaxis genes identified belong to the *che* family. Five *che* genes namely *cheA/B/R/V/W* were found to be present in all 403 and generalist genomes. Also universally present was *mcp4*, however of the same group *mcpB* was only present in one 403CC isolate genome and in 65 of the 121 generalist genomes. There were two lesser established genes present in the list. *pctC* was found in five 403CC genomes and only two generalist genomes. *trg* was present in six 403CC and 20 generalist genomes.

3.2.7.4 Vitamin B5 synthesis genes

Pantothenic acid (vitamin B5) synthesis genes *panB/C/D* were largely absent in the 403CC genomes, found in only one of 14. In the generalist group they were present in 89 of the genomes. The presence rate of the three genes were all identical.

3.2.7.5 Oxidative stress genes

Seven genes linked to resistance to oxidative stress were identified, all of which were present in all genomes in the dataset. *sodB*, *katA*, *tpx*, *bcp*, *luxS*, *msrA* and *msrB* were all present, interestingly *ahpC* previously referred to in this thesis was entirely absent.

3.2.7.6 Other genes of potential relevance

Two other genes were identified that fell outside those that would be related to the phenotypic properties tested in this chapter. *HhaIm* a modification methylase previously identified, was present in 13/14 403CC genomes and was absent from the generalist genomes. *fabG* was absent in all 403CC genomes but present in 53 of the generalist genomes. *fabG* is involved in fatty acid metabolism and has been linked to adaptation to a chicken host, discussed in section 3.4.6.

Gene	403CC Presence (N= 14)	Generalist Presence (N= 121)	Pathway
<i>tal</i>	1 (7%)	116 (96%)	Biofilm formation
<i>bioC</i>	0 (0%)	77 (64%)	Biofilm formation
<i>flaA</i>	14 (100%)	62 (51%)	Motility
<i>flaB</i>	14 (100%)	39 (32%)	Motility
<i>mcpB</i>	1 (7%)	65 (54%)	Chemotaxis
<i>pctC</i>	5 (38%)	2 (2%)	Chemotaxis
<i>trg</i>	6 (43%)	20 (17%)	Chemotaxis
<i>panBCD</i>	1 (7%)	89 (74%)	Vit. B5 Synthesis
<i>hha1m</i>	13 (93%)	0 (0%)	R-M System
<i>fabG</i>	0 (0%)	53 (44%)	Fatty Acid Metabolism

Table 3.1 Summary of genes identified that were not universally present across all genomes of both the 403CC and generalist lineage groups

3.3 Discussion

This thesis aimed to identify possible reasons why *Campylobacter jejuni* strains of the 403CC clonal complex do not colonise chickens. Phenotypic assays and genome analysis were used to determine potential differences in the phenotypic profiles and genome content of 403CC strains compared to chicken isolates (phenotypically) and other host generalist strains (genomically). Isolates of the 403CC are largely uncharacterised in the scientific literature to date. It should be noted that for any further work in this area, strain choice and isolate stocks could be improved. Ideally all strains would have the same country of isolation, as in this work whilst all the 403CC isolates were of UK origin, chicken isolates C2/3, RM1221 and B1/41 were isolated from Canada, U.S.A and Botswana respectively. Not only may isolation methods and stock production not be consistent, but geography may play a role in phenotypic properties of the strain. It is difficult to ascertain geographical *C. jejuni* differences based on clinical reporting. Whilst for example, less developed countries may have more cases due to poor sanitation infrastructure, there is less reporting due to healthcare infrastructure. It is also worth noting that where *C. jejuni* can be endemic particularly in areas of Africa, paediatric exposure can lead to asymptomatic carriage later on in life (Kaakoush *et al* 2015). For the stocks used in this thesis they were produced from a stock provided by a former supervisor. However, it was not established if this was the original master stock direct from isolation. Multiple passage may affect phenotypic properties and is often observed in attenuating the properties of the strain. For example, 23 stocks of type strain NCTC 11168 collected from UK laboratories showed considerable variation in motility, morphology, 37°C growth rate, invasion of chicken and human cell lines and ampicillin resistance (Pascoe *et al* 2019). There is also evidence that repeated passage purely into a rich media devoid of stressors attenuated *C. jejuni* and lead to the loss of motility (Sher *et al* 2020). It would therefore be beneficial for strains of the same country of origin to be used, and for several vials be produced of the master stock, potentially a set amount for each planned assay for consistency and to ensure the phenotypic properties observed would not be skewed or biased pre-testing.

Manning *et al* (2003) initially MLST typed strains of the 403CC and suggested that the clonal complex may be largely specialised to porcine hosts. Further work was conducted by Morley (2014) in the PhD thesis “Niche adaptive evolution of *Campylobacter jejuni*” and corresponding paper (Morley *et al* 2015). The Morley (2014,2015) work focused on phenotypic and genotypic properties of 403CC isolates with respect to how they may be pathogenic to humans, rather than looking at the chicken niche restricted properties of the clonal complex. To try and explain the chicken niche adaptive restricted properties of the 403 clonal complex, the work described in this thesis compared the phenotypic characteristics of 403CC isolates compared with those of chicken origin, with a view to potentially explaining the chicken niche adaptive restricted properties of the 403 clonal complex.

Overall, we demonstrated that phenotypically there were very few statistically significant phenotypic differences in observed phenotypic ability between 403CC strains and chicken isolate strains aside from temperature growth curve discussed below. Genome analysis presented few genes linked to phenotypic performance that showed differences in presence/absence between datasets. The strongest potential indicator of the curious near inability of the 403 clonal complex to colonise chicken hosts in the form of the 403CC exclusive restriction modification system *hha1m*.

3.3.1 Temperature growth curves

There was a high degree of variation in the growth curves at strain level, at both 37°C and 42°C (section 3.2.1, Figures 3.1A & 3.1B). No statistically significant differences in growth patterns were detected between the 403CC and chicken isolate groups (Figures 3.1C & 3.1D) except that the chicken isolates grew significantly faster than the 403CC isolates at 42°C during the earlier timepoints (6-9 h, $p < 0.05$, multiple t-tests).

This suggests that despite 403CC isolates being largely associated with cattle and livestock with a 37°C body temperature, they do not show enhanced growth at 37°C compared to the chicken isolates that are presumably adapted to the chicken body temperature of 42°C. But conversely, the chicken isolates did appear to have an early growth advantage over the 403CC isolates at 42°C, although at later time points the

403CC isolates were also able to reach high densities at 42°C. The rapid growth of chicken isolates at 42°C however was followed by a sharp decrease in OD. The most likely explanation for this would be cell death caused by nutrient depletion, the same decline was also seen in 403CC isolates at later time points albeit less rapidly. The rapid early growth is interesting because broiler chicks have a 42°C body temperature, and established population colonisation of the chick cecum by *C. jejuni* occurs in the first 24 h (Hermans *et al* 2011). Therefore, the growth curve findings are consistent with the hypothesis that the chicken isolates are better adapted to rapid initial growth and thus better subsequent establishment of population in the chicken niche compared to 403CC isolates. This may be one reason that they are more routinely isolated from chickens compared to the rarity of 403CC isolates.

As seen in the data the growth rates even within the strain groups show considerable variation at both 37°C and 42°C which is unsurprising in *C. jejuni* that is highly polymorphic with a high degree of genetic and phenotypic variation between strains. In fact, a recent study into type strain NCTC 11168 found that collection of NCTC type strains from 23 separate laboratories resulted in variation in observed phenotypic ability that included growth rate (Pascoe *et al* 2019).

Since the assay presented in Figure 3.1 was conducted in an atmospheric module-controlled plate reader, the nearest comparable data available in the wider literature is a growth curve ran by BMG Labtech (Haigh & Ketley 2011) using a comparable reader with three *C. jejuni* type strains NCTC 11168, 81176 and 81116. This was a 42°C growth curve assay over 24 h and at the 24 h mark OD_{600nm} ranged from approximately 0.48-0.7. The OD values obtained in the work of this thesis were on average slightly lower, probably due to the use of lower volumes of nutrient broth in the wells (100µl MHB vs 200µl MHB used in the BMG Labtech experiment) and also the absence of shaking vs shaking within the module that promotes growth.

Ideally further work would repeat the assays but with a more nutrient rich media as it may have been a limiting factor. Further work that could be done in this area would include direct competition assays, using a mixed culture of 403 and chicken isolates.

This would be useful to see if at 42°C the initial growth spike observed in the chicken isolates between 6-9 h over the 403CC isolates would be high enough for the chicken isolates to outcompete the 403CC strains. However, such experiments would require a method to distinguish between the isolates upon recovery at the endpoint.

3.3.2 Biofilm formation

Biofilm forming ability was assessed in 12 biofilm formation condition assays with varying combinations of temperature, atmospheric oxygen levels and nutrient availability to simulate different *in-vivo* conditions (Section 3.2.2). There was substantial variation in *C. jejuni* biofilm forming ability across the tested conditions. A statistically significant difference was observed under microaerobic conditions, where the chicken isolate group produced significantly more biofilm than the 403CC isolates at 6°C ($p < 0.05$) and at 37°C ($p < 0.01$). Strain PS857 of the 403CC group demonstrated high biofilm forming ability, which is of interest because at 37°C in the growth curve assays this strain grew faster than the rest of the 403CC strains also.

Given the large variety of conditions tested and the two conditions with statistically significant differences in biofilm forming ability not having the temperature or nutrient variables in common it is most likely that there are no specific conditions under which chicken isolates outperform 403CC isolates in biofilm formation ability.

The biofilm formation of *C. jejuni* strains can be highly variable. In one study it was demonstrated that biofilm OD_{600nm} readings ranged from 0.065-1.005 between strains (Pascoe *et al* 2015). The study used 120 isolates in total a mixture of host generalists, cattle specialists, chicken specialists and some *C. coli* isolates. It also found genomically that the genes involved in biofilm formation were different even between ST-21 and ST-45 isolates. Biofilm formation in general within *C. jejuni* is a highly debatable issue. Although it is recognised that *C. jejuni* can form monospecies biofilms in laboratory settings, the results are often inconsistent, for example RM1221 barely produced any biofilm even under perfect laboratory conditions and thus would be unlikely to have the capacity to in the environment and possibly not even in the intestine as a monospecies. It was concluded that there is limited evidence for the formation of architecturally complex

biofilms like those produced by other bacterial species (Teh, Lee and Dykes 2014). Interestingly there is evidence to suggest that oxidative stress such as from atmospheric levels of oxygen can increase biofilm production by *C. jejuni* (Oh, Kim and Jeon 2016) however biofilm formation in this thesis (figures 3.2&3.3) was remarkably similar in both microaerobic and environmental oxygen conditions for both groups of bacteria. Several papers suggest atmospheric oxygen levels are more favourable to biofilm formation than microaerobic (Reuter *et al* 2010, Zhong *et al* 2020) however others suggest that biofilm is very strain dependant and higher oxygen concentrations were only sometimes a stimulus for biofilm production (Arujo *et al* 2022). Arujo *et al* 2022 also concluded in the setting of a broilerhouse lower temperatures were detrimental to biofilm production, improving at 30°C and peaking at 42°C.

The OD_{600nm} recorded in this study (figures 3.2&3.3) were relatively low, indicating that the majority of the strains were poor biofilm formers. There are several potential explanations for this including growth rate (as discussed in section 3.3.1), motility (as discussed in section 3.3.3) and chemotactic properties (as discussed in section 3.3.4) that can affect biofilm forming ability (Reuter *et al* 2010, 2018).

A recent and comprehensive review on the state of *C. jejuni* biofilm literature suggests that research on this particular facet of the bacteria is “still in its infancy” (Ma *et al* 2022). The review also acknowledges the challenge in the field given that the biofilm formation strength of *C. jejuni* can be highly strain dependant and that in *in-vivo* and *ex-vivo* settings, monospecies biofilm formation is less observed or retrievable than multispecies biofilms such as those formed with *Enterococcus spp.* and *Staphylococcus spp.* Given that the premise of this thesis is to consider that one of the barriers 403CC faces in colonising chickens may be persistence outside a host, further work could include many modifications to the biofilm assay such as introducing a secondary species to look at multispecies biofilm formation ability.

This could follow on from work conducted that showed that under aerobic conditions although *C. jejuni* formed monospecies biofilm granting it some protection over planktonic bacteria. After 48 h exposure it became viable but non-culturable (VBNC) unless co cultured with *Pseudomonas aeruginosa* or *Escherichia coli* in which case the survival rate increased (Zhong *et al* 2020).

It would also be useful to test different substrates on which the biofilm would be permitted to grow such as a metal disk and polystyrene, to in part replicate the *ex-vivo* substrate conditions of a broiler house surface and commercial packaging.

3.3.3 Motility

Agar stab motility assays (section 3.2.3) showed that there was considerable variation in motility between individual strains (figure 3.4A). However grouped analysis found no statistically significant difference in motility between the 403CC and chicken isolate groups ($P= 0.4681$, figure 3.4B, unpaired t-test).

The same 403CC strains used in the Morley thesis (2014) were used in this thesis. There was significant variation in observed motility between the motility assays reported by Morley (2014) that had results ranging from 3-30 mm (mean 14.79 mm) and the assays this thesis with 403CC results ranging from 8-59 mm (mean 33.44 mm). There are several variations in the experimental design between the Morley (2014) assay and the assay described in this thesis (section 2.1.4) that may explain the observed pattern of difference in motility scores. The Morley (2014) assay standardised to an OD_{600nm} of 0.1 with a stab inoculum of 2 μ l, compared with an OD_{600nm} of only 0.05 but increased stab inoculum volume of 10 μ l in the current study, which may account for the increased observed “halo” diameter. The media used was consistent across assays (MHB) but was supplemented with different concentrations of agar (0.4% w/v in Morley (2014) vs 0.6% w/v in this thesis) and strains may be differentially adapted to motility at different viscosities. Finally, the incubation temperature was 42°C in the Morley study and 37°C in the current study. There is evidence to suggest that some strains are more motile at 42°C (Aroori, Cogan and Humphrey 2013) however this phenomenon was only observed with strain PS484 (original mean motility 15 mm vs observed 11 mm mean motility) in the current thesis.

Among the chicken isolates, RM1221 has previously be reported as motile with a mean motility of approximately 43 mm (Sorensen *et al* 2015). In the current study, the motility of strain RM1221 was found to be 53.25 mm, however this was 48 h post incubation whereas the Sorensen study only reported 24 h data that may explain the discrepancy.

Motility is an important factor in the colonisation of hosts and there have been studies on how this relates to the colonisation of the chicken gut. A knockout gene experiment showed that flagellar component gene *flaA* was essential for the colonisation of chickens (Jones *et al* 2004). The same study also showed that knockout of motility accessory factor 5 gene (*maf5*) impaired colonisation. Mutation experiments have also shown that although *flaA* is essential for colonisation, full motility is not achieved when *flaB* is knocked out and this may in turn affect colonisation (Neal-McKinney, Christensen & Konkel 2010).

3.3.4 Chemotaxis

In the chemotaxis assays (Section 3.2.4) there was a linear correlation between increasing fucose concentration from 10 mM to 50 mM to 100 mM and the cfu/ml of viable bacteria recovered from the fucose hard agar plugs. This showed that the assay was working as expected, but there was no statistically significant difference in observed chemotaxis between the 403CC and chicken groups at any of the aforementioned concentrations. Fucosylated glycoproteins of the intestinal mucin are a major chemoattractant of *C. jejuni* that many *C. jejuni* strains can utilise as a substrate for growth, providing them with a competitive advantage (Stahl *et al* 2011). The chemotactic response and subsequent uptake of fucose by *C. jejuni* is mediated by the *fuc* locus that is present in approximately 68% of *C. jejuni* isolates (Dwivedi *et al* 2016). The study also found that the *fuc* locus seemed to be associated with MLST clonal complexes where the majority of strains within a CC group would either be *fuc*⁺ or *fuc*⁻. One example of this in relation to the strains used in this thesis is that RM1221 was observed in the Dwivedi *et al* (2016) study as being *fuc*⁺ as were the majority of strains within the 354CC it belongs to, which may include B1/41 used in this thesis. Of the genes within the *fuc* locus putative gene *cj0485* was found to be of particular importance to chemotaxis and mutant strains with knockouts of this gene were not chemoattracted to fucose. The putative gene *cj0485* was more recently categorised as a fucose dehydrogenase with the nomenclature *fucX* (Garber *et al* 2020).

Although there is little existing data on fucose HAP assays associated with *C. jejuni*, the paper from which the HAP assay method was adapted did perform a HAP fucose assay on strain NCTC11168 and recovered a cfu/ml in the order of 7.47×10^{10} at 100 mM fucose concentration (Elgamoudi *et al* 2018). This is several magnitudes higher than the 10^8 - 10^9 cfu/ml observed in this thesis. These differences may be due to the strain being used. As a type strain, NCTC11168 is routinely cultured and may be better adapted to lab testing, while other strains more recently isolated from hosts may be less viable under laboratory conditions. Another explanation may be in the original protocol where the semi-solid motility agar was added to the bacterial suspension the OD was checked again and adjusted to OD_{600nm} of 0.5-0.6 however this step was not included in the current study, which may have resulted in the use of cultures at slightly lower OD, although a 1:1 dilution was used with an OD_{600nm} 1.0 starter culture used.

A recent paper suggested that HAP assays may have disadvantages in measuring chemotaxis, specifically in relation to *Campylobacter spp.* (Elgamoudi & Korolik 2022). It is suggested that there are more accurate assays for determining level of chemotactic responses such as nutrient-depletion and μ -slide assays, which could be used in further work to confirm or more accurately determine the results of this thesis.

As motility and chemotaxis are intertwined it is worth comparing these results to the motility results as discussed in section 3.3.3. Of the strains that produced the highest chemotaxis viable counts at 100 mM (in the order of 10^9) these were isolates that scored highly or moderately in the motility assay, PS857 (high motility) and PS623 (moderate motility) from the 403CC group and RM1221 (high motility) from the chicken isolate group. The lowest performing strains chemotactically were PS444 (high motility) and B1/41 (low motility) and given the relatively close cfu/ml obtained across all strains there was no definitive pattern in regard to a link between observed motility and chemotactic performance. Although the motility and chemotactic systems work in unison to move away from chemorepellents and/or towards chemoattractants, a review looking at motility and chemotaxis in bacterial physiology recognised an “intricate interplay” and the trade-off between growth and motility. This is due to the energy demand of motility accounting for several percent of the energy budget as observed in the model organism *E. coli* (Colin *et al* 2021).

3.3.5 Vitamin B5 Synthesis

There was no statistically significant difference in growth between the 403CC and chicken isolates over 72 h in different media conditions or comparing the same isolate in media with or without B5. (Section 3.2.5, Figures 3.6A and 3.6B, two-way ANOVA with Tukey's multiple comparisons). There was also no statistically significant difference between the 403CC and chicken isolate groups, when comparing growth change between B5 depleted and B5 enriched media (figure 2.6, $P= 0.3686$, unpaired t-test).

The study that this assay was adapted from reported data after 18 h incubation, for a selection of cattle and chicken isolates (Sheppard *et al* 2013). The OD values reported in this thesis are lower than those obtained in the Sheppard (2013) study. For example, chicken isolates in the Sheppard study grew to an OD of approximately 0.45 in B5+ media, compared to a mean of 0.171 in this thesis. Despite this, in B5- media similar levels of growth were seen in the two studies (0.12 vs 0.155).

The 403CC strains that could be considered "cattle strains" for the purposes of this comparison performed much worse in this thesis (mean 0.10) than the cattle group in the Sheppard study (OD 0.38-0.44). This is not surprising because although 403CC isolates are similar to the cattle isolate generalists they are atypical for the group, lacking the *panBCD* genes required for B5 synthesis (found in only one out of 14 403CC genomes, section 2.3.7).

Differences in growth observed between the Sheppard study and this thesis may also be due to the differences in strain preparation. The Sheppard study used overnight cultures in broth as the inoculum whereas the current study used 48 h on agar plates. The Sheppard study also used a 42°C incubation compared to 37°C in this thesis and as was seen in the temperature growth curves of section 3.2.1 (figures 3.1A) a 42°C incubation provides a significant boost to chicken isolate growth in the early stages (6-9 h). Interestingly the Sheppard study concluded that pantothenate (B5) synthesis may be involved in inter-host niche adaptation for rapid host switching from cattle to chickens, and the absence of *pan* genes in the 403CC may be a clue to their distinctive niche restrictive profile.

A more recent genome wide association study (GWAS) found that the vitamin B5 synthesis pathway was a marker associated with lineages that are known to cause disease in humans and may play an important role in infection that has yet to be elucidated (Buchanan *et al* 2017).

3.3.6 Oxidative stress survival

OD readings rose across both groups over time under atmospheric and microaerobic conditions (Section 3.2.6, Figure 3.7 panels A-B), suggesting that *C. jejuni* was capable of growing even in the presence of 20% oxygen. However, luminescence that relates to ATP and thus cell viability dropped over time under atmospheric oxygen levels for both 403CC and chicken isolate groups (Figure 3.7 panels C-D). No statistically significant differences were found between the 403CC and chicken isolate groups under either microaerobic or atmospheric conditions with either the growth (OD) or viability (luminescence) assays. The Bac-Titer cell viability assay was used to distinguish between turbidity and actual bacterial survival and suggested that despite the rising OD, there were fewer viable cells after exposure to atmospheric oxygen. The study that the methodology was adapted from measured ATP differently but also found ATP concentration fell under atmospheric oxygen conditions (Oh, McMullen and Jeon 2015). The fact that the OD and BacTiter results do not correlate may be due to cells growing and then subsequently dying due to the oxidative stress. This would mean that they would still contribute to the number of cells in the culture and the turbidity as reflected in the OD readings but as they are no longer producing ATP would not be reflected in the BacTiter luminescence readings.

More recent work examining the oxidative stress response of *C. jejuni* focuses on two MarR-type transcriptional regulators, *rrpA* and *rrpB*. Although *rrpA* is conserved and present in 99% of *C. jejuni* isolates, *rrpB* seems to be confined to specific MLST clonal complexes. It was suggested that adaption within different hosts and niches linked *rrpB* to specific MLST clonal complexes (Gundogdu *et al* 2016). This was further elaborated on by Ugarte-Ruiz *et al* (2018) who reported that the genotype *rrpA*⁺ *rrpB*⁻ increased resistance to oxidative stress.

In relation to *C. jejuni* in the food chain as a major foodborne pathogen there is also emerging evidence to suggest that oxidative stress related genes may be involved in the cold shock response as *C. jejuni* does not have genes encoding for cold shock proteins. Hyper aerotolerant and aerotolerant *C. jejuni* strains were found to be more resistant to the effects of refrigeration and the freeze thaw process and this is thought to be due to an increase in superoxide dismutase (SOD) activity, particularly the involvement of the *sodB* gene (Oh *et al* 2019).

3.3.7 Genomic analysis

In this thesis it was decided to compare 403CC genomes to those of ST21/45 under the rationale that they would share predominantly the same core genome as generalists, except perhaps for genes relating to the colonisation of chickens. As previously indicated the presence/absence list can be found in the appendix. The focus of the analysis was known genes that have been linked to phenotypic performance, more specifically the phenotypic assays performed in this chapter. It is important to note although all the genomes of the 403CC isolates used in the phenotypic assays are part of the 403CC isolate group the comparison genomically is against ST21/ST45 genomes which only represents one of the three chicken strains used phenotypically (C2/3 from ST45). It can also be summarised from the phenotypic data that any genes of the 403CC group that have been found to be present or absent did not confer any significant advantage or disadvantage specifically as it relates to observed *in-vitro* phenotypic performance in comparison to the chicken isolates used in those assays.

Biofilm formation as previously highlighted does not have a large established research base in *C. jejuni*. However existing literature that combined phenotypic testing as part of a GWAS found a number of genes that were significantly associated with observed biofilm formation ability (Pascoe *et al* 2015). 11 of these genes were present in all genomes within the dataset, two genes, *tal* and *bioC* were not. *Tal* that was only present in 1/14 403CC genomes and 116/121 generalists was proposed by the author to have a role in chemotaxis. *bioC* was found in 0/14 403CC genomes and 77/121 generalists, it functions as part of biotin synthesis however there is no definitive work that correlates this pathway and biofilm formation.

Motility genes were largely conserved in both genome groups, 19 well characterised flagella genes from the groups *fli* and *flg* were present in all genomes, groups that are usually conserved (Lertsethtakarn *et al* 2011). However, *flaA* and *flaB* whilst present in all 403CC genomes were only present in 51% and 32% of the generalist genomes respectively. Although *flaA/B* are perhaps the most recognisable of the flagella genes their presence as it relates to motile ability is not concrete. For example, a study found deletion of *flaB* can result in inconsistent motility phenotypes, however normal motility, intermediate motility and low motility were all observed (de Vries *et al* 2015).

Chemotaxis genes, specifically those of the Che family were also present in all genomes. There were however three genes identified that were not fully present in either genome group; *mcpB* (1/14 and 65/121), *pctC* (5/14 and 2/121) and *trg* (6/14 and 20/121). These genes either had low or mid-level presence in both the 403 and generalist genome sets. A review by Matilla & Krell (2018) looked at chemotactic properties of bacterium and their effect on host infection and pathogenicity. The three genes above are all chemoreceptors that have been studied in other organisms. *mcpB* is a binding receptor for CheB2 as studied in *P. aeruginosa*, mutants of *mcpB* displayed decreased virulence in mouse lung models (Garvis *et al* 2009). *pctC* also studied in *P. aeruginosa* is part of a trio of genes *pctA/B/C*, mutants displayed reduced cell immobilisation (Schwarzer, Fischer & Machen 2016). *trg* was studied in *Salmonella enterica* sv. Typhimurium where mutants displayed reduced fitness in a mouse colitis model (Zhang & Forbes 2015). The roles of these genes in *C. jejuni* has yet to be elucidated.

The pantothenic acid (Vit. B5) synthesis genes *panB/panC/panD* that were only present in 1 of 14 403CC genomes as previously mentioned were the foundation of the vitamin B5 synthesis phenotypic assays (discussed in section 3.3.5). From the genomic perspective it was unexpected to find such absence of these genes as 403CC is a cattle associated clonal complex and the *pan* genes are part of the “cattle associated region of the *C. jejuni* genome” (Sheppard *et al* 2013). As discussed in section 3.3.5 this may affect the ability of 403CC in host switching.

Oxidative stress genes that have previously been described *sodB* and *katA* (Flint *et al* 2014) were present in all isolate genomes. There were further genes identified that were also present in all genomes; *tpx*, *bcp*, *luxS*, *msrA* and *msrB*. *tpx* and *bcp* work in tandem,

by scavenging and reducing hydrogen peroxide, double mutants of both genes also increase sensitivity to superoxides (Atack *et al* 2008). *luxS* mutation was found to have no increase in OS susceptibility in *C. jejuni* NCTC 11168 but was found that it does confer resistance to hydrogen peroxide and organic peroxides in *C. jejuni* 81176 (He *et al* 2008). *msrA/B* were characterised by Atack & Kelly (2008). Their function is to repair oxidised methionine and mutants of *msr* lead to increased susceptibility to hydrogen peroxide, superoxides, and organic peroxides.

Two genes were also identified that may relate to the lack of chicken colonisation ability of strains of the 403CC. *fabG* was absent in all 403CC genomes but was present in 53/121 of the generalist genomes. Proteomic study by Asakura *et al* 2016 looked at fatty acid production and the relationship to adaptation to chicken colonisation. FabG which was involved in fatty acid biosynthesis showed increased expression during both early and late stages of chicken colonisation. *fabG* deletion resulted in reduced unsaturated fatty acid production and reduced chicken colonisation compared to the wild-type strain. A potential chicken colonisation factor being completely absent in the 403CC genome group is potentially a very interesting discovery. It should be noted that *fabG* was only present in 44% of the generalist genomes. One explanation may be that *fabG* is a host specificity factor, gene loss and gain events are not uncommon in a highly recombinant species such as *C. jejuni* and therefore it is entirely possible accessory genes would not be retained across a whole isolate group. There also should be some consideration that there were only 14 403CC genomes compared to 121 generalist genomes, more 403CC genomes should be included in future work to test if this pattern of absence holds true.

The 403CC exclusive restriction modification system *hhaIM* was already discovered in a PhD thesis (Morley 2014) and thus the finding of this was purely confirmatory. But the exclusivity of *hhaIM* to the 403CC held up to a different data set than previously used in the form of the ST21/ST45 genomes used in this thesis. *HhaIM* was the basis of a subsequent paper (Morley *et al* 2015). The paper demonstrated that strains of the 403CC had multiple R-M systems and combined with phylogenetic modelling that showed tight clustering of 403CC isolates, it was concluded that recombination of 403CC was predominantly intralinear with little exchange outside of the clonal complex. This is perhaps the most compelling evidence of why 403CC isolates that were never adapted to colonise avian hosts as a niche have not made the species jump.

There is some suggestion that generalists may acquire the necessary genes to colonise a new niche from a specialist lineage. Successful generalists like ST21 and ST45 readily recombine with specialist lineages across host lines but not with each other, leading to a puzzle of a “cryptic niche structure” (Sheppard *et al* 2014).

In this thesis it was decided to compare 403CC genomes to those of ST21/45 under the rationale that they would share predominantly the same core genome as generalists, except perhaps for genes relating to the colonisation of chickens. Whilst the logic in this is sound, as previously noted the limited recombination of 403CC isolates due to the R-M systems may make this less accurate than originally anticipated. Further work that could be done in this area is to take a data set of chicken specialist lineage genomes and approach the comparison from a different perspective. Future work should also include more than 14 403CC genomes to ensure that any findings, such as the absence of *fabG* in the dataset applies to the greater clonal complex population.

3.3.8 Conclusions and Recommendations

C. jejuni is a multi-species host pathogen that despite its fastidious growth and microaerophilic lifestyle is present in many organisms within the human food chain and surrounding environment. Grouping *C. jejuni* lineages by MLST clonal complex reveals that whilst some *C. jejuni* complexes use host generalisation as a means by which to persist, others specialise to specific host species niches. The niche adaptive properties between those that can and those that cannot colonise and persist in a specific niche may reveal an insight into how *C. jejuni* remains a successful food/waterborne pathogen. The 403 clonal complex represents a group of isolates that belong to a generalist lineage that are atypical in that they show incredibly low ability to colonise the chicken niche, one of the main sources of *C. jejuni* transmission. In this chapter isolates of the 403CC were comparatively tested against known chicken isolates across a range of phenotypic assays that represent *in-vivo* niche conditions or *ex-vivo* stressors. The genomes of 403CC isolates and the largest generalist groups ST21/ST45 were also compared to look for the presence/absence of genes that may relate to niche adaptation.

The majority of the body of this chapter considered whether there were sufficient phenotypic differences between 403CC and chicken isolates to explain the observed pattern of differing niche transmission/colonisation between the two groups of strains. In this thesis a pattern has emerged that 403CC isolates on the whole behave phenotypically comparably to chicken isolate strains across a range of phenotypic assays. The exception to this is the finding that chicken isolates grew significantly faster in the early stages of growth at 42°C (section 3.2.1, fig 3.1B). This is the only phenotypic indicator that may infer a competitive niche colonising advantage of the chicken isolates over the 403CC strains. Aside from this finding the remaining work is in line with previously reported work (Morley 2014) that also concluded that 403CC isolates behaved similarly to “typical *C. jejuni* isolates” in stress and virulence tests.

Through genome analysis of 403CC isolates many key genes as they relate to the tested phenotypic properties are consistent with ST21/45 generalist genomes. These generalist lineages were chosen as they are the largest groups and have a close colonisation profile with a multi host species spread, albeit with the colonisation of chickens separating them from the 403CC group. Table 3.1. illustrates genes that were found to differ largely in presence absence between the two groups. Two biofilm genes *tal* and *bioC* showed no/low presence in the 403CC genome group. Any potential effect this would have is interesting however speculative as it relates to the phenotypic testing. Firstly, there were only two instances out of 12 where the chicken isolates as a group produced significantly higher biofilm. Secondly, the presence of such genes is not confirmed in the chicken isolates as the genomic comparison is against the generalist group. Similarly, with the *pan* genes involved in vitamin B5 synthesis, the 403CC isolates did not perform significantly worse than the chicken isolate group although they lack the requisite genes for self-synthesis. This perhaps would be where the genome analysis model is not ideal because it is entirely plausible that the chicken isolates, two of which are from a specialist lineage, would not have the *pan* genes either. As mentioned previously *pan* genes are from cattle associated region (Sheppard 2013) and may not be conserved in poultry as the host species is usually supplemented with this. From this it can be concluded that the “typical” performance of 403CC isolates is matched both in observed phenotypic ability and genome content. However, the two exceptions, related to biofilm formation and B5 synthesis, are areas of the *C. jejuni* research space that are yet to be fully elucidated.

Two other genes of relevance *hha1m* and *fabG* are prospective leads into the puzzling colonisation pattern of the 403CC. R-M systems and a diminished capacity to be recombinant outside of the lineage could be a significant stumbling block in acquisition of potential colonisation factors that may be specific to a certain host species. *fabG* which was previously mentioned as part of the fatty acid synthesis pathway also is very interesting, it may potentially be a factor in early and late stage chicken colonisation. Further to that it also challenges the perception of what may be considered relevant when looking at colonisation factors, which traditionally skews towards phenotypic properties such as motility, chemotaxis and adhesins.

The main limitation of the chapter is the sample size. As reported in section 2.1 there were six chicken isolates intended for use in the thesis but three of these were unrecoverable over several culturing attempts from -80°C stocks. For future work ideally a larger number of strains from both groups would be used to help bolster any potential findings. A secondary further suggestion for expansion of work in this area would be competition assays. Co-culturing 403CC with chicken isolates would be useful to see if one group of strains could outcompete the other. Not only would this be a more realistic test of what 403CC isolates would potentially face in an actual chicken niche, but the finding of the rapid early growth of chicken isolates at 42°C as aforementioned indicates a potential scenario in which out-competition could be more likely, thus warranting further investigation. The genomic comparison of the 403CC isolates against host generalists ST21/45 also is a strong indicator of the direction potential research into this extremely unique clonal complex could go. The *hha1m* R-M system, and the part it plays in what has been observed as a predominantly intralinear recombination pattern within the tightly clustered 403CC strains is the most promising lead on the abnormality of what should be a well-rounded host generalist complex. A different genomic analysis of 403CC isolates against known chicken isolates, ideally specialist CC's such as ST354, ST573 or ST464, would supplement the genome analysis in this thesis from a different perspective. Not only would it be useful for a more direct inference of potential genes that relate to phenotypic testing, but it would be interesting to see if for example with *fabG* the putative chicken colonisation factor would be present in such a genome group.

Given the magnitude of *C. jejuni* in relation to the human impact worldwide as the leading causative agent of food poisoning, studies that investigate how zoonotic transmission and environmental survival are paramount in our ability to minimise the introduction of *C. jejuni* into the food chain. The 403 clonal complex and the near inability it has to colonise chickens is an anomaly in nature. It is a truly puzzling discovery that amongst a pathogen that not only successfully colonises many species, but is most commonly isolated from chickens, which the 403CC faces some barrier to chicken colonisation and/or persistence that other lineages do not. It could be theorised from the work in this chapter that the most solid prospect for understanding this clonal complex lies in gene gain/loss events that may be host species specific colonisation factors. Necessary gene gain events that are hampered by 403CC specific R-M systems may be barring this specific lineage from what should be one of its main hosts. It may be, that in the greater context of the field of *C. jejuni* research as a whole, that the “403CC anomaly” may be a piece of the puzzle in understanding why generally *C. jejuni* associates so strongly to chicken hosts.

The next chapter will look at the niche adaptive properties of *H. pylori* strains, and how intra- rather than inter- host adaptation may be present within this species.

Chapter Four: Phenotypic and genomic comparisons within *Helicobacter pylori*

4.1 Introduction

The antrum and corpus of the human stomach may be considered as distinct intra host niches. The topographical structure of cells in each region is distinctly different as shown in chapter one (figure 1.4). Further to this, corpus predominant neutrophil/lymphocyte activity is more strongly associated with gastric cancer whereas antrum predominant gastritis is more common in low gastric cancer rate countries (Miftahussurur *et al* 2019). Acidity also shows variation between the antrum and corpus as the parietal cells that secrete acid are found in the corpus a lower pH is generally maintained. There is also evidence to suggest that these distinct niches affect *H. pylori* evolution based on niche site specific isolates from a single ancestral strain possessing varying antibiotic susceptibility profiles (Selgrad *et al* 2014).

Four sets of antrum/corpus paired *H. pylori* isolates were chosen to investigate potential differences between colonisation site of strain and observed phenotypic ability. It was hypothesised that differences in the intra-gastric niche (antrum vs corpus) may have caused divergence and microevolution from a common ancestral strain and that strains isolated from these distinctly different niches may display differing phenotypic properties. Phenotypic assays were chosen to reflect a general overall view of phenotypic properties of *H. pylori* including potential colonisation barriers when adapting to intra-gastric niches.

4.1.1 Growth

Given that conditions between the antrum and corpus are variable it is not unreasonable to suggest that this may have impacted the rate at which *H. pylori* isolates grow. There is limited scientific data on antrum-corporis paired isolates and most research into *H. pylori* growth is targeted towards developing novel inhibitory agents.

Despite this there is evidence that *H. pylori* uses chemotaxis, specifically TlpD for colonisation in the corpus but it has no effect on growth. In the antrum TlpD is not required for localisation but is required for proliferation, showing growth factors may be variable between the two distinct niche areas (Rolig *et al* 2012). Therefore, standard growth curves will compare the growth rate of the antrum and corpus isolates.

4.1.2 Motility

Motility has been shown to be a key colonisation factor in establishing and maintaining a robust *H. pylori* infection in the gastric environment (Ottemann and Lowenthal 2002). The helical shape of *H. pylori* is advantageous for “corkscrewing” through the viscoelastic gastric mucosa to persist in the gastric niche. Numerous animal studies have demonstrated that motility impaired mutants display reduced colonisation and persistence rates indicating the importance of motility in *H. pylori* infection (Osaki *et al* 2006, Nakajima *et al* 2008). It has also been suggested that the urease activity of *H. pylori* raising pH modifies the viscoelasticity properties of gastric mucosa from a viscoelastic mucosal gel to a viscous liquid, permitting motility (Bansil *et al* 2013). As gastric pH may vary between the two niches of antrum and corpus strains isolated from these regions may be differently adapted to motility therefore it is motility will be compared between the antrum and corpus strain groups.

4.1.3 Oxidative stress

As part of the immune mounted response to *H. pylori* infection, reactive oxygen species (ROS) are produced that are toxic to *H. pylori*. As a microaerophilic bacterium *H. pylori* is also more sensitive to environmental oxygen levels. To counteract oxidative stress *H. pylori* employs enzymes such as KatA, SodB and AhpC in the detoxification of superoxides, hydrogen peroxides and peroxides respectively (Flint, Stintzi and Saraiva 2016). As *H. pylori* persists chronically in the gastric niche, continuous exposure to oxidative stress may represent a selective pressure (Ailloud *et al* 2019) that may show variance in oxidative stress defence across antrum and corpus isolates. Therefore, the oxygen survival capabilities of the antrum and corpus groups will be compared.

4.1.4 Menadione resistance

Menadione is an organic compound that displays oxidant activity by generating reactive oxygen species via redox cycling. Metabolism of menadione by one- electron reducing enzymes generates an unstable semiquinone radical that is then reduced to a hydroquinone. In the presence of molecular oxygen backoxidation generates superoxides. Note that the one step redox involving a two-electron reducing enzyme does not generate ROS (Criddle *et al* 2006) (figure 4.1).

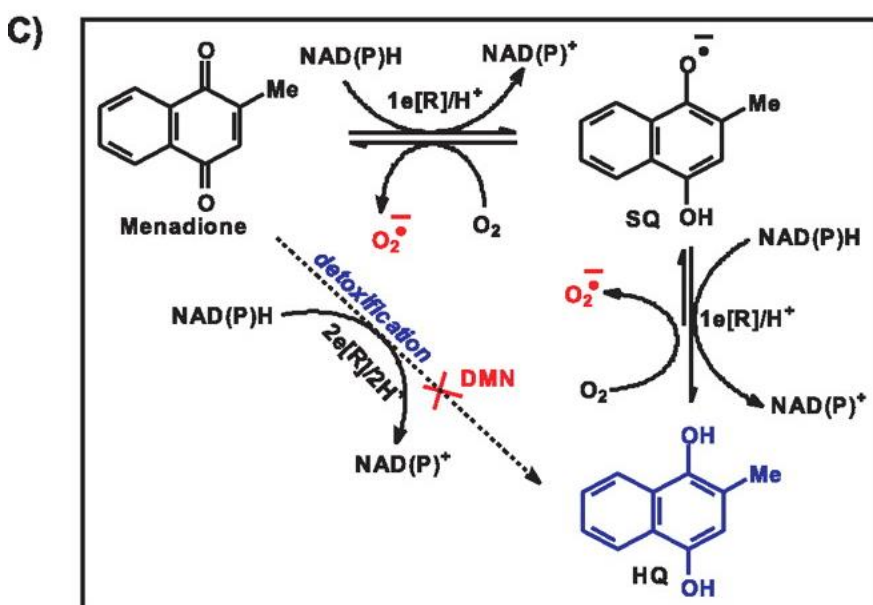


Figure 4.1 adapted from Criddle *et al* 2006 showing the proposed mechanism of reduction of menadione by one-electron and two-electron reducing enzymes and how this may lead to the production of ROS by redox cycling. Figure reproduced under open access creative commons usage.

Menadione has previously been investigated for its anti-bacterial properties on Gram-positive bacteria such as *Staphylococcus aureus*, *Bacillus anthracis* and *Streptococcus spp.* (Schlievert *et al* 2013). Menadione was previously observed as having potential inhibitory effects against *H. pylori* (Park *et al* 2006) and this evidence was bolstered by a 2019 study that demonstrated the anti-bacterial and anti-inflammatory effects of menadione against *H. pylori* (Lee *et al* 2019). Given that menadione can be used to replicate a niche stressor *in-vitro* and its potential anti-bacterial properties, resistance to menadione was tested. This assay is an exception to the grouped analysis of other phenotypic assays, as it was originally a precursor test for potential directed evolution work and became the focus of RNA-Sequencing work (chapter five).

4.1.5 Biofilm formation

One of the less elucidated mechanisms of *H. pylori* pathogenicity is the ability to form monospecies biofilms. A recent review article stated that whilst studies pertaining to biofilm formation of *H. pylori* are on the rise much is unknown about the mechanisms surrounding it (Hathroubi *et al* 2018). *H. pylori* biofilms have been demonstrated to occur *in-vitro* at the air-liquid surface interface or pellicle (Cole *et al* 2004, Yonezawa *et al* 2010). *H. pylori* biofilm formation has also been demonstrated *in-vivo* in mice models (Attaran, Falsafi and Moghaddam 2016) as well as in humans from endoscope gastric mucosal biopsy, where biofilm formation was strongly associated with specimen urease presence (Coticchia *et al* 2006). Biofilm formation by *H. pylori* can be incredibly problematic in eradication therapy as *H. pylori* have been shown to show increased resistance to first line eradication therapy drugs, amoxicillin, clarithromycin and metronidazole when in biofilm compared to in a planktonic state (Yonezawa *et al* 2019). One major factor between antrum/corpus niche conditions is pH. As detailed in section 1.2.2, figure 1.5 the acid secretory parietal cells are located in the corpus and therefore pH levels generally remain more acidic than the antrum. Biofilm formation is partially modulated by pH in *H. pylori*, as pH reduces so does the ability of *H. pylori* to form biofilm structures (Krzyzek *et al* 2020). Based on the fact pH levels vary by gastric niche, and existing research that pH can affect biofilm formation, it was hypothesised that antrum and corpus strains may show differing levels of biofilm formation ability.

4.1.6 Genome analysis

The first whole genome sequence of *H. pylori* was published in 1997 by Tomb *et al* using *H. pylori* strain 26695 originally isolated from a UK patient suffering from gastritis (Tomb *et al* 1997). Similarly to *C. jejuni* it was revealed that *H. pylori* had a relatively modest genome size in this instance 1,667,867 base pairs in length with a low GC content of 39% and approximately 1,590 coding sequences (CDS). The genome was noted to have robust motility systems, and a large number of sequences coding for putative adhesins as well as lipoproteins and other outer membrane proteins (OMPs) eluding to the importance of host pathogen interactions between organism and host. Like *C. jejuni* it was also noted that the *H. pylori* genome contained many homopolymeric nucleotide runs implicated in antigenic variation.

As opposed to *C. jejuni* that had many more biosynthetic pathways the *H. pylori* genome was found to have limited metabolic and biosynthetic capacity and this was thought to be due to its human niche restricted status.

The second whole genome sequence of a *H. pylori* strain, and the first comparison between two *H. pylori* genomes was published in 1999 (Alm *et al* 1999). This study sequenced *H. pylori* strain J99 and compared it to the already sequenced 26695 from the (Tomb *et al* 1997) study. This initial comparison of two *H. pylori* WGS revealed a similar organisation of gene order and predicted proteomes but with a large genomic and allelic diversity. Between 6% and 7% of gene content was specific to each strain with almost half being clustered in a single hypervariable region that suggested a very flexible and diverse accessory genome.

H. pylori is a highly genetically diverse species and this is in part due to a high mutation and recombination rate. Studies have consistently demonstrated a mutation rate in the order of 10^{-5} mutations per site per year (Ailloud *et al* 2019) though this is highly variable between strains. The recombination rate is highly variable between strain lineages and the ratio of recombination to mutation frequency can be as high as 100:1 however it was found in some individuals to be much more modest (Didelot *et al* 2013).

For the genomic analysis of this chapter the paired antrum and corpus strains will be compared. Although it will be assumed that strains will cluster by pair, having the same common ancestor, isolate genomes will be screened to look for any potential genes exclusive to, or more prevalent in the antrum or corpus group. This essentially would be gene gain or loss events that may be due to microevolution to the specific gastric niche.

4.1.7 Aims

The overriding aim of this chapter was to consider the phenotypic properties of strains isolated from the antrum and corpus of patients and to see how they may differ in observed phenotypic ability. Phenotypic assays have been chosen that may reflect niche stressors or properties of the bacterium that are essential to colonisation and persistence. In this chapter growth rate, motility, oxidative stress survival, menadione resistance, and biofilm formation were compared between the antrum and corpus strains. Antrum and corpus genomes were also obtained and heatmapped to look for potential antrum or corpus niche specific genes. The chapter concludes with considering whether across the range of phenotypic assays and genome analysis there is evidence to support the theory that paired isolates from different niches display an altered phenotypic profile or vary in genome content.

4.2 Results

A range of phenotypic assays were undertaken to compare the phenotypic ability of four sets of paired strains isolated from the respective areas (antrum and corpus) of four patients' stomachs. Results are presented for testing of growth rate, motility, oxidative stress survival, menadione resistance and biofilm formation ability. Unless otherwise stated the data presented are means calculated from triplicate data for each isolate. Results are presented with errors bars that represent the standard deviation calculated for the mean and based on the range of data collected for each strain individually.

4.2.1 Growth curves show uniform growth across all isolates

Growth curves were constructed using optical density at 600 nm readings at 24 h intervals for 72 h as described in section 2.2.2. Data shown are the triplicate means at each time point for each strain grouped into their respective groups of antrum isolates and corpus isolates. Results for each individual strain's growth are presented in figure 4.2A. Group-based summary data of growth are shown in figure 4.2B. As can be seen from both figure 4.2A and 4.2B growth rates were tightly clustered across all strains and there were no statistically significant differences between individual strains, or between the antrum and corpus groups (Two-way ANOVA).

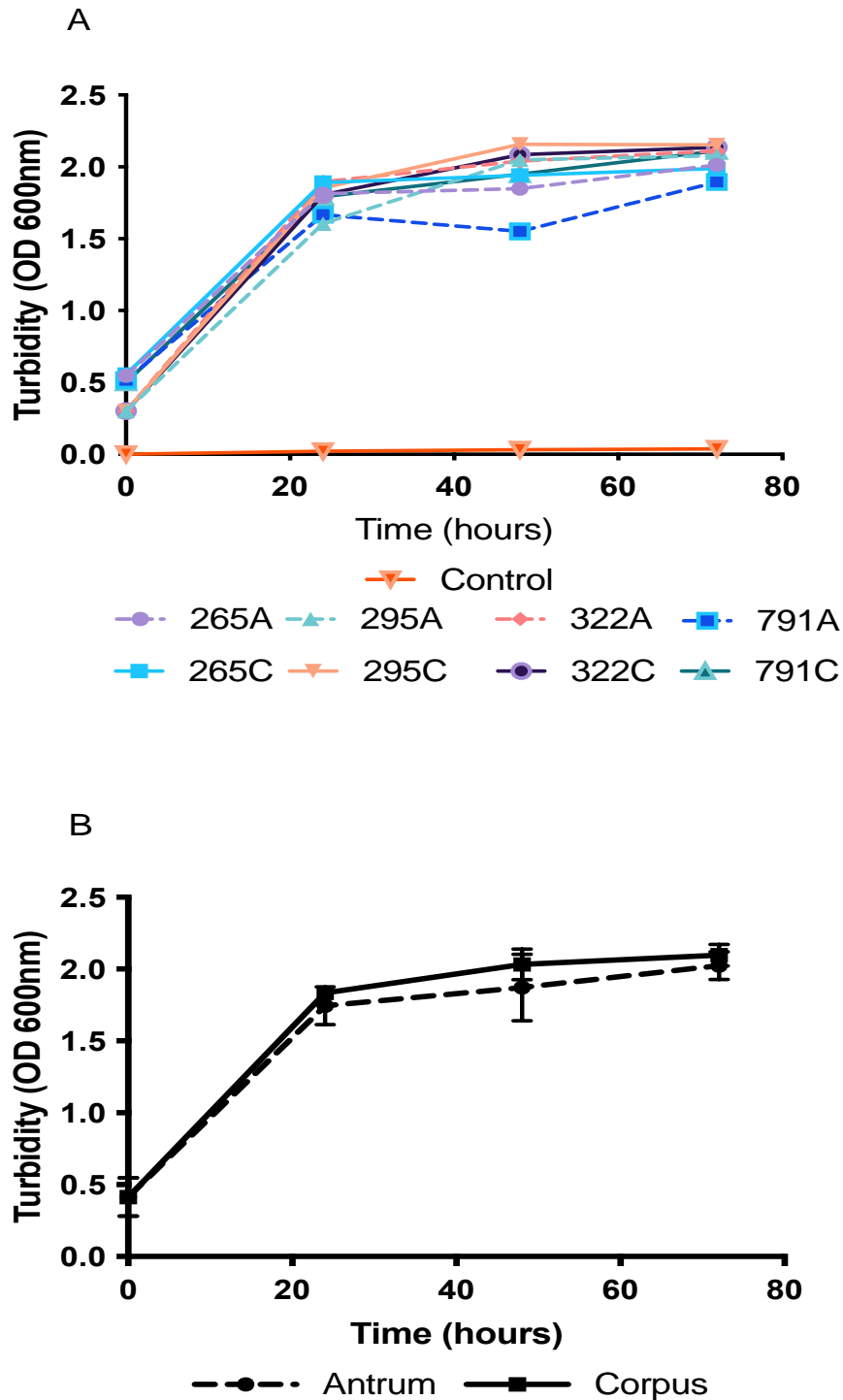


Figure 4.2 Growth curves show very similar growth across all isolates. 37°C growth curves measured at 24 h intervals at OD_{600nm}. (A) Growth curve by individual isolate where dotted lines represent antrum isolates and full lines represent corpus isolates. (B) Growth curve by group where the dotted line with circular points represents the antrum group and the full line with square points represents the corpus isolate group. Error bars are only shown unidirectionally for ease of viewing.

4.2.2 Motile ability shows considerable variation amongst strains with no leaning towards antrum or corpus isolates

Motility data was gathered by an agar stab motility assay as described in section 2.2.3. The motility of individual strains is shown in figure 4.3A and grouped results in figure 4.3B. As can be seen in figure 4.3A there was variation in motility between individual strains found to be statistically significant ($P < 0.0001$, One-way ANOVA) although both antrum and corpus groups had a mixture of more motile and less motile strains. Grouped analysis showed no overall statistically significant difference in motility between the antrum and corpus isolate groups ($P = 0.421$, figure 4.3B, unpaired t-test).

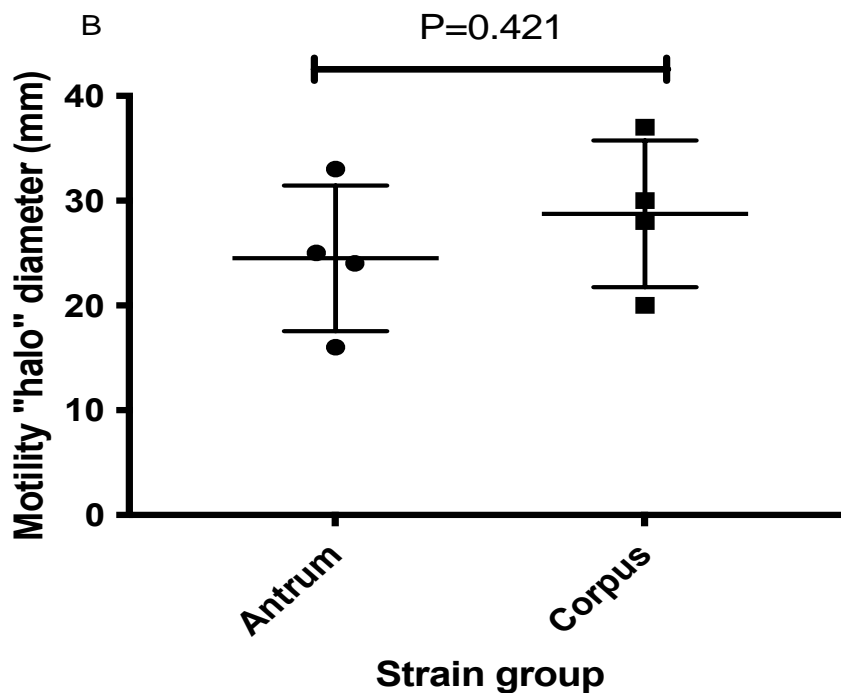
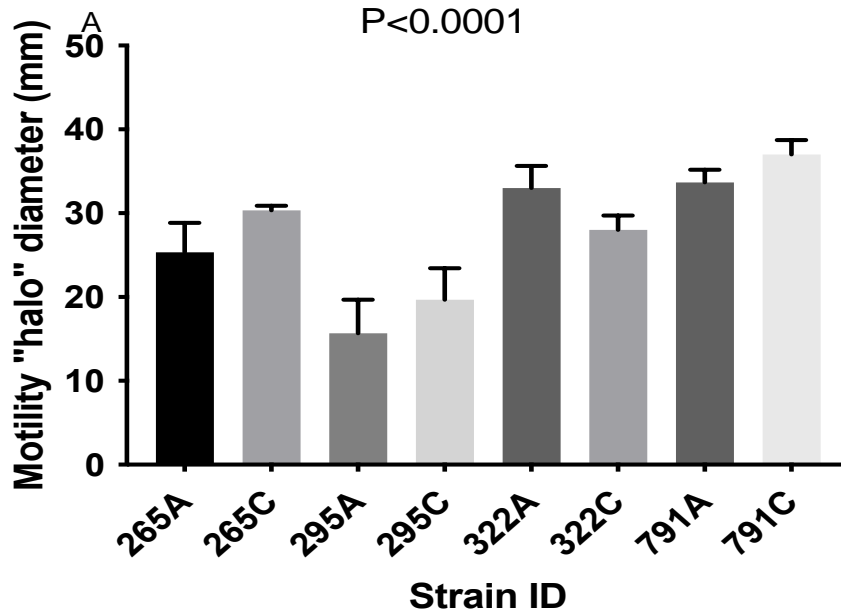


Figure 4.3 Motility varies greatly by isolates but does not cluster by group. Agar stab motility assay results showing diameter of zone of motility in millimetres. Figure 4.3A shows motility by isolate. Error bars show standard deviation from the triplicate mean recorded for each isolate. Figure 4.3B shows motility by strain group where each isolate triplicate mean is displayed as a circle for antrum isolate and square for corpus isolates. Bars show mean for the group and error bars indicate standard deviation.

4.2.3 Oxidative stress survival is not significantly different between antrum and corpus isolates

To assess each strain's ability to survive oxidative stress, bacterial growth and viability in microaerobic (5% O₂) and standard atmospheric (20% O₂) conditions were monitored over time by measuring the OD_{600nm} and BacTiter Glo luminescence (arbitrary units), respectively as described in section 2.2.4. Strains were grouped into antrum and corpus isolates. Figure 4.4 panels A-B show OD readings for the groups under both microaerobic and normal atmospheric oxygen conditions and panels C-D show the corresponding luminescence results. No statistically significant difference was found between the antrum isolate and corpus isolate groups when measuring OD (growth) in both microaerobic and atmospheric conditions (figure 4.4 panels A-B respectively, multiple t-test). No statistically significant difference was found between the groups when measuring luminescence (viability) either (figure 4.4 panels C-D, multiple t-test).

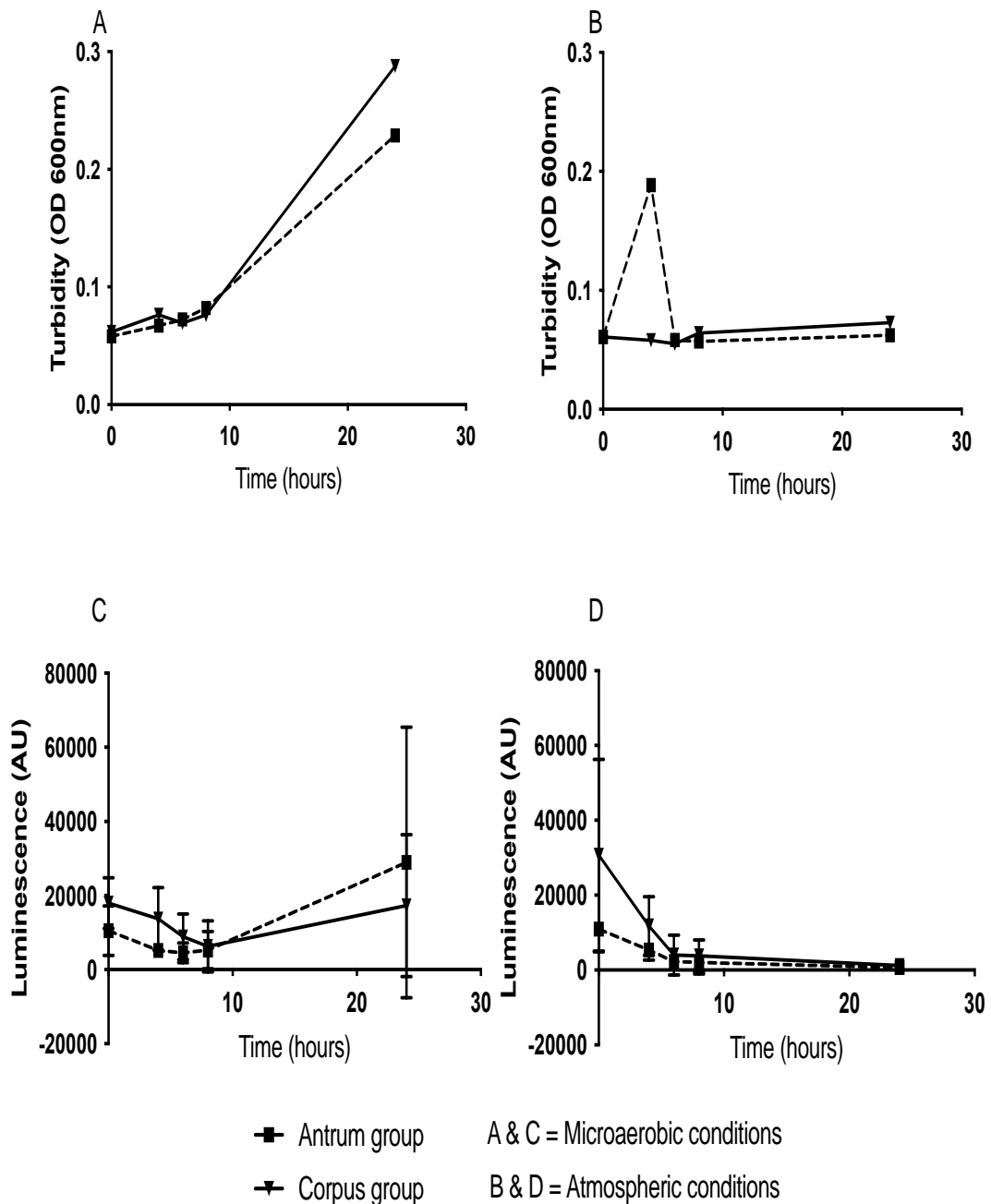


Figure 4.4 Oxidative stress survival does not significantly differ between antrum and corpus groups. Oxidative stress survival assay Figure 4.4(A-B) shows OD_{600nm} at 0, 4, 6, 8 and 24 h for antrum (square time points perforated lines) and corpus isolate groups (triangle time points full line) under microaerobic (A) and atmospheric (B) oxygen conditions. 4.4 (C-D) shows luminescence (arbitrary units) at 0, 4, 6, 8 and 24 h for antrum and corpus isolate groups under microaerobic (4.4C) and standard atmospheric oxygen (4.4D) conditions. The bars and error bars indicate the mean and SD, respectively, for each group.

4.2.4 Menadione minimum inhibitory concentration was consistent across all isolates

A 96 well plate based MIC assay was developed as described (Section 2.2.5) using serial dilution of menadione. OD_{600nm} was measured at 0, 24, 48, 72 and 96 h. Figure 4.5 shows the MIC results for each of the eight individual strains by antrum corpus pair and show a remarkably consistent MIC. At 0.3125 mM concentration the OD observed was markedly lower than the previous serial dilution and therefore this was considered the MIC. Some of the strains had an OD that was similar to the no bacterial control. Confirmatory statistical analysis was conducted and increasing menadione concentration was found to statistically significantly affect growth measured by OD_{600nm} ($P > 0.0001$, ANOVA). As mentioned in the rationale for phenotypic assays in section 4.1, there was no grouped analysis for this assay as it was intended as a preliminary starting point for directed evolution based assays. It was decided that the sub-MIC concentration of 0.15625mM would be suitable for testing and therefore was ultimately used to mimic niche stressors in the RNA-Sequencing work in the next chapter (chapter five).

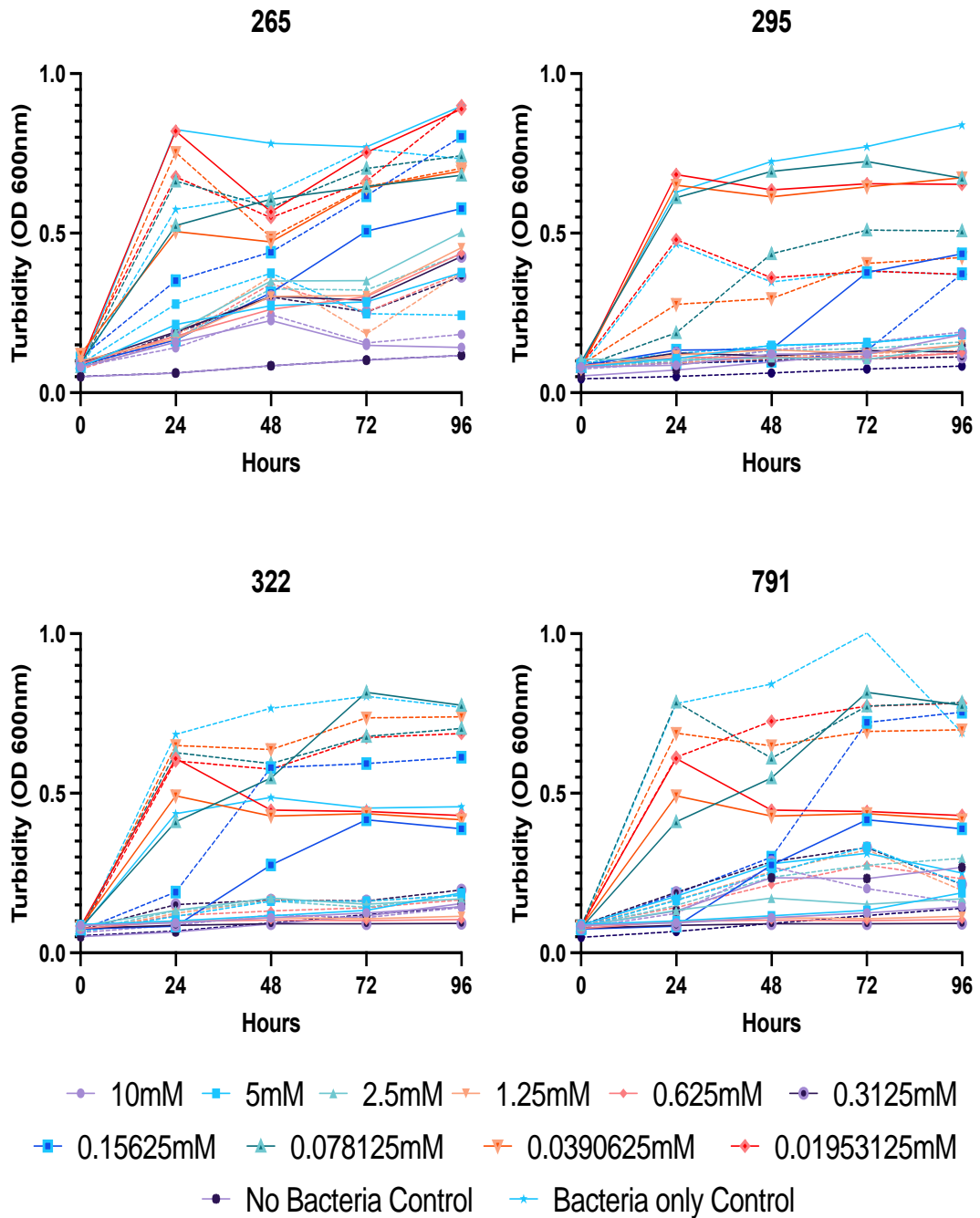


Figure 4.5 Menadione MIC was consistent across all isolates. Turbidity recorded at OD_{600nm}. Results shown by strain pair, corpus strains represented by full lines and antrum by dashed lines. Each coloured line representing a menadione serial dilution concentration, menadione only control or bacteria only control (see key).

4.2.5 Biofilm formation ability is significantly different between isolates but not by antrum corpus group

Biofilm formation ability was investigated as described in section 2.2.6. Strain 265C was not available at the time of this specific assay as during routine purity checks the stock was found to be contaminated. Therefore this assay will only reflect 7 of the 8 strains. Figure 4.6 shows the OD_{600nm} recorded following biofilm formation protocol. Individual strain biofilm formation is shown in figure 4.6A and antrum/corpus grouped results in figure 4.6B. As can be seen in figure 4.6A there is considerable variation in biofilm formation ability across all strains and this was found to be statistically significant (P=0.028, ANOVA). Grouped analysis in figure 4.6B showed that the corpus isolates were much closely clustered in biofilm formation ability, whereas the antrum group had a low biofilm (322A) and high biofilm (295A) strain. Direct comparison of the antrum and corpus groups showed no statistically significant difference (P=0.770, t-test).

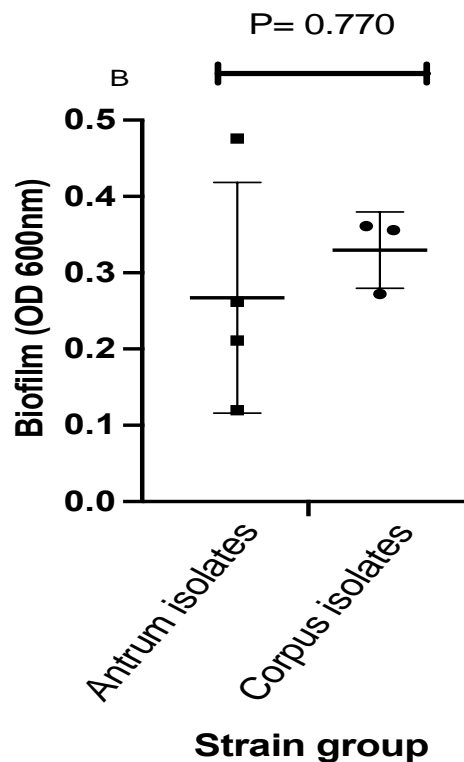
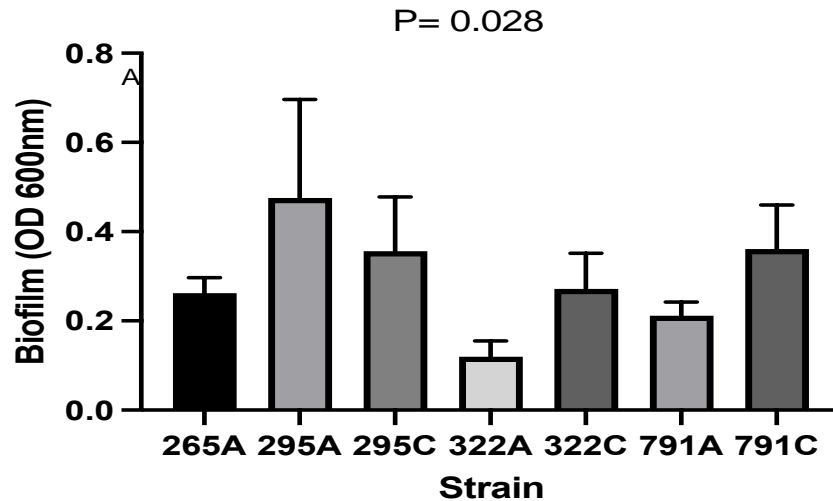


Figure 4.6 Biofilm formation shows significant isolate but not group variance, corpus isolates cluster close than those of the antrum group. Biofilm measured by OD_{600nm} . Figure 4.6A shows biofilm formation by isolate. Error bars show standard deviation from the triplicate mean recorded for each isolate. Figure 4.6B shows biofilm formation by strain group where each isolate triplicate mean is displayed as a square for antrum isolate and a circle for corpus isolates. Bars show mean for the group and error bars indicate standard deviation.

4.2.6 Genome analysis by heatmap shows paired antrum/corpus isolates differ in gene presence/absence

Genome analysis was performed as described in section 2.2.8. 861 genes are found in all samples. There are 414 genes present only in the J99 reference strain. There are 63 genes that are absent from J99 but present in all the other strains.

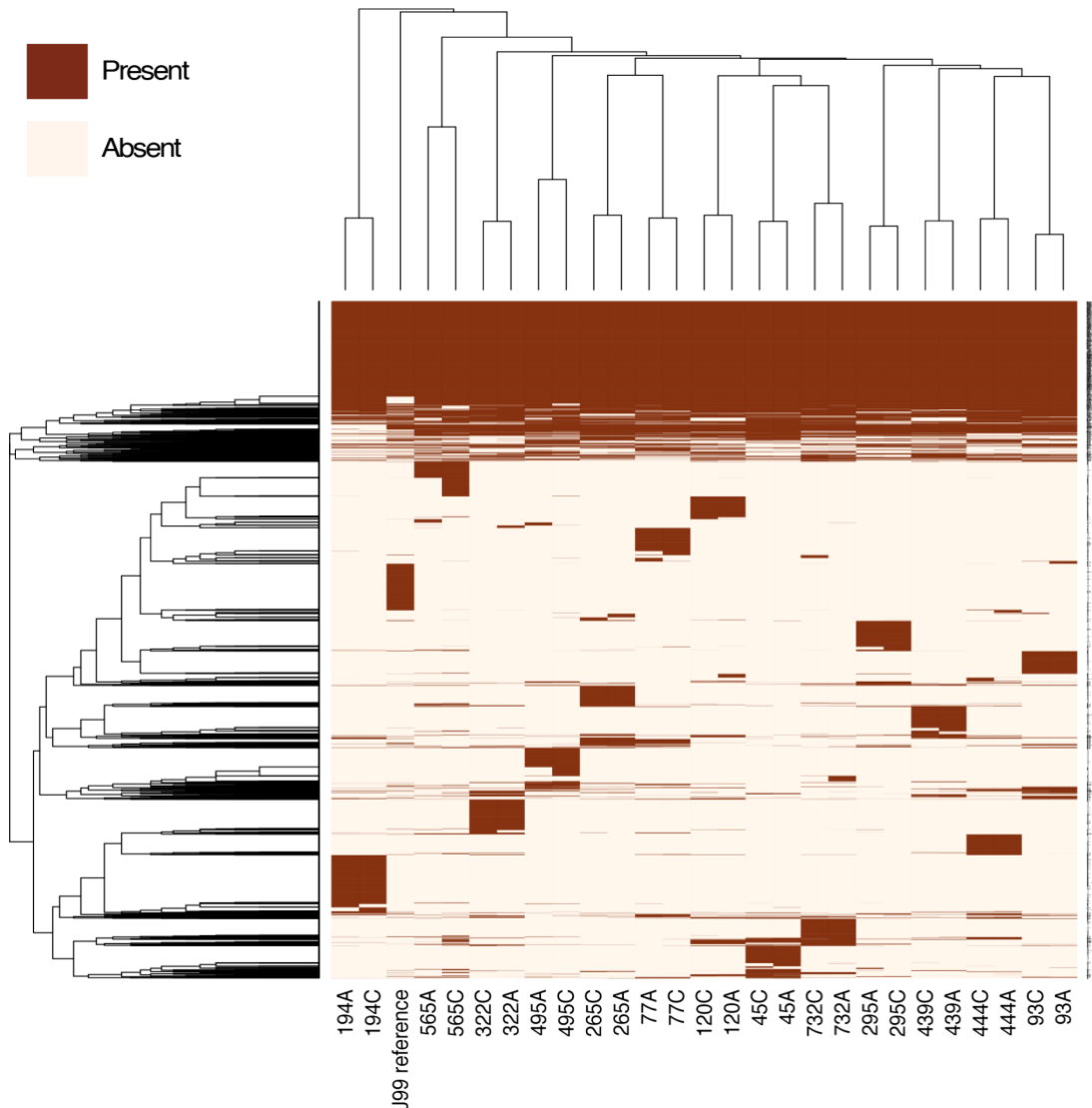


Figure 4.7 Gene presence/absence shows variance within antrum/corpus pair. Produced by Professor Lesley Hoyles. Bidirectional heatmap showing clustering of genes present and absent in *H. pylori* isolates included in this study. The heatmap was created in R using heatmap.2 and the gene data in binary format (1, present; 0, absent). *x* axis, isolate names (same numerical prefix indicates isolates are from the same patient); *y* axis, genes encoded within genomes of isolates. Gene annotations for all isolates were compared with those of the reference strain *H. pylori* J99 (J99 reference). The clustering of the gene profiles shows that corpus (C suffix) and antrum (A suffix) isolates from the same patient cluster together and are distinct from the reference strain. It is clear that there are gene differences from corpus and antrum isolates recovered from the same patient (e.g. 194A and 194C have different profiles from one another).

Even by cursory glance it can be seen that paired strains from the same patient cluster together, and analysis of these heatmaps showed no clustering based on either antrum or corpus isolates. Despite this the heatmap clearly shows very small amounts of gene variation within all antrum corpus pairs, with isolate pairs 194, 495 and 77 being easily observed.

4.3 Discussion

This chapter aimed to identify potential differences between paired antrum and corpus strains that may be a result of adaptation to different niches of the human stomach. Phenotypic assays and genome analysis were used to determine potential differences in the phenotypic profiles and genome content of antrum strains compared to corpus strains. four sets of paired antrum corpus isolates were used across all phenotypic testing. 13 sets of paired antrum corpus isolate genomes plus reference strain J99 were used in genomic comparison. Comparative work between antrum and corpus strains are largely uncharacterised in the scientific literature to date. The primary purpose of these phenotypic assays was to directly compare the growth, motility, oxidative stress resistance, menadione resistance and biofilm formation of paired antrum and corpus isolates with each other. From this work the goal was to determine whether there were any differences in phenotypic characteristics between *H. pylori* isolates taken from different regions of the same patient's stomach. No control strains were included in these assays because the most commonly used reference *H. pylori* strains are lab-adapted, so not directly comparable with clinical isolates, and among the available well-characterised clinical isolates there are no paired antrum and corpus strains, to our knowledge. However, future studies should include a reference *H. pylori* strain or well characterised isolate such as 26695 or 60190, to validate the laboratory assays as far as possible.

There is some limited evidence supporting the potential effects of microevolution of *H. pylori* strains when comparing paired antrum and corpus isolates. For example, a study looking at clarithromycin heteroresistance acknowledged the role of antrum vs corpus microevolution. In chronic infection 17.5% of patients had paired antrum corpus isolates with different levels of clarithromycin resistance (Farzi *et al* 2019).

Similar studies have also found discordance in antibiotic susceptibility between antrum and corpus paired strains in 15.2% of patients tested (Selgrad *et al* 2014).

At the genomic level it has also been reported that paired antrum corpus isolates have shown differences in the number of repeats at the 3'-end of the *cagA* gene (Carroll *et al* 2004). This is the region associated with EPIYA motifs as discussed in section 1.2.2.

4.3.1 Growth curves

Growth curves were constructed using optical density at OD_{600nm} and was shown in section 4.2.1. Results for each individual strain's growth were presented in figure 4.2A and antrum corpus group-based summary data of growth are shown in figure 4.2B. It was apparent from the growth curve construction and subsequently confirmed by statistical analysis that there was no statistically significant difference in growth between both individual strains and the comparison of the antrum and corpus groups. All of the isolates clustered extremely close together.

It is difficult to directly compare results of *H. pylori* growth to existing scientific literature. As *H. pylori* is so fastidious often supplementation of growth media can be extensive in order to reach exponential growth faster. For example, one study used thin layer liquid culture with brucella broth, 10% foetal bovine serum and 0.5% yeast extract. Serum-free RPMI-1640, dimethyl- β -cyclodextrin (200 μ g/ml) and 1% yeast extract. Generating an OD_{600nm} of 3.4 after just 28 h (Joo *et al* 2010). Comparing this to the work done in the thesis the growth curves shown in section 4.2.1 have an OD_{600nm} of approximately 1.8 at the same timepoint.

Given the clustering of all eight isolates it would be interesting to add more sets of paired strains to see if this close growth association holds true. Potentially supplementation of growth media as seen in the above study may affect how well antrum and corpus strains grow with the abundance of nutrients available to them. The alternate route is growth curves with inhibitory agents. For example, the diabetes medication Metformin has been shown to be inhibitory to *H. pylori* growth (Courtois *et al* 2018) however this steps away from the focus of this thesis that is conditions found within the niches of the stomach.

4.3.2 Motility

As seen in section 4.2.2 the agar stab motility assays demonstrated that although there was statistically significant difference between the individuals strains (Figure 4.3A, $P < 0.0001$, ANOVA), there was no statistical significance when comparing the antrum and corpus groups (Figure 4.3B, $P = 0.421$, unpaired t-test).

Both strain groups showed similar variation in motile ability between strains, with some slightly more or less motile properties than others. On the whole however the results were close enough that there were no particularly strong or weak performers within either of the groups.

H. pylori agar stabs are one way in which motility can be observed. There are three types of motility that *H. pylori* possesses; ‘swimming motility’ (movement in liquid media, ‘spreading motility’ (movement in soft agar 0.3% concentration) and ‘swarming motility’ (movement on semi-solid or solid media) (Gu 2017). Swimming velocity can be directly determined through phase-contrast microscopy, spreading motility through agar stab “halo” diameters (as used in this thesis) and swarming motility through “halo” diameters produced on the surface of agar. Testing spreading motility was the most appropriate method in the context of replicating the gastric niche. As a by-product of *H. pylori* raising localised pH using urease, the viscoelasticity of the gastric mucin that *H. pylori* colonises becomes less rigid in its ‘gel-like’ structure and allows successful motility through the mucin layer (Bansil *et al* 2013).

Work looking at creating motile mutants used type strain NCTC11637 for reference as a wild type in agar stab motility assays that produced a ‘halo’ diameter of 15 mm (Chiou *et al* 2013). This is significantly smaller than that observed by strains in this thesis (range 15-35mm). The assay in Chiou *et al* used the same agar-broth composition as in this thesis however the stab inoculate concentration or volume was not described therefore it is difficult to make direct comparison. Further to this, in this thesis stab plates were incubated for seven days compared to 72 h in the aforementioned study and this may also have impacted the observed spread.

4.3.3 Oxidative stress survival

Oxidative stress survival was measured by bacterial growth and viability in microaerobic (5% O₂) and standard atmospheric (20% O₂) conditions measuring OD_{600nm} and BacTiter Glo luminescence (arbitrary units) respectively as shown in section 4.2.3. Figure 4.4 panels A-B showed OD readings for the groups under both microaerobic and normal atmospheric oxygen conditions and panels C-D showed the corresponding luminescence results.

No statistically significant difference was found between the antrum and corpus isolate groups when measuring OD (growth) in both microaerobic and atmospheric conditions (figure 4.4 panels A-B respectively, multiple t-test). No statistically significant difference was found between the groups when measuring luminescence (viability) either (figure 4.4 panels C-D, multiple t-test).

This exact assay was also performed in Chapter 3 (3.2.6 results, 3.3.6 discussion) on *C. jejuni* isolates and the findings are consistent when considering both are microaerophilic organisms that are closely related. The difference is that whilst *C. jejuni* could grow in the 20% O₂ condition, as seen by a steady rise in OD, *H. pylori* did not. This links in with the theme of intra- vs inter- host niche adaptation. *C. jejuni* as a multi host species pathogen is exposed to standard atmospheric oxygen in between hosts, whereas *H. pylori* does not face this specific challenge in chronic infection, despite being exposed to oxidative stressors. In the *C. jejuni* work it was commented that the OD and luminescence readings did not concur. The commentary was that cells had grown and then died from oxidative stress, still contributing to the turbidity and subsequent OD readings. However, when BacTiter Glo was used the cells were not viable and there was no active ATP to bind to, thus showing the discrepancy. In the *H. pylori* dataset whilst the OD continued to rise in the microaerophilic condition as expected, the luminescence seemed to dip gradually during 0-8 h time points before rebounding slightly at the 24 h mark. The OD did not change dramatically between the 0-8 h time frame either that may be an indicator in the initial viability of the strains grown for the purpose of the assay. *H. pylori* combats oxidative stress within the host with an array of well-studied detoxification enzymes including but not limited to; catalase (KatA) (Harris *et al* 2003), superoxide dismutase (SOD) (Seyler *et al* 2001), and NADPH quinone reductase (MdaB)(Wang & Maier 2004).

There are also the peroxiredoxin family of alkyl hydroperoxide reductase (AhpC) thiol peroxidase (Hp-Tpx) and bacterioferritin comigratory protein (Bcp) (Stent, Every & Sutton 2012). There are also less elucidated virulence factors that may play a role in oxidative stress defence such as neutrophil-activating protein A (NapA). NapA has a dual role, stimulating host cell production of reactive oxygen intermediates (ROI) to create a chronic state of inflammation, whilst protecting *H. pylori* from oxidative DNA damage (Wang *et al* 2006).

It was clear from these results that the inability to grow in standard atmospheric oxygen is a clear indicator to how susceptible to high oxidative stress despite all the mechanisms *H. pylori* has to detoxify reactive oxygen species (ROS) and reactive oxygen intermediates (ROI). A potential further area of study therefore may be to focus on a lower oxidative burden, but still true to the state of oxidative stress in chronic inflammation in the host that may be variable between the antrum and corpus. This may be achieved by using agents such as hydrogen peroxide.

4.3.4 Menadione resistance

A MIC 96-well plate assay was conducted to test individual strain sensitivity to menadione, measured by OD_{600nm} across 96 h (results shown in 4.2.4, figure 4.5). At 0.15625mM there is a visible mid ground between the lower concentrations of menadione where growth is more significant and 0.3125mM the where the observed OD is markedly lower. Therefore it was concluded that 0.3215mM is the MIC and 0.15625mM would be the appropriate concentration for transcriptomics work as shown in chapter five. Confirmatory statistical analysis was conducted and menadione concentration was found to be statistically significantly when affecting growth measured by OD_{600nm} (P<0.0001).

There are very few papers on the effects of menadione on *H. pylori*, however it has been shown to be inhibitory in disk diffusion assay form (Park *et al* 2006) and using agar plates supplemented with menadione (Lee *et al* 2019). It was also reported than menadione had antibiotic modifying activity, lowering the MIC of antibiotics against multi-resistant strains of *Staphylococcus aureus*, *Escherichia coli* and *Pseudomonas aeruginosa* (Andrade *et al* 2017).

The findings of the menadione assay were very interesting. There was very little difference in resistance to the compound, all strains displayed an incredibly close MIC profile. This combined with the lack of existing reported literature on the effects of menadione on *H. pylori* makes it a very interesting proposition to further explore. There were two potential novel avenues to further the menadione resistance work on *H. pylori*.

One possible option was to go down the route of directed evolution. Using rounds of menadione based 96 well plate assays and looking for isolates that became more resistant to menadione, past the MIC threshold. These isolates would then be sequenced and compared the previous generation or even several previous generations. Whilst this is work that could still be conducted in the future, directed evolution can be a time exhaustive project and is not guaranteed to provide data or results of note. The second option was to use a sub-MIC concentration of menadione on *H. pylori* isolates and see how inoculum with this compound affects transcription by RNA-Sequencing and this will be reported in the following chapter (Chapter five).

4.3.5 Biofilm formation

Biofilm formation ability was tested by measuring OD_{600nm} and results are shown in section 4.2.5. Individual strain biofilm formation was shown in figure 4.6A. There was considerable variation in biofilm formation ability across all strains and this was statistically significant (P=0.028, ANOVA). Grouped analysis in figure 4.6B showed that the corpus isolates were much closely clustered in biofilm formation ability, whereas the antrum group had low biofilm (322A) and high biofilm (295A) former. Direct comparison of the antrum and corpus groups showed no statistically significant difference (P=0.770, t-test). Biofilm data in this thesis fell within the range of approximately OD_{600nm} (0.2-0.5) from crystal violet assays, which is in line with existing literature. Yonezawa *et al* (2009) were investigating strain TK1402 and how its outer membrane vesicles (OMVs) are involved in biofilm formation. Although TK1402 did produce significantly higher biofilm with an OD_{600nm} of 1.5 the remainder of the strains had biofilm ODs between 0.2-0.5, consistent with the data presented in this thesis.

A recent review on *H. pylori* biofilms suggests that biofilm formation may be one of the critical barriers to eradicating infection (Moghadam *et al* 2021). It further states that biofilms inhibit the penetration of antibiotics and that antibiotics cannot clear biofilm, leading to failed eradication treatment.

A *H. pylori* study was conducted investigating MBEC (minimum biofilm eradication concentration) that looks at bacterial viability after antibiotic exposure, taking into account biofilm. The findings were that MBEC was significantly higher than the MIC for amoxicillin, clarithromycin, tetracycline and metronidazole (Fauzia *et al* 2020).

A second review acknowledges that *H. pylori* biofilm research is still in its infancy (Krzyzek *et al* 2020). The review lists at least 16 factors involved in biofilm formation ranging from morphological transformation to efflux pumps and type 4 secretion systems (T4SS), too diverse to discuss within the scope of this discussion. The review however concluded that *H. pylori* biofilm formation is achieved in a ‘stepwise and highly complex process’.

As the biofilm assay showed results consistent with what is currently observed in existing scientific literature, there is little to adapt upon the original assay. The limitation of the assay is that like many *H. pylori* biofilm experiments the biofilm was formed at the pellicle, or air-liquid interface. This method is popular as early work looked at *H. pylori* and its associated biofilm in water sources, during postulation of the fecal-oral route of *H. pylori* transmission (Percival & Thomas 2009). For the approach this thesis takes, looking at mimicking antrum and corpus conditions using a biotic surface or submersion in a biotic type media may generate more biologically relevant data.

4.3.6 Genome analysis

As shown in section 4.2.6, 13 paired sets of antrum corpus isolate genomes were compared alongside J99. A presence absence gene sheet was generated (see appendix section 8.2) and a bidirectional heatmap was generated for visualisation of gene presence/absence (figure 4.7). As expected paired isolates clustered together, there was no clustering based on either antrum or corpus genomes. Potentially the only way to look at genomic differences potentially caused by microevolution is on a strain-pair basis.

Work has been done using deep sequencing to study microevolution among *H. pylori* populations within patient stomachs (Wilkinson 2019). However based on the initial findings there were few real differences in the number of genes present in the antrum and corpus isolates. It may be that microevolution occurs on such a small scale that there are no observed differences using the gene presence/absence approach. Genes may be present, but highly polymorphic with allelic variation (Wilkinson *et al* 2022). It may also be that no microevolution has taken place despite strains being isolated from different niches of the stomach. Finally it could be that due to the duration of chronic infection in the patients being unknown in this thesis, there has been insufficient time for microevolution to occur.

In a study of mice, *H. pylori* infection is corpus dominant, 5-10 fold over the antrum initially but after a week becomes antrum dominant for approximately two months. After such period antrum growth declines and the infection becomes corpus prominent once more (Keilberg *et al* 2021). It was suggested the antrum switches between challenging and favourable conditions for *H. pylori* growth. This dynamic system may be conducive or detrimental to microevolution.

Niche adaptation to regions of the stomach however does have some supporting evidence. Ailloud *et al* (2019) demonstrated that within-host population structure is influenced by the physical separation of the antrum and the mucosa of the corpus/fundus. It was concluded that niche-specific mutations were largely non-neutral, indicating they are involved in local adaptation. These niche-specific mutations and niche-specific genotypes are the strongest evidence to date of antrum/corpus niche differential adaptation.

4.3.7 Conclusions and Recommendations

H. pylori is a chronically persistent coloniser of the gastric niche. Although the organism is well researched, there is comparatively very little research that considers how the antrum and corpus should be considered two separate niche environments due to the dynamic nature and structure of the stomach. Further to this there is little comparative work between how persistence in these two distinct niche regions of the stomach may alter the properties of the isolates that colonise them.

In this chapter paired patient isolates from the antrum were comparatively tested against isolates from the corpus across a range of phenotypic assays that represent *in-vivo* niche conditions or stressors. The genomes of 13 paired antrum and corpus isolates were also compared to look for the presence/absence of genes that may relate to niche adaptation in either area of the stomach potentially by way of microevolution.

The majority of the body of this chapter considered whether there were sufficient phenotypic differences between antrum and corpus isolates to support the theory of niche adaptation and/or microevolution between the two groups of strains. In this chapter a pattern has emerged that antrum and corpus isolates on the whole behave phenotypically comparably across a range of phenotypic assays.

As with the phenotypic analysis of *C. jejuni* in chapter two one of the main limitations of this particular work is the number of strains used to generate data. For future work ideally a larger number of paired strains would be used to help bolster any potential findings. Recommendations for further phenotypic based work would be the possibility of performing directed evolution work using menadione as mentioned in section 4.3.4. The research space for menadione and potential applications to *H. pylori* treatment is novel and largely neglected. Another set of assays could also look at antibiotic resistance, as aforementioned this is the only phenotypically acknowledged work in scientific literature that has determined significant differences between paired antrum corpus isolates (Selgrad *et al* 2014, Farzi *et al* 2019). Although this work would therefore be derivative it would still be interesting to see if the observed association in other studies is replicable with the paired strains used in this study.

The genomic comparison of the antrum corpus paired strains showed very strict clustering by pair, with no evidence of any kind of niche related genes. As cited previously, Ailloud (2019) shows there is evidence of genomic antrum corpus paired differences. There were 309 niche specific mutations and 232 niche specific genes across 16 patients. 32 niche specific genes were found on average per patient, although two patients showed no significant results.

Wilkinson (2022) identified within clinical isolate pairs, and even single colonies within a niche, genomic diversity was present. However, this was most commonly associated with allelic variation of genes as opposed to the presence/absence of a gene between a clinical antrum/corpus pair. It could therefore be theorised at the phenotypic level it would be harder to spot differences between paired clinical strains if the alleles are functional, than an absent gene which could show a more deleterious effect to phenotypic performance. As mentioned earlier in the discussion, number of isolates used may have also been insufficient to see any phenotypic differences. There is limited work in the *Helicobacter* field on clinical biopsy pairs that could refute or support the phenotypic data in this chapter. There are also fewer number of less pathogenic clinical strains available as *H. pylori* is “test and treat” upon symptomatic complaint as opposed to screening. This also may skew obtainable strains towards those more likely to have worse disease outcomes. Finally, there is no standard by which gastric biopsy is achieved during invasive testing for *H. pylori*. Although it is the position of this thesis and an increasingly common opinion, that dual antrum and corpus biopsy is essential, this is currently not required clinical practice.

H. pylori is one of the most infectious agents in the world, given the sheer magnitude of the global population thought to be colonised the bacteria (as discussed in chapter one, section 1.2). Gastric cancer is the fifth-leading type of cancer and the third-leading cause of cancer related death globally. Of this 60% of cases are attributed to *H. pylori* infection which equates to 5.5% of all cancer cases (Parkin 2006). The global impact of *H. pylori* cannot be ignored, but as much as continuing healthcare science and academic research improves our understanding of *H. pylori* there is still much that we do not know.

One area that is poorly investigated is niche adaptation and differentiation of *H. pylori* to distinctly different regions of the stomach, the antrum and corpus. Although this may seem minimal, there is a larger concern in relation to strains and interplay with the niche they inhabit. As with most bacteria antibiotic resistance rates are on the rise, and as mentioned in the introduction the WHO listed *H. pylori* as a priority pathogen for the development of new antibiotic drugs (Tacconelli *et al* 2018) in response to alarming rise in resistance to clarithromycin. Resistance rates however are now being found not always to be consistent within a patient. Even when mixed culture is not present the paired antrum corpus strains do not always share the same antibiotic resistance profile, as has been

previously mentioned in this chapter. This worrying trend can lead to eradication treatment failure and should be considered where *H. pylori* becomes persistent despite treatment. The second main conclusion of this chapter is that menadione may be a novel antimicrobial or supplementary for an antibiotic. This also ties in with the current concern of adequate antibiotics/antimicrobial agents to eradicate *H. pylori*. Although the menadione work in this chapter (results shown in section 4.2.4) does not consider how applicable menadione would be in terms of suitable concentration and toxicity in a healthcare setting, it does show strong inhibitory properties.

Stemming from this, the next chapter will look at the applications of applying a sub-MIC concentration of menadione and how this affects transcription in *H. pylori*.

Chapter Five: Transcriptomic effect of Menadione on *H. pylori* 322A

5.1 Introduction

Transcriptomics provides a useful snapshot of differentially expressed gene patterns under specific conditions. As shown in chapter four, menadione provided a strong inhibitory effect at certain concentrations against *H. pylori* growth. As mentioned in section 4.1.4 menadione has previously been suggested to have anti-bacterial and anti-inflammatory effects against *H. pylori* (Lee *et al* 2019). There is a gap in the *H. pylori* sphere of knowledge on the use and potential effects of menadione. It was therefore imperative that this work was investigated as any work related to *H. pylori* and menadione is novel, particularly as any large-scale effects of menadione on *H. pylori* transcription have never been reported beyond limited targeting of virulence genes (Lee *et al* 2019).

There are several existing studies that look at *H. pylori* RNA-Sequencing (RNA-Seq) and transcriptional analysis when a stressor is used in the ‘treated’ condition. For example, Marcus, Sachs & Scott (2018) challenged *H. pylori* at differing pH levels. Genes involved with acid acclimation, motility, ROS, and the *Cag* pathogenicity island all showed increased expression at acidic pH, with some gene expression increasing more significantly at different extremes of acidity. A study interested in high-salt diets and the potential effects on *H. pylori* transcription used NaCl as the stressor and found 65 upregulated and 53 downregulated genes in response to high salt conditions. It was noted that prominent outer membrane proteins that act as adhesins SabA, HopQ and HopA had significantly upregulated transcript levels of the genes that encode them (Loh *et al* 2018).

Initially work was undertaken to screen for menadione resistant mutants under an experimental evolution protocol utilising well plate based minimum inhibitory concentration (MIC) assays, and disc diffusion assays. Across many rounds of repeats with over 100 replicates the assays failed to yield viable menadione resistant mutants.

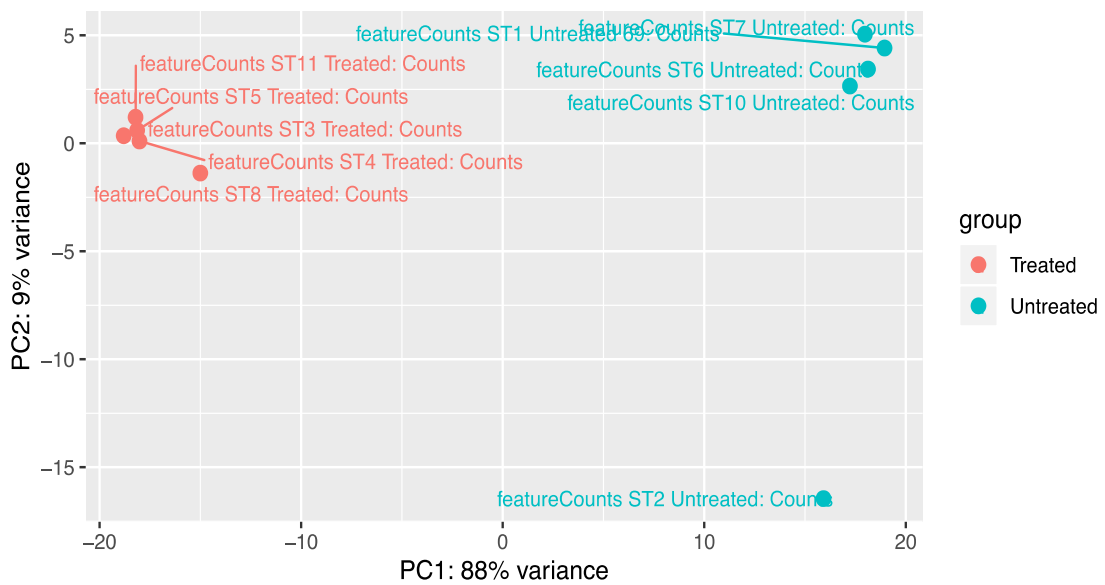
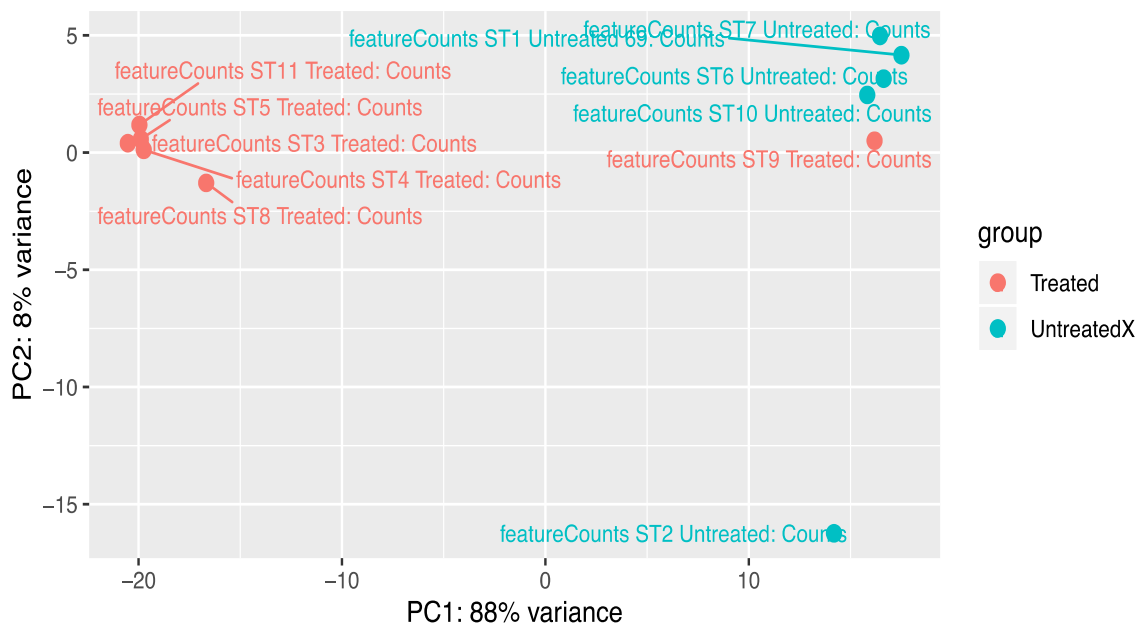
Therefore, it was decided to instead use RNA-Seq to take a snapshot of the *H. pylori* transcriptome when exposed to sub MIC levels of menadione as compared to an untreated control group.

5.2 Results

Transcriptomics work was undertaken by RNA-Seq and subsequent bioinformatics analysis of five untreated and five sub-MIC treated samples of 322A (samples shown in table 2.3). The samples within the treated and untreated groups clustered closely together and the two groups clustered apart and this will be shown by Principal Component Analysis plots. In total there were 1312 significantly differentially expressed genes (adjusted P value <0.05). How these genes clustered by treatment group will be shown by heatmap. The top ten most significant genes will also be shown. Finally, pathway over-representation analysis will show significantly differentially expressed genes that were mapped to the epithelial cell signalling pathway.

5.2.1 Principal Component Analysis shows samples clustering by treatment group

Principal component analysis plots were generated by DESeq2 as described in section 2.3.6, shown in figures 5.1 and 5.2. Both the treated and untreated groups clustered closely together within their sample group along the x-axis aside from menadione treated sample ST9. It was decided at this point ST9 was an anomaly of experimental error (it was in the treated group but menadione was mistakenly not added). DESeq2 was run for a second time, and ST9 was discarded from any further data analysis. Figure 5.1 shows the original PCA plot including ST9 and 5.2 shows the same plot with ST9 omitted. ST2 also did not cluster with other untreated strains on the y-axis and this may ultimately have been due to the sample not receiving the full amount of menadione.



Figures 5.1 and 5.2 PCA plots show samples cluster by treatment group. Principal component analysis plots as generated by DESeq2 showing clustering of samples based on log₂-transformed featureCounts data. Menadione treated samples shown in orange and menadione untreated samples shown in teal. Figure 5.1 shows the original DESeq2 output, and figure 5.2 shows a second DESeq2 run with anomalous sample ST9 omitted.

5.2.2 Heatmap shows 1312 statistically differentially expressed genes, clustered by treatment group

As stated in the introduction to the results section (section 5.2) treatment of 322A with menadione resulted in 1312 differentially expressed genes that were of statistical significance (adjusted P value <0.05). All 1312 differentially expressed genes were visualised by generation of a heatmap (figure 5.3) using GraphPad v9. A second visualisation produced by Professor Lesley Hoyles using R package heatmap.2 from gplots v3.0.1. can be found in the appendix section 8.3. The heatmap shows that the significantly differentially expressed genes, as depicted in the figure by log₂ gene count, are strongly clustered by treatment group. It also shows using the log₂ gene count key, that treatment with menadione caused both significantly differentially expressed genes that were upregulated and genes that were downregulated compared to the untreated sample group.

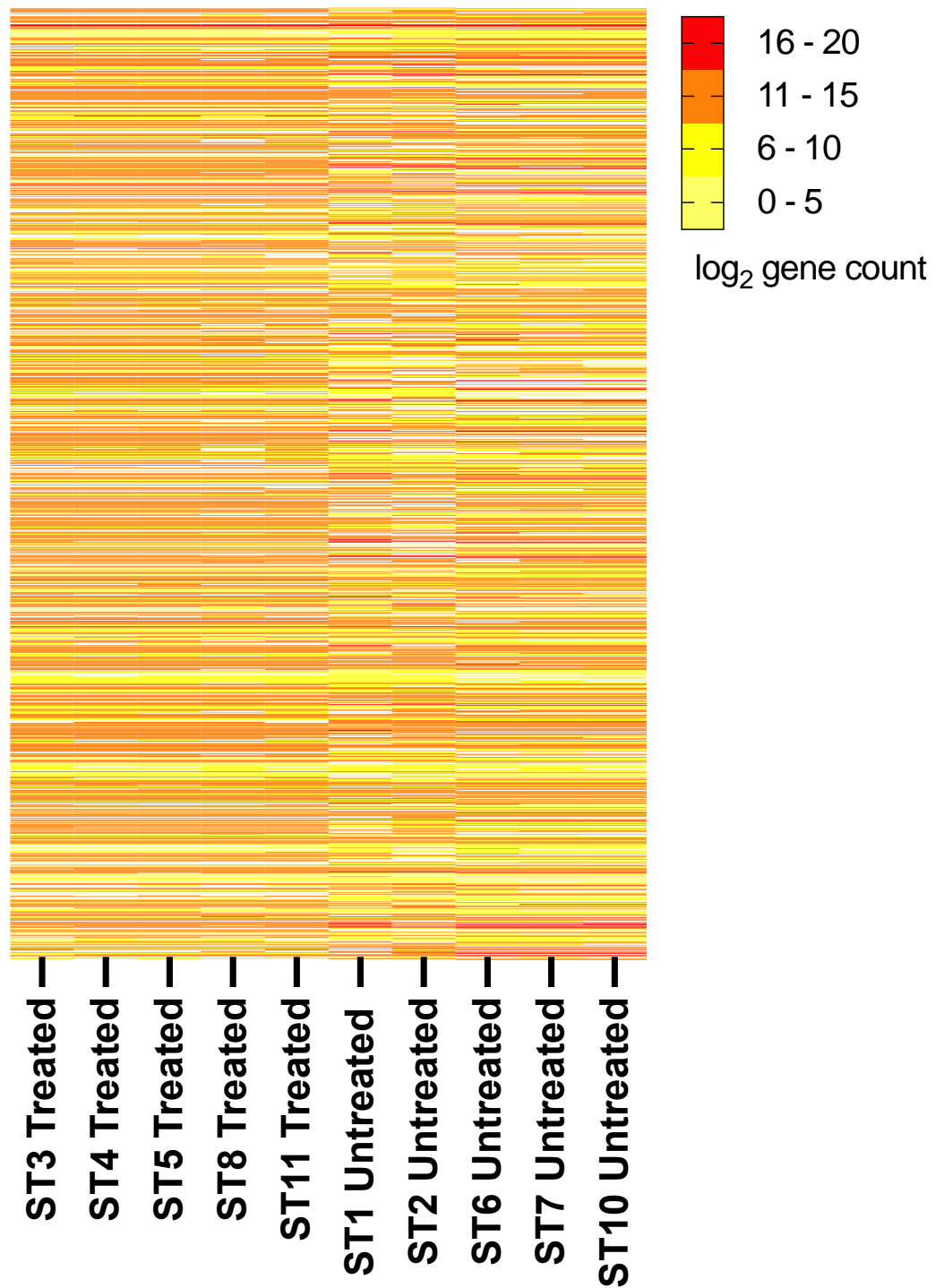


Figure 5.3 Significantly differentially expressed genes show clustering by treatment group. Heatmap showing clustering of the 1312 significantly (adjusted P value < 0.05) differentially expressed genes for the treated and untreated samples. Log₂ transformed gene count information was generated from normalized count data produced using DESeq2.

5.2.3 Top 10 most significantly differentially expressed genes show upregulation and downregulation events when comparing the menadione treated and untreated conditions

Of the 1312 significantly differentially expressed genes, the top ten genes that showed the highest significance were collated in a table 5.1 using log₂ fold change output from DESeq2 as performed by the author. Positive log₂ fold change values indicate upregulated genes in the untreated condition as compared to the menadione treated condition. Negative values therefore demonstrate downregulation as compared to the treated group. Each gene was also plotted on individual box plots using log₂-transformed gene counts (figure 5.4 box plots produced by Professor Lesley Hoyles using the R package tidyverse v1.2.1.).

Gene ID	Gene	Gene Function	Log ₂ Fold Change
322A_00252	N/A	Hypothetical Protein	2.576112303
322A_01003	N/A	Hypothetical Protein	3.32821417
322A_01557	<i>luxS</i>	Ribosylthiomocysteine lyase	4.213385597
322A_00270	<i>mnmE</i>	tRNA modification GTPase	-4.947680923
322A_00940	<i>rnc</i>	Ribonuclease 3	-3.237729269
322A_01444	<i>truA</i>	tRNA pseudouridine synthase A	2.674137729
322A_00054	<i>haeIII</i>	Modification methylase	-2.155654463
322A_00936	<i>glpC</i>	Anaerobic G3P dehydrogenase	-2.379076394
322A_00300	<i>ruvC</i>	Endodeoxyribonuclease	3.023872463
322A_00578	<i>virB10</i>	T4SS Protein	-2.110352745

Table 5.1 Top 10 most significantly differentially expressed genes when comparing untreated and menadione treated groups. Log₂ fold changes in gene expression were obtained from DESeq2 output by transcriptomic data analysis of the author. Positive log₂ fold change values indicate upregulation in the untreated group and negative fold change values downregulation in the untreated group as compared to the menadione treated group.

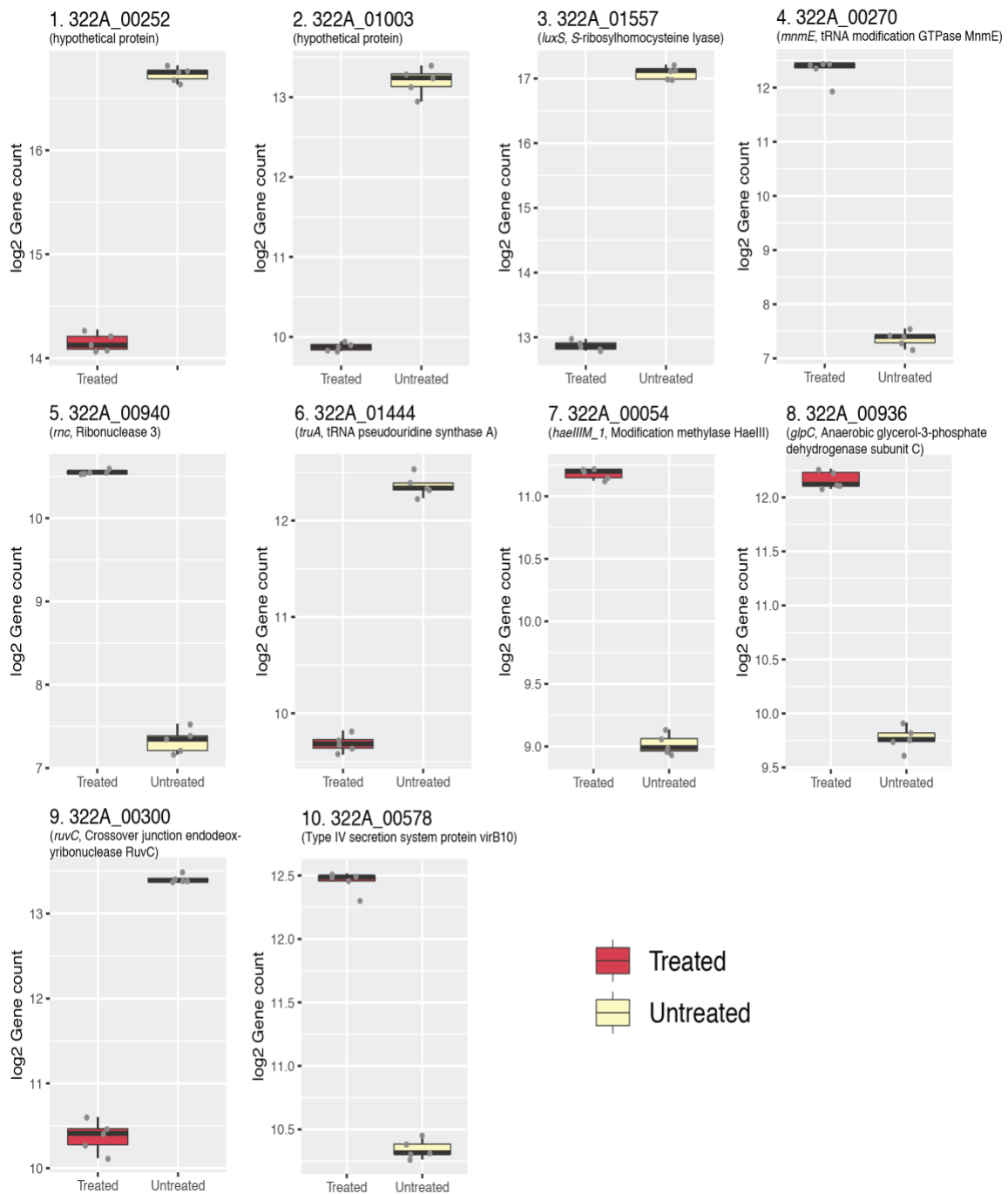


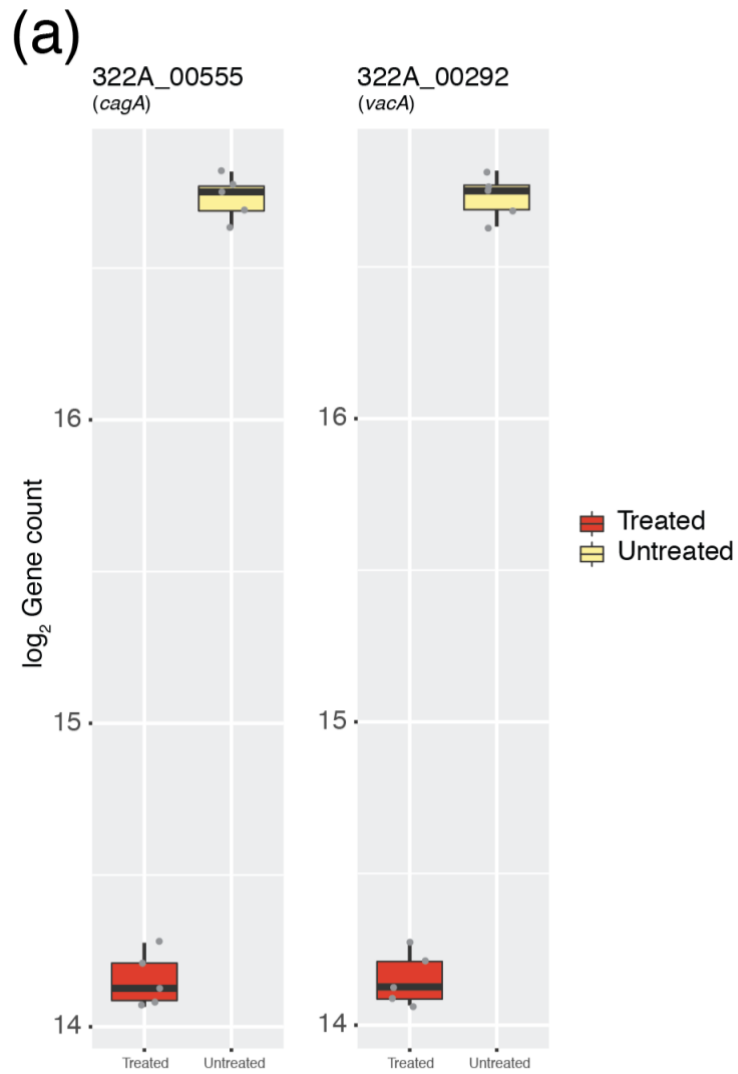
Figure 5.4 Top 10 most significantly differentially expressed genes between menadione treatment conditions. Box plots of log₂-transformed gene count data for the top 10 most significant (adjusted *P* value < 0.05) differentially expressed genes, as determined using DESeq2. Log₂-transformed gene count data was generated from normalized count data produced using DESeq2. Image produced by Professor Lesley Hoyles. N=5 treated, N=5 untreated per gene shown.

5.2.4 Pathway over-representation analysis shows “Epithelial cell signalling in *H. pylori* infection” is the most statistically significantly affected metabolic pathway by menadione treatment

It has been shown so far that the samples clustered by treatment group (principal component analysis section 5.2.1) and 1312 significant differentially expressed genes also cluster by treatment group (heatmap figure 5.3.). The next step is to show the relevance of these differentially expressed genes in relation to the functionality of the organism itself. Pathway over-representation analysis was done by Professor Lesley Hoyles as described in section 2.3.8 using KEGG to map differentially expressed genes against known metabolic pathways using a reference genome in the programme *H. pylori* 26695. Of 93 mapped pathways, 89 were statistically significant (adjusted P value <0.05). 33 of those were statistically significant at an adjusted P value of <0.01 a list of which are shown in table 5.2. Based on the significant differentially expressed genes ‘Epithelial cell signalling in *H. pylori* infection’ was the most statistically over-represented metabolic pathway (adjusted P value <0.01). Figure 5.5A (produced by Professor Lesley Hoyles using the R package tidyverse v1.2.1.), shows that menadione treatment downregulates expression of major virulence genes *cagA* and *vacA* (adjusted P values <0.05). Figure 5.5B shows the pathway for epithelial cell signalling in *H. pylori* infection and log₂ fold changes in gene expression from treatment with menadione.

Pathway	Number of genes in pathway	Adjusted p value
Epithelial cell signaling in Helicobacter pylori infection	35/40	1.02E-07
Oxidative phosphorylation	30/35	1.37E-06
Carbon metabolism	41/53	1.37E-06
Two-component system	28/32	1.37E-06
Flagellar assembly	27/31	2.39E-06
Lipopolysaccharide biosynthesis	24/27	4.62E-06
Peptidoglycan biosynthesis	14/14	4.25E-05
Mismatch repair	14/14	4.25E-05
Aminoacyl-tRNA biosynthesis	22/26	5.93E-05
ABC transporters	23/28	8.68E-05
Bacterial chemotaxis	15/16	1.24E-04
Folate biosynthesis	17/19	1.24E-04
Glyoxylate and dicarboxylate metabolism	12/12	1.57E-04
Protein export	14/15	2.19E-04
Amino sugar and nucleotide sugar metabolism	16/18	2.19E-04
Arginine and proline metabolism	11/11	2.63E-04
Glycerophospholipid metabolism	11/11	2.63E-04
Porphyrin and chlorophyll metabolism	11/11	2.63E-04
Terpenoid backbone biosynthesis	11/11	2.63E-04
Ribosome	36/53	2.74E-04
Phenylalanine, tyrosine and tryptophan biosynthesis	15/17	3.44E-04
Pantothenate and CoA biosynthesis	10/10	5.56E-04
Glycolysis / Gluconeogenesis	15/18	1.17E-03
Methane metabolism	13/15	1.41E-03
Cysteine and methionine metabolism	14/17	2.13E-03
Homologous recombination	14/17	2.13E-03
Quorum sensing	12/14	2.68E-03
Bacterial secretion system	15/19	2.83E-03
Fatty acid metabolism	10/11	2.91E-03
Purine metabolism	17/23	4.29E-03
Fatty acid biosynthesis	9/10	6.09E-03
Lysine biosynthesis	10/12	9.68E-03
Butanoate metabolism	10/12	9.68E-03

Table 5.2 List of significant KEGG over-production pathways when mapped by the 1312 significantly differentially expressed genes. All pathways show adjusted P value of < 0.01.



Log2 fold change

cagA
vacA

1.982795718
1.639242512

(b)

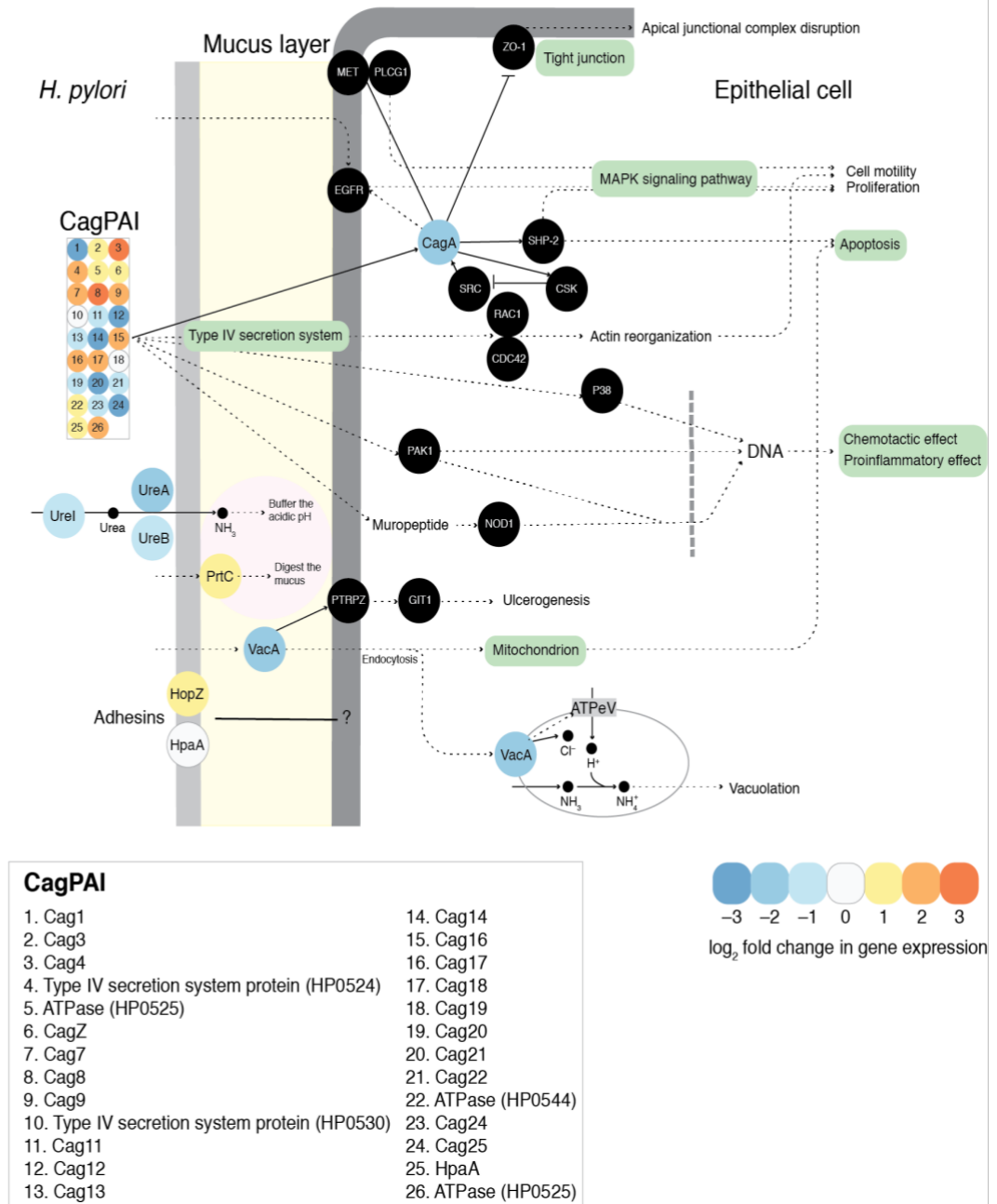


Figure 5.5. Epithelial cell signaling in *H. pylori* 322A is down-regulated in menadione-treated *H. pylori* 322A. (a) Among the 1312 significantly (adjusted P value < 0.05) differentially expressed genes are *cagA* and *vacA*, with expression of both down-regulated in menadione-treated *H. pylori* cells. Box plots generated by Professor Lesley Hoyles, log₂ fold change provided by the author, N=5 treated, N=5 untreated. (b) Pathway analysis showed that ‘Epithelial cell signaling in *Helicobacter pylori* infection’

was the most significantly (adjusted P value < 0.05) over-represented metabolic pathway associated with the set of significantly differentially expressed genes. Both *cagA* and *vacA* are associated with this pathway. Proposed mechanism of action is as follows. Down-regulation of *cagA* prevents inhibition of ZO-1, maintaining tight junction integrity in host epithelial cells, along with preventing activation of MAPK signaling. Down-regulation of *vacA* prevents or reduces ulcerogenesis, and apoptotic effects associated with *H. pylori* infection, and reduces or prevents vacuolation. Down-regulation of urease-associated genes limits *H. pylori*'s ability to protect itself from host-associated acid production within the mucus layer. *H. pylori* genes (35/40 in whole pathway, from the 1312 differentially expressed genes) are shown in terms of their log₂-fold change. Black circles with white text represent host-associated gene products not assayed in this study but with which *H. pylori* gene products interact (note: not all host-associated gene products included in the pathway are shown to aid clarity). The pathway was created based on *H. pylori*-specific information available from KEGG on 13 March 2020. Figure including proposed mechanism produced by Professor Lesley Hoyles using KEGG reference pathway map05120 and modified using Adobe Illustrator. Proposed mechanism of action further described by the author in 5.3.4.

5.3 Discussion

The aim of this chapter was to investigate menadione as a novel agent based on previous MIC data, and test how it may affect transcription in *H. pylori* strain 322A. Random untreated and menadione treated (0.15625 mM) samples were sent to MacroGen Inc, South Korea for RNA extraction and RNA-Seq. Raw sequencing data (FASTQ) was converted through bioinformatics tools into normalised count data that could then be visualised to observe the results.

5.3.1 Principal component analysis

The first piece of visualised data came from the end output of the bioinformatics conversion from FASTQ file to normalised count data (section 2.3.5). DESeq2 generates a principal component analysis (PCA) plot. The PCA plot shows clusters of samples based on their similarity as a pseudo overall expression profile. PCA reduces the number of dimensions (an axis would be required to plot featureCounts reads of all samples for each gene) to 2-D.

By rotating a line through all hypothetical ‘dimensions’ until the distance among all projected points is maximum, PC1 shown on the x-axis (section 5.2.1 figures 5.1 & 5.2) is achieved. PC1 therefore conveys maximum variation among data points with minimum error.

Looking at figure 5.1 (section 5.2.1) all treated and untreated samples clustered together in their respective groups at separate ends of the x-axis aside from ST9 (Treated) (PC1 explains 88 % of the variation in the data). The most logical explanation for this anomaly is that menadione was mistakenly not added to ST9 during the sample preparation phase. Therefore, it was excluded from any further analysis and DESeq2 was run for a second time excluding sample ST9. The PCA plot from this second run is figure 5.2. Removal of ST9 still shows good separation of the data based on treatment group, with PC1 again explaining 88 % of the variation in the data.

5.3.2 Heatmap of 1312 significantly differentially expressed genes

Knowing that the two conditions of samples clustered the next stage was to look at the number of statistically differentially expressed genes. Using the normalised count data from DESeq2 a heatmap showing clustering of 1312 statistically differentially expressed genes (adjusted P value <0.05) was generated (methods section 2.3.7, results section 5.2.2, figure 5.3). A second heatmap generated by Professor Lesley Hoyles using a different visualisation can be found in the appendix (section 8.3). The heatmap showed that the statistically differentially expressed genes clustered by treatment. There was a mixture of higher and lower log₂-transformed gene counts genes comparatively between the two treatment conditions. Therefore, it could be concluded at this point that treatment of *H. pylori* 322A with menadione had caused both upregulation and downregulation of different genes.

5.3.3 Most significantly differentially expressed genes

From the 1312 statistically differentially expressed genes, Professor Lesley Hoyles compiled the top ten most significant differentially expressed genes (methods section 2.3.7) and generated box plots from log₂-transformed gene count data from DESeq2 (figure 5.4). For further clarification, table 5.1 generated by the author shows these ten

genes in relation to log₂ fold change when comparing the treated group to the untreated group. A positive fold change value relates to upregulation in the untreated condition and a negative to downregulation in the untreated group as compared to the menadione treated group. The first two genes 322A_00252 and 322A_01003 respectively were annotated as hypothetical proteins.

The third gene in figure 5.4 is annotated as *luxS* (S-ribosylhomocysteine lyase) and is downregulated in the menadione treated group with a log₂ fold change of 4.213385597. *luxS* a gene commonly associated with quorum sensing is interesting in the context of *H. pylori* research. LuxS has a central metabolic function in the activated methyl cycle (AMC) required for methyltransferases. However, *H. pylori* has no enzyme for catalysing a stage in the cycle (homocysteine to methionine) making the role of LuxS unclear (Doherty *et al* 2010). The same study however concluded that the combination of genes *cysK-metB-luxS* encode the capacity to generate cysteine through reverse transsulfuration. Outside of metabolism deletion of *luxS* has been reported to diminish competitive ability in mice models and motility in soft agar (Lee *et al* 2006). This was also supported by a study that showed *luxS* deletion diminished motility in soft agar and exhibited a reduced infection rate in a Mongolian gerbil model (Osaki *et al* 2006). The likely explanation is that LuxS modulates flagellar transcripts and flagellar biosynthesis via the production of AI-2 a signalling molecule (Shen *et al* 2010).

The fourth gene in figure 5.4 is *mnmE* (tRNA modification GTPase MnmE). Although MnmE is highly conserved amongst bacteria and eukarya (Armengod *et al* 2012), there is no reference to this specific GTPase in *H. pylori* literature. There is some work on *mnmE* in gastrointestinal pathogens. *MnmE* is thought to share a tRNA modification pathway with *gidA*. Although *gidA* or *gidA/mnmE* mutants showed most attenuation. It was found across two studies that *mnmE* deletion mutants are attenuated in both *in vitro* and *in vivo* models of *Salmonella* (Shippy *et al* 2013,2014). The studies concluded growth, motility, intracellular replication and invasiveness were affected, however in this thesis menadione treatment upregulated expression of the gene with a log₂ fold change of -4.97680923.

The fifth gene in figure 5.4 is *rnc* (Ribonuclease 3), for which there is little research in the field of *H. pylori*. A paper looking at the maturation of atypical ribosomal RNA precursors in *H. pylori* stated that whilst maturation of rRNA has been ‘extensively studied in *E. coli* and *B. subtilis*’ nothing was known in *H. pylori* (Iost, Chabas & Darfeuille 2019). Their findings were that the initial processing step by RNase III in *H. pylori* had some similarities but also differences to that of the aforementioned organisms. *Rnc* was upregulated by menadione treatment with a log₂ fold change of -3.237729269.

The sixth gene in figure 5.4 is *truA* (tRNA pseudouridine synthase A) and was downregulated by menadione treatment with a log₂ fold change of 2.674137729. Although there is no research on *truA* in *H. pylori* there is a recent study that looked at the unexpected effect of pseudouridines on *Pseudomonas* spp. (Tagel *et al* 2020). In the study, they observed that lack of pseudouridylation activity by the absence of TruA elevates the mutation frequency in *Pseudomonas putida* and *Pseudomonas aeruginosa* that could not be ascribed to error-prone DNA polymerases or malfunctioning of the DNA repair pathways. It was also found *truA* deletion mutants of *P. putida* had a decreased tolerance to stressors, as evidenced by decreased growth compared to wild-type in the presence of tetracycline, ampicillin and nitroquinoline 1-oxide (ROS production). The deletion of *truA* decreasing tolerance to ROS production could potentially lend to the argument there is an undetermined role in *H. pylori* for the gene, and that TruA may assist in detoxifying oxygen species, potentially even superoxides such as those produced by menadione.

The seventh gene in figure 5.4 is *haeIIIM_1* (Modification methylase HaeIII) and was upregulated by menadione treatment with a log₂ fold change of -2.155654463. It was not possible to find any specific literature on this gene or the enzyme it encodes. However, the UniProt protein database (accessed 4/10/2022) (Wang *et al* 2021) recognises the protein as a cytosine-specific methyltransferase and therefore confirmed as part of a restriction modification system. It is thought that *H. pylori* has many R-M systems, and the complement of them varies by strain. Reference strains J99 and 26695 have more than 20 putative DNA R-M systems between them (Lin *et al* 2001).

The eighth gene in figure 5.4 is *glpC* (Anaerobic glycerol-3-phosphate dehydrogenase subunit C) and was upregulated by menadione treatment with a log₂ fold change of -2.379036394. The role of *glpC* is not well documented in *H. pylori* scientific literature other than a paper that the GlpC protein is predicted to contain iron-sulfur clusters (Benoit *et al* 2018). Outside of *H. pylori* there is a paper that demonstrates GlpC remarkably increases the resistance of *E. coli* to organic solvents, including reducing the hydrophobicity of the cell surface (Shimizu *et al* 2005). It is worthwhile to note that the menadione solution used in this thesis was not dissolved in organic solvents. A study into *Proteus vulgaris* (Wu *et al* 2015) found that *glpC* deletion mutants showed reduced growth compared to wild-type in the presence of organic solvents, mirroring the results of the previously cited study (Shimizu *et al* 2005). The *P. vulgaris* study also concluded that GlpC plays an important role in biofilm formation, pH resistance, antibiotic tolerance and defence against phagocytosis.

The ninth gene in figure 5.4 is *ruvC* (Crossover junction endodeoxyribonuclease RuvC) and was downregulated by menadione treatment with a log₂ fold change of 3.023872463. A definitive study into *ruvC* in *H. pylori* made many findings on the numerous roles RuvC plays. Inactivation of *ruvC* reduced the rate of homologous recombination, increased sensitivity to levofloxacin, metronidazole, oxidative stress and macrophage survival. It was also determined that in a mouse model the 50% infectious dose was 100-fold higher than wild-type and without RuvC infection spontaneously cleared from the murine gastric mucosa over a timeframe of 36-67 days. It was therefore concluded in this huge body of work RuvC is essential for continued *in vivo* survival of *H. pylori* (Loughlin *et al* 2003).

The final gene in figure 5.4. encodes the Type IV secretion system VirB10 and expression of this gene was upregulated by menadione treatment with a log₂ fold change of -2.110352745. The main VirB10 ortholog in *H. pylori* literature is CagY part of the well-researched *cag* pathogenicity island (*cagPAI*). CagY has a large middle repeat region (MRR) with large amounts of repeat sequence motifs. It is suggested that recombination within the MRR of *cagY* can change the functionality of the T4SS like a switch or biological rheostat, to tune the host inflammatory response to maximise persistent infection (Barrozo *et al* 2013). Further study into CagY also suggested a rheostat like model and demonstrated that CagY MRR recombination alters binding to β 1 integrin that

in turn modulates T4SS function and mediation of close contact with host cells (Skoog *et al* 2018).

5.3.4 Pathway over-representation analysis

After confirming samples clustered by treatment group, and that 1312 significantly differentially expressed genes clustered by treatment, significant differentially expressed genes were mapped to a biological pathway in *H. pylori* to determine the impact menadione may have on the functionality/virulence of the organism. Pathway overrepresentation analysis was performed by Professor Lesley Hoyles using KEGG (methods shown in section 2.3.8, figures in section 5.2.4). 33 statistically significant pathways ($P < 0.01$) based on mapping of the 1312 statistically differentially expressed genes were found (table 5.2, full list see appendix 8.4). It was determined the most significant pathway in relation to the 1312 significantly differentially expressed genes was ‘epithelial cell signalling in *H. pylori* infection’ (35/40 genes in whole pathway). Figure 5.5A shows that menadione treatment downregulates expression of major virulence genes *cagA* and *vacA*. Log₂ fold changes were added by the author which were 1.982795718 and 1.639242512 for *cagA* and *vacA* respectively. Figure 5.5B shows the pathway for epithelial cell signalling in *H. pylori* infection and log₂-fold changes in gene expression from treatment with menadione. 24 out of 26 *cag*-pathogenicity island (*cagPAI*) genes were significantly differentially expressed however for more brevity this discussion will focus on the three key genes/gene groups *cagA*, *vacA* and *ureA/B/I*.

CagA and VacA are arguably the two most important virulence factors in *H. pylori* and they have been studied extensively. There is one existing paper that concluded menadione can downregulate *cagA* and *vacA* (Lee *et al* 2019). Aside from this, studies generally compare *cagA*⁺/*cagA*⁻ and *vacA s1/m1* to *vacA s2/m2*. The most recent review available includes an overview of work on these virulence factors (Sharndama and Mba 2022).

Vacuolating cytotoxin A (VacA) is ubiquitous in *H. pylori* and a preliminary overview of VacA is found in the introduction of the thesis (section 1.2.2). As the name suggests VacA creates vacuolation of host cells as an accumulation of large endosome like vesicles. It also disrupts tight junctions and can also enter mitochondria, dissipating mitochondrial transmembrane potential activating Bcl-2 associated protein X (Bax) a pro-apoptotic

factor (Maleki-Kakelar *et al* 2019). The role of VacA in carcinogenesis although not fully elucidated is also demonstrated, for example in chronic infection the presence of VacA disrupts the autophagic pathway resulting in a failure to clear bacteria and allow the accumulation of ROS that may promote carcinogenesis (Raju *et al* 2012). It is suggested in this thesis that downregulation of *vacA* by menadione may prevent or reduce ulcerogenesis, vacuolation and apoptosis.

Cytotoxin-associated gene A (CagA) is considered the most important virulence factor in relation to disease outcomes in patients infected by *H. pylori* (preliminary overview found in introduction section 1.2.2). *cagA*⁺ strains are highly associated with patient outcomes of gastric ulcers and gastric cancers (Khadir *et al* 2017). *cagA* is part of the *cag*-pathogenicity island (*cagPAI*) that encodes the CagA oncoprotein and a T4SS, a syringe-like pilus structure for the translocation of CagA into host cells (Muller 2012). CagA once inside a host cell can induce cellular alterations affecting motility, proliferation, cytoskeletal rearrangement and inducing apoptosis (Baj *et al* 2020). There is a counter suggestion on CagA and apoptosis, in that CagA may actually inhibit apoptosis and that may promote survival of epithelial cells with DNA damage that may contribute to tumorigenesis (Palrasu *et al* 2020). CagA also plays a role in promoting chronic inflammation and exacerbating gastric tissue damage (Chuang *et al* 2011, Teh *et al* 2002). From the work done in this thesis (figure 5.5B) it is suggested that downregulation of *cagA* by menadione may prevent inhibition of zonula occludens (ZO-1) that maintains tight junction integrity in host epithelial cells (Lee *et al* 2011, Palatinus *et al* 2011). Downregulation of *cagA* may also result in the prevention of activating the MAPK signalling pathway. MAPK signalling when induced by CagA can result in hyperproliferation of the cell resulting in increased mutation rate. This combined with a chronic state of inflammation can be linked to tumorigenesis (Magnelli *et al* 2020).

There is also significant interplay between the CagA and VacA proteins themselves that have been suggested to work antagonistically (Jang *et al* 2010). CagA blocks the cytotoxicity of VacA, and the ability of VacA to enter host cells (Akada *et al* 2010). CagA also blocks apoptotic activity of VacA in both a phosphorylated and unphosphorylated manner (Oldani *et al* 2009). One proposed mechanism is that CagA is injected into cells via T4SS in local cells bacteria are bound to and as a by-product protects them from VacA cytotoxicity. VacA attacks distant cells, freeing nutrients, and thus the presence of both

CagA and the most active VacA type (s1, i1, m1) are linked to the most severe disease outcomes in patients (Akada *et al* 2010).

Lastly from figure 5.5's signalling pathway are the group of urease-associated genes *ureA/B/I* that were downregulated when treated with menadione. *H. pylori* produces large amounts of urease that is pumped out into the local environment of the bacteria. Urease is essential in the persistent colonisation of the stomach, by catalysing the hydrolysis of urea to ammonia the local pH of the highly acidic stomach is raised, thus helping *H. pylori* persist (Mobley 2001). It was also explained previously in this thesis that pH change by urease changes the viscoelasticity of the gastric mucus to a less viscous state, permitting increased motility (Bansil *et al* 2013). Beyond the traditional associations of the role of urease it is also suggested that it may have additional properties as a major virulence factor, for example it was determined that *H. pylori* urease can trigger processes initiating pro-angiogenic responses in different cellular models. This could be a potential factor in gastric carcinoma development as angiogenesis is required for tumour growth (Olivera-Severo *et al* 2017). In this thesis it was suggested that the downregulation of urease-associated genes *ureA/B/I* may limit *H. pylori*'s ability to protect itself from host-associated acid production within the mucus layer.

5.3.5 Conclusions and Recommendations

The aim of this chapter was to use menadione as a novel agent as it is poorly reported in existing *H. pylori* literature and mimicked a niche stressor as it produces ROS through redox cycling. It was decided that by using a sub-MIC menadione concentration as determined in chapter 4 (results section 4.2.4), treating random samples of 322A, and performing RNA-Seq the potential effects of this novel agent would be uncovered. From the copious amount of data generated by RNA-Seq it was determined through bioinformatics analysis and visualisation that treatment groups (untreated vs treated with menadione) clustered separately from each other. From this 1312 significantly differentially expressed genes were present (adjusted P value <0.005) and gene expression data also clustered by treatment group. Of the 1312 genes the ten most significantly differentially expressed genes were investigated, three of which were particularly interesting. *luxS* that was downregulated and may affect competitive ability and motility. *ruvC* that was downregulated and is thought to be essential for persistent *in*

vivo colonisation. Finally, *cagY* that was upregulated and is thought to work as a biological rheostat to tune the host inflammatory response by modifying the functionality of the *cag* T4SS. The 1312 genes were also mapped against known most significantly differentially expressed biological pathway ‘epithelial cell signalling in *H. pylori* infection’ (35/40 genes). The pathway showed significant differential expression in 24/26 genes of the *cag*PAI and most importantly downregulation of three of the most important virulence factors of *H. pylori* (*cagA*, *vacA* and urease genes *ureA/B/I*). Therefore, in the epithelial cell signalling pathway, it is demonstrated that menadione downregulates *cagA*, that may prevent inhibition of (ZO-1) that maintains tight junction integrity in host epithelial cells. It may also result in the prevention of activating the MAPK signalling pathway, stopping hyperproliferation. It is also demonstrated that menadione downregulates *vacA* that may prevent or reduce ulcerogenesis, vacuolation and apoptosis. Finally, it is demonstrated that menadione downregulates urease group genes *ureA/B/I* may limit *H. pylori*’s ability to protect itself from host-associated acid production within the mucus layer.

The main recommendation as in the previous two chapters relates to sample size. Although there were initially six replicates for each condition (untreated vs menadione treated) one untreated sample was discarded due to second round purity test contamination (U3/ST12) and one treated sample was rejected from transcriptomic analysis as it appeared to be a ‘treated’ sample that was mistakenly not inoculated with menadione (T2/ST9). There was still sufficient sample size to show clustering of the groups however more replicates are always useful to bolster any findings, although in this thesis cost was a prohibitive factor.

Another further piece of work based on this chapter would be to use a strain other than 322A, or multiple strains with replicates in one run cost permitting. Looking at the aims of chapter four and the overall theme of this thesis the best suggestion would be to look at the transcriptomic profile of 322C with the same menadione treatment. This pulls together the novel findings of menadione’s effect on *H. pylori* transcription and the antrum/corpus paired strain comparison previously investigated in this thesis relating to niche adaptation in the stomach.

With the dataset generated by the RNA-Seq in this chapter, further work could look at more of the 1312 significantly differentially expressed genes. Perhaps the best way to pick out genes that are most relevant would be additional pathway over-representation analysis. There were 89 pathways recognised by KEGG that showed significantly differentially expressed genes mapped to them. Epithelial cell signalling in *H. pylori* infection was the most significant and therefore was used for analysis. Although not fully extensive the following pathways in descending order of significance may be of interest (number of significantly differentially expressed genes shown). Oxidative phosphorylation (30/35), Carbon metabolism (41/53), Two-component system (28/32), Flagellar assembly (27/31), LPS biosynthesis (24/27) and Peptidoglycan biosynthesis (14/14) (Full list of $P < 0.01$ pathways shown in table 5.2).

The body of work presented in this chapter clearly provides strong evidence that menadione is a novel agent that downregulates essential components of *H. pylori* that contribute to the pathogenicity and virulence of the organism. Menadione, which has been demonstrated to downregulate *vacA* and translocation of CagA toxin by downregulation of T4SS *cag* pathogenicity island genes previously by RT-PCR (Lee *et al* 2019) has never been used to our knowledge as a treatment condition in *H. pylori* RNA-Sequencing. What this chapter concludes is that the effect of menadione on *H. pylori* is extensive across 89 metabolic pathways. As shown by the 1312 statistically differentially expressed genes, although discussion of this transcriptomic data focussed on key genes (*cagA*, *vacA*, *ureA/B/I*, *luxS*, *ruvC* and *cagY*), there is a wealth of data still untapped that was beyond the scope of this thesis. Given this, and the limited but promising existing work on menadione as a novel antimicrobial, the potential use of this substance may have a vital use in the future of *H. pylori* eradication therapy.

Chapter Six: Final Discussion

6.1 Discussion

The main aim of this thesis was to look at niche adaptation in two closely related organisms that had poorly elucidated explanations for niche differential phenomena that are not fully explored in existing scientific literature. The 403 clonal complex of *C. jejuni* is somewhat of an enigma in the *C. jejuni* field of research. A generalist complex of a multi host species coloniser that has near inability to colonise/persist in chicken hosts, which form the largest zoonotic reservoir in *C. jejuni* transmission, is indeed a mystery in *C. jejuni* inter-host niche adaptation. By the same token intra-host niche adaptation relating to the distinct areas of the stomach (antrum and corpus), although a growing field, is still largely unexplored within *H. pylori*. The methodology employed in both the *C. jejuni* and *H. pylori* main results chapters (chapter three *C. jejuni*, chapter four *H. pylori*) is a comparative perspective, to be true to the main aim of testing bacteria from a different niche. In *C. jejuni* this meant testing the phenotypic and genome content of 403CC strains against chicken isolates phenotypically and generalist isolates genomically. The main two aims with *C. jejuni* were, firstly; to consider whether across these phenotypic assays, there were sufficient differences between 403CC and chicken isolates to explain the observed pattern of differing niche transmission/colonisation between the two groups of strains. Secondly, to compare the genomes of 403CC isolates to ST21/45 generalist isolates. The phenotypic testing of 403CC strains is limited in scientific literature, aside from (Morley 2014) where the only direct overlap in testing between that thesis and this was motility. Further to this there has never been any published work on 403CC strains being directly compared to isolates from the host they have a near inability to colonise. Comparative genome analysis has been performed on 403CC isolates (Morley 2014) but not against a large number of major host generalist isolates. Again, to continue a consistent theme, the *H. pylori* work had similar aims; Firstly, to consider whether across the range of phenotypic assays there are sufficient differences to conclude a pattern of phenotypic variation between isolates from each of the gastric niches. Secondly, to compare gene contents of the genomes of *H. pylori* antrum and corpus isolates. The direct phenotypic

testing of antrum corpus paired isolates could not be found in existing scientific literature other than reports of variance in antibiotic susceptibility profiles between antrum and corpus paired isolates (Selgrad *et al* 2014), which were therefore not performed in this thesis. Genome work has been done at the deep sequencing level using single colony isolates. The work found that there was extensive genetic diversity both within and between the antrum and corpus gastric niches (Wilkinson *et al* 2022). In this thesis a more surface level genome comparison between antrum and corpus paired isolates was conducted.

In chapter three, the phenotypic and genomic comparisons of *C. jejuni* 403CC vs chicken isolates, the aims were not fully met. 403CC isolates performed phenotypically in line with the chicken isolates across a range of assays. Therefore, it could not be determined that across the phenotypic assays there were not sufficient differences between 403CC isolates and chicken isolates to explain the difference in host niche colonisation ability. The main finding in this chapter however was that in a 42°C growth curve, initial growth (6-9 h) was statistically significantly higher in chicken isolates over 403CC isolates ($P < 0.05$). Applying this to a non-experimental setting this may suggest *in vivo* that 403CC may be outcompeted in a chicken host with mixed isolates, and early out competition may result in inability to persist. In the genomic analysis it was found that most key genes associated with phenotypic fitness were present in both 403CC and host generalist datasets. *hha1M*, a modification methylase, was still found to be 403CC exclusive. This is in line with (Morley 2014, Morley *et al* 2015). It was found for the first time that 403CC isolates largely lacked the *panBCD* genes involved in vitamin B5 synthesis (7% presence). This is a strange finding for a lineage that readily colonises cattle as it is suggested that that B5 synthesis is essential in cattle colonisation as the cattle diet (grass grazing) does not provide the necessary nutrients, compared to grain fed chicken (Sheppard *et al* 2015). *fabG* was also absent in the 403CC genome group and this was linked to potentially being a chicken host colonisation factor (Asakura *et al* 2016). The main limitation of this work was the sample size particularly the fact that at the outset three of the proposed chicken isolates intended for use were unrecoverable. Future work would ideally use more 403CC and chicken isolates to bolster any potential findings. To expand upon the 42°C growth finding direct competition between 403CC and chicken isolates would be useful using growth co-culture, however there would have to be an end output that could distinguish between isolates. Genomically 403CC isolate genomes were

compared to those of ST21/45 generalist groups but comparing the 403CC genomes to those from chicken specialist groups may be another approach to gene presence/absence. It may also be interesting to knockout *hha1M* the 403CC exclusive modification methylase and look for recombination events when mixed with other lineages. 403CC is tightly phylogenetically clustered and does not recombine in an inter-lineage fashion (Morley *et al* 2015). Generalist groups do not recombine in nature with each other but do readily recombine with specialist lineages (Sheppard *et al* 2014).

The pubMLST database of 403CC isolates demonstrates that the lineage is capable of colonising many host species as inferred from subsequent isolation. The work done in this thesis would support that. From the observed pattern of phenotypic performance and genome analysis, the 403CC can still comfortably be considered overall a regular generalist lineage. The phenotypic performance suggests that it is perfectly capable, at least *in-vitro*, to perform necessary functions and have the properties required to transmit between and colonise most host species. Other than early impaired growth at 42°C as compared to the chicken isolates used in this thesis, no more evidence phenotypically has come to light on why 403CC isolates are severely restricted from colonisation of a chicken host. There are however examples such as *panBCD* and *fabG* of which are being described as potential host colonisation or host specificity factors that the 403CC isolates greatly or completely lacked. The R-M systems unique to 403CC may be gatekeeping recombination with specialist lineages, especially chicken specialist lineages, which may result in gene gain events that could be advantageous to chicken colonisation/persistence.

In chapter four, the phenotypic and genomic comparisons of *H. pylori* antrum vs corpus paired isolates, the aims were not fully met. Antrum and corpus paired isolates performed similarly across a range the range of phenotypic assays and clustered within strain pair genomically. Therefore, it could not be determined that across the phenotypic assays or genomic analysis there were not sufficient differences between paired isolates from the antrum and corpus gastric niches. Other than studies outlined in this thesis, regarding antibiotic resistance, there was limited antrum/corpus phenotypic study that would support or contradict that certain phenotypic properties may be observable within clinical paired strains. As mentioned in chapter four deep sequencing showed that a lot of allelic variation occurred between clinical strain pairs and this wouldn't necessarily reflect in the phenotype, certainly not to the degree of a gene gain/loss event. The main limitation

of this chapter also was sample size, ideally a lot more than four pairs of antrum/corpus strains would be used. Also, potentially with more time more phenotypic assays would have been conducted as there is evidence of phenotypic differences between antrum corpus paired isolates for example in levels of antibiotic resistance (Selgrad *et al* 2014, Farzi *et al* 2019). Therefore, the recommendations for further work would be additional phenotypic assays using additional niche mimic stressors with a larger number of strains. Antibiotic susceptibility assays may also be interesting although they are already established as often niche differential, it would be interesting to see if this association holds true for the isolate pairs used in this thesis. Finally, a potential method of directed evolution could be developed to look how particular stressors that may reflect the environment within a niche may cause microevolution of the organism (discussed below).

In chapter five, the initial aim was to perform directed evolution on *C. jejuni* and *H. pylori* bringing together a common niche stressor mimicker for both organisms such as an oxidative stress agent, which would be perfect for two microaerophilic organisms. The plan was to do a series of 96-well plate experiments using gradient concentrations of stressor reagent and screening for mutants. Pyrogallol was initially used, but the rapid colour change from clear to dark brown made it impossible to read. Hydrogen peroxide was used but *H. pylori* catalase caused bubbling and ultimately clearance of the broth. It was around this time the work on menadione in chapter three had been completed. As the menadione MIC was consistent across strains it was used, however across approximately 100 replicates no evidence of evolution of resistance was found. Concurrent to this disc diffusion assays using menadione were also performed, to look for colonies in the zone of clearance. Across a number of replicate plates no colonies were observed. RNA-Seq was chosen to be used in conjunction with menadione treatment in *H. pylori*. RNA-Seq is a much better representation of real-world niche changes.

Transient environmental stressors, like in a dynamic environment such as the human stomach, do not always result in mutation. What they often do cause is fluctuation in gene expression in response to a stressor, and RNA-Seq can take a snapshot of this. The findings of this chapter were that exposure to menadione caused 1312 significantly differentially expressed genes in *H. pylori* 322A (adjusted P value <0.05). Treated and untreated menadione groups clustered tightly in principal component analysis and the 1312 genes also clustered by treatment group when visualised on a heatmap. When

mapped to metabolic pathways the most significantly affected pathway was epithelial cell signalling in *H. pylori* infection. Through this and looking at the most significant differentially expressed genes it was shown that *cagA*, *vacA*, *ureA/B/I*, *luxS*, *ruvC* were downregulated and *cagY* were upregulated. These genes are crucial the virulence and pathogenicity of *H. pylori* and in the case of urease genes *ureA/B/I* and *ruvC* potentially essential for persistent colonisation of a host. The limitation of this chapter was again sample size, although there ended up being five treated and five untreated samples that were enough to show distinct clustering more replicates would be of value. Further study would look at more of the 1312 statistically differentially expressed genes perhaps in the context of the 32 remaining most significant metabolic pathways differentially expressed genes mapped to as suggested in chapter four. Following the main theme of this thesis in regard to *H. pylori* (intra host niche adaptation) it would be interesting to repeat the RNA-Seq experiment with the paired isolate 322C. Although they share a very close profile in regard to menadione resistance in chapter four, the whole transcriptional response may not be the same. Overall in this chapter the findings were very positive in the small field of *H. pylori* menadione treatment and the first known application of RNA-Seq in this area.

Despite not being able to draw direct parallels between inter-host niche adaptation in 403CC *C. jejuni* and intra-host niche adaptation in *H. pylori* (antrum vs corpus), the similarities and differences between the organisms are very interesting. The two closely related organisms have many similar properties; Gram-negative, mesophilic, fastidious, gastrointestinal organisms with overall high mutation and recombination rates. Yet the way in which they colonise niches is so dramatically different.

C. jejuni despite being a microaerobic organism has demonstrated the ability to persevere outside of a host organism and can colonise a wide array of host species. Interestingly across the 44 grouped clonal complexes some groups are largely specialist, and overwhelmingly have a single host species as their niche, and some are generalist and are more evenly distributed across several host species. The major concern for humans with *C. jejuni* is introduction into the food chain, predominantly through chicken reservoirs. Described in this thesis is the 403 clonal complex, a group of isolates that have shown near inability to colonise chickens. Initially described as a ‘mammalian associated specialist lineage’ (Morley 2014) this thesis would categorise the 403CC as a generalist

lineage with poor/no niche colonisation ability in chickens. The real-world applications of this study therefore become incredibly intriguing. If we could determine the barrier to colonisation that 403CC isolates face, the potential applications in farm to fork for the poultry industry could be considerable, and subsequently the number of *C. jejuni* infections worldwide.

H. pylori could be considered the most competent coloniser not just between these two organisms but within the bacterial kingdom. However, the niche it inhabits, or subsequently the niches (antrum and corpus), are changing the properties of the initial infecting strain due to the dynamic nature of the stomach, and the inflammatory response caused by *H. pylori* infection itself. The *H. pylori* research community is starting to pay more attention to the fact that antrum/corpus paired isolates do not always have the same properties. As an organism that demands development for new antibiotics due to the alarming rise in clarithromycin resistance, those in the biomedical field now realise that *H. pylori* eradication treatment can fail, based on antrum vs corpus resistance profiles alone (Selgrad *et al* 2014, Farzi *et al* 2019). Even the treatments themselves can change the niche environments, for example the use of Protein Pump Inhibitors (PPI) in antibiotic triple therapy raises stomach pH by reducing acid secretion. This walks a fine line between making the antibiotics more stable, but also causing a higher rate of growth of *H. pylori* by creating a more favourable niche environment (Scott, Sachs & Marcus 2016). Understanding that *H. pylori* infection is much more nuanced, below the tier of mixed isolate cultures or single isolate cultures are antrum and corpus niche isolates, and their differences should not be underestimated.

Niche adaptation should continue to evolve as a field across many bacterial species. This work shows that at least in the scientific enquiry of *C. jejuni* and *H. pylori*, there is still much we do not know.

5.2 Future work

Future work has been suggested in each of the three results chapters and can be summarised here. Given adequate time and further resources the work conducted in this thesis could easily be expanded on. For work in relation to the 403CC of *C. jejuni* there are now two bodies of work that conclude 403CC isolates perform phenotypically in line with other *C. jejuni* isolate groups. However, the number of isolates used is small and work could be scaled up. The work in this thesis did see significance in rapid early growth at 42°C in chicken isolates as compared to 403CC isolates. The relevancy of this *in-vivo* has been discussed and a mixed culture model would assist to observe potential competitive fitness. If possible, it would also be useful to attain one of the five 403 isolates recovered from a chicken, which for the purposes of genomic comparison may be incredibly insightful. It is theorised that R-M systems unique to the 403CC restrict inter-lineage recombination to the point that acquisition of host species colonisation factors are not attainable. *HhaIm* in particular shows up as 403CC exclusive and a knockout of this gene could prove the concept of the almost exclusive intra-lineage recombinant nature of the lineage. It would also be interesting if one of the 403CC chicken isolates have retained *hhaIm* and other parts of the R-M systems found in the lineage.

Work pertaining to comparison of antrum corpus clinical pairs in chapter four did not demonstrate any significant difference across phenotyping testing between antrum and corpus. This chapter would also benefit from scale, as only four antrum/corpus pairs were used. It has been noted throughout that antimicrobial susceptibility has been found in other scientific literature to show observable phenotypic difference between antrum/corpus pairs which guides this thesis in the assertion that further work may find observable antrum/corpus differences when scale is applied. Chapter four also contained the initial work with menadione, which may prove to be an invaluable supplement to *H. pylori* targeted eradication therapy. The MIC's obtained were uniform across all strains but this would also benefit to being applied to a larger strain cohort. Directed evolution using menadione, which would reflect longer exposure than the work conducted in chapter five, may also be a viable future project given time and resources. The existing literature on menadione use against *H. pylori* which now includes this thesis is small but is promising. The compound needs to be tested for toxicity alongside efficacy to determine whether it would be suitable for use in a clinical setting.

Finally, the transcriptomic work in chapter five, application of menadione against *H. pylori* 322A has many avenues for further work. As whole transcriptome sequencing becomes less cost prohibitive the follow-up work for the data presented in this chapter is more viable. It is recognised that further replicates of the initial work on 322A could be done, however ultimately the clustering of samples showed the robustness of the data. Alternatively, the use of other strains is vital to compare transcription profiles of many isolates when treated with menadione. It is suggested that 322C would be one strain that should undergo the sequencing as this would tie-in with the comparison of clinical strain pairs. The transcriptomic data revealed 1312 statistically significantly differentially expressed genes between treatment groups and these were grouped into known metabolic pathways. The most significant pathway “Epithelial cell signalling in *H. pylori* infection” is very important as it largely focusses around *cagA*. In this thesis for the first time it was shown that the gene was downregulated by menadione treatment. What would be useful further work is Western blotting of bacterial cell lysates to prove the reduced gene expression translates to reduced protein production in the cells. There were 33 pathways listed in chapter five were significant to a P value $p < 0.01$ and 89 pathways were significant to $p < 0.05$ as listed in the appendix. Further work based on this is difficult to quantify as all of these pathways could be mapped and be assistive in many areas of the *H. pylori* research community looking at disruption of any of these pathways.

6.3 Conclusion

This thesis looks at niche adaptation events that are poorly characterised in existing scientific literature. Novel approaches have been made to investigate these niche phenomena to provide further insight and potentially inform further areas of research.

The 403CC of *C. jejuni* remains cryptic and needs further investigation, however this thesis presents the first comparative phenotypic work between isolates of the lineage and those isolated from chicken hosts the 403 lineage has a near inability to colonise. The work demonstrates that across a range of tested phenotypic properties 403CC strains behave “typical” of *C. jejuni* isolates. The main finding in this area was a slower initial growth rate at chicken temperatures compared to isolates from chickens. It is now also theorised by comparing 403CC genomes to those of large generalist groups that host

specificity and/or colonisation factors are important for host association and that 403 lineage R-M systems may impede the ability to colonise chicken hosts.

The analysis of *H. pylori* antrum/corpus paired isolates by phenotype is not covered in the existing literature beyond the bounds of antimicrobial susceptibility. Although no significant differences were found in phenotypic performance, this thesis would conclude that looking at paired isolates is essential both for research and clinical practice. Heteroresistance, particularly to clarithromycin, will become an emerging problem as resistance rates continue to rise. An incomplete clinical profile runs the risk of failed eradication therapy without considering variation between the isolates found in both niches of the stomach. There is an increasing wealth of data on the genomes of paired clinical strains, observed microevolution and allelic variation between strains of the antrum and corpus niche. To get a complete picture of how niche environment will play a role in how we subsequently may need to treat *H. pylori* in the future, phenotypic properties must be married with the genomics.

Finally, this thesis demonstrates for the first time the application of novel antimicrobial menadione in whole transcriptome sequencing. Sub MIC levels of menadione caused 1312 significantly differentially expressed genes when compared to an untreated group using the *H. pylori* strain 322A. Due to the enormity of the data these genes were mapped to 89 metabolic pathways that showed statistically significant difference. Much of the analysis focussed on epithelial cell signalling in *H. pylori* infection, which most importantly showed for the first time that *cagA* is downregulated by menadione treatment. The data generated by RNA-Seq is far too large to fit within the scope of this thesis and therefore is recommended to guide future research and clinical study into the application of menadione.

7.0 References

1. Abdullah, M., Greenfield, L. K., Bronte-Tinkew, D., Capurro, M. I., Rizzuti, D., & Jones, N. L. (2019). VacA promotes CagA accumulation in gastric epithelial cells during *Helicobacter pylori* infection. *Scientific Reports*, 9(1), 38-018-37095-4.
2. Afgan, E., Baker, D., Batut, B., van den Beek, M., Bouvier, D., Cech, M., et al. (2018). The galaxy platform for accessible, reproducible and collaborative biomedical analyses: 2018 update. *Nucleic Acids Research*, 46(W1), W537-W544.
3. Ailloud, F., Didelot, X., Woltemate, S., Pfaffinger, G., Overmann, J., Bader, R. C., et al. (2019). Within-host evolution of *Helicobacter pylori* shaped by niche-specific adaptation, intragastric migrations and selective sweeps. *Nature Communications*, 10(1), 2273-019-10050-1.
4. Akada, J. K., Aoki, H., Torigoe, Y., Kitagawa, T., Kurazono, H., Hoshida, H., et al. (2010). *Helicobacter pylori* CagA inhibits endocytosis of cytotoxin VacA in host cells. *Disease Models & Mechanisms*, 3(9-10), 605-617.
5. Alemka, A., Whelan, S., Gough, R., Clyne, M., Gallagher, M. E., Carrington, S. D., et al. (2010). Purified chicken intestinal mucin attenuates *Campylobacter jejuni* pathogenicity in vitro. *Journal of Medical Microbiology*, 59(Pt 8), 898-903.
6. Alemka A, Corcionivoschi N, Bourke B. Defense and adaptation: the complex inter-relationship between *Campylobacter jejuni* and mucus. *Front Cell Infect Microbiol*. 2012;2:15. Published 2012 Feb 20. doi:10.3389/fcimb.2012.00015

7. Alm, R. A., Ling, L. S., Moir, D. T., King, B. L., Brown, E. D., Doig, P. C., et al. (1999). Genomic-sequence comparison of two unrelated isolates of the human gastric pathogen *Helicobacter pylori*. *Nature*, 397(6715), 176-180.
8. Andrade, J. C., Morais Braga, M. F., Guedes, G. M., Tintino, S. R., Freitas, M. A., Quintans, L. J., Jr, et al. (2017). Menadione (vitamin K) enhances the antibiotic activity of drugs by cell membrane permeabilization mechanism. *Saudi Journal of Biological Sciences*, 24(1), 59-64.
9. Andrews, S. (2010). *FastQC: A quality control tool for high throughput sequence data*
10. Araujo, P. M., Batista, E., Fernandes, M. H., Fernandes, M. J., Gama, L. T., & Fraqueza, M. J. (2022). Assessment of biofilm formation by *Campylobacter* spp. isolates mimicking poultry slaughterhouse conditions. *Poultry Science*, 101(2), 101586.
11. Armengod, M. E., Moukadiri, I., Prado, S., Ruiz-Partida, R., Benitez-Paez, A., Villarroya, M., et al. (2012). Enzymology of tRNA modification in the bacterial MnmEG pathway. *Biochimie*, 94(7), 1510-1520.
12. Arnold, M., Park, J. Y., Camargo, M. C., Lunet, N., Forman, D., & Soerjomataram, I. (2020). Is gastric cancer becoming a rare disease? A global assessment of predicted incidence trends to 2035. *Gut*, 69(5), 823-829.
13. Aroori, S. V., Cogan, T. A., & Humphrey, T. J. (2013). The effect of growth temperature on the pathogenicity of *Campylobacter*. *Current Microbiology*, 67(3), 333-340.
14. Asakura, H., Kawamoto, K., Murakami, S., Tachibana, M., Kurazono, H., Makino, S., et al. (2016). Ex vivo proteomics of *Campylobacter jejuni* 81-176 reveal that FabG affects fatty acid composition to alter bacterial growth fitness in the chicken gut. *Research in Microbiology*, 167(2), 63-71.

15. Atack, J. M., Harvey, P., Jones, M. A., & Kelly, D. J. (2008). The *Campylobacter jejuni* thiol peroxidases tpx and bcp both contribute to aerotolerance and peroxide-mediated stress resistance but have distinct substrate specificities. *Journal of Bacteriology*, 190(15), 5279-5290.
16. Atack, J. M., & Kelly, D. J. (2008). Contribution of the stereospecific methionine sulphoxide reductases MsrA and MsrB to oxidative and nitrosative stress resistance in the food-borne pathogen *Campylobacter jejuni*. *Microbiology (Reading, England)*, 154(Pt 8), 2219-2230.
17. Attaran, B., Falsafi, T., & Moghaddam, A. N. (2016). Study of biofilm formation in C57Bl/6J mice by clinical isolates of *Helicobacter pylori*. *Saudi Journal of Gastroenterology : Official Journal of the Saudi Gastroenterology Association*, 22(2), 161-168.
18. Babu Rajendran, N., Mutters, N. T., Marasca, G., Conti, M., Sifakis, F., Vuong, C., et al. (2019). Mandatory surveillance and outbreaks reporting of the WHO priority pathogens for research & discovery of new antibiotics in european countries. *Clinical Microbiology and Infection : The Official Publication of the European Society of Clinical Microbiology and Infectious Diseases*,
19. Backert, S., Tegtmeyer, N., & Fischer, W. (2015). Composition, structure and function of the *Helicobacter pylori* cag pathogenicity island encoded type IV secretion system. *Future Microbiology*, 10(6), 955-965.
20. Baj, J., Korona-Glowniak, I., Forma, A., Maani, A., Sitarz, E., Rahnama-Hezavah, M., et al. (2020). Mechanisms of the epithelial-mesenchymal transition and tumor microenvironment in *Helicobacter pylori*-induced gastric cancer. *Cells*, 9(4), 10.3390/cells9041055.

21. Bankevich, A., Nurk, S., Antipov, D., Gurevich, A. A., Dvorkin, M., Kulikov, A. S., et al. (2012). SPAdes: A new genome assembly algorithm and its applications to single-cell sequencing. *Journal of Computational Biology: A Journal of Computational Molecular Cell Biology*, 19(5), 455-477.
22. Bansil, R., Celli, J. P., Hardcastle, J. M., & Turner, B. S. (2013). The influence of mucus microstructure and rheology in *Helicobacter pylori* infection. *Frontiers in Immunology*, 4, 310.
23. Barrozo, R. M., Cooke, C. L., Hansen, L. M., Lam, A. M., Gaddy, J. A., Johnson, E. M., et al. (2013). Functional plasticity in the type IV secretion system of *Helicobacter pylori*. *PLoS Pathogens*, 9(2), e1003189.
24. Bartpho, T. S., Wattanawongdon, W., Tongtawee, T., Paoin, C., Kangwantas, K., & Dechsukhum, C. (2020). Precancerous gastric lesions with *Helicobacter pylori vacA (+)/babA2(+)/oipA (+)* genotype increase the risk of gastric cancer. *BioMed Research International*, 2020, 7243029.
25. Benoit, S. L., Holland, A. A., Johnson, M. K., & Maier, R. J. (2018). Iron-sulfur protein maturation in *Helicobacter pylori*: Identifying a nfu-type cluster carrier protein and its iron-sulfur protein targets. *Molecular Microbiology*, 108(4), 379-396.
26. Bolinger, H., & Kathariou, S. (2017). The current state of macrolide resistance in *Campylobacter* spp.: Trends and impacts of resistance mechanisms. *Applied and Environmental Microbiology*, 83(12), 10.1128/AEM.00416-17. Print 2017 Jun 15.

27. Bort, B., Marti, P., Mormeneo, S., Mormeneo, M., & Iranzo, M. (2022). Prevalence and antimicrobial resistance of *Campylobacter* spp. isolated from broilers throughout the supply chain in Valencia, Spain. *Foodborne Pathogens and Disease*,
28. Bragazzi, N. L., Kolahi, A. A., Nejadghaderi, S. A., Lochner, P., Brigo, F., Naldi, A., et al. (2021). Global, regional, and national burden of Guillain-Barre syndrome and its underlying causes from 1990 to 2019. *Journal of Neuroinflammation*, *18*(1), 264-021-02319-4.
29. Bridge, D. R., & Merrell, D. S. (2013). Polymorphism in the *Helicobacter pylori* CagA and VacA toxins and disease. *Gut Microbes*, *4*(2), 101-117.
30. Bronowski, C., James, C. E., & Winstanley, C. (2014). Role of environmental survival in transmission of *Campylobacter jejuni*. *FEMS Microbiology Letters*, *356*(1), 8-19.
31. Brynildsrud, O., Bohlin, J., Scheffer, L., & Eldholm, V. (2016). Rapid scoring of genes in microbial pan-genome-wide association studies with scoary. *Genome Biology*, *17*(1), 238-016-1108-8.
32. Buchanan, C. J., Webb, A. L., Mutschall, S. K., Kruczkiewicz, P., Barker, D. O. R., Hetman, B. M., et al. (2017). A genome-wide association study to identify diagnostic markers for human pathogenic *Campylobacter jejuni* strains. *Frontiers in Microbiology*, *8*, 1224.
33. Burgers, R., Schneider-Brachert, W., Reischl, U., Behr, A., Hiller, K. A., Lehn, N., et al. (2008). *Helicobacter pylori* in human oral cavity and stomach. *European Journal of Oral Sciences*, *116*(4), 297-304.
34. Byrne, C. M., Clyne, M., & Bourke, B. (2007). *Campylobacter jejuni* adhere to and invade chicken intestinal epithelial cells in vitro. *Microbiology (Reading, England)*, *153*(Pt 2), 561-569.

35. Carroll, I. M., Ahmed, N., Beesley, S. M., Khan, A. A., Ghousunnissa, S., Morain, C. A. O., et al. (2004). Microevolution between paired antral and paired antrum and corpus *Helicobacter pylori* isolates recovered from individual patients. *Journal of Medical Microbiology*, 53(Pt 7), 669-677.
36. Cawthraw SA, Newell DG. Investigation of the presence and protective effects of maternal antibodies against *Campylobacter jejuni* in chickens. *Avian Dis.* 2010;54(1):86-93. doi:10.1637/9004-072709-Reg.1
37. Chauhan, N., Tay, A. C. Y., Marshall, B. J., & Jain, U. (2019). *Helicobacter pylori* VacA, a distinct toxin exerts diverse functionalities in numerous cells: An overview. *Helicobacter*, 24(1), e12544.
38. Chiou, P. Y., Luo, C. H., Chang, K. C., & Lin, N. T. (2013). Maintenance of the cell morphology by MinC in *Helicobacter pylori*. *PloS One*, 8(8), e71208.
39. Chuang, C. H., Yang, H. B., Sheu, S. M., Hung, K. H., Wu, J. J., Cheng, H. C., et al. (2011). *Helicobacter pylori* with stronger intensity of CagA phosphorylation lead to an increased risk of gastric intestinal metaplasia and cancer. *BMC Microbiology*, 11, 121-2180-11-121.
40. Cole, S. P., Harwood, J., Lee, R., She, R., & Guiney, D. G. (2004). Characterization of monospecies biofilm formation by *Helicobacter pylori*. *Journal of Bacteriology*, 186(10), 3124-3132.
41. Colin, R., Ni, B., Laganenka, L., & Sourjik, V. (2021). Multiple functions of flagellar motility and chemotaxis in bacterial physiology. *FEMS Microbiology Reviews*, 45(6), 10.1093/femsre/fuab038.

42. Connerton, I. F., & Connerton, P. L. (2017). *Campylobacter* Foodborne disease. *Foodborne diseases 3rd edition* (pp. 209-221)
43. Correa, P., & Piazzuelo, M. B. (2011). *Helicobacter pylori* infection and gastric adenocarcinoma. *US Gastroenterology & Hepatology Review*, 7(1), 59-64.
44. Correa, P., & Piazzuelo, M. B. (2012). The gastric precancerous cascade. *Journal of Digestive Diseases*, 13(1), 2-9.
45. Coticchia, J. M., Sugawa, C., Tran, V. R., Gurrola, J., Kowalski, E., & Carron, M. A. (2006). Presence and density of *Helicobacter pylori* biofilms in human gastric mucosa in patients with peptic ulcer disease. *Journal of Gastrointestinal Surgery : Official Journal of the Society for Surgery of the Alimentary Tract*, 10(6), 883-889.
46. Courtois, S., Benejat, L., Izotte, J., Megraud, F., Varon, C., Lehours, P., et al. (2018). Metformin can inhibit *Helicobacter pylori* growth. *Future Microbiology*, 13, 1575-1583.
47. Criddle, D. N., Gillies, S., Baumgartner-Wilson, H. K., Jaffar, M., Chinje, E. C., Passmore, S., et al. (2006). Menadione-induced reactive oxygen species generation via redox cycling promotes apoptosis of murine pancreatic acinar cells. *The Journal of Biological Chemistry*, 281(52), 40485-40492.
48. de Brito, B. B., da Silva, F. A. F., Soares, A. S., Pereira, V. A., Santos, M. L. C., Sampaio, M. M., et al. (2019). Pathogenesis and clinical management of *Helicobacter pylori* gastric infection. *World Journal of Gastroenterology*, 25(37), 5578-5589.
49. de Martel, C., Georges, D., Bray, F., Ferlay, J., & Clifford, G. M. (2020). Global burden of cancer attributable to infections in 2018: A worldwide incidence analysis. *The Lancet.Global Health*, 8(2), e180-e190.

50. de Vries, Stefan P W, Gupta, S., Baig, A., L'Heureux, J., Pont, E., Wolanska, D. P., et al. (2015). Motility defects in *Campylobacter jejuni* defined gene deletion mutants caused by second-site mutations. *Microbiology (Reading, England)*, *161*(12), 2316-2327.
51. Dearlove, B. L., Cody, A. J., Pascoe, B., Meric, G., Wilson, D. J., & Sheppard, S. K. (2016). Rapid host switching in generalist *Campylobacter* strains erodes the signal for tracing human infections. *The ISME Journal*, *10*(3), 721-729.
52. Didelot, X., Nell, S., Yang, I., Woltemate, S., van der Merwe, S., & Suerbaum, S. (2013). Genomic evolution and transmission of *Helicobacter pylori* in two south african families. *Proceedings of the National Academy of Sciences of the United States of America*, *110*(34), 13880-13885.
53. Dingle, K. E., Colles, F. M., Wareing, D. R., Ure, R., Fox, A. J., Bolton, F. E., et al. (2001). Multilocus sequence typing system for *Campylobacter jejuni*. *Journal of Clinical Microbiology*, *39*(1), 14-23.
54. Dixon, M. F., Genta, R. M., Yardley, J. H., & Correa, P. (1996). Classification and grading of gastritis. the updated sydney system. international workshop on the histopathology of gastritis, Houston 1994. *The American Journal of Surgical Pathology*, *20*(10), 1161-1181.
55. Doherty, N. C., Shen, F., Halliday, N. M., Barrett, D. A., Hardie, K. R., Winzer, K., et al. (2010). In *Helicobacter pylori*, LuxS is a key enzyme in cysteine provision through a reverse transsulfuration pathway. *Journal of Bacteriology*, *192*(5), 1184-1192.

56. Duangnumsawang, Y., Zentek, J., & Goodarzi Boroojeni, F. (2021). Development and functional properties of intestinal mucus layer in poultry. *Frontiers in Immunology*, *12*, 745849.
57. Dwivedi, R., Nothaft, H., Garber, J., Xin Kin, L., Stahl, M., Flint, A., et al. (2016). L-fucose influences chemotaxis and biofilm formation in *Campylobacter jejuni*. *Molecular Microbiology*, *101*(4), 575-589.
58. El Khadir, M., Alaoui Boukhris, S., Benajah, D. A., El Rhazi, K., Ibrahimi, S. A., El Abkari, M., et al. (2017). VacA and CagA status as biomarker of two opposite end outcomes of *Helicobacter pylori* infection (gastric cancer and duodenal ulcer) in a Moroccan population. *PloS One*, *12*(1), e0170616.
59. Elgamoudi, B. A., Ketley, J. M., & Korolik, V. (2018). New approach to distinguishing chemoattractants, chemorepellents and catabolised chemoeffectors for *Campylobacter jejuni*. *Journal of Microbiological Methods*, *146*, 83-91.
60. Elgamoudi, B. A., & Korolik, V. (2022). A review of the advantages, disadvantages and limitations of chemotaxis assays for *Campylobacter* spp. *International Journal of Molecular Sciences*, *23*(3), 10.3390/ijms23031576.
61. Eusebi, L. H., Telese, A., Marasco, G., Bazzoli, F., & Zagari, R. M. (2020). Gastric cancer prevention strategies: A global perspective. *Journal of Gastroenterology and Hepatology*,
62. Farhadkhani, M., Nikaeen, M., Hassanzadeh, A., & Nikmanesh, B. (2019). Potential transmission sources of *Helicobacter pylori* infection: Detection of *H. pylori* in various environmental samples. *Journal of Environmental Health Science & Engineering*, *17*(1), 129-134.

63. Farzi, N., Behzad, C., Hasani, Z., Alebouyeh, M., Zojaji, H., & Zali, M. R. (2019). Characterization of clarithromycin heteroresistance among *Helicobacter pylori* strains isolated from the antrum and corpus of the stomach. *Folia Microbiologica*, 64(2), 143-151.
64. Fauzia, K. A., Miftahussurur, M., Syam, A. F., Waskito, L. A., Doohan, D., Rezkitha, Y. A. A., et al. (2020). Biofilm formation and antibiotic resistance phenotype of *Helicobacter pylori* clinical isolates. *Toxins*, 12(8), 10.3390/toxins12080473.
65. Feng, J., Lamour, G., Xue, R., Mirvakliki, M. N., Hatzikiriakos, S. G., Xu, J., et al. (2016). Chemical, physical and morphological properties of bacterial biofilms affect survival of encased *Campylobacter jejuni* F38011 under aerobic stress. *International Journal of Food Microbiology*, 238, 172-182.
66. Ferwana, M., Abdulmajeed, I., Alhajahmed, A., Madani, W., Firwana, B., Hasan, R., et al. (2015). Accuracy of urea breath test in *Helicobacter pylori* infection: Meta-analysis. *World Journal of Gastroenterology*, 21(4), 1305-1314.
67. Flint, A., Stintzi, A., & Saraiva, L. M. (2016). Oxidative and nitrosative stress defences of *Helicobacter* and *Campylobacter* species that counteract mammalian immunity. *FEMS Microbiology Reviews*, 40(6), 938-960.
68. Flint, A., Sun, Y. Q., Butcher, J., Stahl, M., Huang, H., & Stintzi, A. (2014). Phenotypic screening of a targeted mutant library reveals *Campylobacter jejuni* defenses against oxidative stress. *Infection and Immunity*, 82(6), 2266-2275.
69. Garber, J. M., Nothaft, H., Pluvinaige, B., Stahl, M., Bian, X., Porfirio, S., et al. (2020). The gastrointestinal pathogen *Campylobacter jejuni* metabolizes sugars with potential help from commensal *Bacteroides vulgatus*. *Communications Biology*, 3(1), 2-019-0727-5.

70. Garvis, S., Munder, A., Ball, G., de Bentzmann, S., Wiehlmann, L., Ewbank, J. J., et al. (2009). *Caenorhabditis elegans* semi-automated liquid screen reveals a specialized role for the chemotaxis gene cheB2 in *Pseudomonas aeruginosa* virulence. *PLoS Pathogens*, 5(8), e1000540.
71. Gebara, E. C., Faria, C. M., Pannuti, C., Chehter, L., Mayer, M. P., & Lima, L. A. (2006). Persistence of *Helicobacter pylori* in the oral cavity after systemic eradication therapy. *Journal of Clinical Periodontology*, 33(5), 329-333.
72. Gisbert, J. P., Arata, I. G., Boixeda, D., Barba, M., Canton, R., Plaza, A. G., et al. (2002). Role of partner's infection in reinfection after *Helicobacter pylori* eradication. *European Journal of Gastroenterology & Hepatology*, 14(8), 865-871.
73. Goodwin, C. S., Armstrong, J. A., Chilvers, T., Peters, M., Collins, D., Sly, L., et al. (1989). Transfer of *Campylobacter pylori* and *Campylobacter mustelae* to *Helicobacter* gen. nov. as *Helicobacter pylori* comb. nov. and *Helicobacter mustelae* comb. nov. respectively *International Journal of Systematic Bacteriology*, 39(4), 397-405.
74. Gu, H. (2017). Role of flagella in the pathogenesis of *Helicobacter pylori*. *Current Microbiology*, 74(7), 863-869.
75. Gundogdu, O., da Silva, D. T., Mohammad, B., Elmi, A., Wren, B. W., van Vliet, A. H., et al. (2016). The *Campylobacter jejuni* oxidative stress regulator RrpB is associated with a genomic hypervariable region and altered oxidative stress resistance. *Frontiers in Microbiology*, 7, 2117.

76. Habib, I., Uyttendaele, M., & De Zutter, L. (2010). Survival of poultry-derived *Campylobacter jejuni* of multilocus sequence type clonal complexes 21 and 45 under freeze, chill, oxidative, acid and heat stresses. *Food Microbiology*, 27(6), 829-834.
77. Haigh, R. D., & Ketley, J. M. (2011). Growth of *Campylobacter* using a microplate reader equipped with ACU. *University of Leicester*,
78. Hara-Kudo, Y., & Takatori, K. (2011). Contamination level and ingestion dose of foodborne pathogens associated with infections. *Epidemiology and Infection*, 139(10), 1505-1510.
79. Harris, A. G., Wilson, J. E., Danon, S. J., Dixon, M. F., Donegan, K., & Hazell, S. L. (2003). Catalase (KatA) and KatA-associated protein (KapA) are essential to persistent colonization in the *Helicobacter pylori* SS1 mouse model. *Microbiology (Reading, England)*, 149(Pt 3), 665-672.
80. Hathroubi, S., Servetas, S. L., Windham, I., Merrell, D. S., & Ottemann, K. M. (2018). *Helicobacter pylori* biofilm formation and its potential role in pathogenesis. *Microbiology and Molecular Biology Reviews: MMBR*, 82(2), 10.1128/MMBR.00001-18. Print 2018 Jun.
81. He, Y., Frye, J. G., Strobaugh, T. P., & Chen, C. (2008). Analysis of AI-2/LuxS-dependent transcription in *Campylobacter jejuni* strain 81-176. *Foodborne Pathogens and Disease*, 5(4), 399-415.
82. Hendrixson, D. R., & DiRita, V. J. (2004). Identification of *Campylobacter jejuni* genes involved in commensal colonization of the chick gastrointestinal tract. *Molecular Microbiology*, 52(2), 471-484.

83. Hermans, D., Van Deun, K., Martel, A., Van Immerseel, F., Messens, W., Heyndrickx, M., et al. (2011). Colonization factors of *Campylobacter jejuni* in the chicken gut. *Veterinary Research*, 42, 82-9716-42-82.
84. Ho, T. W., McKhann, G. M., & Griffin, J. W. (1998). Human autoimmune neuropathies. *Annual Review of Neuroscience*, 21, 187-226.
85. Hofreuter, D., Tsai, J., Watson, R. O., Novik, V., Altman, B., Benitez, M., et al. (2006). Unique features of a highly pathogenic *Campylobacter jejuni* strain. *Infection and Immunity*, 74(8), 4694-4707.
86. Humphrey S, Chaloner G, Kemmett K, et al. *Campylobacter jejuni* is not merely a commensal in commercial broiler chickens and affects bird welfare. *mBio*. 2014;5(4):e01364-14. Published 2014 Jul 1. doi:10.1128/mBio.01364-14
87. Huang, Y., Wang, Q. L., Cheng, D. D., Xu, W. T., & Lu, N. H. (2016). Adhesion and invasion of gastric mucosa epithelial cells by *Helicobacter pylori*. *Frontiers in Cellular and Infection Microbiology*, 6, 159.
88. Huizinga, R., van den Berg, B., van Rijs, W., Tio-Gillen, A. P., Fokkink, W. J., Bakker-Jonges, L. E., et al. (2015). Innate immunity to *Campylobacter jejuni* in Guillain-Barre syndrome. *Annals of Neurology*, 78(3), 343-354.
89. Ica, T., Caner, V., Istanbulu, O., Nguyen, H. D., Ahmed, B., Call, D. R., et al. (2012). Characterization of mono- and mixed-culture *Campylobacter jejuni* biofilms. *Applied and Environmental Microbiology*, 78(4), 1033-1038.
90. Igwaran, A., & Okoh, A. I. (2019). Human campylobacteriosis: A public health concern of global importance. *Heliyon*, 5(11), e02814.
91. Iost, I., Chabas, S., & Darfeuille, F. (2019). Maturation of atypical ribosomal RNA precursors in *Helicobacter pylori*. *Nucleic Acids Research*, 47(11), 5906-5921.

92. Jang, S., Jones, K. R., Olsen, C. H., Joo, Y. M., Yoo, Y. J., Chung, I. S., et al. (2010). Epidemiological link between gastric disease and polymorphisms in VacA and CagA. *Journal of Clinical Microbiology*, *48*(2), 559-567.
93. Johnson, K. S., & Ottemann, K. M. (2018). Colonization, localization, and inflammation: The roles of *H. pylori* chemotaxis *in vivo*. *Current Opinion in Microbiology*, *41*, 51-57.
94. Jolley, K. A., Bray, J. E., & Maiden, M. C. J. (2018). Open-access bacterial population genomics: BIGSdb software, the PubMLST.org website and their applications. *Wellcome Open Research*, *3*, 124.
95. Jones, F. S., Orcutt, M., & Little, R. B. (1931). Vibrios (*Vibrio jejuni*, N.sp.) associated with intestinal disorders of cows and calves. *The Journal of Experimental Medicine*, *53*(6), 853-863.
96. Jones, M. A., Marston, K. L., Woodall, C. A., Maskell, D. J., Linton, D., Karlyshev, A. V., et al. (2004). Adaptation of *Campylobacter jejuni* NCTC11168 to high-level colonization of the avian gastrointestinal tract. *Infection and Immunity*, *72*(7), 3769-3776.
97. Joo, J. S., Park, K. C., Song, J. Y., Kim, D. H., Lee, K. J., Kwon, Y. C., et al. (2010). A thin-layer liquid culture technique for the growth of *Helicobacter pylori*. *Helicobacter*, *15*(4), 295-302.
98. Kaakoush, N. O., Castano-Rodriguez, N., Mitchell, H. M., & Man, S. M. (2015). Global epidemiology of *Campylobacter* infection. *Clinical Microbiology Reviews*, *28*(3), 687-720.

99. Kabir, S. M. L., Chowdhury, N., Asakura, M., Shiramaru, S., Kikuchi, K., Hinenoya, A., et al. (2019). Comparison of established PCR assays for accurate identification of *Campylobacter jejuni* and *Campylobacter coli*. *Japanese Journal of Infectious Diseases*, 72(2), 81-87.
100. Kamata, K., & Tokuda, Y. (2014). Rapid diagnosis of *Campylobacter jejuni* by stool gram stain examination. *BMJ Case Reports*, 2014, 10.1136/bcr-2013-202876.
101. Kamogawa-Schifter, Y., Yamaoka, Y., Uchida, T., Beer, A., Tribl, B., Schoniger-Hekele, M., et al. (2018). Prevalence of *Helicobacter pylori* and its CagA subtypes in gastric cancer and duodenal ulcer at an Austrian tertiary referral center over 25 years. *PloS One*, 13(5), e0197695.
102. Kanehisa, M., & Goto, S. (2000). KEGG: Kyoto encyclopedia of genes and genomes. *Nucleic Acids Research*, 28(1), 27-30.
103. Kayali, S., Manfredi, M., Gaiani, F., Bianchi, L., Bizzarri, B., Leandro, G., et al. (2018). *Helicobacter pylori*, transmission routes and recurrence of infection: State of the art. *Acta Bio-Medica: Atenei Parmensis*, 89(8-S), 72-76.
104. Keilberg, D., Steele, N., Fan, S., Yang, C., Zavros, Y., & Ottemann, K. M. (2021). Gastric metabolomics detects *Helicobacter pylori* correlated loss of numerous metabolites in both the corpus and antrum. *Infection and Immunity*, 89(2), 10.1128/IAI.00690-20. Print 2021 Jan 19.
105. Kenyon, J., Inns, T., Aird, H., Swift, C., Astbury, J., Forester, E., et al. (2020). *Campylobacter* outbreak associated with raw drinking milk, north west england, 2016. *Epidemiology and Infection*, 148, e13.

106. Kim, D., Paggi, J. M., Park, C., Bennett, C., & Salzberg, S. L. (2019). Graph-based genome alignment and genotyping with HISAT2 and HISAT-genotype. *Nature Biotechnology*, *37*(8), 907-915.
107. Klancnik, A., Vuckovic, D., Jamnik, P., Abram, M., & Mozina, S. S. (2014). Stress response and virulence of heat-stressed *Campylobacter jejuni*. *Microbes and Environments*, *29*(4), 338-345.
108. Krzyzek, P., Grande, R., Migdal, P., Paluch, E., & Gosciniak, G. (2020). Biofilm formation as a complex result of virulence and adaptive responses of *Helicobacter pylori*. *Pathogens (Basel, Switzerland)*, *9*(12), 10.3390/pathogens9121062.
109. Lackner, J., Schlichting, D., Muller-Graf, C., & Greiner, M. (2019). Systematic review of the burden of *Campylobacter*-associated disease. [Systematischer Review zur Krankheitslast durch *Campylobacter* spp] *Gesundheitswesen (Bundesverband Der Arzte Des Offentlichen Gesundheitsdienstes (Germany))*, *81*(7), e110-e120.
110. Lake, R. J., Campbell, D. M., Hathaway, S. C., Ashmore, E., Cressey, P. J., Horn, B. J., et al. (2021). Source attributed case-control study of campylobacteriosis in New Zealand. *International Journal of Infectious Diseases : IJID : Official Publication of the International Society for Infectious Diseases*, *103*, 268-277.
111. Larson, C. L., Shah, D. H., Dhillon, A. S., Call, D. R., Ahn, S., Haldorson, G. J., et al. (2008). *Campylobacter jejuni* invade chicken LMH cells inefficiently and stimulate differential expression of the chicken CXCLi1 and CXCLi2 cytokines. *Microbiology* *154*, 3835–3847. doi: 10.1099/mic.0.2008/ 021279-0
112. Lee, K. H., Kim, J. Y., Kim, W. K., Shin, D. H., Choi, K. U., Kim, D. W., et al. (2011). Protective effect of rebamipide against *Helicobacter pylori*-CagA-induced effects on gastric epithelial cells. *Digestive Diseases and Sciences*, *56*(2), 441-448.

113. Lee, M. H., Yang, J. Y., Cho, Y., Woo, H. J., Kwon, H. J., Kim, D. H., et al. (2019). Inhibitory effects of menadione on *Helicobacter pylori* growth and *Helicobacter pylori*-induced inflammation via NF-kappaB inhibition. *International Journal of Molecular Sciences*, 20(5), 10.3390/ijms20051169.
114. Lee, S. Y., Moon, H. W., Hur, M., & Yun, Y. M. (2015). Validation of western *Helicobacter pylori* IgG antibody assays in Korean adults. *Journal of Medical Microbiology*, 64(Pt 5), 513-518.
115. Lee, W. K., Ogura, K., Loh, J. T., Cover, T. L., & Berg, D. E. (2006). Quantitative effect of *luxS* gene inactivation on the fitness of *Helicobacter pylori*. *Applied and Environmental Microbiology*, 72(10), 6615-6622.
116. Lee, Y. C., Chen, T. H., Chiu, H. M., Shun, C. T., Chiang, H., Liu, T. Y., et al. (2013). The benefit of mass eradication of *Helicobacter pylori* infection: A community-based study of gastric cancer prevention. *Gut*, 62(5), 676-682.
117. Lee, Y. C., Chiang, T. H., Liou, J. M., Chen, H. H., Wu, M. S., & Graham, D. Y. (2016). Mass eradication of *Helicobacter pylori* to prevent gastric cancer: Theoretical and practical considerations. *Gut and Liver*, 10(1), 12-26.
118. Lertsethtakarn, P., Ottemann, K. M., & Hendrixson, D. R. (2011). Motility and chemotaxis in *Campylobacter* and *Helicobacter*. *Annual Review of Microbiology*, 65, 389-410.
119. Liao, Y., Smyth, G. K., & Shi, W. (2014). featureCounts: An efficient general-purpose program for assigning sequence reads to genomic features. *Bioinformatics (Oxford, England)*, 30(7), 923-930.
120. Lin, L. F., Posfai, J., Roberts, R. J., & Kong, H. (2001). Comparative genomics of the restriction-modification systems in *Helicobacter pylori*. *Proceedings of the National Academy of Sciences of the United States of America*, 98(5), 2740-2745.

121. Lin, T. F., & Hsu, P. I. (2018). Second-line rescue treatment of *Helicobacter pylori* infection: Where are we now? *World Journal of Gastroenterology*, *24*(40), 4548-4553.
122. Liu, H., Wu, J., Lin, X. C., Wei, N., Lin, W., Chang, H., et al. (2014). Evaluating the diagnoses of gastric antral lesions using magnifying endoscopy with narrow-band imaging in a Chinese population. *Digestive Diseases and Sciences*, *59*(7), 1513-1519.
123. Loh, J. T., Beckett, A. C., Scholz, M. B., & Cover, T. L. (2018). High-salt conditions alter transcription of *Helicobacter pylori* genes encoding outer membrane proteins. *Infection and Immunity*, *86*(3), 10.1128/IAI.00626-17. Print 2018 Mar.
124. Looft, T., Cai, G., Choudhury, B., Lai, L. X., Lippolis, J. D., Reinhardt, T. A., et al. (2019). Avian intestinal mucus modulates *Campylobacter jejuni* gene expression in a host-specific manner. *Frontiers in Microbiology*, *9*, 3215.
125. Loughlin, M. F., Barnard, F. M., Jenkins, D., Sharples, G. J., & Jenks, P. J. (2003). *Helicobacter pylori* mutants defective in RuvC holliday junction resolvase display reduced macrophage survival and spontaneous clearance from the murine gastric mucosa. *Infection and Immunity*, *71*(4), 2022-2031.
126. Love, M. I., Huber, W., & Anders, S. (2014). Moderated estimation of fold change and dispersion for RNA-seq data with DESeq2. *Genome Biology*, *15*(12), 550-014-0550-8.
127. Luning, G. (1989). *Campylobacter pylori* becomes *Helicobacter pylori*. *Lancet (London, England)*, *2*(8670), 1019-1020.

128. Lynch, C. T., Lynch, H., Egan, J., Whyte, P., Bolton, D., Coffey, A., et al. (2020). Antimicrobial resistance of *Campylobacter* isolates recovered from broilers in the republic of Ireland in 2017 and 2018: An update. *British Poultry Science*, , 1-7.
129. Ma, L., Feng, J., Zhang, J., & Lu, X. (2022). *Campylobacter* biofilms. *Microbiological Research*, 264, 127149.
130. Magira, E. E., Papaioakim, M., Nachamkin, I., Asbury, A. K., Li, C. Y., Ho, T. W., et al. (2003). Differential distribution of HLA-DQ beta/DR beta epitopes in the two forms of Guillain-Barre syndrome, acute motor axonal neuropathy and acute inflammatory demyelinating polyneuropathy (AIDP): Identification of DQ beta epitopes associated with susceptibility to and protection from AIDP. *Journal of Immunology (Baltimore, Md.: 1950)*, 170(6), 3074-3080.
131. Magnelli, L., Schiavone, N., Staderini, F., Biagioni, A., & Papucci, L. (2020). MAP kinases pathways in gastric cancer. *International Journal of Molecular Sciences*, 21(8), 10.3390/ijms21082893.
132. Maleki Kakelar, H., Barzegari, A., Dehghani, J., Hanifian, S., Saeedi, N., Barar, J., et al. (2019). Pathogenicity of *Helicobacter pylori* in cancer development and impacts of vaccination. *Gastric Cancer : Official Journal of the International Gastric Cancer Association and the Japanese Gastric Cancer Association*, 22(1), 23-36.
133. Man, S. M. (2011). The clinical importance of emerging *Campylobacter* species. *Nature Reviews.Gastroenterology & Hepatology*, 8(12), 669-685.
134. Manning, G., Dowson, C. G., Bagnall, M. C., Ahmed, I. H., West, M., & Newell, D. G. (2003). Multilocus sequence typing for comparison of veterinary and human isolates of *Campylobacter jejuni*. *Applied and Environmental Microbiology*, 69(11), 6370-6379.

135. Marcus, E. A., Sachs, G., & Scott, D. R. (2018). Acid-regulated gene expression of *Helicobacter pylori*: Insight into acid protection and gastric colonization. *Helicobacter*, 23(3), e12490.
136. Marshall, B. J., Armstrong, J. A., McGeachie, D. B., & Glancy, R. J. (1985). Attempt to fulfil Koch's postulates for pyloric *Campylobacter*. *The Medical Journal of Australia*, 142(8), 436-439.
137. Matilla, M. A., & Krell, T. (2018). The effect of bacterial chemotaxis on host infection and pathogenicity. *FEMS Microbiology Reviews*, 42(1), 10.1093/femsre/fux052.
138. Medema, G. J., Teunis, P. F., Havelaar, A. H., & Haas, C. N. (1996). Assessment of the dose-response relationship of *Campylobacter jejuni*. *International Journal of Food Microbiology*, 30(1-2), 101-111.
139. Mentis, A., Lehours, P., & Megraud, F. (2015). Epidemiology and diagnosis of *Helicobacter pylori* infection. *Helicobacter*, 20 Suppl 1, 1-7.
140. Miftahussurur, M., Waskito, L. A., Syam, A. F., Nusi, I. A., Wibawa, I. D. N., Rezkitha, Y. A. A., et al. (2019). Analysis of risks of gastric cancer by gastric mucosa among Indonesian ethnic groups. *PloS One*, 14(5), e0216670.
141. Mobley, H. L. T. (2001). Urease. In H. L. T. Mobley, G. L. Mendz & S. L. Hazell (Eds.), *Helicobacter pylori: Physiology and genetics* (). Washington (DC): ASM Press.
142. Moghadam, M. T., Chegini, Z., Khoshbayan, A., Farahani, I., & Shariati, A. (2021). *Helicobacter pylori* biofilm and new strategies to combat it. *Current Molecular Medicine*, 21(7), 549-561.

143. Moller, H., Heseltine, E., & Vainio, H. (1995). Working group report on schistosomes, liver flukes and *Helicobacter pylori*. *International Journal of Cancer*, 60(5), 587-589.
144. Montano, V., Didelot, X., Foll, M., Linz, B., Reinhardt, R., Suerbaum, S., et al. (2015). Worldwide population structure, long-term demography, and local adaptation of *Helicobacter pylori*. *Genetics*, 200(3), 947-963.
145. Morelli, G., Didelot, X., Kusecek, B., Schwarz, S., Bahlawane, C., Falush, D., et al. (2010). Microevolution of *Helicobacter pylori* during prolonged infection of single hosts and within families. *PLoS Genetics*, 6(7), e1001036.
146. Morley, L. (2014). *Niche adaptive evolution in Campylobacter jejuni*. Unpublished PhD Thesis, Nottingham Trent University,
147. Morley, L., McNally, A., Paszkiewicz, K., Corander, J., MERIC, G., Sheppard, S. K., et al. (2015). Gene loss and lineage-specific restriction-modification systems associated with niche differentiation in the *Campylobacter jejuni* sequence type 403 clonal complex. *Applied and Environmental Microbiology*, 81(11), 3641-3647.
148. Mourkas, E., Taylor, A. J., MERIC, G., Bayliss, S. C., Pascoe, B., Mageiros, L., et al. (2020). Agricultural intensification and the evolution of host specialism in the enteric pathogen campylobacter jejuni. *Proceedings of the National Academy of Sciences of the United States of America*, 117(20), 11018-11028.
149. Muller, A. (2012). Multistep activation of the *Helicobacter pylori* effector CagA. *The Journal of Clinical Investigation*, 122(4), 1192-1195.
150. Nakajima, K., Inatsu, S., Mizote, T., Nagata, Y., Aoyama, K., Fukuda, Y., et al. (2008). Possible involvement of *putA* gene in *Helicobacter pylori* colonization in the stomach and motility. *Biomedical Research (Tokyo, Japan)*, 29(1), 9-18.

151. Nakamura, S., & Matsumoto, T. (2013). *Helicobacter pylori* and gastric mucosa-associated lymphoid tissue lymphoma: Recent progress in pathogenesis and management. *World Journal of Gastroenterology*, *19*(45), 8181-8187.
152. Narayanan, M., Reddy, K. M., & Marsicano, E. (2018). Peptic ulcer disease and *Helicobacter pylori* infection. *Missouri Medicine*, *115*(3), 219-224.
153. Neal-McKinney, J. M., Christensen, J. E., & Konkel, M. E. (2010). Amino-terminal residues dictate the export efficiency of the *Campylobacter jejuni* filament proteins via the flagellum. *Molecular Microbiology*, *76*(4), 918-931.
154. Oderda, G., Rapa, A., Ronchi, B., Lerro, P., Pastore, M., Staiano, A., et al. (2000). Detection of *Helicobacter pylori* in stool specimens by non-invasive antigen enzyme immunoassay in children: Multicentre italian study. *BMJ (Clinical Research Ed.)*, *320*(7231), 347-348.
155. Oh, E., Andrews, K. J., McMullen, L. M., & Jeon, B. (2019). Tolerance to stress conditions associated with food safety in *Campylobacter jejuni* strains isolated from retail raw chicken. *Scientific Reports*, *9*(1), 11915-019-48373-0.
156. Oh, E., Kim, J. C., & Jeon, B. (2016). Stimulation of biofilm formation by oxidative stress in *Campylobacter jejuni* under aerobic conditions. *Virulence*, *7*(7), 846-851.
157. Oh, E., McMullen, L., & Jeon, B. (2015). Impact of oxidative stress defense on bacterial survival and morphological change in *Campylobacter jejuni* under aerobic conditions. *Frontiers in Microbiology*, *6*, 295.

158. Oldani, A., Cormont, M., Hofman, V., Chiozzi, V., Oregioni, O., Canonici, A., et al. (2009). *Helicobacter pylori* counteracts the apoptotic action of its VacA toxin by injecting the CagA protein into gastric epithelial cells. *PLoS Pathogens*, 5(10), e1000603.
159. Olivera-Severo, D., Uberti, A. F., Marques, M. S., Pinto, M. T., Gomez-Lazaro, M., Figueiredo, C., et al. (2017). A new role for *Helicobacter pylori* urease: Contributions to angiogenesis. *Frontiers in Microbiology*, 8, 1883.
160. Osaki, T., Hanawa, T., Manzoku, T., Fukuda, M., Kawakami, H., Suzuki, H., et al. (2006). Mutation of *luxS* affects motility and infectivity of *Helicobacter pylori* in gastric mucosa of a mongolian gerbil model. *Journal of Medical Microbiology*, 55(Pt 11), 1477-1485.
161. Ottemann, K. M., & Lowenthal, A. C. (2002). *Helicobacter pylori* uses motility for initial colonization and to attain robust infection. *Infection and Immunity*, 70(4), 1984-1990.
162. Page, A. J., Cummins, C. A., Hunt, M., Wong, V. K., Reuter, S., Holden, M. T., et al. (2015). Roary: Rapid large-scale prokaryote pan genome analysis. *Bioinformatics (Oxford, England)*, 31(22), 3691-3693.
163. Palatinus, J. A., O'Quinn, M. P., Barker, R. J., Harris, B. S., Jourdan, J., & Gourdie, R. G. (2011). ZO-1 determines adherens and gap junction localization at intercalated disks. *American Journal of Physiology. Heart and Circulatory Physiology*, 300(2), H583-94.
164. Palrasu, M., Zaika, E., El-Rifai, W., Garcia-Buitrago, M., Piazuolo, M. B., Wilson, K. T., et al. (2020). Bacterial CagA protein compromises tumor suppressor mechanisms in gastric epithelial cells. *The Journal of Clinical Investigation*, 130(5), 2422-2434.

165. Park, B. S., Lee, H. K., Lee, S. E., Piao, X. L., Takeoka, G. R., Wong, R. Y., et al. (2006). Antibacterial activity of *tabebuia impetiginosa martius ex DC* (taheebo) against *Helicobacter pylori*. *Journal of Ethnopharmacology*, *105*(1-2), 255-262.
166. Parker, C. T., Quinones, B., Miller, W. G., Horn, S. T., & Mandrell, R. E. (2006). Comparative genomic analysis of *Campylobacter jejuni* strains reveals diversity due to genomic elements similar to those present in *C. jejuni* strain RM1221. *Journal of Clinical Microbiology*, *44*(11), 4125-4135.
167. Parkhill, J., Wren, B. W., Mungall, K., Ketley, J. M., Churcher, C., Basham, D., et al. (2000). The genome sequence of the food-borne pathogen *Campylobacter jejuni* reveals hypervariable sequences. *Nature*, *403*(6770), 665-668.
168. Parkin, D. M. (2006). The global health burden of infection-associated cancers in the year 2002. *International Journal of Cancer*, *118*(12), 3030-3044.
169. Pascoe, B., Meric, G., Murray, S., Yahara, K., Mageiros, L., Bowen, R., et al. (2015). Enhanced biofilm formation and multi-host transmission evolve from divergent genetic backgrounds in *Campylobacter jejuni*. *Environmental Microbiology*, *17*(11), 4779-4789.
170. Pascoe, B., Williams, L. K., Calland, J. K., Meric, G., Hitchings, M. D., Dyer, M., et al. (2019). Domestication of *Campylobacter jejuni* NCTC 11168. *Microbial Genomics*, *5*(7), 10.1099/mgen.0.000279. Epub 2019 Jul 16.
171. Patel, S. K., Pratap, C. B., Jain, A. K., Gulati, A. K., & Nath, G. (2014). Diagnosis of *Helicobacter pylori*: What should be the gold standard? *World Journal of Gastroenterology*, *20*(36), 12847-12859.

172. Peiffer, S., Pelton, M., Keeney, L., Kwon, E. G., Ofosu-Okromah, R., Acharya, Y., et al. (2020). Risk factors of perioperative mortality from complicated peptic ulcer disease in Africa: Systematic review and meta-analysis. *BMJ Open Gastroenterology*, 7(1), e000350.
173. Peleteiro, B., Bastos, A., Ferro, A., & Lunet, N. (2014). Prevalence of *Helicobacter pylori* infection worldwide: A systematic review of studies with national coverage. *Digestive Diseases and Sciences*, 59(8), 1698-1709.
174. Percival, S. L., & Thomas, J. G. (2009). Transmission of *Helicobacter pylori* and the role of water and biofilms. *Journal of Water and Health*, 7(3), 469-477.
175. Raju, D., Hussey, S., Ang, M., Terebiznik, M. R., Sibony, M., Galindo-Mata, E., et al. (2012). Vacuolating cytotoxin and variants in Atg16L1 that disrupt autophagy promote *Helicobacter pylori* infection in humans. *Gastroenterology*, 142(5), 1160-1171.
176. Rapp D, Ross C, Hea SY, Brightwell G. Importance of the Farm Environment and Wildlife for Transmission of *Campylobacter jejuni* in A Pasture-Based Dairy Herd. *Microorganisms*. 2020;8(12):1877. Published 2020 Nov 27. doi:10.3390/microorganisms8121877
177. Reuter, M., Mallett, A., Pearson, B. M., & van Vliet, A. H. (2010). Biofilm formation by *Campylobacter jejuni* is increased under aerobic conditions. *Applied and Environmental Microbiology*, 76(7), 2122-2128.
178. Rolig, A. S., Shanks, J., Carter, J. E., & Ottemann, K. M. (2012). *Helicobacter pylori* requires TlpD-driven chemotaxis to proliferate in the antrum. *Infection and Immunity*, 80(10), 3713-3720.

179. Saenz, J. B., & Mills, J. C. (2018). Acid and the basis for cellular plasticity and reprogramming in gastric repair and cancer. *Nature Reviews.Gastroenterology & Hepatology*, *15*(5), 257-273.
180. Sahin O, Luo N, Huang S, Zhang Q. Effect of Campylobacter-specific maternal antibodies on *Campylobacter jejuni* colonization in young chickens. *Appl Environ Microbiol.* 2003;69(9):5372-5379. doi:10.1128/AEM.69.9.5372-5379.2003
181. Savoldi, A., Carrara, E., Graham, D. Y., Conti, M., & Tacconelli, E. (2018). Prevalence of antibiotic resistance in *Helicobacter pylori*: A systematic review and meta-analysis in world health organization regions. *Gastroenterology*, *155*(5), 1372-1382.e17.
182. Schlievert, P. M., Merriman, J. A., Salgado-Pabon, W., Mueller, E. A., Spaulding, A. R., Vu, B. G., et al. (2013). Menaquinone analogs inhibit growth of bacterial pathogens. *Antimicrobial Agents and Chemotherapy*, *57*(11), 5432-5437.
183. Schwarz, S., Morelli, G., Kusecek, B., Manica, A., Balloux, F., Owen, R. J., et al. (2008). Horizontal versus familial transmission of *Helicobacter pylori*. *PLoS Pathogens*, *4*(10), e1000180.
184. Schwarzer, C., Fischer, H., & Machen, T. E. (2016). Chemotaxis and binding of *Pseudomonas aeruginosa* to scratch-wounded human cystic fibrosis airway epithelial cells. *PloS One*, *11*(3), e0150109.
185. Scott, D. R., Marcus, E. A., Weeks, D. L., & Sachs, G. (2002). Mechanisms of acid resistance due to the urease system of *Helicobacter pylori*. *Gastroenterology*, *123*(1), 187-195.
186. Scott, D. R., Sachs, G., & Marcus, E. A. (2016). The role of acid inhibition in *Helicobacter pylori* eradication. *F1000research*, *5*, 10.12688/f1000research.8598.1. eCollection 2016.

187. Sebald, M., & Veron, (1963). Base dna content and classification of vibrios. *Annales De l'Institut Pasteur*, 105, 897-910.
188. Seemann, T. (2014). Prokka: Rapid prokaryotic genome annotation. *Bioinformatics (Oxford, England)*, 30(14), 2068-2069.
189. Selgrad, M., Tammer, I., Langner, C., Bornschein, J., Meissle, J., Kandulski, A., et al. (2014). Different antibiotic susceptibility between antrum and corpus of the stomach, a possible reason for treatment failure of *Helicobacter pylori* infection. *World Journal of Gastroenterology*, 20(43), 16245-16251.
190. Seyler, R. W., Jr, Olson, J. W., & Maier, R. J. (2001). Superoxide dismutase-deficient mutants of *Helicobacter pylori* are hypersensitive to oxidative stress and defective in host colonization. *Infection and Immunity*, 69(6), 4034-4040.
191. Sharndama, H. C., & Mba, I. E. (2022). *Helicobacter pylori*: An up-to-date overview on the virulence and and pathogenesis mechanisms. *Brazilian Journal of Microbiology*, 53(1), 33-50.
192. Shen, F., Hogley, L., Doherty, N., Loh, J. T., Cover, T. L., Sockett, R. E., et al. (2010). In *Helicobacter pylori* auto-inducer-2, but not LuxS/MccAB catalysed reverse transsulphuration, regulates motility through modulation of flagellar gene transcription. *BMC Microbiology*, 10, 210-2180-10-210.
193. Sheppard, S. K., Cheng, L., Meric, G., de Haan, C. P., Llarena, A. K., Marttinen, P., et al. (2014). Cryptic ecology among host generalist *Campylobacter jejuni* in domestic animals. *Molecular Ecology*, 23(10), 2442-2451.
194. Sheppard, S. K., Didelot, X., Meric, G., Torralbo, A., Jolley, K. A., Kelly, D. J., et al. (2013). Genome-wide association study identifies vitamin B5 biosynthesis as a host specificity factor in *Campylobacter*. *Proceedings of the National Academy of Sciences of the United States of America*, 110(29), 11923-11927.

195. Sher, A.A, Jerome, J.P, Bell, J.A, Yu, J, Kim, H.Y, Barrick, J.E and Mansfield, L.S (2020) Experimental Evolution of *Campylobacter jejuni* Leads to Loss of Motility, rpoN (σ 54) Deletion and Genome Reduction. *Front. Microbiol.* *11*:579989. doi: 10.3389/fmicb.2020.579989
196. Shimizu, K., Hayashi, S., Kako, T., Suzuki, M., Tsukagoshi, N., Doukyu, N., et al. (2005). Discovery of *glpC*, an organic solvent tolerance-related gene in *Escherichia coli*, using gene expression profiles from DNA microarrays. *Applied and Environmental Microbiology*, *71*(2), 1093-1096.
197. Shippy, D. C., Eakley, N. M., Lauhon, C. T., Bochler, P. N., & Fadl, A. A. (2013). Virulence characteristics of *Salmonella* following deletion of genes encoding the tRNA modification enzymes GidA and MnmE. *Microbial Pathogenesis*, *57*, 1-9.
198. Shippy, D. C., & Fadl, A. A. (2014). tRNA modification enzymes GidA and MnmE: Potential role in virulence of bacterial pathogens. *International Journal of Molecular Sciences*, *15*(10), 18267-18280.
199. Skoog, E. C., Morikis, V. A., Martin, M. E., Foster, G. A., Cai, L. P., Hansen, L. M., et al. (2018). CagY-dependent regulation of type IV secretion in *Helicobacter pylori* is associated with alterations in integrin binding. *Mbio*, *9*(3), 10.1128/mBio.00717-18.
200. Sorensen, M. C., Gencay, Y. E., Birk, T., Baldvinsson, S. B., Jackel, C., Hammerl, J. A., et al. (2015). Primary isolation strain determines both phage type and receptors recognised by *Campylobacter jejuni* bacteriophages. *PloS One*, *10*(1), e0116287.

201. Stahl, M., Friis, L. M., Nothaft, H., Liu, X., Li, J., Szymanski, C. M., et al. (2011). L-fucose utilization provides *Campylobacter jejuni* with a competitive advantage. *Proceedings of the National Academy of Sciences of the United States of America*, *108*(17), 7194-7199.
202. Stent, A., Every, A. L., & Sutton, P. (2012). *Helicobacter pylori* defense against oxidative attack. *American Journal of Physiology. Gastrointestinal and Liver Physiology*, *302*(6), G579-87.
203. Stintzi, A. (2003). Gene expression profile of *Campylobacter jejuni* in response to growth temperature variation. *Journal of Bacteriology*, *185*(6), 2009-2016.
204. Sugano, K., Tack, J., Kuipers, E. J., Graham, D. Y., El-Omar, E. M., Miura, S., et al. (2015). Kyoto global consensus report on *Helicobacter pylori* gastritis. *Gut*, *64*(9), 1353-1367.
205. Tacconelli, E., Carrara, E., Savoldi, A., Harbarth, S., Mendelson, M., Monnet, D. L., et al. (2018). Discovery, research, and development of new antibiotics: The WHO priority list of antibiotic-resistant bacteria and tuberculosis. *The Lancet. Infectious Diseases*, *18*(3), 318-327.
206. Tagel, M., Ilves, H., Leppik, M., Jurgenstein, K., Remme, J., & Kivisaar, M. (2020). Pseudouridines of tRNA anticodon stem-loop have unexpected role in mutagenesis in *Pseudomonas* spp. *Microorganisms*, *9*(1), 10.3390/microorganisms9010025.
207. Teh, A. H., Lee, S. M., & Dykes, G. A. (2014). Does *Campylobacter jejuni* form biofilms in food-related environments? *Applied and Environmental Microbiology*, *80*(17), 5154-5160.

208. Teh, A. H. T., Lee, S. M., & Dykes, G. A. (2017). The influence of dissolved oxygen level and medium on biofilm formation by *Campylobacter jejuni*. *Food Microbiology*, *61*, 120-125.
209. Teh, M., Tan, K. B., Seet, B. L., & Yeoh, K. G. (2002). Study of p53 immunostaining in the gastric epithelium of *cagA*-positive and *cagA*-negative *Helicobacter pylori* gastritis. *Cancer*, *95*(3), 499-505.
210. Tenenbaum, D., & Maintainer, B. (2022). *KEGGREST: Client-side REST access to the kyoto encyclopedia of genes and genomes (KEGG)*. R package version 1.36.3.
211. Testerman, T. L., & Morris, J. (2014). Beyond the stomach: An updated view of *Helicobacter pylori* pathogenesis, diagnosis, and treatment. *World Journal of Gastroenterology*, *20*(36), 12781-12808.
212. Tomb, J. F., White, O., Kerlavage, A. R., Clayton, R. A., Sutton, G. G., Fleischmann, R. D., et al. (1997). The complete genome sequence of the gastric pathogen *Helicobacter pylori*. *Nature*, *388*(6642), 539-547.
213. Ugarte-Ruiz, M., Dominguez, L., Corcionivoschi, N., Wren, B. W., Dorrell, N., & Gundogdu, O. (2018). Exploring the oxidative, antimicrobial and genomic properties of *Campylobacter jejuni* strains isolated from poultry. *Research in Veterinary Science*, *119*, 170-175.
214. Veron, M., & Chatelainm R,. (1973). Taxonomic study of the Genus *Campylobacter* Sebald and Véron and designation of the neotype strain for the type species, *Campylobacter fetus* (smith and taylor) sebald and véron. *International Journal of Systematic and Evolutionary Microbiology*, *23*(2), 122-134.

215. Vucic, S., Kiernan, M. C., & Cornblath, D. R. (2009). Guillain-Barre syndrome: An update. *Journal of Clinical Neuroscience: Official Journal of the Neurosurgical Society of Australasia*, 16(6), 733-741.
216. Wang, G., & Maier, R. J. (2004). An NADPH quinone reductase of *Helicobacter pylori* plays an important role in oxidative stress resistance and host colonization. *Infection and Immunity*, 72(3), 1391-1396.
217. Wang, G., & Maier, R. J. (2015). A novel DNA-binding protein plays an important role in *Helicobacter pylori* stress tolerance and survival in the host. *Journal of Bacteriology*, 197(5), 973-982.
218. Wang, Y., Wang, Q., Huang, H., Huang, W., Chen, Y., McGarvey, P. B., et al. (2021). A crowdsourcing open platform for literature curation in UniProt. *PLoS Biology*, 19(12), e3001464.
219. Warnes, G. R., Bolker, B., Bonebakker, L., Gentleman, R., Wolfgang, H. A. L., Lumley, T., et al. (2015). *Gplots: Various R programming tools for plotting data*
220. Warren, J. R., & Marshall, B. (1983). Unidentified curved bacilli on gastric epithelium in active chronic gastritis. *Lancet (London, England)*, 1(8336), 1273-1275.
221. Weyermann, M., Rothenbacher, D., & Brenner, H. (2009). Acquisition of *Helicobacter pylori* infection in early childhood: Independent contributions of infected mothers, fathers, and siblings. *The American Journal of Gastroenterology*, 104(1), 182-189.
222. Whelan, M. V. X., Ardill, L., Koide, K., Nakajima, C., Suzuki, Y., Simpson, J. C., et al. (2019). Acquisition of fluoroquinolone resistance leads to increased biofilm formation and pathogenicity in *Campylobacter jejuni*. *Scientific Reports*, 9(1), 18216-019-54620-1.

223. Wilkinson, D. J., Dickins, B., Robinson, K., & Winter, J. (2022). Genomic diversity of *Helicobacter pylori* populations from different regions of the human stomach. *BioRxiv (Preprint)*,
224. Williams, L. K., Fonseca, B. B., & Humphrey, T. J. (2016). Chapter 5, *Campylobacter jejuni* in poultry: A commensal or a pathogen? In B.B. Fonseca et al (Ed.), *Campylobacter spp. and related organisms in poultry* (pp. 75-88)
225. Willison, H. J., Jacobs, B. C., & van Doorn, P. A. (2016). Guillain-barre syndrome. *Lancet (London, England)*, 388(10045), 717-727.
226. Wilson, D. J., Gabriel, E., Leatherbarrow, A. J., Cheesbrough, J., Gee, S., Bolton, E., et al. (2009). Rapid evolution and the importance of recombination to the gastroenteric pathogen *Campylobacter jejuni*. *Molecular Biology and Evolution*, 26(2), 385-397.
227. World Health Organisation. (2013). *The global view of campylobacteriosis* World Health Organisation.
228. Wu, Y. L., Liu, K. S., Yin, X. T., & Fei, R. M. (2015). *glpC* gene is responsible for biofilm formation and defense against phagocytes and imparts tolerance to pH and organic solvents in *Proteus vulgaris*. *Genetics and Molecular Research: GMR*, 14(3), 10619-10629.
229. Yonezawa, H., Osaki, T., Hojo, F., & Kamiya, S. (2019). Effect of *Helicobacter pylori* biofilm formation on susceptibility to amoxicillin, metronidazole and clarithromycin. *Microbial Pathogenesis*, 132, 100-108.
230. Yonezawa, H., Osaki, T., Kurata, S., Zaman, C., Hanawa, T., & Kamiya, S. (2010). Assessment of in vitro biofilm formation by *Helicobacter pylori*. *Journal of Gastroenterology and Hepatology*, 25 Suppl 1, S90-4.

231. Zhang, M., & Forbes, N. S. (2015). Trg-deficient *Salmonella* colonize quiescent tumor regions by exclusively penetrating or proliferating. *Journal of Controlled Release: Official Journal of the Controlled Release Society*, 199, 180-189.
232. Zhong, X., Wu, Q., Zhang, J., Ma, Z., Wang, J., Nie, X., et al. (2020). *Campylobacter jejuni* biofilm formation under aerobic conditions and inhibition by ZnO nanoparticles. *Frontiers in Microbiology*, 11, 207.
233. Zhou, X., Su, J., Xu, G., & Zhang, G. (2014). Accuracy of stool antigen test for the diagnosis of *Helicobacter pylori* infection in children: A meta-analysis. *Clinics and Research in Hepatology and Gastroenterology*, 38(5), 629-638.

8.0 Appendix

8.1 *H. pylori* ethical approval

Patients gave written consent that clinical isolates of *H. pylori* from the patients will be used for the purpose of study. College Ethical Review Committee approval not required. Approval granted by the NHS National Research Ethics Service, Nottingham Research Ethics Committee 2 (Ref: 08/H0408/195)

7.1.2 *C. jejuni* presence/absence list comparing 403CC genomes (N=14) against ST21/45 generalist genomes (N=121). Designation of a gene as either 403, non-403 or “both” based on an arbitrary 70% cut off. 437 hypothetical proteins were present in this list but are now omitted.

Gene	Non-unique gene name	Group	Annotation
fdx_2		403	Ferredoxin
hhalM		403	Modification methylase Hhal
group_7191		403	putative type I restriction enzyme P M protein
group_3612		Non 403	4-sulfomuconolactone hydrolase
yfhL		Non 403	putative ferredoxin-like protein YfhL
group_7090	dpnA	403	Modification methylase DpnIIB
group_6972		403	ATP/GTP phosphatase
group_3892		403	Putative type-1 restriction enzyme specificity protein MPN_089
group_6032	epsJ_2	403	putative glycosyltransferase EpsJ
group_1671	mepA	403	Multidrug export protein MepA
tal		Non 403	Transaldolase
tenI		Non 403	Regulatory protein TenI
obg		Non 403	GTPase Obg
group_5498	tenI	403	Thiazole tautomerase
group_5952	murG	403	UDP-N-acetylglucosamine--N-acetylmuramyl-(pentapeptide) pyrophosphoryl-undecaprenol N-acetylglucosaminyl transferase MurG
proB		Non 403	Glutamate 5-kinase
murG		Non 403	UDP-N-acetylglucosamine--N-acetylmuramyl-(pentapeptide) pyrophosphoryl-undecaprenol N-acetylglucosaminyl transferase MurG
yycB_2		403	putative transporter YycB
hsdR_1		403	Type I restriction enzyme EcoR124II R protein
group_4579	obg	403	GTPase Obg
nimT		403	2-nitroimidazole transporter
tupA		403	Tungstate-binding protein TupA
group_3897	radD	403	Putative DNA repair helicase RadD

group_5586	hsdR_2	403	Type I restriction enzyme EcoR124II R protein
group_6251		Non 403	PBP superfamily domain protein
group_4858	proB	403	Glutamate 5-kinase
group_1817		403	hypothetical protein
group_4455	tal	Non 403	Transaldolase
hsdS_2		403	Type-1 restriction enzyme EcoKI specificity protein
cocE		403	Cocaine esterase
group_4230	yafP	403	putative N-acetyltransferase YafP
group_5368	porA	403	Major outer membrane protein
group_3287	intA	403	Prophage CP4-57 integrase
group_7770	epsN	403	Putative pyridoxal phosphate-dependent aminotransferase EpsN
group_1116		Non 403	Major Facilitator Superfamily protein
lldP		Non 403	L-lactate permease
epsJ_2		403	putative glycosyltransferase EpsJ
eptB		403	Phosphoethanolamine transferase EptB
kipA_2		403	KipI antagonist
group_992	epsJ_1	403	putative glycosyltransferase EpsJ
group_728	vacA	403	Vacuolating cytotoxin autotransporter
ccsA		Non 403	Cytochrome c biogenesis protein CcsA
hsdS_1		403	Type-1 restriction enzyme EcoKI specificity protein
group_631	pgtP_2	403	Phosphoglycerate transporter protein
group_757		Non 403	Bacteriohemerythrin
arsR		Non 403	Arsenical resistance operon repressor
group_1448	hsdM	403	Type I restriction enzyme EcoKI M protein
torZ_1		403	Trimethylamine-N-oxide reductase 2
group_3558		403	putative type I restriction enzyme P M protein
pepD		Non 403	Cytosol non-specific dipeptidase
group_5064	lldP	403	L-lactate permease

group_5906		403	Gene 25-like lysozyme
group_5457		403	hypothetical protein
group_37			Capsule polysaccharide biosynthesis protein
group_3014		403	Alpha-2,3-sialyltransferase (CST-I)
mepA			Multidrug export protein MepA
group_6605		403	Type VI secretion lipoprotein
dcuD_4		403	Putative cryptic C4-dicarboxylate transporter DcuD
group_4574	fic	403	Adenosine monophosphate-protein transferase SoFic
group_2237	vatD	403	Streptogramin A acetyltransferase
group_3538	yihN_1	403	Inner membrane protein YihN
group_2812		403	CAAX amino terminal protease self- immunity
lex1		403	Glycosyltransferase family 25 (LPS biosynthesis protein)
yhjE		403	Proline/betaine transporter
group_3806		403	LamB/YcsF family protein
group_3539	yihN_2	403	Inner membrane protein YihN
neuA		403	N-acylneuraminate cytidyltransferase
group_3968	yagU	403	Inner membrane protein YagU
group_4648	hddC_2	403	D-glycero-alpha-D-manno-heptose 1-phosphate guanylyltransferase
group_2071		403	Intracellular multiplication and human macrophage-killing
nhaA_1		Non 403	Na()/H() antiporter NhaA
group_4078		403	molybdate ABC transporter periplasmic molybdate-binding protein
group_1166	pepD	403	Cytosol non-specific dipeptidase
vacA		403	Vacuolating cytotoxin autotransporter precursor
group_3912	ccsA	403	Cytochrome c biogenesis protein CcsA
dinB		403	DNA polymerase IV
hcpA_2		403	Major exported protein
group_770	dsbL_1	403	Thiol:disulfide interchange protein DsbL precursor
bla		Non 403	Beta-lactamase OXA-10 precursor

yihN_1		403	Inner membrane protein YihN
yihN_2		403	Inner membrane protein YihN
pdxA		Non 403	4-hydroxythreonine-4-phosphate dehydrogenase
group_1678	espC	403	Serine protease EspC
kdpA_5		403	Potassium-transporting ATPase potassium-binding subunit
panC		Non 403	Pantothenate synthetase
panB		Non 403	3-methyl-2-oxobutanoate hydroxymethyltransferase
panD		Non 403	Aspartate 1-decarboxylase precursor
epsJ_1		Non 403	putative glycosyltransferase EpsJ
bioC		Non 403	biotin biosynthesis protein BioC
rimO		Non 403	Ribosomal protein S12 methylthiotransferase RimO
group_4593		403	Xylose isomerase-like TIM barrel
dltA		Non 403	D-alanine--poly(phosphoribitol) ligase subunit 1
yafP		Non 403	putative N-acetyltransferase YafP
group_1926	bioC	403	Malonyl-[acyl-carrier protein] O-methyltransferase
group_4499	ttcA	403	tRNA 2-thiocytidine biosynthesis protein TtcA
dcuD_1		Non 403	Putative cryptic C4-dicarboxylate transporter DcuD
group_508		Non 403	putative type I restriction enzyme P M protein
group_5543		403	Acetyltransferase (GNAT) family protein
lgrD		403	Linear gramicidin synthase subunit D
group_1818		Non 403	aminoalkylphosphonic acid N-acetyltransferase
legI_2		403	N,N'-diacetyllegionaminic acid synthase
siaA		403	UDP-N-acetylglucosamine 2-epimerase
group_518	kdpA_2	403	Potassium-transporting ATPase potassium-binding subunit
mftC		403	Putative mycofactocin radical SAM maturase MftC
yfIS_2		Non 403	Putative malate transporter YfIS
group_5482		403	protoporphyrinogen oxidase
group_857	yfkO	403	Putative NAD(P)H nitroreductase YfkO

exsA		Non 403	Exoenzyme S synthesis regulatory protein ExsA
pgtP_2		403	Phosphoglycerate transporter protein
group_1429	rfaF	403	ADP-heptose--LPS heptosyltransferase 2
yfIS		403	Putative malate transporter YfIS
group_4978		403	Beta-1,4-N-acetylgalactosaminyltransferase (CgtA)
group_2408	fliD	403	Flagellar hook-associated protein 2
group_2753	pdxA	403	4-hydroxythreonine-4-phosphate dehydrogenase
group_2116	nhaA_1	403	Na()/H() antiporter NhaA
rfaF		Non 403	ADP-heptose--LPS heptosyltransferase 2
fokIM_2		403	Modification methylase FokI
group_429	strE	403	GDP-6-deoxy-D-mannose reductase
yfkO		both	Putative NAD(P)H nitroreductase YfkO
kdpA_4		403	Potassium-transporting ATPase A chain
group_3763	rimO	403	Ribosomal protein S12 methylthiotransferase RimO
tsh		Non 403	Temperature-sensitive hemagglutinin tsh autotransporter precursor
group_5491		403	putative tautomerase
kdpD_1		403	Sensor protein KdpD
group_1496	dcuD_1	403	Putative cryptic C4-dicarboxylate transporter DcuD
nrgA		403	Ammonium transporter NrgA
cysE		Non 403	Serine acetyltransferase
hindIIIM		403	Modification methylase HindIII
group_4980		403	Beta-1,4-N-acetylgalactosaminyltransferase (CgtA)
yxeP_2		both	putative hydrolase YxeP
group_4232		403	Beta-1,4-N-acetylgalactosaminyltransferase (CgtA)
group_445	strE	403	dTDP-glucose 4,6-dehydratase
group_3393		Non 403	YheO-like PAS domain protein
group_1436	mcp4_1	403	Methyl-accepting chemotaxis protein 4
group_1820		403	aminoalkylphosphonic acid N-acetyltransferase

group_1658	citN	403	Citrate transporter
cysA_2		Non 403	Sulfate/thiosulfate import ATP-binding protein CysA
group_6137		403	putative metallo-hydrolase
besA		403	Ferri-bacillibactin esterase BesA
group_5137	queF	403	NADPH-dependent 7-cyano-7-deazaguanine reductase
group_4503	pctC_1	403	Methyl-accepting chemotaxis protein PctC
rmd_1		403	GDP-6-deoxy-D-mannose reductase
ttcA		both	tRNA 2-thiocytidine biosynthesis protein TtcA
group_1058	proP_1	both	Proline/betaine transporter
group_5698	ansZ	403	L-asparaginase 2 precursor
group_2151		403	OPT oligopeptide transporter protein
group_2403	cysA_1	403	Sulfate/thiosulfate import ATP-binding protein CysA
pgtP_1		Non 403	Phosphoglycerate transporter protein
kdpA		Non 403	Potassium-transporting ATPase A chain
group_2602		both	DNA polymerase III subunit delta
xerH_2		403	Tyrosine recombinase XerH
yicL		Non 403	putative inner membrane transporter YicL
fliD		Non 403	Flagellar hook-associated protein 2
group_3054	fmt_2	Non 403	Methionyl-tRNA formyltransferase
group_7785	gspA	Non 403	General stress protein A
group_7787	fcl	Non 403	GDP-L-fucose synthase
group_5008		Non 403	putative metallo-hydrolase
dsbL_1		Non 403	Thiol:disulfide interchange protein DsbL precursor
ymfD		Non 403	Bacillibactin exporter
group_4528		Non 403	Gram-negative bacterial tonB protein
hrcA		Non 403	Heat-inducible transcription repressor HrcA
ansZ		Non 403	L-asparaginase 2 precursor
cirA_3		Non 403	Colicin I receptor precursor

fdol		Non 403	Formate dehydrogenase, cytochrome b556(fdo) subunit
bcr		Non 403	Bicyclomycin resistance protein
group_1811		403	transport protein TonB
group_1602	pseI	403	Pseudaminic acid synthase
epsJ_3		403	putative glycosyltransferase EpsJ
gspA		403	General stress protein A
kdpA_2		403	Potassium-transporting ATPase A chain
group_1061	proP_1	403	Proline/betaine transporter
group_653	assT_1	403	Arylsulfate sulfotransferase AssT precursor
group_3500	tetO	403	Tetracycline resistance protein TetO
lexA_2		403	DNA polymerase V subunit UmuD
group_3994		Non 403	putative inner membrane protein
group_5139		Non 403	TMAO/DMSO reductase
group_2711	bsdB	Non 403	Phenolic acid decarboxylase subunit B
rhaM		Non 403	L-rhamnose mutarotase
uxaA_2		Non 403	Altronate dehydratase
kdgR		Non 403	Pectin degradation repressor protein KdgR
strE		Non 403	dTDP-glucose 4,6-dehydratase
group_3480		Non 403	Amidohydrolase
uxaA_1		Non 403	Altronate dehydratase
dapA_1		Non 403	4-hydroxy-tetrahydrodipicolinate synthase
fabG_2		Non 403	3-oxoacyl-[acyl-carrier-protein] reductase FabG
group_3335	cysE	403	Serine acetyltransferase
group_3391		403	YheO-like PAS domain protein
moeZ		both	putative adenylyltransferase/sulfurtransferase MoeZ
group_4213	nimT	Non 403	2-nitroimidazole transporter
group_7772	moeZ	Non 403	putative adenylyltransferase/sulfurtransferase MoeZ
group_4640	hsdS_1	Non 403	Type-1 restriction enzyme EcoKI specificity protein

ribD		Non 403	Riboflavin biosynthesis protein RibD
group_1875		403	putative transporter
rbr1		both	Rubrerythrin-1
group_1485	dcuD_3	403	Putative cryptic C4-dicarboxylate transporter DcuD
group_5124	yxeP_2	403	putative hydrolase YxeP
group_785	proP_4	Non 403	Proline/betaine transporter
yfIS_1		Non 403	Putative malate transporter YfIS
mcpB		Non 403	Cache domain protein
group_2594	ymfD	403	Bacillibactin exporter
group_1987	fcl	403	GDP-L-fucose synthase
group_1447	hsdM	403	Type I restriction enzyme EcoKI M protein
group_2984		Non 403	Putative transposase DNA-binding domain protein
group_5043	rbr1	403	Rubrerythrin-1
group_2523	dsbl	403	Protein-disulfide oxidoreductase Dsbl
group_2434	pIdA	Non 403	Phospholipase A1 precursor
pIdA		403	Phospholipase A1 precursor
group_4034	fhuC	Non 403	Iron(3 ⁻)-hydroxamate import ATP-binding protein FhuC
rhmT		Non 403	Inner membrane transport protein RhmT
fliY		both	Cystine-binding periplasmic protein precursor
mcp4_1		403	Methyl-accepting chemotaxis protein 4
cysC		both	putative adenylyl-sulfate kinase
ynfE		Non 403	Putative dimethyl sulfoxide reductase chain YnfE precursor
group_1312	torZ	403	Trimethylamine-N-oxide reductase 2 precursor
group_3795	exbB_1	Non 403	Biopolymer transport protein ExbB
group_6414	exbD_1	Non 403	Biopolymer transport protein ExbD
group_4512		Non 403	Gram-negative bacterial tonB protein
group_3543	bcr	403	Bicyclomycin resistance protein
group_5769	hrcA	403	heat-inducible transcription repressor

metA		Non 403	Homoserine O-succinyltransferase
mdeA		Non 403	Methionine gamma-lyase
group_5468		Non 403	protoporphyrinogen oxidase
group_3891		Non 403	Putative type-1 restriction enzyme specificity protein MPN_089
hsdR_3		Non 403	Type I restriction enzyme EcoR124II R protein
group_3557		Non 403	putative type I restriction enzymeP M protein
group_206	flaB_3	Non 403	Flagellin B
group_427	strE	Non 403	dTDP-glucose 4,6-dehydratase
ssa1_2		Non 403	Serotype-specific antigen 1
group_2460	pgIC	Non 403	Undecaprenyl phosphate N,N'-diacetylbacillosamine 1-phosphate transferase
group_865	dtpT_2	403	Di-/tripeptide transporter
group_4581	fdol	403	Formate dehydrogenase, cytochrome b556(fdo) subunit
group_2648		Non 403	putative TonB-dependent receptor precursor
era_1		403	GTPase Era
rfbC		403	dTDP-4-dehydrorhamnose 3,5-epimerase
group_3995		403	putative inner membrane protein
group_5140	yedY	403	TMAO/DMSO reductase
group_1168		Non 403	putative glycosyltransferase involved in capsule biosynthesis
group_3687		Non 403	twin-arginine leader-binding protein DmsD
sunS		Non 403	SPBc2 prophage-derived glycosyltransferase SunS
group_5228		Non 403	Plasmid stabilisation system protein
ygdH		403	putative lysine decarboxylase
fucP		Non 403	L-fucose-proton symporter
group_3808		Non 403	MORN repeat variant
group_1170	fliY	Non 403	Cystine-binding periplasmic protein precursor
group_729	vacA	Non 403	Vacuolating cytotoxin autotransporter precursor
hsdR		Non 403	Type I restriction enzyme EcoR124II R protein
xerD_2		403	Tyrosine recombinase XerD

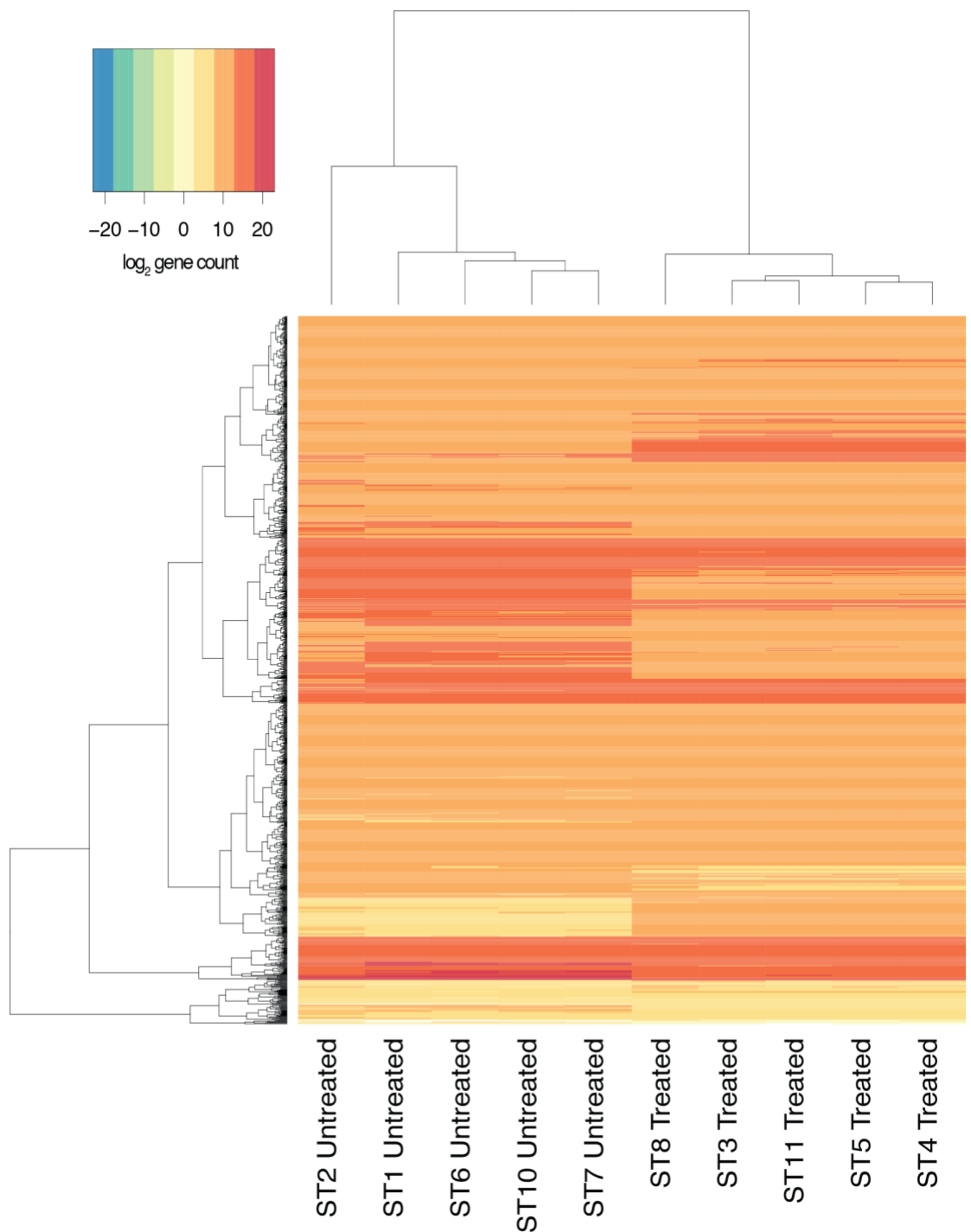
adhR		Non 403	HTH-type transcriptional regulator AdhR
group_4234		403	Beta-1,4-N-acetylgalactosaminyltransferase (CgtA)
group_1416		403	MmgE/PrpD family protein
bsdB		403	Phenolic acid decarboxylase subunit B
group_633	pgtP_2	Non 403	Phosphoglycerate transporter protein
group_3405	ribD	403	Riboflavin biosynthesis protein RibD
hxB		403	Heme/hemopexin transporter protein HuxB precursor
group_1839	kdpC	Non 403	Potassium-transporting ATPase C chain
group_1109		403	putative MFS family transporter protein
group_1795	xerD_2	Non 403	Tyrosine recombinase XerD
group_2281	sepA	Non 403	Serine protease SepA autotransporter
porA		Non 403	Major outer membrane protein precursor
group_1013	topB	403	DNA topoisomerase 3
group_5416		403	YcfA-like protein
kdpC		403	Potassium-transporting ATPase C chain
group_1409	pcaB	403	3-carboxy-cis,cis-muconate cycloisomerase
kdpA_1		403	Potassium-transporting ATPase A chain
group_4577	fic	Non 403	Adenosine monophosphate-protein transferase SoFic
group_2617	tusA	Non 403	Sulfurtransferase TusA
group_1675	pic	Non 403	Serine protease pic autotransporter
group_3464	epsJ_2	Non 403	putative glycosyltransferase EpsJ
group_5587	hsdR_2	Non 403	Type I restriction enzyme EcoR124II R protein
group_7791	tsdA_2	Non 403	Thiosulfate dehydrogenase
group_215	flaB_1	Non 403	Flagellin B
aldA		Non 403	Lactaldehyde dehydrogenase
group_2723	cdtA	Non 403	Cytolethal distending toxin subunit A precursor
cas9		Non 403	CRISPR-associated endonuclease Cas9
group_1539	hsdR	Non 403	Type-1 restriction enzyme R protein

group_3363		Non 403	3',5'-cyclic-nucleotide phosphodiesterase
wfgD		Non 403	UDP-Glc:alpha-D-GlcNAc-diphosphoundecaprenol beta-1,3-glucosyltransferase WfgD
rmlA1		Non 403	Glucose-1-phosphate thymidyltransferase 1
hsdS		Non 403	Type-1 restriction enzyme EcoKI specificity protein
group_4288	guaB	Non 403	Inosine-5'-monophosphate dehydrogenase
group_4185	assT	Non 403	Arylsulfate sulfotransferase AssT precursor
group_6686		Non 403	putative type I restriction enzyme P M protein
rfbB		Non 403	dTDP-glucose 4,6-dehydratase
group_5672		Non 403	Glycosyltransferase family 25 (LPS biosynthesis protein)
group_6687		Non 403	Divergent AAA domain protein
group_5022		Non 403	putative methyltransferase
group_2544		Non 403	Putative NAD(P)H nitroreductase
group_978	cas9	Non 403	CRISPR-associated endonuclease Cas9
group_3958		Non 403	Capsular polysaccharide synthesis protein
fdtB		Non 403	dTDP-3-amino-3,6-dideoxy-alpha-D-galactopyranose transaminase
fdtC		Non 403	dTDP-3-amino-3,6-dideoxy-alpha-D-galactopyranose 3-N-acetyltransferase
group_6631		403	TrbM
group_3505		403	Relaxase/Mobilisation nuclease domain protein
group_5870		403	Type IV secretion system protein VirB11
ssb_1		403	Single-stranded DNA-binding protein
group_984	cas9	403	CRISPR-associated endonuclease Cas9
group_1265		403	Type IV secretion system proteins
group_790	proP_1	403	Proline/betaine transporter
group_7375		Non 403	PIN domain protein
group_1810		Non 403	transport protein TonB
group_287		403	hypothetical protein
group_6633		403	Type IV secretion system protein virB10
virB2		403	Type IV secretion system protein virB2 precursor

virB8		403	Type IV secretion system protein virB8
virB9		403	Type IV secretion system protein virB9 precursor
fhuC		403	Iron(3)-hydroxamate import ATP-binding protein FhuC
rfbE		403	CDP-paratose 2-epimerase
group_3580	exsA	Non 403	Exoenzyme S synthesis regulatory protein ExsA
group_4825	sdaC	Non 403	Serine transporter
ymfD_2		403	Bacillibactin exporter
espP		Non 403	Serine protease EspP precursor
feuC		Non 403	Iron-uptake system permease protein FeuC
group_5479		Non 403	EcoKI restriction-modification system protein HsdS
dmsB		Non 403	Anaerobic dimethyl sulfoxide reductase chain B
group_6244		Non 403	putative lysine decarboxylase
group_3138	feuB	Non 403	Iron-uptake system permease protein FeuB
group_3623	glnD	Non 403	Bifunctional uridylyltransferase/uridylyl-removing enzyme
pseH		both	UDP-4-amino-4,6-dideoxy-N-acetyl-beta-L-altrosamine N-acetyltransferase
fhuB		both	Iron(3)-hydroxamate import system permease protein FhuB
group_892	dcuD_2	Non 403	Putative cryptic C4-dicarboxylate transporter DcuD
rmd		Non 403	GDP-6-deoxy-D-mannose reductase
fumC		both	Fumarate hydratase class II
virB4		403	Type IV secretion system protein virB4
kdpB		Non 403	Potassium-transporting ATPase B chain
tsdA_1		403	Cytochrome c
group_2880		Non 403	sn-glycerol-3-phosphate dehydrogenase subunit C
pglC		both	Undecaprenyl phosphate N,N'-diacetylbacillosamine 1-phosphate transferase
lexA_4		403	DNA polymerase V subunit UmuD
group_4192	traG	403	Conjugal transfer protein TraG
group_5110	hsdM	403	Type I restriction enzyme EcoKI M protein
group_105	flaA_2	403	Flagellin A

epsN		both	Putative pyridoxal phosphate-dependent aminotransferase EpsN
gph		both	Phosphoglycolate phosphatase
ileS		both	Isoleucine--tRNA ligase
group_227	flaB_1	Non 403	Flagellin A
group_1057	yfIS	Non 403	Putative malate transporter YfIS
group_3895	radD	Non 403	Putative DNA repair helicase RadD
ywaC		Non 403	GTP pyrophosphokinase YwaC
group_180	trg	403	Methyl-accepting chemotaxis protein III
group_5571	aroH	Non 403	Phospho-2-dehydro-3-deoxyheptonate aldolase
group_4486		Non 403	Sodium Bile acid symporter family protein
arsC2		Non 403	Arsenate-mycothioli transferase ArsC2
fepA		Non 403	Ferrienterobactin receptor precursor
cas1		both	CRISPR-associated endonuclease Cas1
kfoC		both	Chondroitin synthase
epsM		Non 403	Putative acetyltransferase EpsM
pet		Non 403	Serine protease pet autotransporter precursor
group_4190	traC	403	DNA primase TraC
frdB_1		both	Fumarate reductase iron-sulfur subunit
pncB2		both	Nicotinate phosphoribosyltransferase pncB2
group_1717	yycB	Non 403	putative transporter YycB
hddC_2		both	D-glycero-alpha-D-manno-heptose 1-phosphate guanylyltransferase
legF_2		both	CMP-N,N'-diacetyllegionaminic acid synthase
ccsA_1		Non 403	Cytochrome c biogenesis protein CcsA
ycdF		both	Glucose 1-dehydrogenase 2
group_5289		Non 403	thiol:disulfide interchange protein precursor
ugpA		Non 403	sn-glycerol-3-phosphate transport system permease protein UgpA
gph_1		Non 403	Phosphoglycolate phosphatase
group_5722		Non 403	conjugal transfer mating pair stabilization protein TraN

group_2150		Non 403	OPT oligopeptide transporter protein
group_6321		Non 403	formate dehydrogenase-O subunit gamma
araQ		Non 403	L-arabinose transport system permease protein AraQ
group_2099	cas1	Non 403	CRISPR-associated endonuclease Cas1
group_2521	dsbl	Non 403	Protein-disulfide oxidoreductase Dsbl
group_1050	yfIS_2	Non 403	Putative malate transporter YfIS
group_6541	legI_1	Non 403	N,N'-diacetyllegionaminic acid synthase
group_6540	siaA	Non 403	UDP-N-acetylglucosamine 2-epimerase
group_5176	fumC	Non 403	Fumarate hydratase class II
recG_2		Non 403	putative permease
ggt		Non 403	Gamma-glutamyltranspeptidase precursor
aldA_2		Non 403	Lactaldehyde dehydrogenase
group_6174	cysC	Non 403	putative adenyllyl-sulfate kinase
group_2103	epsJ_1	Non 403	putative glycosyltransferase EpsJ
group_6542		Non 403	Alpha-2,3-sialyltransferase (CST-I)
group_2444	ydhP_1	Non 403	Inner membrane transport protein YdhP



8.3 Heatmap showing bidirectional clustering of the 1312 significantly (adjusted P value < 0.05) differentially expressed genes for the treated and untreated samples. Log₂ transformed gene count information was generated from normalized count data produced using DESeq2. The image was produced by Professor Lesley Hoyles.

8.4 KEGG over-representation metabolic pathways with menadione treated significantly differentially expressed genes mapped to them

Pathway	Genes in pathway	Number of genes in pathway	P value	Adjusted p value
Epithelial cell signaling in Helicobacter pylori infection	HP0073, HP0072, HP0071, HP0009, HP0887, HP0410, HP0492, HP0797, HP0547, HP0520, HP0522, HP0523, HP0524, HP1421, HP0525, HP0526, HP0527, HP0528, HP0529, HP0530, HP0531, HP0532, HP0534, HP0535, HP0537, HP0538, HP0539, HP0540, HP0541, HP0542, HP0543, HP0544, HP0545, HP0546, HP0169	35/40	1.15E-09	1.02E-07
Oxidative phosphorylation	HP1540, HP1539, HP1538, HP0828, HP1010, HP1260, HP1261, HP1264, HP1265, HP1267, HP1268, HP1269, HP1270, HP1271, HP1272, HP1273, HP1212, HP0193, HP0192, HP0191, HP0147, HP0146, HP0145, HP0144, HP1131, HP1132, HP1133, HP1134, HP1137, HP1136	30/35	5.49E-08	1.37E-06
Carbon metabolism	HP0027, HP0026, HP1385, HP1386, HP0485, HP0875, HP0779, HP0742, HP0589, HP0577, HP0574, HP0557, HP1045, HP1325, HP0690, HP0652, HP0974, HP0950, HP1210, HP1238, HP0193, HP0192, HP0191, HP0183, HP0397, HP1166, HP0154, HP0121, HP1346, HP0921, HP1108, HP1109, HP1111, HP0371, HP1099, HP1100, HP1102, HP1103, HP0176, HP0107, HP1345	41/53	6.01E-08	1.37E-06
Two-component system	HP0103, HP0082, HP0099, HP0019, HP0616, HP0393, HP1540, HP1539, HP1538, HP1529, HP1442, HP0815, HP0601, HP0115, HP0512, HP1032, HP1067, HP0714, HP0693, HP0690, HP0193, HP0192, HP0191, HP0392, HP0147, HP0146, HP0145, HP0144	28/32	6.16E-08	1.37E-06
Flagellar assembly	HP1558, HP1557, HP1477, HP0908, HP0870, HP0816, HP0815, HP0770, HP0753, HP0601, HP0115, HP1030, HP0584, HP1031, HP1032, HP1041, HP1092, HP1585, HP0353, HP0352, HP0351, HP0325, HP0246, HP1119, HP0173, HP1419, HP1420	27/31	1.34E-07	2.39E-06
Lipopolysaccharide biosynthesis	HP0022, HP0021, HP0003, HP1580, HP1570, HP0867, HP0860, HP0859, HP0858, HP0857, HP0580, HP0579, HP1039, HP1052, HP0328, HP0230, HP0270, HP0279, HP0280, HP0394, HP1416, HP0159, HP1375, HP1429	24/27	3.11E-07	4.62E-06
Peptidoglycan biosynthesis	HP1565, HP1556, HP1494, HP0851, HP0740, HP0738, HP0648, HP0623, HP0597, HP1221, HP1155, HP0494, HP0493, HP1418	14/14	3.82E-06	4.25E-05
Mismatch repair	HP1387, HP1482, HP0911, HP1478, HP1460, HP0621, HP0615, HP0348, HP0259, HP1245, HP1247, HP0717, HP1231, HP0500	14/14	3.82E-06	4.25E-05
Aminoacyl-tRNA biosynthesis	HP1547, HP1513, HP1480, HP0886, HP0830, HP0774, HP0617, HP0238, HP1253, HP0658, HP0975, HP0972, HP1190, HP1241, HP0182, HP0417, HP0403, HP1153, HP0123, HP1422, HP0643, HP0476	22/26	6.00E-06	5.93E-05
ABC transporters	HP1577, HP1576, HP1564, HP1498, HP1466, HP1465, HP1464, HP0818, HP0749, HP0748, HP1082, HP0251, HP0298, HP0299, HP0300, HP0301, HP0302, HP1251, HP1252, HP0940, HP0939, HP0362, HP0475	23/28	9.76E-06	8.68E-05

Bacterial chemotaxis	HP0103, HP0082, HP0099, HP0019, HP0616, HP0393, HP0816, HP0815, HP1030, HP0584, HP1031, HP1067, HP0352, HP0298, HP0392	15/16	1.54E-05	1.24E-04
Folate biosynthesis	HP1545, HP1510, HP0804, HP0802, HP0800, HP0798, HP0768, HP0639, HP1036, HP0293, HP0959, HP0934, HP0933, HP0928, HP1232, HP0172, HP1413	17/19	1.68E-05	1.24E-04
Glyoxylate and dicarboxylate metabolism	HP0026, HP0485, HP0875, HP0779, HP0512, HP1045, HP0690, HP1238, HP0183, HP0509, HP1099, HP1434	12/12	2.30E-05	1.57E-04
Protein export	HP0074, HP1551, HP1550, HP1549, HP1450, HP0786, HP0763, HP0576, HP1060, HP1061, HP0320, HP1255, HP1300, HP1152	14/15	3.55E-05	2.19E-04
Amino sugar and nucleotide sugar metabolism	HP0075, HP0045, HP0044, HP1532, HP0840, HP0648, HP0646, HP0327, HP1275, HP0683, HP0178, HP1166, HP0366, HP0360, HP1103, HP1418	16/18	3.70E-05	2.19E-04
Arginine and proline metabolism	HP0056, HP0049, HP0020, HP1399, HP0832, HP0757, HP0294, HP0695, HP0672, HP0422, HP1158	11/11	5.62E-05	2.63E-04
Glycerophospholipid metabolism	HP1509, HP0871, HP0737, HP1016, HP1071, HP0700, HP0961, HP0215, HP0499, HP1357, HP1348	11/11	5.62E-05	2.63E-04
Porphyrin and chlorophyll metabolism	HP0604, HP0237, HP0239, HP0306, HP0665, HP1224, HP0418, HP0376, HP0163, HP0643, HP0476	11/11	5.62E-05	2.63E-04
Terpenoid backbone biosynthesis	HP1443, HP0625, HP1020, HP0354, HP0240, HP0690, HP0929, HP1221, HP0216, HP0400, HP0382	11/11	5.62E-05	2.63E-04
Ribosome	HP0084, HP0083, HP0076, HP1554, HP1496, HP0562, HP0551, HP0514, HP1040, HP0296, HP0297, HP1244, HP1246, HP1292, HP1294, HP1295, HP1296, HP1301, HP1313, HP1314, HP1315, HP1316, HP1317, HP1318, HP1319, HP1320, HP1197, HP1199, HP1200, HP1202, HP1204, HP0200, HP0399, HP1151, HP0491, HP0126	36/53	6.16E-05	2.74E-04
Phenylalanine, tyrosine and tryptophan biosynthesis	HP1038, HP0276, HP0291, HP1249, HP1282, HP1281, HP1280, HP1279, HP1278, HP0672, HP0663, HP0401, HP0157, HP0134, HP1380	15/17	8.11E-05	3.44E-04
Pantothenate and CoA biosynthesis	HP0034, HP0006, HP1475, HP1468, HP0862, HP0841, HP0831, HP0808, HP1058, HP0330	10/10	1.37E-04	5.56E-04
Glycolysis / Gluconeogenesis	HP1385, HP0589, HP1045, HP1275, HP0974, HP1166, HP0154, HP1346, HP0921, HP1108, HP1109, HP1111, HP1103, HP0176, HP1345	15/18	3.02E-04	1.17E-03
Methane metabolism	HP1385, HP1045, HP0652, HP0974, HP0183, HP0407, HP0397, HP0154, HP0121, HP1108, HP1109, HP1111, HP0176	13/15	3.80E-04	1.41E-03
Cysteine and methionine metabolism	HP1121, HP0051, HP0054, HP1468, HP0832, HP0822, HP0672, HP1189, HP1210, HP0197, HP0397, HP0107, HP0106, HP0105	14/17	6.21E-04	2.13E-03
Homologous recombination	HP1387, HP1523, HP1460, HP0877, HP1059, HP0348, HP1245, HP1247, HP0717, HP0925, HP1231, HP0387, HP0500, HP0153	14/17	6.21E-04	2.13E-03
Quorum sensing	HP1551, HP1450, HP0802, HP0786, HP0763, HP1255, HP1282, HP1281, HP1300, HP1152, HP0134, HP0105	12/14	8.13E-04	2.68E-03
Bacterial secretion system	HP1551, HP1550, HP1549, HP1450, HP0887, HP0786, HP0763, HP1421, HP0525, HP1060, HP1061, HP0320, HP1255, HP1300, HP1152	15/19	8.89E-04	2.83E-03

Fatty acid metabolism	HP0090, HP0561, HP0558, HP0557, HP0690, HP0950, HP0202, HP0195, HP1376, HP0371	10/11	9.50E-04	2.91E-03
Purine metabolism	HP0073, HP0072, HP0854, HP0829, HP0775, HP0742, HP0735, HP0572, HP0321, HP0278, HP1275, HP0930, HP0198, HP0409, HP1179, HP0364, HP0104	17/23	1.45E-03	4.29E-03
Fatty acid biosynthesis	HP0090, HP0561, HP0558, HP0557, HP0950, HP0202, HP0195, HP1376, HP0371	9/10	2.12E-03	6.09E-03
Lysine biosynthesis	HP1507, HP1494, HP0822, HP0740, HP0626, HP1013, HP0290, HP1189, HP0212, HP0510	10/12	3.59E-03	9.68E-03
Butanoate metabolism	HP0589, HP0692, HP0691, HP0690, HP0193, HP0192, HP0191, HP1108, HP1109, HP1111	10/12	3.59E-03	9.68E-03
Pyruvate metabolism	HP0589, HP0557, HP1045, HP1325, HP0690, HP0950, HP0193, HP0192, HP0191, HP0121, HP1108, HP1109, HP1111, HP0371	14/19	4.12E-03	1.08E-02
Arginine biosynthesis	HP0073, HP0072, HP1399, HP0512, HP0672, HP0380	6/6	4.87E-03	1.18E-02
Nitrogen metabolism	HP0004, HP0773, HP0512, HP1238, HP0380, HP1186	6/6	4.87E-03	1.18E-02
Pentose phosphate pathway	HP1385, HP1386, HP0742, HP0574, HP1275, HP1166, HP1179, HP1099, HP1100, HP1102, HP0176	11/14	5.04E-03	1.18E-02
DNA replication	HP0012, HP1387, HP1460, HP0615, HP1245, HP1247, HP1323, HP0717, HP0661, HP1231, HP0500	11/14	5.04E-03	1.18E-02
Pyrimidine metabolism	HP0005, HP1474, HP0865, HP0581, HP0266, HP1011, HP1084, HP0349, HP0930, HP0198, HP0919, HP0372, HP0364, HP0104	14/20	8.58E-03	1.96E-02
Alanine, aspartate and glutamate metabolism	HP0056, HP1398, HP1532, HP0649, HP0512, HP1084, HP0672, HP0380, HP0919, HP0723	10/13	9.82E-03	2.07E-02
Glycine, serine and threonine metabolism	HP0098, HP0822, HP1050, HP1071, HP1278, HP0652, HP0974, HP1189, HP0183, HP0397	10/13	9.82E-03	2.07E-02
Nicotinate and nicotinamide metabolism	HP1394, HP0329, HP1337, HP0952, HP0930, HP1356, HP1355	7/8	1.03E-02	2.07E-02
2-Oxocarboxylic acid metabolism	HP0027, HP0026, HP1468, HP0779, HP0330, HP0672, HP1189	7/8	1.03E-02	2.07E-02
Sulfur relay system	HP0013, HP1335, HP0801, HP0800, HP0798, HP0768, HP0220	7/8	1.03E-02	2.07E-02
Selenocompound metabolism	HP1513, HP0825, HP1164, HP0417, HP0106	5/5	1.19E-02	2.29E-02
Vancomycin resistance	HP0740, HP0738, HP0941, HP1155, HP0493	5/5	1.19E-02	2.29E-02
Biotin metabolism	HP0029, HP0598, HP0561, HP0558, HP1254, HP0195, HP1406, HP1376	8/10	1.50E-02	2.83E-02
Propanoate metabolism	HP0779, HP0557, HP1045, HP0690, HP0950, HP1108, HP1109, HP1111, HP0371	9/12	1.88E-02	3.48E-02
Citrate cycle (TCA cycle)	HP0027, HP0026, HP0779, HP0589, HP1325, HP0193, HP0192, HP0191, HP1108, HP1109, HP1111	11/16	2.41E-02	4.37E-02
Galactose metabolism	HP0646, HP1275, HP0360, HP1103	4/4	2.88E-02	4.56E-02
Valine, leucine and isoleucine degradation	HP1468, HP0692, HP0691, HP0690	4/4	2.88E-02	4.56E-02

Tryptophan metabolism	HP0485, HP0875, HP0294, HP0690	4/4	2.88E-02	4.56E-02
Cyanoamino acid metabolism	HP1238, HP0183, HP1118, HP0723	4/4	2.88E-02	4.56E-02
Starch and sucrose metabolism	HP0646, HP1275, HP1166, HP1103	4/4	2.88E-02	4.56E-02
Glycerolipid metabolism	HP1509, HP0700, HP0201, HP1348	4/4	2.88E-02	4.56E-02
Fructose and mannose metabolism	HP0045, HP0044, HP1385, HP0574, HP1275, HP0176, HP0112	7/9	2.97E-02	4.56E-02
Base excision repair	HP1526, HP0650, HP0615, HP0585, HP0348, HP0142, HP1347	7/9	2.97E-02	4.56E-02
Nucleotide excision repair	HP1541, HP0911, HP1478, HP0821, HP0615, HP0705, HP1114	7/9	2.97E-02	4.56E-02
RNA degradation	HP0010, HP1010, HP0247, HP1248, HP1213, HP1228, HP0154, HP0109	8/11	3.52E-02	5.30E-02
Riboflavin metabolism	HP0002, HP1574, HP0804, HP0802, HP1087	5/6	4.68E-02	6.94E-02
Thiamine metabolism	HP0845, HP0844, HP0843, HP0354, HP1287, HP0220	6/8	5.76E-02	8.41E-02
Synthesis and degradation of ketone bodies	HP0692, HP0691, HP0690	3/3	7.01E-02	9.31E-02
Phenylalanine metabolism	HP0294, HP0672, HP0943	3/3	7.01E-02	9.31E-02
D-Glutamine and D-glutamate metabolism	HP0623, HP0549, HP0494	3/3	7.01E-02	9.31E-02
beta-Lactam resistance	HP1565, HP1556, HP0597	3/3	7.01E-02	9.31E-02
Cationic antimicrobial peptide (CAMP) resistance	HP0022, HP0772, HP1375	3/3	7.01E-02	9.31E-02
RNA polymerase	HP0776, HP1293, HP1198	3/3	7.01E-02	9.31E-02
Glutathione metabolism	HP0027, HP0832, HP0570, HP1118	4/5	9.67E-02	1.27E-01
Pentose and glucuronate interconversions	HP1386, HP0646	2/2	1.70E-01	1.92E-01
Valine, leucine and isoleucine biosynthesis	HP1468, HP0330	2/2	1.70E-01	1.92E-01
Lysine degradation	HP1507, HP0690	2/2	1.70E-01	1.92E-01
Benzoate degradation	HP0690, HP0924	2/2	1.70E-01	1.92E-01
Novobiocin biosynthesis	HP0672, HP1380	2/2	1.70E-01	1.92E-01
beta-Alanine metabolism	HP0034, HP0006	2/2	1.70E-01	1.92E-01
D-Alanine metabolism	HP0738, HP0941	2/2	1.70E-01	1.92E-01

Streptomycin biosynthesis	HP1275, HP1103	2/2	1.70E-01	1.92E-01
Aminobenzoate degradation	HP1476, HP0294	2/2	1.70E-01	1.92E-01
Sulfur metabolism	HP1210, HP0107	2/2	1.70E-01	1.92E-01
Degradation of aromatic compounds	HP1476, HP0924	2/2	1.70E-01	1.92E-01
Monobactam biosynthesis	HP1013, HP1189, HP0510	3/4	1.94E-01	2.16E-01
Taurine and hypotaurine metabolism	HP1398, HP1118	2/3	3.70E-01	4.02E-01
Vitamin B6 metabolism	HP0098, HP1582	2/3	3.70E-01	4.02E-01
Ubiquinone and other terpenoid-quinone biosynthesis	HP1483, HP1476, HP0654, HP0396, HP0152	5/10	3.99E-01	4.17E-01
Fatty acid degradation	HP0690	1/1	4.13E-01	4.17E-01
Secondary bile acid biosynthesis	HP1014	1/1	4.13E-01	4.17E-01
Ether lipid metabolism	HP0499	1/1	4.13E-01	4.17E-01
alpha-Linolenic acid metabolism	HP0499	1/1	4.13E-01	4.17E-01
Styrene degradation	HP0294	1/1	4.13E-01	4.17E-01
One carbon pool by folate	HP0577, HP0183, HP1434	3/6	4.82E-01	4.82E-01

